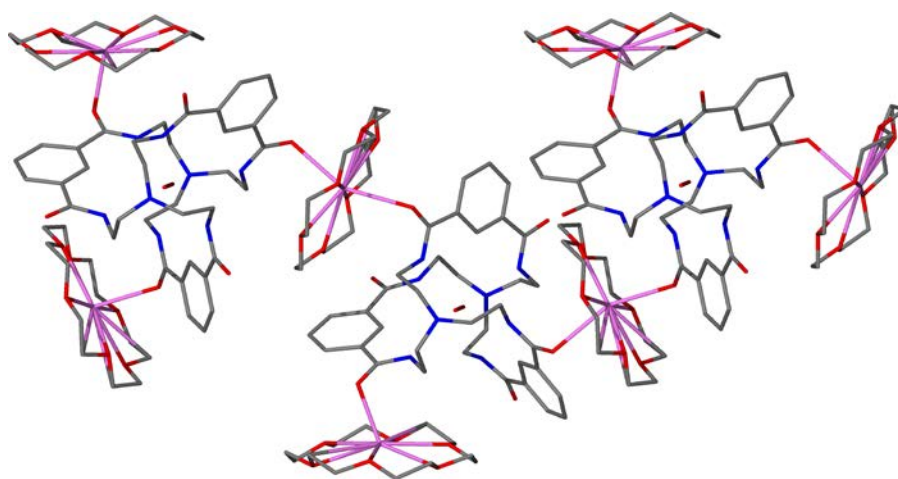
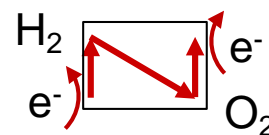
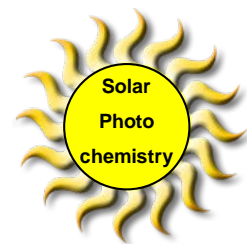
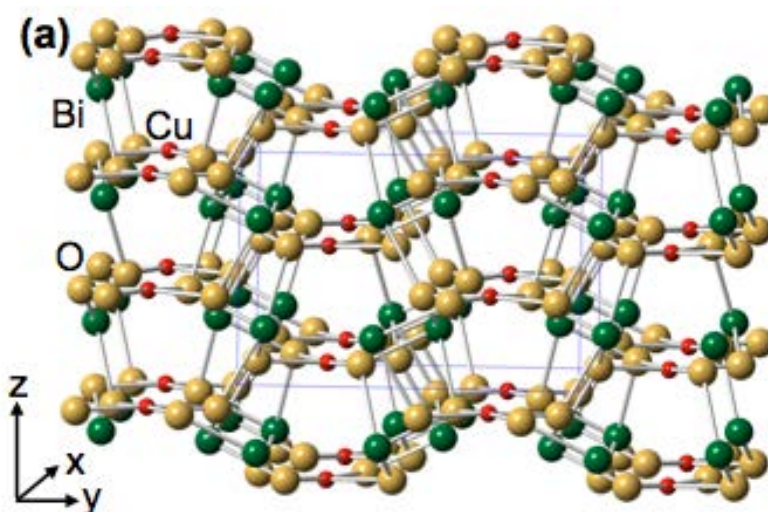


Proceedings of the  
**Thirty-Sixth**  
**DOE Solar Photochemistry**  
**Research Meeting**



The Westin Annapolis, Annapolis, Maryland, June 1-4, 2014



**Sponsored by:**  
**Chemical Sciences, Geosciences, and Biosciences Division**  
**U.S. Department of Energy**



# Program and Abstracts

## Solar Photochemistry Program Research Meeting

Westin Annapolis Hotel  
Annapolis, Maryland  
June 1- 4, 2014

Chemical Sciences, Geosciences, and Biosciences Division  
Office of Basic Energy Sciences  
Office of Science  
U.S. Department of Energy

**Cover Graphics:**

The cover figures are drawn from the abstracts of this meeting. One represents the crystal structure of a hexacarboxamide cryptand to be used as a “hangman” platform for catalysis (Nocera *et al.*, p. 92.) Another depicts the crystal structure of  $\text{CuBi}_2\text{O}_4$  semiconductor which serves as a photocathode for hydrogen production (Choi, p. 38.)

## FOREWORD

The 36<sup>th</sup> Department of Energy Solar Photochemistry Research Meeting, sponsored by the Chemical Sciences, Geosciences, and Biosciences Division of the Office of Basic Energy Sciences, is being held June 1-4, 2014 at the Westin Annapolis Hotel in Annapolis, Maryland. These proceedings include the meeting agenda, abstracts of the formal presentations and posters of the conference, and an address list for the participants.

This Conference is the annual meeting of the grantees who perform research in solar photochemical energy conversion with the support of the Chemical Sciences, Geosciences, and Biosciences Division. This gathering is intended to enable the exchange of new ideas and research concepts between attendees and to further the collaboration and cooperation required for progress in such a difficult field.

This year, the emphasis of the Solar Photochemistry Research Meeting will be on the scientific problem of producing fuels from sunlight. The central program on solar fuels in the Office of Basic Energy Sciences is the Energy Innovation Hub, the Joint Center for Artificial Photosynthesis, and this year, its Director Carl Koval will be a guest lecturer in our opening session on Monday morning. In addition, the meeting is also structured during its daily oral presentation sessions to feature opportunities for discussion of the critical research problems in this topic. A dynamic and instructive exchange is expected.

We would like to express our appreciation to Nada Dimitrijevic for her help in the assembly of this abstract book, to Diane Marceau of the Division of Chemical Sciences, Geosciences, and Biosciences, and to Connie Langston of the Oak Ridge Institute of Science and Education for their assistance with the coordination of the logistics of this meeting. We must also thank all of the researchers whose energy and dedication have made the advances in solar photoconversion of this meeting possible.

Chris Fecko  
Mark T. Spitler  
Chemical Sciences, Geosciences,  
and Biosciences Division  
Office of Basic Energy Sciences

| Solar Photochemistry Research Conference Overview |                              |  |   |   |       |                 |      |
|---|------------------------------|--|---|---|-------|-----------------|------|
| Time  | Sunday, June 1               | Monday, June 2                                       | Tuesday, June 3                               | Wednesdat, June 4   |       |                 |      |
| 7:00  |                              | Breakfest  | Breakfast (7:00-8:00)                         | Breakfast   | 7:00  |                 |      |
| 8:00  |                              | 7:00-8:15  |   | 7:00-8:15   | 8:00  |                 |      |
| 8:15  |                              | Opening Remarks                                      | Session III<br><i>Homogeneous Catalysis</i>   | Session VI<br><i>Catalysis Fundamentals</i>                   | 8:15  |                 |      |
| 8:30  |                              | Session I  |   |   | 8:30  |                 |      |
| 8:45  |                              | <i>Systems for Solar Photoconversion</i>             |   |   | 8:45  |                 |      |
| 9:00  |                              |  |   |   | 9:00  |                 |      |
| 9:15  |                              |  |   |   | 9:15  |                 |      |
| 9:30  |                              | Break  |   |   | 9:30  |                 |      |
| 9:45  |                              | 9:30-10:00   | Session III Discussion                        | Session VI Discussion   | 9:45  |                 |      |
| 10:00   |                              | Session I Continues                                  | Break (10:15-10:30)                           | Break (10:15-10:30)   | 10:00 |                 |      |
| 10:15   |                              |  | 10:15   |   |       |                 |      |
| 10:30   |                              |  | Session IV                                    | Session VII<br><i>Theoretical and Experimental Techniques</i> |       | 10:30           |      |
| 10:45   |                              |  | <i>Heterogeneous Catalysis</i>                |   |       | 10:45           |      |
| 11:00   |                              |  |   |   |       | 11:00           |      |
| 11:15   |                              |  | 11:15   |   |       |                 |      |
| 11:30   |                              |  | 11:30   |   |       |                 |      |
| 11:45   |                              |  | 11:45   |   |       |                 |      |
| 12:00   |                              |  | Session IV Discussion                         |   | 12:00 |                 |      |
| 12:15   |                              | Lunch  |   | Lunch   | 12:15 |                 |      |
| 12:30   |                              | 12:00-1:00   |   | 12:00-1:00  | 12:30 |                 |      |
| 12:45   |                              |  | Lunch   |   | 12:45 |                 |      |
| 1:00  |                              |  | 12:30-1:30                                    | Session VII continues   | 1:00  |                 |      |
| 1:15  |                              |  |   |   | 1:15  |                 |      |
| 1:30  |                              | Individual Time                                      |   |   | 1:30  |                 |      |
| 1:45  |                              |  |   |   | 1:45  |                 |      |
| 2:00  |                              |  |   | Session VII Discussion  | 2:00  |                 |      |
| 2:15  |                              |  | Individual Time                               |   | 2:15  |                 |      |
| 2:30  |                              |  |   | Session I Discussion  | 2:30  |                 |      |
| 2:45  |                              |  |   |   | 2:45  |                 |      |
| 3:00  | Registration                 | Session II<br><i>Photoelectrochemical Subsystems</i> | Session V<br><i>Nanostructured Subsystems</i> |   | 3:00  |                 |      |
| 3:15  | 3:00-6:00                    |  |   |   |       | Closing Remarks | 3:15 |
| 3:30  |                              |  |   |   |       |                 | 3:30 |
| 3:45  |                              |  |   |   |       |                 | 3:45 |
| 4:00  | No Host Reception            |  |   |   |       |                 | 4:00 |
| 4:15  | 5:00-6:00                    |  |   |   | 4:15  |                 |      |
| 4:30  | <i>at the bar</i>            |  |   |   | 4:30  |                 |      |
| 4:45  |                              |  |   |   | 4:45  |                 |      |
| 5:00  |                              | Session II Discussion                                | Session V Discussion                          |   | 5:00  |                 |      |
| 5:15  |                              |  |   |   | 5:15  |                 |      |
| 5:30  |                              |  |   |   | 5:30  |                 |      |
| 5:45  |                              |  |   |   | 5:45  |                 |      |
| 6:00  |                              |  |   |   | 6:00  |                 |      |
| 6:15  |                              | Dinner   |   |   | 6:15  |                 |      |
| 6:30  | Dinner                       | 5:45-8:00  |   |   | 6:30  |                 |      |
| 6:45  | 6:00-7:15                    | <i>on the town</i>                                   | Dinner  |   | 6:45  |                 |      |
| 7:00  |                              |  | 6:15-7:30                                     |   | 7:00  |                 |      |
| 7:15  |                              |  |   |   | 7:15  |                 |      |
| 7:30  | Welcome                      |  |   |   | 7:30  |                 |      |
| 7:45  |                              |  |   |   | 7:45  |                 |      |
| 8:00  | After Dinner Session         | Posters  | Posters                                       |   | 8:00  |                 |      |
| 8:15  | <i>Sensitized Electrodes</i> |  |   |   | 8:15  |                 |      |
| 8:30  |                              | Odd numbers  | Even Numbers                                  |   | 8:30  |                 |      |
| 8:45  | Reception Continues          |  |   |   | 8:45  |                 |      |
| 9:00  | 8:45-10:00                   |  |   |   | 9:00  |                 |      |
| 9:30  | <i>at the bar</i>            | 8:00-10:00   | 8:00-10:00                                    |   | 9:30  |                 |      |
| 10:00   |                              |  |   |   | 10:00 |                 |      |

# *Table of Contents*



# TABLE OF CONTENTS

|                       |     |
|-----------------------|-----|
| <b>Foreword</b> ..... | iii |
| <b>Overview</b> ..... | iv  |
| <b>Program</b> .....  | xv  |

## Abstracts of Oral Presentations

### **Sunday Evening – After Dinner Session: Sensitized Electrodes**

|  |   |
|--|---|
| Light-Stimulated Hole Injection at Dye-Sensitized Phosphide Photocathodes<br><b>Stephen Maldonado</b> , University of Michigan.....  | 3 |
| Molecular and Material Approaches to Overcome Kinetic and Energetic Constraints in Dye-Sensitized Solar Cells<br>Josh Baillargeon, Dhritabrata Mandal, Jesse Ondersma, Suraj Soman, Yuling Xie, and <b>Thomas W. Hamann</b> , Michigan State University..... | 5 |

### **Session I – Systems for Solar Photoconversion**

|  |    |
|--|----|
| Development of Scalably Manufacturable Solar-Fuels Generators<br><b>Carl A. Koval</b> , Joint Center for Artificial Photosynthesis (JACP), California Institute of Technology.....   | 11 |
| Combining Chemical and Biological Strategies to Solar Energy Conversion<br><b>David M. Tiede</b> , Karen L. Mulfort, Lisa M. Utschig, Oleg G. Poluektov, and Lin X. Chen, Argonne National Laboratory.....   | 16 |
| A Tandem Photoelectrochemical Cell for Water Splitting<br><b>Thomas A. Moore</b> , <b>Ana L. Moore</b> , and Devens Gust, Arizona State University.....  | 20 |
| MLCT Excited States at Interfaces and in Rigid Media: Applications in Energy Conversion<br><b>Thomas J. Meyer</b> , Dennis Ashford, Alex Lapides, Byron Farnum, Sheng Zhang, Akitaka Ito, and John Papanikolas, University of North Carolina at Chapel Hill..... | 24 |
| The Challenges of Photoelectrochemical Water Splitting<br><b>John A. Turner</b> , National Renewable Energy Laboratory.....  | 29 |

## Session II – Photoelectrochemical Subsystems

- Nano-Structured Photo-Materials and Electrocatalysts for Conversion of Solar Energy to Fuels  
Allen J. Bard, and **C. Buddie Mullins**, University of Texas at Austin.....33
- Electrochemical Synthesis of Polycrystalline Semiconductor Electrodes with Optimum Compositions and Morphologies for Use in Solar Fuel Production  
**Kyoung-Shin Choi**, University of Wisconsin-Madison.....38
- Design, Discovery and Evaluation of Semiconductors for Visible Light Harvesting  
Polina Burmistrova, Huafeng Huang, Bingfei Cao, Limin Wang, James Ciston, Yimei Zhu, Qixi Mi, Nathan Lewis, John Lofaro, Michael White, Mark Hybertsen, and **Peter Khalifah**, Stony Brook University..... 41
- Functionalization and Modification of Transition Metal Dichalcogenide, GaP, and WO<sub>3</sub> Photoelectrodes  
Joshua D. Wiensch, Victoria Dix, James McKone, Craig Wiggernhorn, and **Nathan S. Lewis**, California Institute of Technology..... 44

## Session III – Homogeneous Catalysis

- Mixed-Metal Supramolecular Complexes as Photocatalysts for Hydrogen Production: Light Capture, Charge Separation, Electron Collection and Catalysis in Single Molecules  
Rongwei Zhou, Hannah Mallalieu, Gerald Manbeck, Skye King, and **Karen J. Brewer**, Virginia Polytechnic Institute.....49
- A Concerted Synthetic, Spectroscopic, and Computational Approach towards Water Splitting by Heterometallic Complexes  
**Cláudio N. Verani**, **John F. Endicott**, and **H. Bernhard Schlegel**, Wayne State University..... 53
- A Systematic Approach to a Molecular Light-driven Water Splitting Catalyst  
Nattawut Kaveevivitchai, Lars Kohler, Ruifa Zong, Lianpeng Tong, and **Randolph P. Thummel**, University of Houston..... 57

## Session IV – Heterogeneous Catalysis

- CO<sub>2</sub> Reduction to Organics in an Aqueous Photoelectrochemical Environment  
Jing Gu, Yong Yan, Amanda J. Morris, Elizabeth L. Zeitler, Yuan Hu, and **Andrew B. Bocarsly**, Princeton University..... 63
- Oxomanganese Catalysts for Solar Fuel Production  
**Gary W. Brudvig**, **Charles A. Schmuttenmaer**, Robert H. Crabtree, and Victor S. Batista, Yale University.....66

|  |    |
|--|----|
| Nanostructured Photocatalytic Water Splitting Systems<br>John R. Swierk, Nicholas S. McCool, Nella M. Vargas-Barbosa, Timothy Saunders,<br>Dongdong Qin, Greg D. Barber, Christopher Gray, Jennifer Dysart, Pengtao Xu, <b>Thomas E. Mallouk</b> , Dalvin D. Mendez-Hernandez, Ana L. Moore, Thomas A. Moore, and<br>Devens Gust, The Pennsylvania State University..... | 71 |
|--|----|

### **Session V – Nanostructured Systems**

|  |    |
|--|----|
| Nanotechnological and Biological Systems for Light-Driven Hydrogen Evolution<br><b>Kara L. Bren, Richard Eisenberg, and Todd D. Krauss</b> , University of Rochester.....                                  | 77 |
| Inorganic Assemblies for Closing the Photosynthetic Cycle on the Nanoscale<br><b>Heinz Frei</b> , Lawrence Berkeley National Laboratory.....   | 80 |
| Solar Energy-Driven Multi-Electron-Transfer Catalysts for Water Splitting: Robust and<br>Carbon-Free Nano-Triads<br><b>Craig L. Hill, Tianquan Lian, and Djamaladdin G. Musaev</b> , Emory University..... | 83 |

### **Session VI – Catalysis Fundamental Research**

|  |    |
|--|----|
| Mechanochemistry and Fuel-Forming Mechano-Electrocatalysis on Spring Electrodes<br>Drazenka Svedruzic, Suzanne Ferrere, and <b>Brian A. Gregg</b> , National Renewable Energy<br>Laboratory..... | 89 |
| Hangman Catalysis for the Activation of Small Molecules<br>Dilek K. Dogutan, Daniel Graham, Manolis Roupelakis, and <b>Daniel G. Nocera</b> , Harvard<br>University.....                         | 92 |
| Artificial Photosynthesis for Photogeneration of Fuels<br><b>Etsuko Fujita</b> , Dmitry E. Polyansky, David C. Grills, and James T. Muckerman,<br>Brookhaven National Laboratory.....            | 95 |

### **Session VII – Theoretical and Experimental Techniques**

|   |     |
|---|-----|
| Semiconductor-Electrocatalyst Contacts: Theory, Experiment, and Applications to Solar<br>Water Photoelectrolysis<br><b>Shannon W. Boettcher</b> , Fuding Lin, and Thomas J. Mills, University of Oregon.....  | 103 |
| Photo- and Electrochemical Water Oxidation: New Water Oxidation Chemistry of<br>Ruthenium Complexes with Polypyridyl Ligands<br><b>James T. Muckerman</b> , Javier J. Concepcion, Dmitry Polyansky, and Etsuko Fujita,<br>Brookhaven National Laboratory..... | 106 |
| Pulse Radiolysis as a Tool for Unraveling Mechanistic Details of Redox Processes<br>Relevant to Solar Energy Conversion<br><b>David C. Grills</b> , Dmitry E. Polyansky, and Etsuko Fujita, Brookhaven National<br>Laboratory.....                            | 110 |

Visible Light Photoactivity of a Mixed  $\alpha$ -(Fe,Cr)<sub>2</sub>O<sub>3</sub>(0001) Surface  
**Michael A. Henderson**, S. E. Chamberlin, Y. Wang, T. C. Kaspar, P. V. Sushko, and  
S.A. Chambers, Pacific Northwest National Laboratory..... 113

Structural Control and Dynamics of Excited State Cu(I) Diimine Complexes for  
Interfacial Photoinduced Charge Transfer and Other Solar Energy Conversion Systems  
**Lin X. Chen**, J. Huang, M. W. Mara, M. R. Harpham, N. M. Dimitrijevic, and K.  
Fransted, Argonne National Laboratory..... 117

**Poster Abstracts** (by poster number)

1. Molecular Origins of Electronic Structure in Inorganic Systems for Solar Photoconversion  
Robert J. Stewart, Christopher Grieco, Adam D. Rimshaw, and John B. Asbury ..... 125
2. Linker Rectifiers for Covalent Attachment of Catalysts to Semiconductor Surfaces  
Wendu Ding, Christian Negre, Laura J. Allen, Rebecca L. Milot, Gary W. Brudvig, Charles A. Schmittenmaer, Robert H. Crabtree, and Victor S. Batista..... 126
3. Photo-Induced Electron Transfer and Electrons in Ionic Liquids  
Edward W. Castner, Jr., Min Liang, Boning Wu, Luiz Felipe O'Faria, and Sufia Khatun ..... 127
4. Molecular Water Oxidation Catalysis: Homogeneous vs Heterogeneous  
Javier J. Concepcion, Etsuko Fujita, and James T. Muckerman..... 128
5. Relating Structure and Photoelectrochemical Properties: Electron Injection by Structurally and Theoretically Characterized Transition-Metal-Doped Polyoxotitanate Nanoparticles  
Philip Coppens, Yang Chen, Katarzyna N. Jarzemska, and Elzbieta Trzop..... 129
6. Hydroxamates as Enhanced Stability Anchors in Solar Cells  
Christopher Koenigsmann, Bradley J. Brennan, Christian F.A. Negre, Matthieu Koepf, Alec C. Durrell, Rebecca L. Milot, Victor S. Batista, Gary W. Brudvig, Robert H. Crabtree, Charles A. Schmittenmaer, Teresa S. Ripolles, Jose A. Torre, and Juan Bisquert ..... 130
7. A Cobalt Perfluoropinacolate Complex for WOC  
Laleh Tahsini, Sarah E. Specht, Mehmed Z. Ertem, Victor S. Batista, and Linda H. Doerrer..... 131
8. Dirhodium Complexes for H<sub>2</sub> Production Using Visible Light Irradiation  
Zhanyong Li, Jarett Martin, Nicholas Leed, Suzanne Witt, Kim R. Dunbar, and Claudia Turro..... 132
9. Polymer Mechanochemistry of Metal Bipyridyls  
Suzanne Ferrere, Drazenka Svedruzic, and Brian Gregg..... 133
10. Trap-free Transport in Ordered and Disordered TiO<sub>2</sub> Nanostructures  
Julio Villanueva-Cab, Song-Rim Jang, Adam F. Halverson, Kai Zhu, and Arthur J. Frank ..... 134
11. Quantum Chemical Calculations on Transition Metal Containing Systems: Redox Potentials, pK<sub>a</sub>'s, and Application to Modeling Electron Trapping and Transport in the Gratzel Cell  
Jing Zhang, Steve Jerome, Mike Steigerwald, Louis Brus, and Richard A. Friesner.... 135

|     |  |     |
|-----|--|-----|
| 12. | Homogeneous Approaches to Photochemically Driving the Reverse Water Gas Shift Reaction<br>Nathan T. La Porte, Mark Westwood, Davis B. Moravec and <u>Michael D. Hopkins</u> .....  | 136 |
| 13. | Mapping Morphology Dependent Charge Separation Pathways in Conjugated Polymer Blends<br>Zhi Guo, Chris Wong, Doyun Lee, Richard Schaller, Xiaobing Zuo, Byeongdu Lee, TengFei Luo, Haifeng Gao, and <u>Libai Huang</u> .....   | 137 |
| 14. | Visible Light Induced Electron Transfer with Thiolated Gold Clusters<br>Yong-Siou Chen, Kevin Stamplecoskie, and <u>Prashant V. Kamat</u> .....  | 138 |
| 15. | Photoinduced Charge Separation and Charge Transport in DNA<br><u>Frederick D. Lewis</u> .....  | 139 |
| 16. | Auger Assisted Electron Transfer from Quantum Dots and Plasmon Induced Hot Electron Transfer in CdS-Au Nanorods<br>Haiming Zhu, Ye Yang, Kaifeng Wu, Zheyuan Chen, and <u>Tianquan Lian</u> .....  | 140 |
| 17. | Controlled Growth and Transport Properties of Indium Tin Oxide Nanoforest<br>Timothy Garvey, Byron Farnum, and <u>Rene Lopez</u> .....   | 141 |
| 18. | Modular Homogeneous and Framework Chromophore-Catalyst Assemblies<br><u>Karen L. Mulfort</u> , Anusree Mukherjee, Oleksandr Kokhan, Jens Niklas, Lin X. Chen, Oleg G. Poluektov, and David M. Tiede.....   | 142 |
| 19. | Efficient Solar Photoelectrolysis by Nanoporous Mo:BiVO <sub>4</sub> through Controlled Electron Transport<br>Jason A. Seabold, Kai Zhu, and <u>Nathan R. Neale</u> .....  | 143 |
| 20. | Formal and Computational Assessment of the ‘States’ Involved in Donor/Acceptor Coupling<br><u>Marshall D. Newton</u> .....   | 144 |
| 21. | Novel Approaches to Efficient Production of Solar Fuels<br>Candy Mercado, Andriy Zakutayev, Kai Zhu, and <u>Arthur J. Nozik</u> .....  | 145 |
| 22. | Photoelectrochemical Studies of Metal Oxide Single Crystals<br>Lauren King, Meghan Kern, Ted Kraus, Alexander Nepomnyashchii, Kevin Watkins, and <u>Bruce Parkinson</u> .....  | 146 |
| 23. | CO <sub>2</sub> Capture by Metal Supported Metal-Organic Frameworks<br><u>Hrvoje Petek</u> , Min Feng, Hao Sun, and Jin Zhao.....  | 147 |
| 24. | Electronic Structure of Molecular Based Co and Ni Catalysts for Solar Fuel Production as Revealed by EPR and DFT<br><u>Oleg G. Poluektov</u> , Jens Niklas, Karen L. Mulfort, Lisa M. Utschig, David M. Tiede, Michael D. Hopkins, Mark Westwood, Claudio N. Verani, and Kristy L. Mardis..... | 148 |

|     |  |     |
|-----|--|-----|
| 25. | Mechanistic Insights into Concerted Proton-Electron Transfer Reactions in the Excited States of NADH-like Transition Metal Complexes<br><u>Dmitry E. Polyansky</u> , Etsuko Fujita, and James T. Muckerman.....  | 149 |
| 26. | Photoinduced Dynamics at Interfaces: Time-Domain Ab Initio Studies<br><u>Oleg V. Prezhdo</u> .....   | 150 |
| 27. | Catalytic Water Oxidation with Monomeric Ru Complexes: Analysis of Reactive Intermediates<br>Lifen Yan, Guibo Zhu, and <u>Yulia Pushkar</u> .....  | 151 |
| 28. | Time Resolved X-ray Analysis of Water Splitting in Photosystem II<br>Katherine Davis, Lifen Yan, and <u>Yulia Pushkar</u> .....  | 152 |
| 29. | Photo-Induced Electron Transfer of Silicon-Phthalocyanines Dispersed in a Conjugated Polymer<br><u>Garry Rumbles</u> , Adam Brunell, Jaehong Park, and Obadiah Reid.....   | 153 |
| 30. | Photocatalysts for H <sub>2</sub> Evolution: Combination of the Light Absorbing Unit and Catalytic Center in a Single Molecule<br>Nicholas Leed, Zhanyong Li, Suzanne Witt, Kim R. Dunbar, and <u>Claudia Turro</u> .....  | 154 |
| 31. | Understanding the effect of catalyst on the photovoltage of an electrodeposited n - Si/SiO <sub>x</sub> /Co/CoOOH photoanode for water oxidation<br>James C. Hill, Alan T. Landers, and <u>Jay A. Switzer</u> .....  | 155 |
| 32. | Simple Photochemical Systems for the Detailed Evaluation of Homogeneous Water Reduction Catalysts<br>Bing Shan, Rebecca Adams, and <u>Russell Schmehl</u> .....  | 156 |
| 33. | Reactivity Mechanisms in New Cobalt Catalysts for Proton Reduction<br>Debashis Basu, Marco Allard, Xuetao Shi, Shivnath Mazumder, <u>H. Bernhard Schlegel</u> and <u>Cláudio N. Verani</u> .....   | 157 |
| 34. | Photosystem I-Molecular Catalyst Complexes for Light-Driven Hydrogen Production: New Acceptor Protein Based Strategies for Hybrid Formation<br><u>Lisa M. Utschig</u> , Sunshine C. Silver, Sarah R. Soltau, Jens Niklas, Karen L. Mulfort, David M. Tiede, and Oleg G. Poluektov..... | 158 |
| 35. | Studies on the <sup>3</sup> MLCT Excited State and Catalytic Water Oxidation Properties of Mono and Multimetallic Ruthenium Complexes<br><u>Cláudio N. Verani</u> , <u>John F. Endicott</u> , and <u>H. Bernhard Schlegel</u> .....  | 159 |
| 36. | Photoinitiated Charge Separation and Transport in Self-assembled Charge Conduits<br><u>Michael R. Wasielewski</u> , Vladimir Roznyatovskiy, Yi-Lin Wu, Raanan Carmieli, Scott M. Dyar, and Kristen E. Brown.....   | 160 |
| 37. | Exciton Delocalization at Nanoscopic Organic/Inorganic Interfaces<br>Matthew Frederick, Victor Amin, Rachel Harris, Ken Aruda, Shengye Jin, and <u>Emily A. Weiss</u> .....  | 161 |

**LIST OF PARTICIPANTS..... 163**

**AUTHOR INDEX..... 171**

# *Program*



**36<sup>th</sup> DOE SOLAR PHOTOCHEMISTRY  
RESEARCH MEETING**

**June 1-4, 2014**

**Westin Annapolis Hotel  
Annapolis, Maryland**

**PROGRAM**

**Sunday, June 1**

- 3:00 – 6:00 p.m.      Registration
- 5:00 – 10:00 p.m.    No Host Reception
- 6:00 – 7:15 p.m.      Dinner

**After Dinner Session – Sensitized Electrodes**

Mark T. Spitler, Chair

- 7:30 p.m.      Welcome
- 7:45 p.m.      Light-Stimulated Hole Injection at Dye-Sensitized Phosphide Photocathodes  
**Stephen Maldonado**, University of Michigan
- 8:15 p.m.      Molecular and Material Approaches to Overcome Kinetic and Energetic  
Constraints in Dye-Sensitized Solar Cells  
Josh Baillargeon, Dhritabrata Mandal, Jesse Ondersma, Suraj Soman, Yuling Xie,  
and **Thomas W. Hamann**, Michigan State University

**Monday Morning, June 2**

- 7:00 a.m.      Breakfast

**Session I**

**Systems for Solar Photoconversion**

Mark T. Spitler, Chair

- 8:15 a.m.      Opening Remarks  
**B. Gail McLean** and **Mark T. Spitler**, US Department of Energy
- 8:30 a.m.      Development of Scalably Manufacturable Solar-Fuels Generators  
**Carl A. Koval**, Joint Center for Artificial Photosynthesis (JACP), California  
Institute of Technology

- 9:30 a.m. Coffee Break
- 10:00 a.m. Combining Chemical and Biological Strategies to Solar Energy Conversion  
**David M. Tiede**, Karen L. Mulfort, Lisa M. Utschig, Oleg G. Poluektov, and Lin X. Chen, Argonne National Laboratory
- 10:30 a.m. A Tandem Photoelectrochemical Cell for Water Splitting  
**Thomas A. Moore, Ana L. Moore**, and Devens Gust, Arizona State University
- 11:00 a.m. MLCT Excited States at Interfaces and in Rigid Media: Applications in Energy Conversion  
**Thomas J. Meyer**, Dennis Ashford, Alex Lapides, Byron Farnum, Sheng Zhang, Akitaka Ito, and John Papanikolas, University of North Carolina at Chapel Hill
- 11:30 a.m. The Challenges of Photoelectrochemical Water Splitting  
**John A. Turner**, National Renewable Energy Laboratory

### Monday Afternoon, June 2

- 12:00 p.m. Lunch

#### Session II Photoelectrochemical Subsystems Jay A. Switzer, Chair

- 3:00 p.m. Nano-Structured Photo-Materials and Electrocatalysts for Conversion of Solar Energy to Fuels  
Allen J. Bard, and **C. Buddie Mullins**, University of Texas at Austin
- 3:30 p.m. Electrochemical Synthesis of Polycrystalline Semiconductor Electrodes with Optimum Compositions and Morphologies for Use in Solar Fuel Production  
**Kyoung-Shin Choi**, University of Wisconsin-Madison
- 4:00 p.m. Design, Discovery and Evaluation of Semiconductors for Visible Light Harvesting  
Polina Burmistrova, Huafeng Huang, Bingfei Cao, Limin Wang, James Ciston, Yimei Zhu, Qixi Mi, Nathan Lewis, John Lofaro, Michael White, Mark Hybertsen, and **Peter Khalifah**, Stony Brook University
- 4:30 p.m. Functionalization and Modification of Transition Metal Dichalcogenide, GaP, and WO<sub>3</sub> Photoelectrodes  
Joshua D. Wiensch, Victoria Dix, James McKone, Craig Wiggernhorn, and **Nathan S. Lewis**, California Institute of Technology

5:00 p.m. Discussion on Challenges and Priorities in Photoelectrochemical Subsystems -  
Program Manager

### **Monday Evening, June 2**

5:45 p.m. Dinner on the town

8:00 - 10:00 p.m. **Posters: Odd numbers**

### **Tuesday Morning, June 3**

7:00 a.m. Breakfast

#### **Session III Homogeneous Catalysis Kim R. Dunbar, Chair**

8:00 a.m. Mixed-Metal Supramolecular Complexes as Photocatalysts for Hydrogen Production: Light Capture, Charge Separation, Electron Collection and Catalysis in Single Molecules  
Rongwei Zhou, Hannah Mallalieu, Gerald Manbeck, Skye King, and **Karen J. Brewer**, Virginia Polytechnic Institute

8:30 a.m. A Concerted Synthetic, Spectroscopic, and Computational Approach towards Water Splitting by Heterometallic Complexes  
**Cláudio N. Verani, John F. Endicott, and H. Bernhard Schlegel**, Wayne State University

9:15 a.m. A Systematic Approach to a Molecular Light-driven Water Splitting Catalyst  
Nattawut Kaveevivitchai, Lars Kohler, Ruifa Zong, Lianpeng Tong, and **Randolph P. Thummel**, University of Houston

9:45 a.m. Discussion on Challenges and Priorities in Homogeneous Catalysis - Program Manager

10:15 a. m. Coffee Break

#### **Session IV Heterogeneous Catalysis Nathan R. Neale, Chair**

10:30 a.m. CO<sub>2</sub> Reduction to Organics in an Aqueous Photoelectrochemical Environment  
Jing Gu, Yong Yan, Amanda J. Morris, Elizabeth L. Zeitler, Yuan Hu, and **Andrew B. Bocarsly**, Princeton University

- 11:00 a.m. Oxomanganese Catalysts for Solar Fuel Production  
**Gary W. Brudvig, Charles A. Schmuttenmaer**, Robert H. Crabtree, and Victor S. Batista, Yale University
- 11:30 a.m. Nanostructured Photocatalytic Water Splitting Systems  
John R. Swierk, Nicholas S. McCool, Nella M. Vargas-Barbosa, Timothy Saunders, Dongdong Qin, Greg D. Barber, Christopher Gray, Jennifer Dysart, Pengtao Xu, **Thomas E. Mallouk**, Dalvin D. Mendez-Hernandez, Ana L. Moore, Thomas A. Moore, and Devens Gust, The Pennsylvania State University
- 12:00 p.m. Discussion on Challenges and Priorities in Heterogeneous Catalysis - Program Manager

### **Tuesday Afternoon, June 3**

- 12:30 p.m. Lunch

#### **Session V** **Nanostructured Subsystems** Prashant V. Kamat, Chair

- 3:00 p.m. Nanotechnological and Biological Systems for Light-Driven Hydrogen Evolution  
**Kara L. Bren, Richard Eisenberg, and Todd D. Krauss**, University of Rochester
- 3:45 p.m. Inorganic Assemblies for Closing the Photosynthetic Cycle on the Nanoscale  
**Heinz Frei**, Lawrence Berkeley National Laboratory
- 4:15 p.m. Solar Energy-Driven Multi-Electron-Transfer Catalysts for Water Splitting: Robust and Carbon-Free Nano-Triads  
**Craig L. Hill, Tianquan Lian, and Djameladdin G. Musaeu**, Emory University
- 5:00 p.m. Discussion on Challenges and Priorities in Nanostructured Subsystems - Program Manager

### **Tuesday Evening, June 3**

- 6:15 p.m. Dinner

- 8:00 – 10:00 p.m. **Posters: Even numbers**

## Wednesday Morning, June 4

7:00 a.m. Breakfast

### **Session VI** **Catalysis Fundamental Research** Michael D. Hopkins, Chair

8:15 a.m. Mechanochemistry and Fuel-Forming Mechano-Electrocatalysis on Spring Electrodes  
Drazenka Svedruzic, Suzanne Ferrere, and **Brian A. Gregg**, National Renewable Energy Laboratory

8:45 a.m. Hangman Catalysis for the Activation of Small Molecules  
Dilek K. Dogutan, Daniel Graham, Manolis Roupelakis, and **Daniel G. Nocera**, Harvard University

9:15 a.m. Artificial Photosynthesis for Photogeneration of Fuels  
**Etsuko Fujita**, Dmitry E. Polyansky, David C. Grills, and James T. Muckerman, Brookhaven National Laboratory

9:45 a.m. Discussion on Challenges and Priorities in Catalysis Fundamental Research - Program Manager

10:15 a.m. Coffee Break

### **Session VII** **Theoretical and Experimental Techniques** H. Bernhard Schlegel, Chair

10:30 a.m. Semiconductor-Electrocatalyst Contacts: Theory, Experiment, and Applications to Solar Water Photoelectrolysis  
**Shannon W. Boettcher**, Fuding Lin, and Thomas J. Mills, University of Oregon

11:00 a.m. Photo- and Electrochemical Water Oxidation: New Water Oxidation Chemistry of Ruthenium Complexes with Polypyridyl Ligands  
**James T. Muckerman**, Javier J. Concepcion, Dmitry Polyansky, and Etsuko Fujita, Brookhaven National Laboratory

11:30 a.m. Pulse Radiolysis as a Tool for Unraveling Mechanistic Details of Redox Processes Relevant to Solar Energy Conversion  
**David C. Grills**, Dmitry E. Polyansky, and Etsuko Fujita, Brookhaven National Laboratory

## Wednesday Afternoon, June 4

12:00 p.m. Lunch

**Session VII**  
**Theoretical and Experimental Techniques**  
**(continued)**

Hrvoje Petek, Chair

- 1:00 p.m. Visible Light Photoactivity of a Mixed  $\alpha$ -(Fe,Cr)<sub>2</sub>O<sub>3</sub>(0001) Surface  
**Michael A. Henderson**, S.E. Chamberlin, Y. Wang, T.C. Kaspar, P.V. Sushko,  
and S.A. Chambers, Pacific Northwest National Laboratory
- 1:30 p.m. Structural Control and Dynamics of Excited State Cu(I) Diimine Complexes for  
Interfacial Photoinduced Charge Transfer and Other Solar Energy Conversion  
Systems  
**Lin X. Chen**, J. Huang, M. W. Mara, M. R. Harpham, N. M. Dimitrijevic, and K.  
Fransted, Argonne National Laboratory
- 2:00 p.m. Discussion on Challenges and Priorities in Theoretical and Experimental  
Techniques - Program Manager
- 2:30 p.m. Discussion on Challenges and Priorities in Systems for Solar Photoconversion -  
Program Manager
- 3:15 p.m. Closing Remarks  
**Mark T. Spitler**, U.S. Department of Energy

*Sunday Evening*

*After Dinner Session: Sensitized Electrodes*



# Light-Stimulated Hole Injection at Dye-Sensitized Phosphide Photocathodes

Stephen Maldonado  
 Department of Chemistry  
 University of Michigan  
 Ann Arbor, MI 48109-1055

This talk will highlight accomplishments to date of our work on developing sensitized photocathodes based on adsorbed chromophores on p-type gallium phosphide (GaP, Figure 1). The intent of the project is to identify and elucidate kinetic, chemical, and electrochemical properties that favor sensitized hole injection with high internal quantum yields and large photovoltage. These features will then be used to design high surface area sensitized photocathode architectures capable of sustaining high total energy conversion efficiency.

First, a quantitative model for describing dye sensitization at a planar semiconductor photoelectrode was developed.<sup>1</sup> A finite-difference simulation program originally designed to model solid-state photovoltaics was modified by changing the boundary conditions at the interfaces to follow explicitly the Marcus-Gerischer theory of heterogeneous charge transfer. In this way, steady-state response characteristics of a planar semiconductor photoelectrode in the dark and under illumination could be modeled through an analysis of all the possible generation and recombination processes with values of experimentally controllable parameters (e.g. charge-carrier lifetimes, hole injection rate constant...etc; Figure 1a) as input parameters. The effects of a complete monolayer of a photoactive molecule capable of injecting holes into a p-type GaP were simulated.

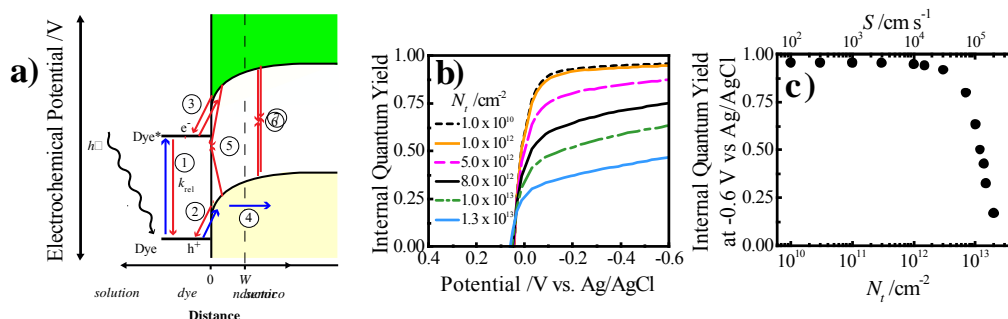


**Figure 1.** (a) Dye-sensitized hole injection from a photoexcited chromophore at the surface of a phosphide semiconductor under depletion conditions. The constituent processes that (blue) favor and (red) limit the magnitude of the net sensitized photocurrent are indicated. These processes are (1) optical excitation/relaxation of the dye, (2) hole transfer between the dye and semiconductor, (3) electron transfer between the dye and semiconductor, (4) electric-field-induced transport within the semiconductor, (5) charge recombination at surface states at the semiconductor interface, (6) charge recombination in the depletion region, and (7) charge recombination in the bulk of the semiconductor. (b) Modeling results for the potential dependence of the internal quantum yield for hole injection at various GaP surface trap densities. (c) The modeled internal quantum yield for hole injection as a function of surface trap density. The corresponding values for surface recombination velocity are also shown. Major simulation parameters:  $N_D = 1.1 \times 10^{18} \text{ cm}^{-3}$ ;  $\mu_n = \mu_p = 100 \text{ cm}^2 \text{ V}^{-1} \text{ s}^{-1}$ ;  $k_{inj} = 3.8 \times 10^{14} \text{ s}^{-1}$ .

A major finding in this phase was the explicit description of the effect that values of each system property has on the efficiency for sensitization. The model specifically showed the benefit of operating under depletion conditions. Strong internal electric fields lower the rates of deleterious ‘reverse’ charge-transfer back in to the dye and electrolyte, favoring the prospects for efficient hole injection and relaxing the demands on other system properties. Figures 1b and c highlight results that identify the minimum surface defect density required for efficient sensitization at a p-GaP photoelectrode. Under strong depletion conditions, the tolerances towards surface defects

(traps) is relaxed, suggesting that even normally ‘defective’ native GaP surfaces should support sensitization with reasonably high internal quantum yields. Further, only moderate levels of passivation should be necessary to attain hole injection with unity quantum yield. Accordingly, we identified conditions that facilitated the first measurement of sensitized hole injection from a quantum dot into a semiconductor photoelectrode.<sup>2</sup>

Second, we developed new wet chemistries for the functionalization of GaP amenable for dye sensitization.<sup>3-6</sup> One example is functionalization of GaP(111)A surfaces with short organic groups attached through covalent Ga-C surface bonds (Figure 2).<sup>3,4</sup> Following modification, a profound change in the flat-band potential of GaP(111) electrodes modified with either methyl or allyl groups immersed in water was observed relative to native GaP interfaces, along with an insensitivity of the flat-band potential towards changes in solution pH. Further, both types of modified GaP surfaces were chemically stabilized against chemical degradation in air and water and also demonstrated a lowered content of surface trap states, implying the allyl group was as effective as stabilizing the surface but with the capacity for further derivitization. Recent results with allyl-terminated surfaces show molecular species can be grafted without perturbing the underlying Ga-C surficial bonding.

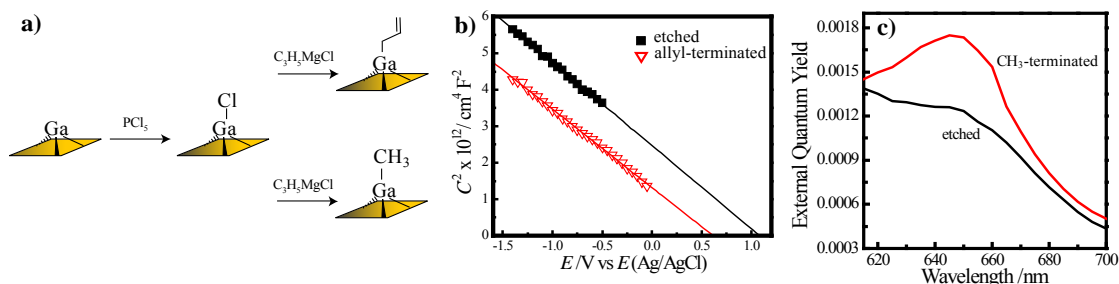


**Figure 2.** (a) Schematic depiction of GaP functionalization. (b) Representative reciprocal squared capacitance-potential plots for p-GaP(111)A electrodes that were either just etched (solid black squares) or reacted with C<sub>3</sub>H<sub>5</sub>MgCl (open red triangles) in 1M KCl, 20 mM EuCl<sub>2</sub>, 20 mM EuCl<sub>3</sub>. (c) Wavelength-dependent external quantum yields measured for etched and CH<sub>3</sub>-terminated GaP(111)A photoelectrodes immersed in a solution with [Brilliant Green] = 16 μM.

Studies on the extent that electronic coupling between GaP and the sensitizer (molecular and quantum dot) have on the attainable internal quantum yields are ongoing using the aforementioned functionalization route as well as grafting with N-heterocyclic carbenes and Williamson-ether coupling (i.e. P-O-C surface bonds). These findings will then be applied to high-aspect-ratio GaP photocathode architectures that support both high sensitizer loadings and operate under depletion conditions. The intent is to determine which modification strategy or strategies are best suited for high surface-area GaP materials that can function with high external quantum yields.

#### DOE Sponsored Publications 2011-2014

1. Chitambar, M. J.; Wang, Z.; Liu, Y.; Rockett, A.; **Maldonado, S. J. Am. Chem. Soc. 2012, 134, 10670-10681.**
2. Wang, Z.; Shakya, A.; Gu, J.; Lian, S.; **Maldonado, S. J. Am. Chem. Soc. 2013, 135, 9275-9278.**
3. Peczonczyk, S.; Brown, E. S.; **Maldonado, S. Langmuir 2014, 30, 156-164.**
4. Eady, S. C.; Peczonczyk, S. L.; **Maldonado, S.; Lehnert, N. Chem. Comm. 2014, submitted (in revision stage).**
5. Brown, E. S.; Peczonczyk, S.; Wang, Z.; **Maldonado, S. J. Phys. Chem. C 2014, submitted.**
6. Brown, E. S.; **Maldonado, S. 2014, in preparation (target submission April 2014).**

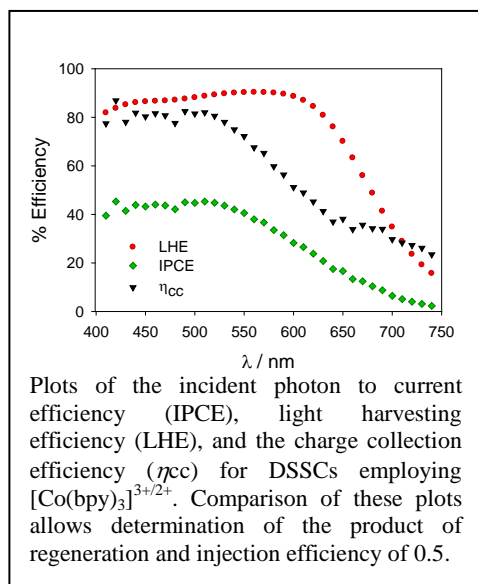
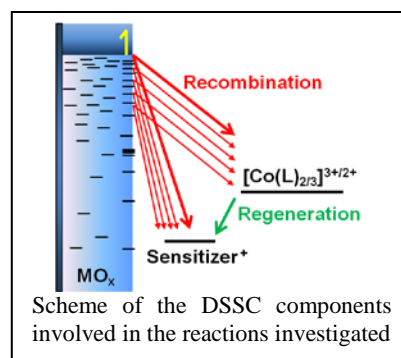
# Molecular and Material Approaches to Overcome Kinetic and Energetic Constraints in Dye-Sensitized Solar Cells

Josh Baillargeon, Dhritabrata Mandal, Jesse Ondersma, Suraj Soman, Yuling Xie,

Thomas W. Hamann

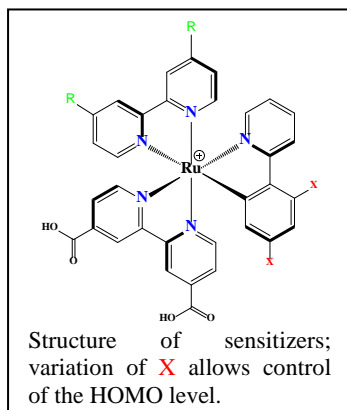
Department of Chemistry  
Michigan State University  
East Lansing, MI 48824

The general goal of this project is to understand the fundamental role of the relevant dye-sensitized solar cell, DSSC, components (redox shuttle, photoanode and sensitizer) involved in key efficiency-determining processes. Ultra-fast electron injection from a photoexcited sensitizer into a photoanode produces a charge separated state with typically high quantum efficiency. We are primarily interested in the subsequent processes of dye regeneration and recombination which control the charge collection. We systematically vary the components involved in each reaction and interrogate them with a series of photoelectrochemical measurements. The general lessons learned will ultimately be used to develop design rules for next generation DSSCs comprised of molecules and materials which are capable of overcoming the kinetic and energetic constraints of current generation cells.



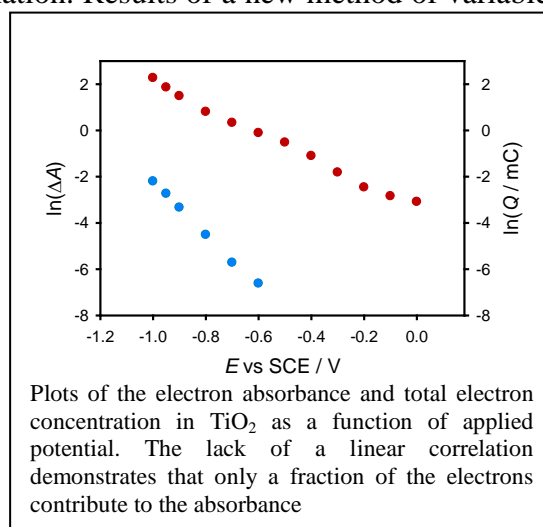
The  $\text{I}_3^-/\text{I}^-$  redox couple has been the predominant redox shuttle in DSSCs partially due to quantitative regeneration when used with conventional ruthenium based sensitizers such as N3. The regeneration efficiency is determined by the kinetic competition between dye regeneration by the redox shuttle and recombination of electrons in the photoanode with the oxidized sensitizer. Achieving quantitative regeneration with  $\text{I}_3^-/\text{I}^-$ , however, comes at an energy penalty of  $>500$  meV, and is not generally compatible with all sensitizers. Thus, our aim is to elucidate the interplay of redox shuttle and sensitizer in controlling regeneration and the photoanode and sensitizer in controlling recombination, in order to minimize the energy lost in driving these reactions. We utilize one-electron outersphere redox shuttles that are amenable to systematic variation. Recent results

comparing the regeneration efficiency of cells employing cobalt bis-trithiacyclonane,  $[\text{Co}(\text{ttcn})_2]^{3+/2+}$ , and cobalt tris-bipyridine,  $[\text{Co}(\text{bpy})_3]^{3+/2+}$ , redox shuttles in combination with organic sensitizers will be presented. We found that  $[\text{Co}(\text{ttcn})_2]^{2+}$  is capable of quantitative dye regeneration with only a  $\sim 200$  meV driving force, whereas regeneration with  $[\text{Co}(\text{bpy})_3]^{3+/2+}$  is suboptimal with a  $\sim 300$  meV driving force. These results can be understood in the context of Marcus cross exchange reactions. The rates of regeneration and recombination are also affected



by the oxidation potential (HOMO) of the sensitizer. We have therefore synthesized a series of cyclometalated sensitizers which allow for the control of HOMO level (x) as well as the steric bulk (R) through introduction of substituents on the phenylpyridine or bipyridine ligands, respectively. Recent results of examining the regeneration of this series of sensitizers will also be presented.

Additional current efforts are aimed at measuring recombination both to the sensitizer and outersphere redox shuttles under operational conditions of a cell. The photoanode plays a central role as the electron donor in these recombination reactions. We have therefore been pursuing spectroelectrochemical methods to determine the energetics and density of trap states of photoanode materials. The results of these measurements show a clear discrepancy between electrons in trap states and free conduction band electrons. The conduction band edge,  $E_{CB}$ , is arguably the most important physical property of the photoanode in determining the rate of recombination. Results of a new method of variable temperature spectroelectrochemistry employed to determine  $E_{CB}$  of  $TiO_2$  photoanodes, as well as the extinction coefficient of electrons delocalized in the conduction band, will also be presented. The recombination of electrons from trap states and from the conduction band determined by measuring the electron lifetime in contact with very positive, low reorganization energy redox shuttles and moderate potential, high reorganization energy redox shuttles, respectively. The results from a similar set of experiments on alternative photoanode materials, such as  $SrTiO_3$ , will also be presented. The combined results of this research will ultimately allow us to make detailed structure–function relationships of the photoanode.



Future work involves developing new methods to measure the recombination rate under operational (steady state) conditions, opposed to the high light intensity transient absorption measurements typically employed. Success will allow simultaneous determination of recombination to dye and redox shuttles, in addition to regeneration, for the systematically varied sensitizer, photoanode and redox shuttle. Leveraging results derived from this comprehensive approach will allow the development of the next-generation DSSC.

## DOE Sponsored Publications 2011-2014

1. Soman, S., Xie, Y., Hamann, T.W.; “Cyclometalated Sensitizers for DSSCs Employing Cobalt Redox Shuttles” *Polyhedron*, 2014, submitted.
2. Xie, Y., Hamann, T.W.; “Fast Low Spin Cobalt Complex Redox Shuttles for Dye-Sensitized Solar Cells.” *Journal of Physical Chemistry Letters*, 2013, 4, 328–332.
3. Ondersma, J.W.; Hamann, T.W.; “Recombination and Redox Couples in Dye-Sensitized Solar Cells.” *Coordination Chemistry Reviews* 2013, 257, 1533–1543.
4. Ondersma, J.W.; Hamann, T.W.; “Conduction Band Energy Determination by Variable Temperature Spectroelectrochemistry.” *Energy and Environmental Science* 2012, 5 (11), 9476–9480.
5. Hamann, T.W.; “The End of Iodide? Cobalt Complex Redox Shuttles in DSSCs.” *Dalton Transactions*, 2012, 41 (11), 3111 – 3115.
6. Ondersma, J.W.; Hamann, T.W.; “Spatially-Resolved Sources of Dark Current in Nanoparticle TiO<sub>2</sub> Electrodes.” *Langmuir* 2011, 27 (21), 13361–13366.



*Session I*

*Systems for Solar Photoconversion*



## Development of Scalably Manufacturable Solar-Fuels Generators

Carl A. Koval

Joint Center for Artificial Photosynthesis (JCAP)

California Institute of Technology

Pasadena, CA 91125

JCAP's mission is to build fully integrated solar-fuels generators that utilize earth-abundant semiconductors and catalysts for efficient conversion of water to O<sub>2</sub> and H<sub>2</sub> and for the reduction of CO<sub>2</sub> to liquid fuels. JCAP prototypes are designed to enable separation of products and therefore require membranes and complex interfaces between various material components that will function under realistic operating conditions. JCAP's long-term goal is to develop a commercially viable, solar-generation technology that simultaneously satisfies the following four criteria: high efficiency, multi-year stability, low module cost, and safe operation. JCAP's approach to assembling complete artificial photosynthetic systems is to develop robust concepts for complete solar-fuels generators, then to break them down into essential assemblies of components, and finally to adapt or discover the materials needed to fabricate those assemblies. JCAP bridges basic and applied sciences as well as engineering associated with prototype construction and consideration of scale-up challenges.

JCAP's prototyping activity involves conceptual design, detailed modeling, comprehensive design, fabrication, assembly and testing.<sup>1-5</sup> Multi-dimensional, multi-physics models that couple light absorption, electronic transport, catalysis, and solution transport have been developed. These modeling tools allow JCAP to optimize geometries of prototype designs, guide materials development, define operational conditions and constraints, understand cell performance in real life environments, and evaluate the viability of new design concepts. In addition, JCAP performs studies aimed at understanding requirements for solar-fuels generating facilities at the GW scale, and also manufacturing strategies for solar water-splitting modules.<sup>6</sup>

In order to assemble solar-fuels generators, JCAP needs to develop and understand the integration of materials and processes over a wide range of length scales. One of JCAP's most important accomplishments has been the development of n-p<sup>+</sup>-Si/n-WO<sub>3</sub> and n-p<sup>+</sup>-Si/n-TiO<sub>2</sub> core-shell microwire devices for solar water splitting under both acidic and basic conditions.<sup>7</sup> Preparation of these complex structures requires optimization and control of a series of processing techniques and instruments. A second critical integration issue is the ability to protect materials from corrosion and other damaging processes during operation in a complete device. JCAP has utilized atomic layer deposition (ALD) and nanostructuring methods to protect both photocathodes and photoanodes for up to hundreds of hours.<sup>8-11</sup>

Materials with the optimal properties required to construct solar-fuels generators do not yet exist. JCAP's materials discovery research utilizes both traditional (i.e., directed) and high-throughput experimentation methods, and also takes advantage of computational theory and DOE User Facilities. In order to make meaningful performance comparisons between materials, JCAP develops and implements uniform methods and protocols for benchmarking the activities of oxygen evolution reaction (OER), hydrogen evolution reaction (HER), and

CO<sub>2</sub> reduction reaction (CO<sub>2</sub>RR) catalysts under solar-fuels generator operating conditions.<sup>12</sup> JCAP is also heavily invested in a coordinated effort that involves the high-throughput synthesis, screening, characterization and analysis of light absorbing and catalyst materials. Composition libraries are prepared by ink-jet printing and physical vapor deposition, and subsequently screened using a suite of instruments invented by JCAP such as a parallel catalyst screening instrument that can quantify catalytic activity based on bubble imaging,<sup>13</sup> a high-throughput scanning droplet electrochemical cell that allows for full 3-electrode (photo)electrochemical measurements,<sup>14</sup> and a photoabsorber screening instrument that fills the technological gap between optical characterization and photoelectrochemical water splitting.<sup>15</sup> Using this approach, JCAP has recently discovered and rapidly developed a new class of cerium-rich OER catalysts comprised entirely of earth-abundant elements and having catalytic activities approaching those of the best known noble-metal based catalysts.<sup>16</sup>

JCAP has a portfolio of research projects aimed at the directed discovery, characterization and understanding of light absorber, catalyst and membrane materials. Through directed research, JCAP has developed suitable materials for photocathodes, including Si and WSe<sub>2</sub>, that are relatively stable and that have demonstrated high efficiency for the solar-driven production of H<sub>2</sub> from H<sub>2</sub>O. Also, JCAP has discovered a technique for preparing nanopillar photocathodes composed of p-type InP for efficient solar-driven hydrogen production, and developed a thin-film, polycrystalline InP photocathode material using non-epitaxial growth methods combined with a nanotexturing and atomic layer deposition protection process.<sup>17</sup> Guided by a detailed understanding of optical interactions, JCAP researchers, working in collaboration with researchers from the Center for Energy Nanoscience, a DOE Energy Frontier Research Center, have demonstrated that a sparse array of GaAs nanowires (<10% areal coverage) has nearly 100% photoelectrochemical charge conversion efficiency.<sup>18</sup> Moreover, JCAP has discovered and characterized a new class of light absorbers comprised of ZnSn<sub>x</sub>Ge<sub>1-x</sub>N<sub>2</sub>.<sup>19</sup> The direct gap can be tuned from 2 eV to 3.1 eV by simple control of the composition, and these materials can be deposited in high quality thin film form by a scalable process. Two new and scalable thin-film deposition methods for BiVO<sub>4</sub>, a photoanode material composed of earth-abundant elements, were also developed.<sup>10,20,21</sup> Both methods provide control of stoichiometry, which is important for both understanding the basic properties of the materials and maximizing OER performance.

Each half reaction in solar water-splitting requires discovery of stable catalysts that promote the oxidation of water and the reduction of protons at low overpotentials. These catalytic systems must also be composed of inexpensive, scalable, and earth-abundant materials. *In situ* studies of highly active FeNiOx catalysts for the electrochemical oxidation of water in basic electrolytes have been investigated in order to identify the composition and local environment of the active sites.<sup>22</sup> Combined experimental and theoretical studies suggest that the high activity of these catalysts arises from Fe<sup>3+</sup> cations contained in strained octahedral environments within a matrix of  $\gamma$ -NiOOH. Currently only IrO<sub>2</sub> can reach JCAP's performance goals under acidic conditions. In order to develop catalysts with low Ir loading and/or to find a replacement for Ir, the mechanism of OER under acidic conditions was probed by ambient pressure X-ray photoelectron spectroscopy using a customized electrochemical cell. It was demonstrated that, under OER conditions, iridium undergoes a change in oxidation state from Ir(IV) to Ir(V) that takes place predominantly at the surface of

the catalyst. Under acidic conditions, cobalt phosphide HER catalysts showed an overpotential of only 85 mV at a current density of 10 mA cm<sup>-2</sup>. Molybdenum and cobalt selenide catalysts were also prepared and investigated for HER.<sup>23</sup>

A fully integrated solar-fuels generator requires separation of products for both safety and efficiency, while allowing for sufficient ion-conduction between the reduction and oxidation chambers. In solar fuel generators, the gas back diffusion becomes a primary concern due to the comparable rate of hydrogen production and permeation across the membrane. Device geometry requirements dictated by the light absorption also limit the tolerable crossover of product gases, and elevate the importance of good mechanical properties.<sup>24</sup> In light of the unique membrane requirements for solar fuel generators, JCAP is focused on developing new material systems that have balanced and tunable ion and gas transport properties necessary for a solar-fuels generator membrane.<sup>25</sup>

## References

1. Modestino, M. A.; Diaz-Botia, C. A.; Haussener, S.; Gomez-Sjoberg, R.; Ager, J. W.; Segalman, R. A., "Integrated microfluidic test-bed for energy conversion devices". *Physical Chemistry Chemical Physics* 2013, 15, 7050-7054.
2. Modestino, M. A.; Walczak, K. A.; Berger, A.; Evans, C. M.; Haussener, S.; Koval, C.; Newman, J. S.; Ager, J. W.; Segalman, R. A., Robust production of purified H<sub>2</sub> in a stable, self-regulating, and continuously operating solar fuel generator. *Energy & Environmental Science* 2014, 7, 297-301.
3. Xiang, C. X.; Chen, Y. K.; Lewis, N. S., Modeling an integrated photoelectrolysis system sustained by water vapor. *Energy & Environmental Science* 2013, 6, 3713-3721.
4. Coridan, R. H.; Shaner, M.; Wiggernhorn, C.; Brunschwig, B. S.; Lewis, N. S., Electrical and Photoelectrochemical Properties of WO<sub>3</sub>/Si Tandem Photoelectrodes. *Journal of Physical Chemistry C* 2013, 117, 6949-6957.
5. Berger, A.; Segalman, R. A.; Newman, J., Material Requirements for Membrane Separators in a Water-Splitting Photoelectrochemical Cell. *Energy & Environmental Science* 2014.
6. Zhai, P.; Haussener, S.; Ager, J.; Sathre, R.; Walczak, K.; Greenblatt, J.; McKone, T., Net primary energy balance of a solar-driven photoelectrochemical water-splitting device. *Energy & Environmental Science* 2013, 6, 2380-2389.
7. Shaner, M.; Foutaine, K.; Ardo, S.; Atwater, H.; Lewis, N., Photoelectrochemistry of Core-Shell Tandem Junction n-p<sup>+</sup>-Si/n-WO<sub>3</sub> Microwire Array Photoelectrodes. *Energy and Environmental Science* 2013.
8. Lin, Y. J.; Battaglia, C.; Boccard, M.; Hettick, M.; Yu, Z. B.; Ballif, C.; Ager, J. W.; Javey, A., Amorphous Si Thin Film Based Photocathodes with High Photovoltage for Efficient Hydrogen Production. *Nano Letters* 2013, 13, 5615-5618.
9. Hu, S.; Shaner, M.; Beardslee, J.; Lichterman, M.; Brunschwig, B.S.; Lewis, N.S., Quantitative, sustained, efficient solar-driven water oxidation with "leaky" TiO<sub>2</sub>

10. Lichterman, M. F.; Shaner, M. R.; Handler, S. G.; Brunschwig, B. S.; Gray, H. B.; Lewis, N. S.; Spurgeon, J. M., Enhanced Stability and Activity for Water Oxidation in Alkaline Media with Bismuth Vanadate Photoelectrodes Modified with a Cobalt Oxide Catalytic Layer Produced by Atomic Layer Deposition. *Journal of Physical Chemistry Letters* 2013, 4, 4188-4191.
11. Javey, A.; Ager, J.; Lee, M. H.; Kuniharu, T. Nanotexturing and Oxide Surface Passivation for Improved Photoelectrochemical Performance. 2012.
12. McCrory, C. C. L.; Jung, S. H.; Peters, J. C.; Jaramillo, T. F., Benchmarking Heterogeneous Electrocatalysts for the Oxygen Evolution Reaction. *Journal of the American Chemical Society* 2013, 135, 16977-16987.
13. Xiang, C.; Suram, S. K.; Haber, J. A.; Guevarra, D. W.; Soedarmadji, E.; Jin, J.; Gregoire, J. M., High-Throughput Bubble Screening Method for Combinatorial Discovery of Electrocatalysts for Water Splitting. *ACS Combinatorial Science* 2014, 16, 47-52.
14. Gregoire, J. M.; Xiang, C. X.; Liu, X. N.; Marcin, M.; Jin, J., Scanning droplet cell for high throughput electrochemical and photoelectrochemical measurements. *Review of Scientific Instruments* 2013, 84, 6.
15. Gregoire, J. M.; Xiang, C.; Mitrovic, S.; Liu, X.; Marcin, M.; Cornell, E. W.; Fan, J.; Jin, J., Combined Catalysis and Optical Screening for High Throughput Discovery of Solar Fuels Catalysts. *Journal of the Electrochemical Society* 2013, 160, F337-F342.
16. (a) Haber, J. A.; Cai, Y.; Jung, S.; Xiang, C.; Mitrovic, S.; Jin, J.; Bell, A. T.; Gregoire, J. M., High Throughput Mapping of Electrochemical Properties of (Ni-Fe-Co-Ce)Ox Oxygen Evolution Catalysts. *CHemElectroChem* 2013; (b) Haber, J. A.; Cai, Y.; Jung, S.; Xiang, C.; Mitrovic, S.; Jin, J.; Bell, A. T.; Gregoire, J. M., Discovering Ce-rich oxygen evolution catalysts, from high throughput screening to water electrolysis. *Energy & Environmental Science*, 2014.
17. Lee, M. H.; Takei, K.; Zhang, J. J.; Kapadia, R.; Zheng, M.; Chen, Y. Z.; Nah, J.; Matthews, T. S.; Chueh, Y. L.; Ager, J. W.; Javey, A., p-Type InP Nanopillar Photocathodes for Efficient Solar-Driven Hydrogen Production. *Angewandte Chemie-International Edition* 2012, 51, 10760-10764.
18. Hu, S.; Chi, C. Y.; Fountaine, K. T.; Yao, M. Q.; Atwater, H. A.; Dapkus, P. D.; Lewis, N. S.; Zhou, C. W., Optical, electrical, and solar energy-conversion properties of gallium arsenide nanowire- array photoanodes. *Energy & Environmental Science* 2013, 6, 1879-1890.
19. (a) Chen, S.; Narang, P.; Atwater, H.; Wang, L. W., Phase Stability and Defect Physics of Ternary ZnSnN<sub>2</sub> Semiconductor: First Principles Insights. *Advanced Materials* 2013; (b) Narang, P.; Chen, S.; Coronel, N.; Gul, S.; Yano, J.; Wang, L. W.; Lewis, N. S.; Atwater, H. A., Band Gap Tunability in Zn(Sn,Ge)N<sub>2</sub> Semiconductor Alloys. *Advanced Materials* 2013.
20. Chen, L.; Aarcon-Lado, E.; Hettick, M.; Sharp, I. D.; Lin, Y. J.; Javey, A.; Ager, J. W., Reactive Sputtering of Bismuth Vanadate Photoanodes for Solar Water Splitting. *Journal*

of Physical Chemistry C 2013, 117, 21635-21642.

21. Alarcon-Llado, E.; Chen, L.; Hettick, M.; Mashouf, N.; Lin, Y. J.; Javey, A.; Ager, J. W., BiVO<sub>4</sub> thin film photoanodes grown by chemical vapor deposition. *Physical Chemistry Chemical Physics* 2014, 16, 1651-1657.
22. (a) Yeo, B. S.; Bell, A. T., In Situ Raman Study of Nickel Oxide and Gold-Supported Nickel Oxide Catalysts for the Electrochemical Evolution of Oxygen. *Journal of Physical Chemistry C* 2012, 116, 8394-8400; (b) Louie, M. W.; Bell, A. T., An Investigation of Thin-Film Ni-Fe Oxide Catalysts for the Electrochemical Evolution of Oxygen. *Journal of the American Chemical Society* 2013, 135, 12329- 12337.
23. Velazquez, J. M.; Saadi, F. H.; Pieterick, A. P.; Spurgeon, J. M.; Soriaga, M. P.; Brunschwig, B. S.; Lewis, N. S., Synthesis and hydrogen-evolution activity of tungsten selenide thin films deposited on tungsten foils. *Journal of Electroanalytical Chemistry* 2014.
24. Haussener, S.; Xiang, C.; Spurgeon, J. M.; Ardo, S.; Lewis, N. S.; Weber, A. Z., Modeling, simulation, and design criteria for photoelectrochemical water-splitting systems. *Energy & Environmental Science* 2012, 5 (12), 9922-9935.
25. (a) Hoarfrost, M. L.; Tyagi, M.; Segalman, R. A.; Reimer, J. A., Proton Hopping and Long-Range Transport in the Protic Ionic Liquid [Im][TFSI], Probed by Pulsed-Field Gradient NMR and Quasi-Elastic Neutron Scattering. *The Journal of Physical Chemistry B* 2012, 116 (28), 8201-8209; (b) Schneider, Y.; Modestino, M. A.; McCulloch, B. L.; Hoarfrost, M. L.; Hess, R. W.; Segalman, R. A., Ionic Conduction in Nanostructured Membranes Based on Polymerized Protic Ionic Liquids. *Macromolecules* 2013, 46, 1543-1548; (c) Sudre, G.; Inceoglu, S.; Cotanda, P.; Balsara, N. P., Influence of Bound Ion on the Morphology and Conductivity of Anion-Conducting Block Copolymers. *Macromolecules* 2013, 46, 1519-1527.

## Combining Chemical and Biological Strategies to Solar Energy Conversion

David M. Tiede, Karen L. Mulfort, Lisa M. Utschig, Oleg G. Poluektov, and Lin X. Chen  
Chemical Sciences and Engineering Division  
Argonne National Laboratory  
Argonne, IL, 60439

This program investigates fundamental mechanisms for coupling the solar photon produced excited-states to multiple-electron, proton-coupled fuels catalysis in natural and artificial photosynthesis. The comparison between natural and artificial photosynthesis is used to identify fundamental principles for solar energy conversion and to develop strategies for the design of sustainable photosynthetic systems for solar energy conversion. The program investigates mechanisms for solar energy conversion at the most fundamental level by the development and application of advanced synchrotron X-ray techniques, electron paramagnetic resonance spectroscopy, and ultrafast transient optical spectroscopy for structure-function analyses. Synthetic approaches are developed that implement both biologically-inspired chemical designs and chemically-inspired biohybrid designs to test concepts derived from fundamental studies in natural and artificial photosynthesis. This presentation will provide examples of chemically-inspired biohybrid designs for multi-electron solar fuels catalysis, and present results on X-ray characterization of amorphous oxide water-oxidation catalyst films as an approach for resolving metal-oxo coordination chemistry underlying photosynthetic water-splitting. The X-ray studies have further relevance for the development of capabilities for structure resolution linked to photochemical energy conversion at electrode interfaces.

*1. Supramolecular bio-hybrid assemblies for investigation of fundamental mechanisms for solar energy to fuels conversion.* Supramolecular architectures solar fuels catalysis include designs that link photosensitizer and catalyst molecular modules. Current research points to the challenges of creating architectures that support the multiple electron and proton transfers needed for solar fuels catalysis, while avoiding a variety of excited-state quenching and charge recombination pathways. Synthetic biology approaches have demonstrated opportunities to create hybrid molecular architectures of precisely controlled structure that incorporate molecular recognition, host-guest chemistry, repair, and sustainability of biology-based frameworks, and combine these with the robustness and tunability of chemical systems. Our program investigates the opportunities to exploit protein “molecular wires” as components in supramolecular biohybrid synthesis, and to investigate fundamental mechanisms for multiple-electron, proton-coupled, solar-driven catalysis using sequential, single turn-over light pulses and high-resolution structural characterization in homogeneous phase and crystalline samples. Our on-going work has investigated a variety of self-assembly and covalent linking strategies for coupling

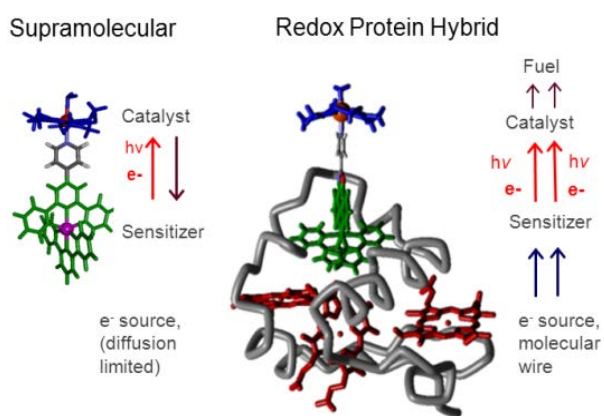
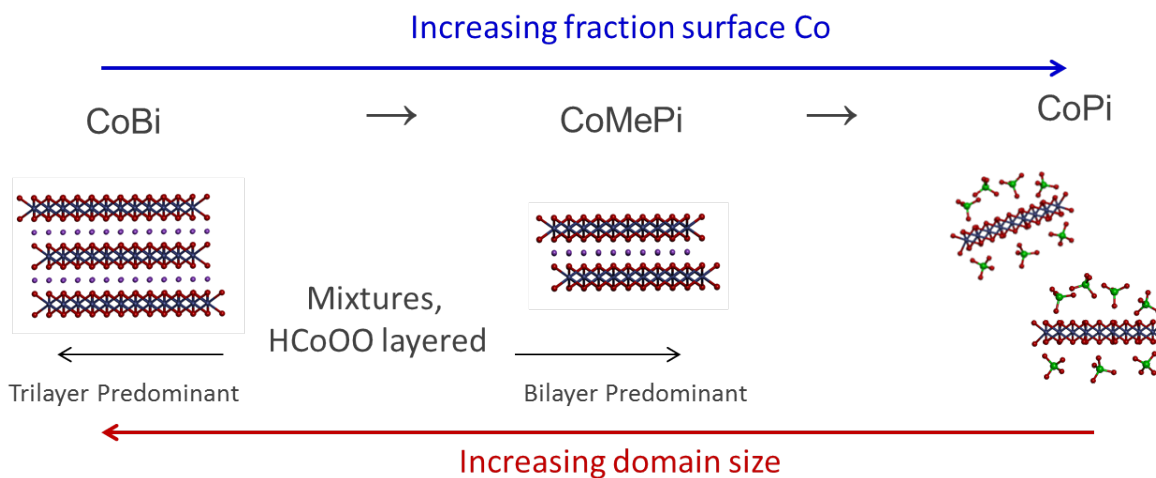


**Figure 1.** Comparison of supramolecular (left) and redox protein hybrid (right) architectures for solar fuels catalysis. Adjacent are electron transport schemes.

photosensitizers to the tri-heme cytochromes *c7* from *Geobacter sulfurreducens*. This work has mapped out site-dependent photo-sensitized electron transfer to cofactor hemes using Ru(bpy)<sub>3</sub> derivatives that are covalently linked to cysteine residues placed at a variety of positions on the cytochrome *c7* surface through site-directed mutagenesis. Rates of electron transfer were found to vary from 10<sup>11</sup> s<sup>-1</sup> to 10<sup>6</sup> s<sup>-1</sup> depending upon the site and pathway for electron transfer. Photochemical quenching processes are found to track in parallel the site-dependent electron transfer, indicating that both processes follow similar pathway dependences. These results establish a criteria for constructing photocatalytic pathways in multi-heme proteins, one that requires multi-step electron transfer to prevent heme-based sensitizer quenching and rapid charge recombination pathways.

2. *Amorphous oxides as models for deciphering the chemistry underlying photosynthetic water-splitting and interfacial photochemistry.* Amorphous thin film oxygen evolving catalysts (OECs) of first-row transition metals are of wide-spread interest for artificial leaf applications, and further serve as models for investigating metal-oxo coordination chemistry underlying photosynthetic water-splitting. We have developed X-ray atomic pair distribution function analysis techniques for the characterization of the "molecular-dimensioned" domain structures within amorphous oxide water-oxidation catalyst films. Our recent work has extended these measurements to electrode-supported films to resolve structure n linked to photochemical energy conversion at electrode interfaces and to develop capabilities that can be extended to molecular-based systems.



Specific current findings include an examination of the role of oxyanions and metal ion precursors in the electrolytic assembly of amorphous cobalt oxide catalyst films (Co-OEC) films. Catalyst films formed under different buffer solutions: pH = 7.0, phosphate (Pi); pH = 8.0, methylphosphate (MePi), and pH = 9.2, borate (Bi) were found to be composed of equivalent cobaltate domains that increase in size following the sequence phosphate < methylphosphate < borate. The increases in domain size for Co-MPi and Co-Bi are correlated to a transition to layered domains with structures intermediate between those in CoOOH and LiCoOO mineral forms, and have limited stacking coherence length corresponding to a mixture of 1 to 3 layers. In contrast, the CoPi domains are found not to be close stacked, but instead correspond to small, hydrous layers, consistent with a model for phosphate intercalation and disordered stacking. The domain structure changes measured are correlated with changes in electrocatalytic activity.

## DOE Sponsored Publications 2011-2014

1. Multimerization of Solution-State Proteins by Tetrakis(4-Sulfonatophenyl) Porphyrin. Oleksandr Kokhan, Nina Ponomarenko, P. Raj Pokkuluri, Marianne Schiffer, and David M. Tiede\*, (2014) *Biochemistry*, *submitted*.
2. Oxyanion Determined Domain Structure for Electrodeposited Amorphous Cobalt Oxide Oxygen Evolving Catalyst Films, Du, P., Ali Han, Gihan Kwon, Oleksandr Kokhan, Karena W. Chapman, Peter J. Chupas, and David M. Tiede, (2014) *submitted*.
3. Resolving the Domain Structure for the Amorphous Iridium-oxide Water Oxidation Catalyst by X-ray Pair Distribution Function Analysis, Jier Huang, James D. Blakemore, Oleksandr Kokhan, Nathan D. Schley, Robert H. Crabtree,\* Gary W. Brudvig,\* and David M. Tiede\*, (2014) *Phys. Chem. Chem. Phys.*, **16** (5): 1814-1819.
4. Detection of a charge-separated catalyst precursor state in a linked photosensitizer-catalyst assembly, Anusree Mukherjee, Oleksandr Kokhan, Jier Huang, Jens Niklas, Lin X. Chen, David M. Tiede, Karen L. Mulfort\* (2013) *Phys. Chem. Chem. Phys.*, **15**, 21070-21076.
5. Protein Delivery of a Ni Catalyst to Photosystem I for Light-Driven Hydrogen Production, Silver, S. C., Niklas, J., Du, P., Poluektov, O.G., Tiede, D.M., and Utschig, L.M, (2013) *J. Amer. Chem. Soc.* **135** (36), 13246-13249.
6. Nanostructured TiO<sub>2</sub>/Polypyrrole for Visible Light Photocatalysis, Dimitrijevic, N. M.; Tepavcevic, S.; Liu, Y.; Rajh, T.; Silver, S. C.; Tiede, D. M. (2013) *J. Phys. Chem. C* **117**: 15540-15544.
7. Artificial Photosynthesis as a Frontier Technology for Energy Sustainability, T. Faunce, S. Styring, M. R Wasielewski, G. W. Brudvig, A. W. Rutherford, J. Messinger, A. F. Lee, C. L. Hill, H. deGroot, M. Fontecave, D. R. MacFarlane, B. Hankamer, D. G Nocera, D. M. Tiede, H. Dau, W. Hillier, L. Wang (2013) *Energy Environ. Sci.* **6**, 1074–1076.
8. Characterization of an amorphous iridium water oxidation catalyst electrodeposited from organometallic precursors, J. D. Blakemore, M. W. Mara, M. N. Kushner-Lenhoff,† N. D. Schley, S.J. Konezny, I. Rivalta, C. F. A. Negre, R. C. Snoeberger, O. Huang, A. Stickrath, L. A. Tran, M. L. Parr, L. X. Chen,\* D. M. Tiede,\* V. S. Batista,\* R. Crabtree,\* and G.W. Brudvig\*, (2013) *Inorgan. Chem.* **52**: 1860-1871.
9. Structure-based analysis of solar fuels catalysts using *in-situ* X-ray scattering analyses, Karen L. Mulfort\*, Anusree Mukherjee, Oleksandr Kokhan, Pingwu Du, David M. Tiede\* (2013) *Chem. Soc. Rev.* **42**, 2215-2227.
10. A novel ruthenium(II)–cobaloxime supramolecular complex for photocatalytic H<sub>2</sub> evolution: synthesis, characterisation and mechanistic studies, Donald M. Cropek, Anja Metz, Astrid M. Müller, Harry B. Gray, Toyketa Horne, Dorothy C. Horton, Oleg Poluektov, David M. Tiede, Ralph T. Weber, William L. Jarrett, Joshua D. Phillips, and Alvin A. Holder (2012) *Dalton Trans.*, **41**, 13060-13073.
11. Elucidating the Domain Structure of the Cobalt-oxide Water Splitting Catalyst by X-ray Pair Distribution Function Analysis, Pingwu Du, Oleksandr Kokhan, Karena W. Chapman, Peter J. Chupas, and David M. Tiede\* (2012) *J. Am. Chem. Soc.* **134** (27):11096-11099.

12. Resolution of Cofactor-Specific Excited States and Charge Separation Pathways in Photosynthetic Reaction Centers by Single Crystal Spectroscopy, Libai Huang, Nina Ponomarenko, Gary P. Wiederrecht, and David M. Tiede (2012) *Proc. Nat. Acad. Sci. USA* **109** (13), 4851-4856.
13. X-ray Capabilities on the Picosecond Timescale at the Advanced Photon Source, B. Adams, M. Borland, L. X. Chen, P. Chupas, N. Dashdor, G. Doumy, E. Dufresne, S. Durbin, H. Dürr, P. Evans, T. Graber, R. Henning, E. P. Kanter, D. Keavney, C. Kurtz, Y. Li, A. M. March, K. Moffat, A. Nassiri, S. H. Southworth, V. Srajer, D. M. Tiede, D. Walko, J. Wang, H. Wen, L. Young, X. Zhang, and A. Zholents, (2012) *Synchrotron Rad. News* **25** (2): 6-10.
14. Highly Efficient Ultrafast Electron Injection from the Singlet MLCT Excited State of CuI-Diimine Complexes to TiO<sub>2</sub> Nanoparticles, Jier Huang, Onur Buyukcakil, Michael W. Mara, Ali Coskun, Nada M. Dimitrijevic, Gokhan Barin, Oleksandr Kokhan, Andrew B. Stickrath, Romain Ruppert, David M. Tiede, J. Fraser Stoddart, Jean-Pierre Sauvage, and Lin X. Chen, (2012) *Angew. Chem. Intl. Ed.* **51**, 12711–12715.
15. The Hydrogen Catalyst Cobaloxime – a Multifrequency EPR and DFT Study of Cobaloxime's Electronic Structure, Niklas, J., Mulfort, K. L., Rakhimov, R. R., Mardis, K. L., Tiede, D. M., and Poluektov, O. G. (2012) *J. Phys. Chem. B*, **116**, 2943-2957.
16. Nature-Driven Photochemistry for Catalytic Solar Hydrogen Production: A Photosystem I–Transition Metal Catalyst Hybrid, Lisa M. Utschig, Sunshine C. Silver, Karen L. Mulfort, and David M. Tiede (2011) *J. Am. Chem. Soc.* **133**:16334-16337.
17. Metal Nanoparticle Plasmon-Enhanced Light-Harvesting in a Photosystem I Thin Film, I. Kim, S. L. Bender, J. Hranisavljevic, L. M. Utschig, L. Huang, G. P. Wiederrecht, and D.M. Tiede (2011) *Nano Letts.* **11** (8): 3091–3098.
18. Comparing Photosynthetic and Photovoltaic Efficiencies and Recognizing the Potential for Improvement, R. E. Blankenship\*, D. M. Tiede\*, J. Barber, G. W. Brudvig, G. Fleming, M. Ghirardi, M. R. Gunner, W. Junge, D. M. Kramer, A. Melis, T. A. Moore, C. C. Moser, D. G. Nocera, A. J. Nozik, D. R. Ort, W. W. Parson, R. C. Prince, R. T. Sayre (2011) *Science* **332**: 805-809.
19. Photocatalytic Hydrogen Production from Noncovalent Biohybrid Photosystem I/Pt Nanoparticle Complexes, L.M. Utschig, N.M. Dimitrijevic, O.G. Poluektov, S.D. Chemerisov, K.L. Mulfort, and D.M. Tiede (2011) *J. Phys. Chem. Letts.* **2**: 236-241. *Highlighted in Chemical & Engineering News*, **2011**, 89(5), 44-45.

## A Tandem Photoelectrochemical Cell for Water Splitting

Thomas A. Moore, Ana L. Moore, Devens Gust

Center for Bio-Inspired Solar Fuel Production, Department of Chemistry and Biochemistry  
Arizona State University  
Tempe, AZ 85202

The Center for Bio-Inspired Solar Fuel Production, BISfuel, is designing and constructing complete systems that couple light absorption to the oxidation of water and the use of the resulting reducing equivalents for the synthesis of hydrogen or carbon-based fuels.<sup>1,2</sup> In order to use the solar spectrum efficiently, a tandem, two-junction photoelectrochemical cell was designed that uses two dye-sensitized nanoparticulate wide band gap semiconductor photoelectrodes, one absorbing in the visible and the other in the near IR (Fig. 1). The photoanode, inspired by photosynthetic photosystem II (PSII), comprises a high potential sensitizer with an absorption threshold at the red edge of the VIS, the semiconductor, and a bio-inspired redox relay and colloidal  $\text{IrO}_2$ , or molecular catalysts for water oxidation. Sufficient potential for proton reduction to hydrogen, catalyzed at a cathode by Pt or molecular catalysts, is provided by a tandem dye-sensitized solar cell (DSSC) whose phthalocyanine sensitizer has an absorption threshold in the near IR and whose spectrum is complementary to that of the photoanode.

Initial work in collaboration with T. Mallouk led to a single junction water oxidizing cell which, when biased at  $\geq 210$  mV, oxidized water and reduced protons to hydrogen.<sup>3</sup> The quantum yield was  $\sim 1\%$  as a result of unfavorable competition between fast charge recombination at the dye-semiconductor interface and slow oxidation of the  $\text{IrO}_2$  water oxidizing catalyst.

Inspired by nature's solution to a similar problem in PSII, we devised a redox relay<sup>4,5</sup> that shuttles electrons between the oxygen evolving catalyst and the oxidized sensitizer using proton coupled electron transfer (PCET). The relay comprises a benzimidazole-phenol (BiP) similar to that of the Tyr<sub>2</sub>-His redox relay of PSII. In the second generation of the BiP-porphyrin dyad, an unusually short, strong internal hydrogen bond involving the phenolic proton and the imidazole nitrogen emerged when the BiP was linked to a high potential porphyrin (PF<sub>10</sub>). These dyads were attached to  $\text{TiO}_2$  nanoparticles to form triad-like constructs.<sup>6</sup> Upon illumination at 13K, EPR measurements at Argonne National Laboratory clearly show formation of the neutral phenoxyl radical and an electron in the  $\text{TiO}_2$  nanoparticle. From the  $g_x$  value it is clear that the proton has moved away from the phenoxyl oxygen. The observation that both electron and proton transfer processes occur at 13 K strongly suggests that either the proton tunnels from the phenolic oxygen to the imidazole nitrogen or its zero-point energy is higher than the proton

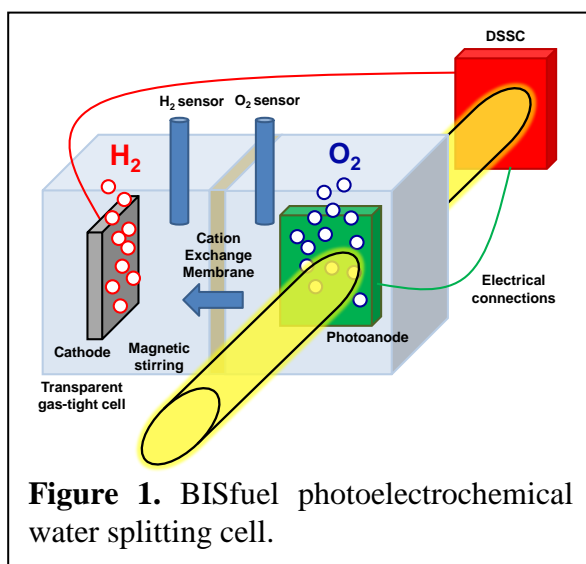


**Figure 1.** BISfuel photoelectrochemical water splitting cell.

transfer barrier. Electrochemical measurements with model systems and theoretical calculations in collaboration with S. Hammes-Schiffer are being conducted to understand the PCET better. The initially formed phenoxyl radical, upon annealing at 100 K, undergoes relaxation characterized by a shift in its  $g_x$  value. A similar relaxation has been reported in PSII preparations.

At room temperature, a PF<sub>10</sub>-BiP dyad attached to SnO<sub>2</sub> nanoparticles undergoes sequential photo-induced electron transfer reactions and an associated proton transfer process that yield a final long lived charge separated state characterized by an electron in the semiconducting SnO<sub>2</sub> nanoparticle and a neutral phenoxyl radical.<sup>7</sup> The long lifetime (93  $\mu$ s) of this state should facilitate the coupling of its high oxidation potential (~1.0 V vs. SCE) to the relatively slow steps of catalytic water oxidation. Indeed, incorporation of a BiP redox mediator/relay in the photoanode of the photoelectrochemical cell reported in 2009 nearly tripled the photocurrent.<sup>8</sup> Transient kinetic studies showed unequivocally that the improvement can be attributed to the BiP providing a more efficient match between the fast electron transfer processes associated with the sensitizer and the relatively slow electron transfer processes associated with IrO<sub>2</sub> oxidation.

Having developed a water oxidation catalyst and using a Pt electrode for hydrogen production, we have constructed the tandem cell shown in Fig. 1. The initial versions of the cell use either porphyrins or ruthenium sensitizers for the water oxidizing photoanode. The cell generates photocurrent under simulated sunlight without any external bias, and both hydrogen and oxygen are produced, as verified using gas detectors.

The water-splitting tandem cell can be used as a platform for examining systems engineering aspects of a complete solar fuel production system. However, it is inefficient, and uses rare metals as catalysts at both electrodes. BISfuel scientists and collaborators are developing alternative sensitizers<sup>9-13</sup> and catalysts.<sup>14,15</sup> Several molecular catalysts for proton reduction inspired by hydrogenase enzymes have been developed. Some achieve very small overpotentials by using redox-non-innocent ligands coupled to the metal at the active site.<sup>16,17</sup> Others use synthetic proteins to control environments and coupling of redox components and to increase catalyst turnover number.<sup>18,19</sup> In addition to these hydrogenase mimics, which are based on Fe and Ni complexes, BISfuel is investigating a Ru-based catalyst in collaboration with V. Artero of CEA, Grenoble, France.

For water oxidation, BISfuel is developing Mn based catalysts that are loosely based on the oxygen evolving complex (OEC) of PSII. These studies are being guided by recent information on the structure of intermediate oxidation states of the OEC obtained from laser pump – femtosecond X-ray probe structures obtained by BISfuel member P. Fromme and colleagues.<sup>20</sup> We are also collaboratively investigating Ru-based water oxidation catalysts developed by J. Concepcion of Brookhaven National Laboratory. In preliminary results, one of these performs comparably to IrO<sub>2</sub> in the tandem cell.

The tandem cell requires high surface area conducting and semiconducting electrodes to function efficiently. BISfuel scientists have developed methods for preparation of such electrodes, including those made of antimony tin oxide<sup>21,22</sup> and Zr-doped TiO<sub>2</sub>, which has a larger band gap than TiO<sub>2</sub> itself. The team is also developing *p*-type semiconductors for use on the fuel production side of the cell, in part through a collaboration with P. Maggard at North Carolina State University.

## DOE Sponsored Publications Relevant to This Presentation

1. Gust, D.; Moore, T. A.; Moore, A. L. Solar fuels via artificial photosynthesis. *Acc. Chem. Res.* **2009**, *42*, 1890-1898.
2. Gust, D.; Moore, T. A.; Moore, A. L. Realizing artificial photosynthesis. *Faraday Discuss.* **2012**, *155*, 9-26.
3. Youngblood, W. J.; Lee, S.-H. A.; Kobayashi, Y.; Hernandez-Pagan, E. A.; Hoertz, P. G.; Moore, T. A.; Moore, A. L.; Gust, D.; Mallouk, T. E. Photoassisted overall water splitting in a visible light-absorbing dye-sensitized photoelectrochemical cell. *J. Am. Chem. Soc.* **2009**, *131*, 926-927.
4. Moore, G. F.; Hambourger, M.; Kodis, G.; Michl, W.; Gust, D.; Moore, T. A.; Moore, A. L. Effects of protonation state on a tyrosine-histidine bioinspired redox mediator. *J. Phys. Chem. B* **2010**, *114* (45), 14450-14457.
5. Moore, G. F.; Hambourger, M.; Gervaldo, M.; Poluektov, O. G.; Rajh, T.; Gust, D.; Moore, T. A.; Moore, A. L. A bioinspired construct that mimics the proton coupled electron transfer between P680(center dot)+ and the Tyr(z)-His190 pair of photosystem II. *J. Am. Chem. Soc.* **2008**, *130* (32), 10466-10467.
6. Megiatto, J. D.; Mendez-Hernandez, D. D.; Tejada-Ferrari, M. E.; Teillout, A.-L.; Llansola Portoles, M. J.; Kodis, G.; Poluektov, O. G.; Rajh, T.; Mujica, V.; Groy, T. L.; Gust, D.; Moore, T. A.; Moore, A. L. A bioinspired redox relay that mimics radical interactions of the Tyr-His pairs of photosystem II. *Nature Chem.* **2014**, DOI: 10.1038/NCHEM.1862.
7. Megiatto, J. D.; Antoniuk-Pablant, A.; Sherman, B. D.; Kodis, G.; Gervaldo, M.; Moore, T. A.; Moore, A. L.; Gust, D. Mimicking the electron transfer chain in photosystem II with a molecular triad thermodynamically capable of water oxidation. *Proc. Natl. Acad. Sci. U. S. A.* **2012**, *109*, 15578-15583.
8. Zhao, Y.; Swierk, J. R.; Megiatto, J. D.; Sherman, B. D.; Youngblood, W. J.; Qin, D.; Lentz, D. M.; Moore, A. L.; Moore, T. A.; Gust, D.; Mallouk, T. E. Improving the efficiency of water splitting in dye-sensitized solar cells by using a biomimetic electron transfer mediator. *Proc. Natl. Acad. Sci. U. S. A.* **2012**, *109*, 15612-15616.
9. Brennan, B. J.; Llansola Portoles, M. J.; Liddell, P. A.; Moore, T. A.; Moore, A. L.; Gust, D. Comparison of silatrane, phosphonic acid, and carboxylic acid functional groups for attachment of porphyrin sensitizers to TiO<sub>2</sub> in photoelectrochemical cells. *Phys. Chem. Chem. Phys.* **2013**, DOI:10.1039/C3CP52156G.
10. Garg, V.; Kodis, G.; Liddell, P. A.; Terazono, Y.; Moore, T. A.; Moore, A. L.; Gust, D. Artificial photosynthetic reaction center with a coumarin-based antenna system. *J. Phys. Chem. B* **2013**, *117* (38), 11299-11308.
11. Terazono, Y.; North, E. J.; Moore, A. L.; Moore, T. A.; Gust, D. Base-catalyzed direct conversion of dipyrromethanes to 1,9-dicarbinoles: A [2+2] approach for porphyrins. *Org. Lett.* **2012**, *14* (7), 1776-1779.
12. Bergkamp, J.; Sherman, B. D.; Mariño-Ochoa, E.; Palacios, R. E.; Cosa, G.; Moore, T. A.; Gust, D.; Moore, A. L. Synthesis and characterization of silicon phthalocyanines bearing axial phenoxyl groups for attachment to semiconducting metal oxides. *J. Porphyrins Phthalocyanines* **2011**, *15*, 1-8.
13. Garg, V.; Kodis, G.; Chachisvilis, M.; Hambourger, M.; Moore, A. L.; Moore, T. A.; Gust, D. Conformationally constrained macrocyclic diporphyrin-fullerene artificial photosynthetic reaction center. *J. Am. Chem. Soc.* **2011**, *133* (9), 2944-2954.

14. Wee, T.-L.; Sherman, B. D.; Gust, D.; Moore, A. L.; Moore, T. A.; Liu, Y.; Scaiano, J. Photochemical synthesis of a water oxidation catalyst based on cobalt nanostructures. *J. Am. Chem. Soc.* **2011**, *133*, 16742-16745.
15. Sherman, B. D.; Pillai, S.; Kodis, G.; Bergkamp, J.; Mallouk, T. E.; Gust, D.; Moore, T. A.; Moore, A. L. A porphyrin-stabilized iridium oxide water oxidation catalyst. *Can. J. Chem.* **2011**, *89* (2), 152-157.
16. Roy, S.; Groy, T. L.; Jones, A. E. Biomimetic model for [FeFe]-hydrogenase: asymmetrically disubstituted diiron complex with a redox-active 2,2'-bipyridyl ligand. *Dalton Trans.* **2013**, *42*, 3843-3853.
17. Dutta, A.; Hamilton, G. A.; Hartnett, H. E.; Jones, A. K. Construction of heterometallic clusters in a small peptide scaffold as [NiFe]-hydrogenase models: Development of a synthetic methodology. *Inorg. Chem.* **2013**, *51*, 9580-9588.
18. Roy, A.; Sarrou, I.; Vaughn, M.; Astashkin, A. V.; Ghirlanda, G. De novo design of an artificial bis-[4Fe4S] binding protein. *Biochemistry* **2013**, *52*, 7586-7594.
19. Roy, A.; Madden, C.; Ghirlanda, G. Photo-induced hydrogen production in a helical peptide incorporating a [FeFe] hydrogenase active site mimic. *Chem. Commun.* **2013**, *48*, 9816-9818.
20. Kupitz, C.; Basu, S.; Grotjohann, I.; Fromme, R.; Zatsepin, N. A.; Rendek, K. N.; Hunter, M.; Shoeman, R. L.; White, T. A.; Wang, D.; James, D.; Yang, J.-H.; Cobb, D. E.; Reeder, B.; Sierra, R. G.; Liu, H.; Barty, A.; Aquila, A. L.; DePonte, D. P.; Kirian, R. A.; Baril, S.; Bergkamp, J. J.; Beyerlein, K. R.; Bogan, M. J.; Caleman, C.; Chao, T.-Z.; Conrad, C. E.; Davis, K. M.; Fleckenstein, H.; Galli, L.; Haupt-Riege, S. P.; Kassemeyer, S.; Laksmono, H.; Liang, M.; Lomb, L.; Marchesini, S.; Martin, A. V.; Messerschmidt, M.; Milanthianaki, D.; Nass, K.; Ros, A.; Roy-Chowdhury, S.; Schmidt, K.; Seibert, M.; Steinbrener, J.; Stellato, F.; Yan, L.; Yoon, C.; Moore, T. A.; Moore, A. L.; Pushkar, Y.; Williams, G. J.; Boutet, S.; Doak, R. B.; Weierstall, U.; Frank, M.; Chapman, H. N.; Spence, J. H. C.; Fromme, P. Serial time-resolved crystallography of photosystem II using a femtosecond X-ray laser. *Nature* **2014**, in press.
21. Sharma, S.; Volosin, A. M.; Schmitt, D.; Seo, D. K. Preparation and electrochemical properties of nanoporous transparent antimony-doped tin oxide (ATO) coatings. *J. Mater. Chem. A* **2013**, *1*, 699-706.
22. Volosin, A. M.; Sharma, S.; Traverse, C.; Newman, N.; Seo, D. K. One-pot synthesis of highly mesoporous antimony-doped tin oxide from interpenetrating inorganic/organic networks. *J. Mater. Chem.* **2011**, *21* (35), 13232-13240.

# MLCT Excited States at Interfaces and in Rigid Media: Applications in Energy Conversion

Thomas J. Meyer, Dennis Ashford, Alex Lapides, Byron Farnum, Sheng Zhang, Akitaka Ito, and John Papanikolas

Department of Chemistry  
University of North Carolina at Chapel Hill  
Chapel Hill, NC 27599

**nanoITO**-Photo-induced electron transfer to and from conductive Sn-doped In<sub>2</sub>O<sub>3</sub> nanoparticles in mesoporous thin films (*nanoITO*) has been investigated on surfaces derivatized with surface-bound chromophores and assemblies. The goal of the work is to explore interfacial electron transfer dynamics in this class of oxide materials for possible applications in energy conversion processes. The unique features of *nanoITO* thin films (*i.e.* transparency and conductivity) allow

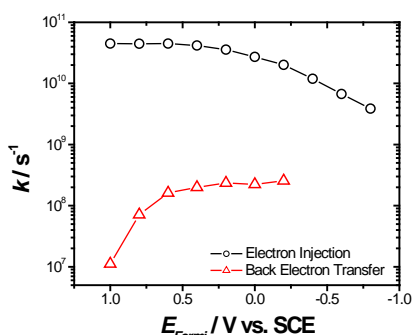
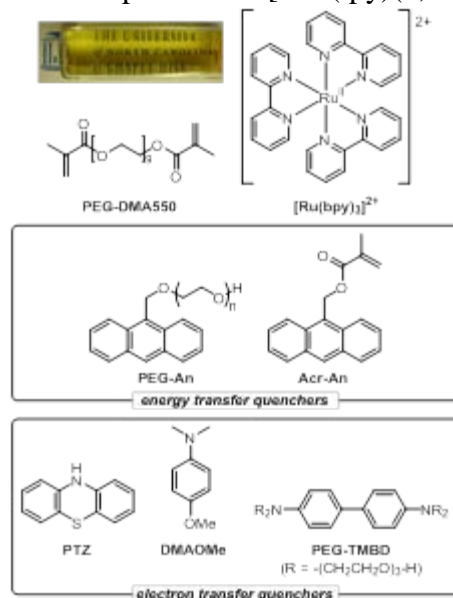


**Figure 1.** Rate constants for electron injection and back electron for RuP<sup>2+</sup>-derivatized *nanoITO* films in 0.1 M LiClO<sub>4</sub> acetonitrile as a function of applied bias.

for an investigation of interfacial dynamics, both electron injection and back electron transfer, as a function of Fermi level. The Fermi level is controlled by both thermal pre-treatment and externally applied bias. Ultrafast injection and back electron transfer dynamics measurements on surface-bound [Ru(bpy)<sub>2</sub>(4,4'-PO<sub>3</sub>H<sub>2</sub>-bpy)]<sup>2+</sup> (RuP<sup>2+</sup>) have been investigated by transient absorption measurements over a 1.8 V range in Fermi level potentials, Figure 1. From these data electron injection follows an expected Marcus dependence, as previously reported on TiO<sub>2</sub>, but back electron transfer becomes “diffusion limited”, independent of driving force due to trap-state limited electron transport. Measurements on *nanoITO* have been extended to a layer-by-layer based molecular

assembly consisting of a phosphonate-derivatized porphyrin chromophore and [Ru<sup>II</sup>(tpy)(4,4'-PO<sub>3</sub>H<sub>2</sub>-bpy)(OH<sub>2</sub>)]<sup>2+</sup> water oxidation catalyst linked through Zr(IV). These studies will be extended to the preparation and characterization of molecular p/n junctions for possible energy conversion applications based on spatially controlled arrays of electron transfer donor (D), chromophore (C), acceptor (A), catalyst (Cat) subunits in configurations such as *nanoITO*|A-C-D-Cat.

**PEG-DMA Films.** Polymerization of poly(ethyleneglycol)dimethacrylate (PEG-DMA) fluids provides a means for preparing thin (mm to cm), chemically inert PEG-DMA films that are optically transparent throughout the visible and conformable to surface structure on the nanoscale. The structure of PEG-DMA550 with nine ethylene glycol spacers is shown below along with the structures of the chromophore, [Ru(bpy)<sub>3</sub>]<sup>2+</sup> (bpy = 2,2'-bipyridine), and reductive and energy transfer



quenchers. We have studied photophysical and photochemical characteristics of the Metal-to-Ligand Charge Transfer (MLCT) excited state(s) of a series of polypyridyl complexes of Ru(II) and Os(II) in semi-rigid PEG-DMA550 films.

MLCT emission energies for  $[\text{Ru}(\text{bpy})_3]^{2+*}$  and a series of Os(II) polypyridyl complexes increase upon polymerization of PEG-DMA550 fluids with film formation due to a rigid medium effect. In the film, enhanced emission quantum yields and longer excited-state lifetimes are observed. They are quantitatively consistent with the Energy Gap Law for nonradiative decay. In semi-rigid PEG-DMA550 films with the added anthracene derivatives, energy transfer quenching of  $[\text{Ru}(\text{bpy})_3]^{2+*}$  occurs to give triplet anthracene by,  $[\text{Ru}(\text{bpy})_3]^{2+*} + -\text{An} \rightarrow [\text{Ru}(\text{bpy})_3]^{2+} + -^3\text{An}$ , by both rapid, static, and slow, diffusional quenching processes. Long-range, static energy transfer occurs with a distance dependence consistent with the Dexter (exchange) energy transfer mechanism. In films with added  $[\text{Ru}(\text{bpy})_3]^{2+}$ , Acr-An and methylviologen dication ( $\text{MV}^{2+}$ ), with the latter added as an electron acceptor, excitation of the complex is followed by energy transfer quenching, long-range  $-^3\text{An}$  to  $-\text{An}$  energy transfer migration, and  $\text{MV}^{2+}$  reduction by  $-^3\text{An}$  to give  $\text{MV}^+$  with a net electron transfer distance of  $>90 \text{ \AA}$ ! Reductive electron transfer quenching of  $[\text{Ru}(\text{bpy})_3]^{2+*}$  in PEG-DMA550 films, e.g.,  $[\text{Ru}(\text{bpy})_3]^{2+*} + \text{D} \rightarrow [\text{Ru}(\text{bpy})_3]^{2+} + \text{D}^+$ , also occurs by static and dynamic quenching. Kinetics of fixed-site electron transfer quenching were analyzed by an electron tunneling model with a distance attenuation factor,  $\beta$ , of  $\sim 0.47 \text{ \AA}^{-1}$  and a notable decrease to  $\beta = 0.16 \text{ \AA}^{-1}$  with the quencher incorporated into the PEG backbone. The fixed-site electron transfer quenching rate constant varies with driving force and back electron,  $[\text{Ru}(\text{bpy})_3]^{2+} + \text{D}^+ \rightarrow [\text{Ru}(\text{bpy})_3]^{2+} + \text{D}$ , is also distance dependent with data analyzed by power law kinetics.

**Electropolymerized Films** We have investigated stabilization of interfacial structures for possible dye-sensitized solar and photoelectrochemical cells by electropolymerization. The complex  $[\text{Fe}(v\text{-tpy})_2]^{2+}$  ( $v\text{-tpy} = 4'\text{-vinyl-2,2':6',2''-terpyridine}$ ) can be reductively electropolymerized on nanocrystalline  $\text{TiO}_2$  pre-derivatized with the surface-bound, phosphonate- and vinyl-derivatized Ru(II) polypyridyl chromophore,  $\text{Ru}(5,5'\text{-divinyl-2,2'-bipyridine})_2(4,4'\text{-(H}_2\text{O}_3\text{P)}_2\text{-2,2'-bipyridine})^{2+}$  (**RuPdvb**<sup>2+</sup>, Figure 2). The outer:inner Fe:Ru ratio was controlled by varying electropolymerization conditions and monitored by both UV-Visible and energy dispersive X-ray spectroscopy measurements. The resulting surface-bound bilayer assemblies were shown to be highly stabilized photochemically and electrochemically. Transient absorbance measurements have been used to demonstrate that photo-excitation and electron

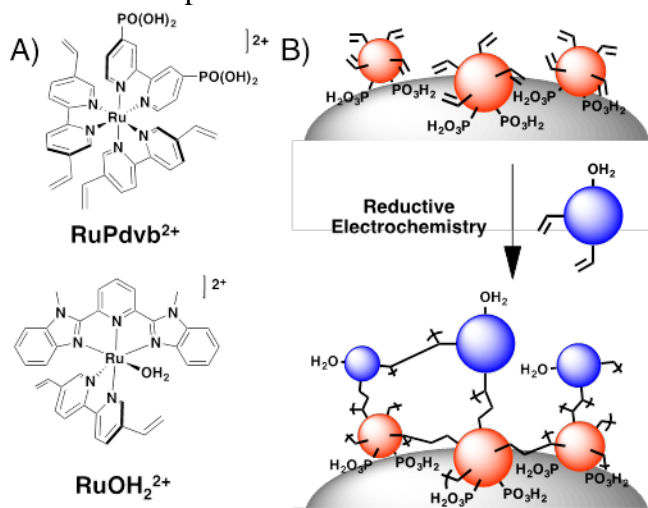


**Fig. 2.** (A) The phosphonate- and vinyl-functionalized chromophore (**RuPdvb**) and the vinyl-functionalized water oxidation catalyst (**RuOH<sub>2</sub><sup>2+</sup>**); (B) Schematic representation of reductive electropolymerization in which the vinyl-functionalized catalyst polymerizes atop the phosphonate-bound chromophore.

injection by the MLCT excited state(s) of the surface-bound Ru<sup>II</sup> complex is followed by directional, outside-to-inside, Fe<sup>II</sup> → Ru<sup>III</sup> electron transfer. In current and future work, the electropolymerization technique will be extended to chromophore-catalyst bilayer assemblies and to more complex molecular assembly structures on both semiconductor and transparent conducting oxides.

Published:

1. Influence of the Fluid-to-Film Transition on Photophysical Properties of MLCT Excited States in a Polymerizable Dimethacrylate Fluid; Knight, T.E.; Goldstein, A.P.; Brennaman, M.K.; Cardolaccia, T.; Pandya, A.; DeSimone, J.M.; Meyer, T.J. *J Phys. Chem. B* **2011**, 115(1), 64-70.
2. Formation of Assemblies Comprising Ru-polypyridine Complexes and CdSe Nanocrystals Studied by ATR-FTIR Spectroscopy and DFT Modeling. Kuposov, A.; Cardolaccia, T.; Albert, V.; Badaeva, E.; Kilina, S.; Meyer, T.; Tretiak, S.; Sykora, M. *Langmuir* **2011**, 27 (13), 8377-8383
3. Understanding the Electronic Structure of 4d Metal Complexes: From Molecular Spinors to L-Edge Spectra of a di-Ru Catalyst. Alperovich, I.; Smolentsev, G.; Moonshiram, D.; Jurss, J. W.; Concepcion, J. J.; Meyer, T. J.; Soldatov, A.; Pushkar, Y.; *J. Am. Chem. Soc.*, **2011**, 133 (39), 15786-15794.
4. Electronic Structure of the Water Oxidation Catalyst, cis,cis-[(bpy)<sub>2</sub>(H<sub>2</sub>O)Ru<sup>III</sup>ORu<sup>III</sup>(OH<sub>2</sub>)(bpy)<sub>2</sub>]<sup>4+</sup>, The Blue Dimer; Jurss, J.W.; Concepcion, J.J.; Butler, J.M.; Omberg, K.M.; Baraldo, L.M.; Thompson, D.G.; Lebeau, E.L.; Hornstein, B.; Schoonover, J.R.; Jude, H.; Thompson, J.D.; Dattelbaum, D.M.; Rocha, R.C.; Templeton, J.L.; Meyer, T.J. *J. Am. Chem. Soc.* **2011**, 133, 1345-1358.
5. Deactivation Pathways for Metal-to-Ligand Charge Transfer Excited States of Ru Polypyridyl Complexes with Triphenylphosphine as a Ligand. Litke, S.V.; Ershov, A.Y.; Meyer, T.J. *J Phys. Chem. A*, **2011**, 115, 14235-14242.
6. Electronic Properties and Structure of Assemblies of CdSe Nanocrystal Quantum Dots and Ru-Polypyridine Complexes Probed by Steady State and Time-Resolved Photoluminescence. Kuposov, A.Y.; Szymanski, P.; Cardolaccia, T.; Meyer, T.J.; Klimov, V.I.; Sykora, M.; *Adv. Funct. Mater.* **2011**, 21(16), 3159-3168.
7. The Golden Rule. Application for Fun and Profit in Electron Transfer, Energy Transfer, and Excited-State Decay; Ito, A.; Meyer, T.J. *Phys. Chem. Chem. Phys.* **2012**, 13731-13745.
8. Self-assembled Bilayer Films of Ru(II) Polypyridyl Complexes by Layer-by-Layer Deposition on Nanostructured Metal Oxides; Hanson, K.; Torelli, D.; Vannucci, A.; Brennaman M.K.; Luo, H.; Alibabaei, L.; Song, W.; Ashford, D.; Norris, M.; Glasson, C.; Concepcion, J.; Meyer, T.J. *Angew. Chem.* **2012**, 51(51), 12782-12785.
9. Sensitized Photodecomposition of Organic Bisphosphonates by Singlet Oxygen; Hanson, K.; Ashford, D.; Concepcion, J.; Binstead, R.; Habibi, S.; Luo, H.; Glasson, C.R.K.; Templeton, J.L.; Meyer, T.J. *J. Am. Chem. Soc.* **2012**, 134, 16975-16978.
10. Sensitization of ultra-long-range excited-state electron transfer by energy transfer in a polymerized film. Ito, A.; Stewart, D. J.; Fang, Z.; Brennaman, M. K.; Meyer, T. J. *Proc. Nat. Acad. Sci.* **2012**, 109 (38), 15132-15135.

11. Interfacial Dynamics and Solar Fuel Formation in Dye Sensitized Photoelectrosynthesis Cells. Song, W.; Chen, Z.; Glasson, C.R.K.; Hanson, K.; Luo, H.; Norris, M.; Ashford, D.; Concepcion, J.; Brennaman, M.K.; Meyer, T.J. *ChemPhysChem*. **2012**, 13 (12), 2882-2890.
12. Structure-Property Relationships in Phosphonate-Derivatized, Ru<sup>II</sup> Polypyridyl Dyes on Metal Oxide Surfaces in an Aqueous Environment. Hanson, K.; Brennaman, M.K.; Ito, A.; Luo, H.; Wenjing, S.; Parker, K.; Ghosh, R.; Norris, M.; Glasson, C.K.; Concepcion, J.; Lopez, R.; Meyer, T.J. *J. Phys. Chem. C*. **2012**, 116 (28), 14837-14847.
13. Spectroscopy and Dynamics of Phosphonate-Derivatized Ruthenium Complexes on TiO<sub>2</sub>. Giokas, P.; Miller, S.; Hanson, K.; Norris, M.; Glasson, C.; Concepcion, J.; Bettis, S.; Meyer, T.; Moran, A. *J. Phys. Chem. C*. **2012**, 117(2) 812-824.
14. Electron Transfer Dynamics of Peptide-Derivatized Ru<sup>II</sup>-polypyridyl Complexes on Nanocrystalline Metal Oxide Films. Hanson, K.; Wilger, D.J.; Jones, S.T.; Harrison, D.P.; Bettis, S.E.; Luo, H.; Brennaman, M.K.; Papanikolas, J.M.; Waters, M.L.; Meyer, T.J. *Pept. Sci.* **2013**, 100 (1), 25-31.
15. Stabilization of [Ru(bpy)<sub>2</sub>(4,4'-(PO<sub>3</sub>H<sub>2</sub>)bpy)]<sup>2+</sup> on Mesoporous TiO<sub>2</sub> with Atomic Layer Deposition of Al<sub>2</sub>O<sub>3</sub>. Hanson, K.; Losego, M.; Kalanyan, B.; Ashford, D.; Parsons, G.; Meyer, T. *Chem. Mater.* **2013**, 25 (1) 3-5.
16. Mechanism of Catalytic Water Oxidation by the Ruthenium Blue dimer catalyst: comparative study in D<sub>2</sub>O versus H<sub>2</sub>O. Moonshiram, D.; Purohit, V.; Concepcion, J.; Meyer, T.J., Pushkar, Y. *Materials* **2013**, 6, 392-409.
17. Experimental Demonstration of Radicaloid Character in a Ru<sup>V</sup>=O Intermediate in Catalytic Water Oxidation. Moonshiram, D.; Alperovich, I.; Concepcion, J.; Meyer, T.J.; Pushkar, Y. *Proc. Nat. Acad. Sci.* **2013**, 110 (10) 3765-3770.
18. Excited-State Dynamics in Rigid Media: Evidence for Long-Range Energy Transfer. Ito, A.; Stewart, D.; Knight, T.; Fang, Z.; Brennaman, M.K.; Meyer, T.J. *J. Phys. Chem. B*. **2013**, 117, 3428-3438.
19. Coordination Chemistry of Single-Site Catalysts in Electropolymerized Vinyl-Bpy Films. Harrison, D.P.; Lapides, A.M.; Binstead, R.A.; Concepcion, J.C.; Mendez, M.A.; Torelli, D.A.; Templeton, J.L.; Meyer, T.J. *Inorg. Chem.* **2012**, 52, 4747-4749.
20. [Ru(bpy)<sub>3</sub>]<sup>2+\*</sup> and Other Remarkable MLCT Excited States. Thompson, D.W.; Ito, A.; Meyer, T.J. *Pure and Applied Chem.* **2013**, 85 (7), 1257-1305.
21. Atom Transfer Radical Polymerization Preparation and Photophysical Properties of Polypyridylruthenium Derivatized Polysyrenes. Fang, Z.; Ito, A.; Kenan, S.; Chen, Z.; Watson, Z.; Rochette, J.; Kanai, Y.; Taylor, D.; Schanze, K.; Meyer, T.J. *Inorg. Chem.* **2013**, 52, 8511-8520.
22. Accumulation of Multiple Oxidative Equivalents at a Single Site by Cross-Surface Electron Transfer on TiO<sub>2</sub>. Song, W.; Ito, A.; Binstead, R.; Hanson, K.; Luo, H.; Brennaman, M.K.; Concepcion, J.; Meyer, T.J. *J. Am. Chem. Soc.* **2013**, 135, 11587-11594.
23. Strategies for Stabilization of Electrodeposited Metal Particles in Electropolymerized Films for H<sup>+</sup> Reduction. Torelli, D.; Harrison, D.; Lapides, A.; Meyer, T.J. *Appl. Mat & Interfaces*. **2013**, 5, 7050-7057.

24. Stabilization of a Ruthenium(II) Polypyridyl Dye on Nanocrystalline TiO<sub>2</sub> by an Electropolymerized Overlayer. Lapides, A.; Ashford, D.; Hanson, K.; Torelli, D.; Templeton, J.; Meyer, T.J. *J. Am. Chem. Soc.* **2013**, 135 (41), 15450-15458.
25. Synthesis of Phosphonic Acid-Derivatized Bipyridine Ligands and Their Ruthenium Complexes. Norris, M.; Concepcion, J.; Glasson, C.; Fang, Z.; Lapides, A.; Ashford, D.; Templeton, J.; Meyer, T.J. *Inorg. Chem.* **2013**, 52 (21), 12492-12501.
26. Rapid Energy Transfer in Non-Porous Metal-Organic Frameworks with Caged Ru(bpy)<sub>3</sub><sup>2+</sup> Chromophores: Oxygen Trapping and Luminescence Quenching. Kent, C.; Liu, D.; Ito, A.; Zhang, T.; Brennaman, K.; Meyer, T.J.; Lin, W. *J. Mat. Chem A.* **2013**, 1, 14982-14989.
27. Soluble Reduced Graphene Oxide Sheets Grafted with Polypyridylruthenium Derivatized Polystyrene Brushes as Light Harvesting Antenna for Photovoltaic Applications. Fang, Z.; Ito, A.; Stuart, A.; Luo, H.; Chen, Z.; Vinodgopal, K.; You, W.; Meyer, T.J.; Taylor, D. *ACS Nano.* **2013**, 7 (9), 7992-8002.
28. Long-Range Photoinduced Electron Transfer Dynamics in Rigid Media. Ito, A.; Fang, Z.; Brennaman, M.K.; Meyer, T.J. *Phys Chem Chem Phys.* **2014**, 16 (10), 4880-4891.
29. Photoinduced Interfacial Electron Transfer within a Mesoporous Transparent Conducting Oxide Film. Farnum, B.; Morseth, Z.; Lapides, A.; Reith, A.; Hoertz, P.; Brennaman, M.K.; Papanikolas, J.; Meyer, T.J. *J. Am. Chem. Soc.* **2014**, 136, 2208-2211.
30. Controlled Electropolymerization of Ruthenium(II) Vinylbipyridyl Complexes in Mesoporous Nanoparticle Films of TiO<sub>2</sub>. Fang, Z.; Keinan, S.; Alibabaei, L.; Luo, H.; Ito, A.; Meyer, T.J. *Angew. Chem. Int. Ed.* **2014**. in press, doi: 10.1002/anie.201402309.
31. Blue-Green Iridium(III) Emitter and Comprehensive Photophysical Elucidation of Heteroleptic Cyclometalated Iridium(III) Complexes. Zanoni, K.; Kariyazaki, B.; Ito, A.; Brennaman, M.K.; Meyer, T.J.; Murakami Iha, N. *Inorg. Chem.* **2014**. in press, doi: 10.1021/ic500070s.

Submitted:

1. Layer-by-Layer Synthesis of a Porphyrin-Ru(Polypyridyl) Chromophore Catalyst Assembly on Mesoporous Metal Oxides. Nayak, A.; Knauf, R.; Hanson, K.; Alibabaei, L.; Concepcion, J.; Ashford, D.; Dempsey, J.; Meyer, T.J. *Chem. Sci.* **2014**.
2. Rigid Medium Effects on Photophysical Properties of MLCT Excited States of Polypyridyl Os(II) Complexes in Polymerized Poly(ethyleneglycol)dimethacrylate Monoliths. Ito, A.; Knight, T.E.; Stewart, D.J.; Brennaman, M.K.; Meyer, T.J. *J. Phys. Chem. A* **2014**.

## The Challenges of Photoelectrochemical Water Splitting

John A. Turner  
Chemical and Material Sciences Center  
National Renewable Energy Laboratory  
Golden, CO 80401

Forty years after the first reported photoelectrochemical (PEC) water splitting experiment, hydrogen production from PEC is still a promise. Thousands of papers later and no material system has yet been identified that has the potential for commercial hydrogen production from water splitting by PEC. The majority of the past research has been directed at metal oxides due to their expected low costs, ease of synthesis and stability. Little progress has been made, however efficiencies for these oxide systems are abysmally low, primarily due to poor electronic structure.

Recent technoeconomic analysis studies indicate that a 20% solar-to-hydrogen PEC conversion efficiency is necessary for a commercially viable system. Additional requirements of lifetime (years), and cells costs ( $< \$400/\text{m}^2$ ) make a working device extremely challenging.

If one considers the photoelectrochemical water splitting process, we have the following order of events: light adsorption, carrier generation, separation and delivery to the interface, electron transfer (electrocatalysis), and product formation. The first four events all depend on the electronic structure of the semiconductor and if a high efficiency device is required then that must be optimized. Clearly then one must decide whether to use an existing PV-based semiconductor or search for a new material with the necessary electronic structure.

The highest efficiency to-date for PEC water splitting using visible light is the III-V-based GaAs/GaInP<sub>2</sub> PV/PEC tandem cell with a published efficiency of 12.4%. The high efficiency stems from the excellent electronic properties of III-Vs, but cell costs are high and lifetime is low. Work is on-going though to stabilize the interface and significantly reduce the manufacturing costs.

Multi-component transition metal oxides are complex materials, making intuitive guesses difficult and a focused search very challenging. A computational approach that will narrow the composition space could greatly decrease the time it takes leading towards a successful material. This presentation will discuss the impact of the PEC system and the cost of the produced hydrogen has on the most fruitful direction of research. The discussion will include metal oxides, surface treatments and tandem cells for PEC water splitting



## *Session II*

### *Photoelectrochemical Subsystems*



## Nano-Structured Photo-Materials and Electrocatalysts for Conversion of Solar Energy to Fuels

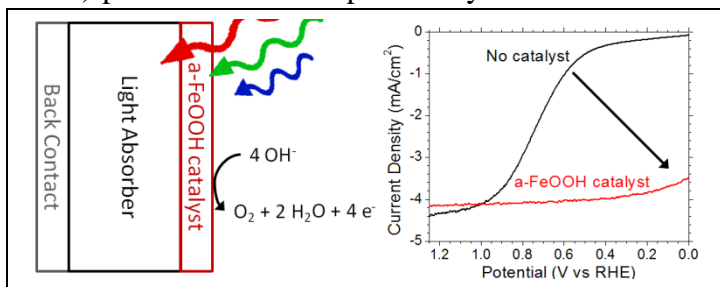
Allen J. Bard and C. Buddie Mullins

Departments of Chemistry and Chemical Engineering  
University of Texas at Austin  
Austin, TX 78712

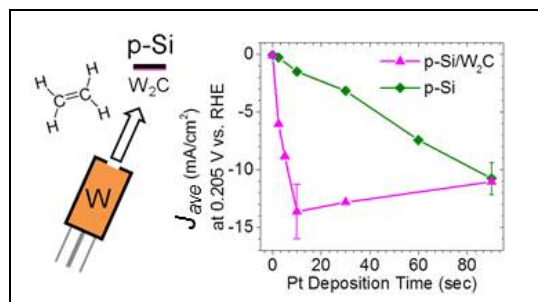
**Project Scope:** Our project has focused on the discovery and characterization of new nanostructured semiconductor photo-materials and electrocatalysts for photoelectrochemical (PEC) systems for the production of H<sub>2</sub>. The morphology of the photo-material is important just as is its compositional make-up; both interactively determine optical and charge-transport characteristics. We have continued to expand our search for new material compositions (including the effects of dopants) and also to synthesize films of candidate photo-materials for physical and photoelectrochemical characterization. We have also studied the performance of amorphous silicon triple junction photovoltaic cells with electrocatalytic and protective coatings.

**Recent Results:** We have undertaken many activities over the past three years and in the limited space of this abstract we will highlight a few of our recent studies:

1. **Amorphous FeOOH oxygen evolution reaction catalyst for photoelectrochemical water splitting:** Reaching the goal of economical photoelectrochemical (PEC) water splitting will likely require the combination of efficient solar absorbers with high activity electrocatalysts for the hydrogen and oxygen evolution reactions (HER and OER). Towards this goal, we synthesized an amorphous FeOOH (a-FeOOH) phase that has not previously been studied as an OER catalyst. The a-FeOOH films show activity comparable to another OER co-catalyst, Co-borate (Co-B<sub>i</sub>), in 1 M Na<sub>2</sub>CO<sub>3</sub>, reaching 10 mA/cm<sup>2</sup> at an overpotential of ~550 mV for 10 nm thick films. Additionally, the a-FeOOH thin films absorb less than 3% of the solar photons (AM1.5G) with energy greater than 1.9 eV, are homogenous over large areas, and act as a protective layer separating the solution from the solar absorber. The utility of a-FeOOH in a realistic system was tested by depositing on amorphous Si triple junction solar cells with a photovoltaic efficiency of 6.8%. The resulting a-FeOOH/a-Si devices achieved a total water splitting efficiency of 4.3% at 0 V vs RHE in a 3 electrode configuration and show no decrease in efficiency over the course of 4 hours.



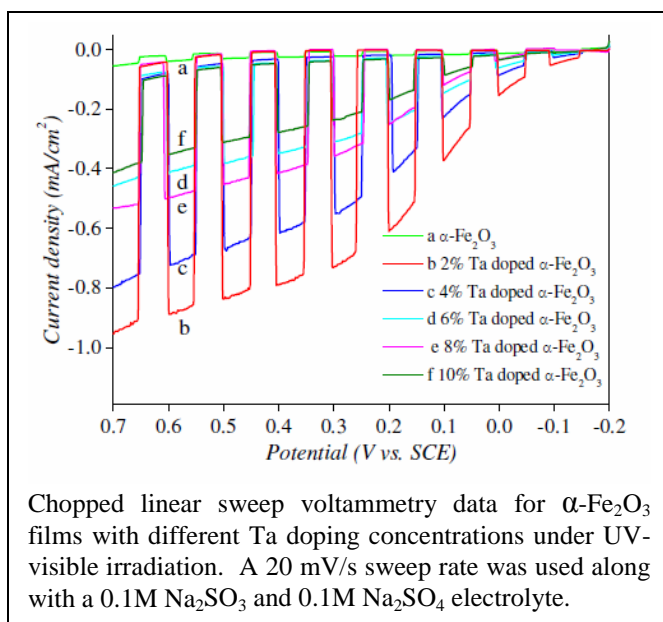
2. **p-Si/W<sub>2</sub>C and p-Si/W<sub>2</sub>C/Pt photocathodes for the hydrogen evolution reaction:** p-Si/W<sub>2</sub>C photocathodes were synthesized by evaporating tungsten metal in an ambient of ethylene gas to form tungsten semicarbide (W<sub>2</sub>C) thin films on top of p-type silicon (p-Si) substrates. As deposited the thin films contained crystalline W<sub>2</sub>C with a bulk W:C atomic ratio of approximately 2:1. The W<sub>2</sub>C films demonstrate catalytic activity for the hydrogen evolution reaction (HER) and p-Si/W<sub>2</sub>C photocathodes produce cathodic photocurrent at potentials more



positive than 0.0 V vs. RHE while bare p-Si photocathodes do not. The W<sub>2</sub>C films are an effective support for Pt nanoparticles allowing for a considerable reduction in Pt loading. p-Si/W<sub>2</sub>C/Pt photocathodes with Pt nanoparticles achieve photocurrent onset potentials and limiting photocurrent densities that are comparable to p-Si/Pt photocathodes with Pt loading nine times higher. This makes W<sub>2</sub>C an earth abundant alternative to

pure Pt for use as an electrocatalyst on photocathodes for the HER.

**3. Improvement of hematite as photocatalyst by doping with Tantalum:** The use of tantalum as a highly effective dopant for hematite photoelectrochemistry (PEC) has shown contradictory results in previous reports. We have shown through screening of different compositions by scanning electrochemical microscopy (SECM), that Ta-doping significantly improves the PEC performance of drop cast films on fluorine-doped tin oxide (FTO). In studies with larger electrodes, a 2% Ta doped hematite photoanode fabricated at 500 °C shows the highest improvement of photoactivity, which is approximately 32 times higher than pure hematite even under visible light. At fabrication temperatures higher than 500 °C (e.g., 600 °C, 680 °C), the FTO substrate becomes more resistive and the dopant Ta prefers to segregate from the bulk phase ( $\alpha$ -Fe<sub>2</sub>O<sub>3</sub>) and forms tantalum fluoride oxide (TaO<sub>2</sub>F), which may act as charge-carrier recombination centers, and the corresponding Ta doped samples show much lower photoactivities. Ta doped hematite samples show stronger (110) diffraction as compared with the pure  $\alpha$ -Fe<sub>2</sub>O<sub>3</sub>. We show that the doping of Ta induced a preferential growth along the {001} basal plane, which has been reported to have good conductivity. We found the conductivity of the Ta doped hematite was improved up to at least ~1 order of magnitude after the incorporation of Ta, with the improved carrier mobility decreasing recombination of the photogenerated holes and electrons.



Chopped linear sweep voltammetry data for  $\alpha$ -Fe<sub>2</sub>O<sub>3</sub> films with different Ta doping concentrations under UV-visible irradiation. A 20 mV/s sweep rate was used along with a 0.1M Na<sub>2</sub>SO<sub>3</sub> and 0.1M Na<sub>2</sub>SO<sub>4</sub> electrolyte.

**Future Plans:** We will continue to study Surface Interrogation-Scanning ElectroChemical Microscopy of photomaterials and electrocatalysts searching for photogenerated intermediates. We will also continue to investigate the behavior of semiconductor composites. Finally, we will continue working on the development and characterization of electrocatalysts for both OER and HER and the effect of photomaterial support on electrocatalytic behavior.

## DOE Sponsored Publications 2011-2014 (Allen J. Bard and C. Buddie Mullins, UT-Austin)

1. H. Ye, H. S. Park, V. Akhavan, B. W. Goodfellow, M. G. Panthani, B. A. Korgel, and A. J. Bard "Photoelectrochemical Characterization of CuInSe<sub>2</sub> and Cu(In<sub>1-x</sub>Ga<sub>x</sub>)Se<sub>2</sub> Thin Films for Solar Cells" *J. Phys. Chem. C* **115**(1), 234-240 (2011). <http://pubs.acs.org/doi/abs/10.1021/jp108170g>
2. H. S. Park, K. E. Kweon, H. Ye, E. Paek, G. S. Hwang, and A. J. Bard "Factors in the Metal Doping of BiVO<sub>4</sub> for Improved Photoelectrocatalytic Activity as Studied by Scanning Electrochemical Microscopy and First-Principles Density-Functional Calculation" *J. Phys. Chem. C* **115**, 17870-17879 (2011). <http://pubs.acs.org/doi/abs/10.1021/jp204492r>
3. David W. Flaherty, Nathan T. Hahn, Sean M. Berglund, Yong-Mao Lin, R. Alan May, Keith J. Stevenson, Zdenek Dohnalek, Bruce D. Kay, and C. Buddie Mullins, "Reactive ballistic deposition of nanostructured model materials for electrochemical energy conversion and storage," *Acc. Chem. Res.* **45**, 434-443 (2012). <http://dx.doi.org/10.1021/ar200164u>
4. Son Hoang, Siwei Guo, Nathan T. Hahn, Allen J. Bard, and C. Buddie Mullins, "Visible-light Driven Photoelectrochemical Water Oxidation on Nitrogen-doped TiO<sub>2</sub> Nanowires," *Nano Lett.* **12**, 26-32 (2012). <http://dx.doi.org/10.1021/nl2028188>
5. Son Hoang, Sean P. Berglund, Nathan T. Hahn, Allen J. Bard, and C. Buddie Mullins, "Enhancing visible light photo-oxidation of water with TiO<sub>2</sub> nanowire arrays via co-treatment with H<sub>2</sub> and NH<sub>3</sub>: Synergistic effects between Ti<sup>3+</sup> and N," *J. Am. Chem. Soc.* **134**, 3659-3662 (2012). <http://dx.doi.org/10.1021/ja211369s>
6. Nathan T. Hahn, Vincent C. Holmberg, Brian A. Korgel, and C. Buddie Mullins, "Electrochemical synthesis and characterization of p-CuBi<sub>2</sub>O<sub>4</sub> thin film photocathodes," *J. Phys. Chem. C* **116**, 6459-6466 (2012). <http://dx.doi.org/10.1021/jp210130v>
7. Sean P. Berglund, Alex J. E. Rettie, Son Hoang, and C. Buddie Mullins, "Incorporation of Mo and W into Nanostructured BiVO<sub>4</sub> Films to Improve Photoelectrochemical Water Oxidation Performance," *Phys. Chem. Chem. Phys.* **14**, 7065-7075 (2012). <http://dx.doi.org/10.1039/C2CP40807D>
8. Nathan T. Hahn, Jeffrey L. Self, and C. Buddie Mullins, "BiSI micro-rod thin films: Efficient solar absorber electrodes," *J. Phys. Chem. Lett.* **3**, 1571-1576 (2012). <http://dx.doi.org/10.1021/jz300515p>
9. Yanqing Cong, Shijun Wang, Hoang X. Dang, Fu-Ren F. Fan, C. Buddie Mullins, and Allen J. Bard, "Synthesis of Ta<sub>3</sub>N<sub>5</sub> nanotube arrays modified with electrocatalysts for photoelectrochemical water oxidation," *J. Phys. Chem. C* **116**, 14541-14550 (2012). <http://dx.doi.org/10.1021/jp304340a>
10. Nathan T. Hahn, Son Hoang, Jeffrey L. Self, and C. Buddie Mullins, "Spray pyrolysis deposition and photoelectrochemical properties of n-type BiOI nano-platelet thin films," *ACS Nano* **6**, 7712-7722 (2012). <http://dx.doi.org/10.1021/nn3031063>
11. Son Hoang, Siwei Guo, and C. Buddie Mullins, "Co-incorporation of Ta, N into TiO<sub>2</sub> nanowires for visible-light driven photoelectrochemical water oxidation," *J. Phys. Chem. C* **116**, 23283-23290 (2012). <http://dx.doi.org/10.1021/jp309743u>

12. Nathan T. Hahn, Alexander J. E. Rettie, Susanna K. Beal, Raymond R. Fullon, and C. Buddie Mullins, "n-BiSI thin films: Selenium doping and solar cell behavior," *J. Phys. Chem. C*. **116**, 24878-24886 (2012). <http://dx.doi.org/10.1021/jp3088397>
13. Son Hoang, Sean P. Berglund, Raymond R. Fullon, Ryan L. Minter, and C. Buddie Mullins, "Chemical bath deposition of vertically aligned TiO<sub>2</sub> nanoplatelet arrays for solar energy conversion applications," *J. Mater. Chem. A*. **1**, 4307-4315 (2013). <http://dx.doi.org/10.1039/C3TA01384G>
14. Sean P. Berglund, Heung Chan Lee, Paul D. Nunez, Allen J. Bard, and C. Buddie Mullins, "Screening of transition and post-transition metals to incorporate into copper oxide and copper bismuth oxide for photoelectrochemical hydrogen evolution," *Phys. Chem. Chem. Phys.* **15**, 4554-4565 (2013). <http://dx.doi.org/10.1039/C3CP50540E>
15. Son Hoang, Thong Q. Ngo, Sean P. Berglund, Raymond R. Fullon, John G. Ekerdt, and C. Buddie Mullins, "Improvement of solar energy conversion with Nb-incorporated TiO<sub>2</sub> hierarchical microspheres," *ChemPhysChem* **14**, 2270-2276 (2013). <http://dx.doi.org/10.1002/cphc.201201092>
16. Alexander J. E. Rettie, Heung-Chan Lee, Luke G. Marshall, Jung-Fu Lin, Cigdem Capan, Jeffrey Lindemuth, John S. McCloy, Jianshi Zhou, Allen J. Bard, and C. Buddie Mullins, "Combined charge carrier transport and photoelectrochemical characterization of BiVO<sub>4</sub> single crystals: Intrinsic behavior of a complex metal oxide," *J. Am. Chem. Soc.* **135**, 11389-11396 (2013). <http://dx.doi.org/10.1021/ja405550k>
17. Huichao He, Sean P. Berglund, Peng Xiao, William D. Chemelewski, Yunhuai Zhang, and C. Buddie Mullins, "Nanostructured Bi<sub>2</sub>S<sub>3</sub>/WO<sub>3</sub> heterojunction films exhibiting enhanced photoelectrochemical performance," *J. Mater. Chem. A*. **1**, 12826-12834 (2013). <http://dx.doi.org/10.1039/C3TA13239K>
18. Sean P. Berglund, Son Hoang, Ryan L. Minter, Raymond R. Fullon, and C. Buddie Mullins, "Investigation of 35 elements as single metal oxides, mixed metal oxides, or dopants for titanium dioxide for dye-sensitized solar cells," *J. Phys. Chem. C*. **117**, 25248-25258 (2013). <http://dx.doi.org/10.1021/jp4073747>
19. M. M. Najafpour, K. C. Leonard, F.-R. F. Fan, M. A. Tabrizi, A. J. Bard, C. K. King'andu, S. L. Suib, B. Haghghia, and S. I. Allakhverdiev, "Nano-Size Layered Manganese-Calcium Oxide as an Efficient and Biomimetic Catalyst for Water Oxidation under Acidic Conditions: Comparable to Platinum" *Dalton Trans.* **42**, 5085-5091 (2013). <http://pubs.rsc.org/en/content/articlelanding/2013/dt/c3dt32864c#!divAbstract>
20. C. Bhattacharya, H. C. Lee, A. J. Bard "Rapid Screening by Scanning Electrochemical Microscopy (SECM) of Dopants for Bi<sub>2</sub>WO<sub>6</sub> Improved Photocatalytic Water Oxidation with Zn Doping" *J. Phys. Chem. C* **117**, 9633-9640 (2013). <http://pubs.acs.org/doi/abs/10.1021/jp308629q>
21. H. S. Park, K. C. Leonard, A. J. Bard "Surface Interrogation Scanning Electrochemical Microscopy (SI-SECM) of Photoelectrochemistry at a W/Mo-BiVO<sub>4</sub> Semiconductor Electrode: Quantification of Hydroxyl Radicals during Water Oxidation" *J. Phys. Chem. C* **117**, 12093-12102 (2013). <http://pubs.acs.org/doi/abs/10.1021/jp400478z>

22. K. C. Leonard, K. M. Nam, H. C. Lee, S. H. Kang, H. S. Park, and A. J. Bard “ZnWO<sub>4</sub>/WO<sub>3</sub> Composite for Improving Photoelectrochemical Water Oxidation” *J. Phys. Chem. C* 117(31), 15901-15910 (2013). <http://pubs.acs.org/doi/abs/10.1021/jp403506q>
23. H. S. Park, H. C. Lee, K. C. Leonard, G. Liu, and A. J. Bard “Unbiased Photoelectrochemical Water Splitting in Z-Scheme Device Using W/Mo-Doped BiVO<sub>4</sub> and Zn<sub>x</sub>Cd<sub>1-x</sub>Se” *ChemPhysChem* 14(10), 2277-2287 (2013). <http://onlinelibrary.wiley.com/doi/10.1002/cphc.201201044/abstract>
24. K. M. Nam, H. S. Park, H. C. Lee, B. H. Meekins, K. C. Leonard, and A. J. Bard “Compositional Screening of the Pb-Bi-Mo-O System. Spontaneous Formation of a Composite of p-PbMoO<sub>4</sub> and n-Bi<sub>2</sub>O<sub>3</sub> with Improved Photoelectrochemical Efficiency and Stability” *J. Phys. Chem. Lett.* 4(16), 2707-2710 (2013). <http://pubs.acs.org/doi/abs/10.1021/jz401334k>
25. S. K. Cho, H. S. Park, H. C. Lee, K. M. Nam, A. J. Bard “Metal Doping of BiVO<sub>4</sub> by Composite Electrodeposition with Improved Photoelectrochemical Water Oxidation” *J. Phys. Chem. C* 117, 23048-23056 (2013). <http://pubs.acs.org/doi/abs/10.1021/jp408619u>
26. K. C. Leonard, A. J. Bard “Pattern Recognition Correlating Materials Properties of the Elements to Their Kinetics for the Hydrogen Evolution Reaction” *J. Am. Chem. Soc.* 135(42), 15885-15889 (2013). <http://pubs.acs.org/doi/abs/10.1021/ja407394q>
27. Hyun S. Park, Hyung-Wook Ha, Rodney S. Ruoff, and Allen J. Bard, “On the improvement of photoelectrochemical performance and finite element analysis of reduced graphene oxide-BiVO<sub>4</sub> composite electrodes,” *J. Electroanalytical Chem.* **716**, 8-15 (2014). <http://www.sciencedirect.com/science/article/pii/S1572665713003962>
28. Sean P. Berglund, Huichao He, William D. Chemelewski, Hugo Celio, and C. Buddie Mullins, “p-Si/W<sub>2</sub>C and p-Si/W<sub>2</sub>C/Pt photocathodes for the hydrogen evolution reaction,” *J. Am. Chem. Soc.* **136**, 1535-1544 (2014). <http://dx.doi.org/10.1021/ja411604k>
29. William C. Chemelewski, Heung-Chan Lee, Allen J. Bard, and C. Buddie Mullins, “Amorphous FeOOH Oxygen Evolution Reaction Catalyst for Photoelectrochemical Water Splitting,” *J. Am. Chem. Soc.* **136**, 2843-2850 (2014). <http://dx.doi.org/10.1021/ja411835a>
30. Alexander J. E. Rettie, Kyle C. Klavetter, Jung-Fu Lin, Andrei Dolocan, Hugo Celio, Ashioma Ishiekwene, Heather L. Bolton, Kristen N. Pearson, Nathan T. Hahn, and C. Buddie Mullins, “Improved visible light harvesting of WO<sub>3</sub> by incorporation of sulfur or iodine: A tale of two impurities,” *Chem. Mater.* **26**, 1670-1677 (2014). <http://dx.doi.org/10.1021/cm403969r>
31. Yiqing Sun, William D. Chemelewski, Sean P. Berglund, Chun Li, Huichao He, Gaoquan Shi, and C. Buddie Mullins, “Antimony doped tin oxide nanorods as a transparent conducting electrode for enhancing photoelectrochemical oxidation of water by hematite,” accepted by *ACS Appl. Mater. Interfaces* (2014). <http://dx.doi.org/10.1039/C4TA01167H>
32. Xinsheng Zhang, Huicheng Li, Shijun Wang, Fu-Ren F. Fan, and Allen J. Bard, “Improvement of Hematite as Photocatalyst by Doping with Tantalum,” accepted by *J. Phys. Chem. C* (2014). <http://pubs.acs.org/doi/abs/10.1021/jp500395a>

# Electrochemical Synthesis of Polycrystalline Semiconductor Electrodes with Optimum Compositions and Morphologies for Use in Solar Fuel Production

Kyoung-Shin Choi  
Department of Chemistry  
University of Wisconsin-Madison  
Madison, WI 53706

The overall objective of our project is to bring about a marked advancement in the synthesis and understanding of inexpensive polycrystalline semiconductor electrodes (photoelectrodes) for use in solar fuel production. Identifying inexpensive and easily processable semiconductors (e.g. oxides or sulfides) that can achieve high solar energy conversion efficiencies and developing facile synthesis methods to produce them as high quality photoelectrodes are critical steps to considerably reduce the production cost of solar fuels. We achieve this goal by developing simple and practical electrochemical synthesis methods/conditions that can produce promising selective semiconductors as high quality photoelectrodes with systematically varying compositions and morphologies. During the past funding period, we focused on extending our synthesis ability to produce ternary oxide-based semiconductors and have established various new synthesis conditions for highly promising photoanodes (n-BiVO<sub>4</sub>, n-ZnFe<sub>2</sub>O<sub>4</sub>, n-type CuWO<sub>4</sub>, n-Bi<sub>2</sub>WO<sub>6</sub>) and photocathodes (p-CuFeO<sub>2</sub>, p-CuBi<sub>2</sub>O<sub>4</sub>). The resulting high quality electrodes enabled us to accurately evaluate their photoelectrochemical properties and develop new strategies to address their main limitations. The most significant achievements made during the past funding period are summarized below.

**1) Studies on n-type BiVO<sub>4</sub> Photoanode for Efficient and Stable Solar Water Oxidation** Bismuth vanadate (BiVO<sub>4</sub>), an n-type semiconductor, has been recently identified as a promising photoanode for use in a photoelectrochemical water splitting cell. It has a direct bandgap of 2.4 eV and an appropriate valence band position for O<sub>2</sub> evolution. In addition, the conduction band of BiVO<sub>4</sub> is located near the H<sub>2</sub> evolution potential, allowing the photocurrent onset to occur near 0.0 V vs. RHE. Due to this feature, BiVO<sub>4</sub> can generate much higher photocurrent in the low bias region than other photoanodes having a smaller bandgap but a more positive conduction band edge.

We have developed several different electrochemical synthesis conditions to prepare BiVO<sub>4</sub> electrodes, which include (i) direct deposition of Bi-V-O and (ii) deposition of BiOI followed by its chemical conversion to BiVO<sub>4</sub> (Figure 1a). Since each of these deposition mechanisms involves different nucleation and growth

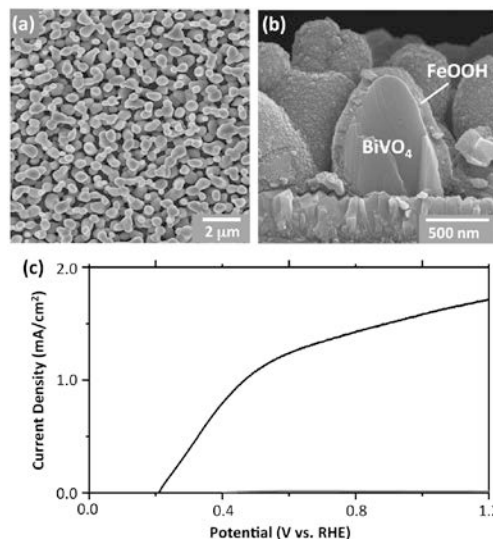


**Figure 1.** (a) SEM of BiVO<sub>4</sub> electrode prepared from electrodeposited BiOI electrode and (b) side-view SEM of BiVO<sub>4</sub>/FeOOH electrode showing a conformal coating of FeOOH on BiVO<sub>4</sub>. (c) *J-V* curve for BiVO<sub>4</sub>/FeOOH photoanode in 0.1 M phosphate buffer (pH 7) (AM 1.5G illumination). Dark current is shown as a gray line.

processes, they resulted in  $\text{BiVO}_4$  electrodes with varying morphologies. Also, each deposition condition allowed for composition tuning with different sets of dopants, increasing the freedom of the composition tuning.

When combined with an appropriate oxygen evolution catalyst such as  $\text{FeOOH}$  (Figure 1b), the electrochemically prepared  $\text{BiVO}_4$  photoanodes showed excellent photoelectrochemical properties for solar water oxidation with an early photocurrent onset potential ( $\leq 0.2$  V vs. RHE) and a high fill factor, achieving the maximum power point at a potential as low as  $\sim 0.6$  V vs. RHE with a current density higher than  $1 \text{ mA/cm}^2$  (Figure 1c). Further photocurrent enhancement was achieved when the composition was optimized by doping, which enhanced the electron-hole separation yield. The promising water oxidation performance achieved by the inexpensive system prepared by simple synthesis procedures presents enormous potential to achieve efficient solar water oxidation by further optimizing morphologies and compositions of the  $\text{BiVO}_4$ -based photoanodes.

## 2) Studies on p-type $\text{CuFeO}_2$ and $\text{CuBi}_2\text{O}_4$ Photocathode for Solar Hydrogen Production

Among various semiconductor photoelectrodes, metal oxides hold the most promise in terms of long-term stability and easy synthesis. However, most of the well-studied oxide electrodes that can utilize visible light for solar water splitting are n-type with the conduction band edge not suitable for hydrogen production. In order to photoelectrolyze water using these materials, application of an external bias or coupling them with a p-type semiconductor electrode having a suitable conduction band position to form photoelectrochemical diodes is necessary. Most p-type semiconductor electrodes extensively studied to date are not oxide-based materials (e.g. Si, GaP, GaInP<sub>2</sub>) and are relatively difficult to process. Therefore, there is a tremendous interest in identifying and preparing cost-effective p-type oxide-based photocathodes with narrow bandgaps ( $E_g < 2$  eV), good charge transport properties, and suitable conduction band positions for hydrogen production.

We have developed electrochemical synthesis conditions to produce p-type  $\text{CuFeO}_2$  and  $\text{CuBi}_2\text{O}_4$  electrodes (Figure 2a), which have a suitable conduction band position to photoreduce water to  $\text{H}_2$  while absorbing the entire range of the visible spectrum ( $E_g = \sim 1.5$  eV for both compounds). Furthermore, these photocathodes show a very positive photocurrent onset potential, achieving a photovoltage of  $\sim 1.0$  V, which is much higher than those of p-Si photocathodes (Figure 2b). Further systematic investigations on these highly promising systems (e.g. composition tuning, identifying and placing proper  $\text{H}_2$  evolution catalysts on the photocathode surface) will make it possible to construct a photoelectrochemical cell with all oxide-based photocathodes and photoanodes.

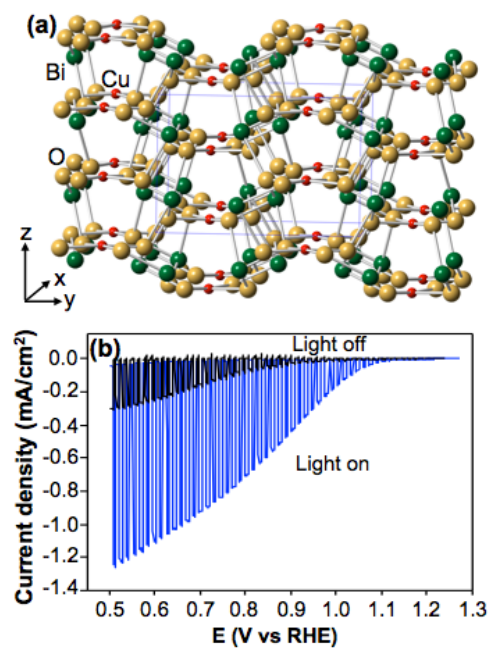


**Figure 2.** (a) Crystal structure of  $\text{CuBi}_2\text{O}_4$  and (b) its  $J$ - $V$  curves for  $\text{O}_2$  reduction (blue) and water reduction to  $\text{H}_2$  (black) measured in  $\text{O}_2$  purged and  $\text{N}_2$  purged 0.1 M of NaOH (pH 12.8), respectively, with a scan rate of 10 mV/s under AM 1.5G illumination.

## DOE Sponsored Publications 2011-2014

1. Spray, R. L. McDonald, K. J.; Choi, K.-S. “Enhancing Photoresponse of Nanoparticulate  $\alpha$ - $\text{Fe}_2\text{O}_3$  Electrodes by Surface Composition Tuning” *J. Phys. Chem C* **2011**, 115, 3497 – 3506.
2. McDonald, K. J.; Choi, K.-S. “Synthesis and Photoelectrochemical Properties of  $\text{Fe}_2\text{O}_3/\text{ZnFe}_2\text{O}_4$  Composite Photoanodes for Use in Solar Water Oxidation” *Chem. Mater.* **2011**, 23, 4863 – 4869.
3. McShane, C. M.; Choi, K.-S. “Junction Studies on Electrochemically Fabricated p-n  $\text{Cu}_2\text{O}$  Homojunction Solar Cells for Efficiency Enhancement” *Phys. Chem. Chem. Phys.* **2012**, 14, 6112 – 6118.
4. Read, C. G.; Park, Y.; Choi, K.-S. “Electrochemical Synthesis of p-type  $\text{CuFeO}_2$  Electrodes for Use in a Photoelectrochemical Cell” *J. Phys. Chem. Lett.* **2012**, 3, 1872 – 1876.
5. McDonald, K. J.; Choi, K.-S. “Electrochemical Synthesis of  $\text{BiOI}$  Electrode and Its Conversion to Highly Efficient Porous n- $\text{BiVO}_4$  Photoanode for Solar Water Oxidation” *Energy Environ. Sci.* **2012**, 5, 8553-8557.
6. Huang, Z.; Lin, Y.; Xiang, X.; Rodriguez Cordoba, W.; McDonald, K. J.; Hagen, K.; Choi, K.-S.; Brunschwig, B. S.; Musaev, D.; Hill, C. L.; Wang, D.; Lian, T. “In situ probe of photocarrier dynamics in water-splitting hematite ( $\alpha$ - $\text{Fe}_2\text{O}_3$ ) electrodes” *Energy Environ. Sci.* **2012**, 5, 8923 – 8926.
7. Hill, J. C.; Choi, K.-S. “Synthesis and Characterization of High Surface Area  $\text{CuWO}_4$  and  $\text{Bi}_2\text{WO}_6$  Electrodes for use as Photoanodes for Solar Water Oxidation” *J. Mat. Chem. A* **2013**, 1, 5006 – 5014.
8. Maijenburg, A.; Hattori, A.; De Respinis, M.; McShane, C.; Choi, K.-S.; Dam, B.; Tanaka, H.; ten Elshof, A. “Ni and p- $\text{Cu}_2\text{O}$  nanocubes with a small size distribution by templated electrodeposition, and their characterization by photocurrent measurement” *ACS Appl. Mater. Interfaces*, **2013**, 5, 10938 – 10945.
9. Maijenburg, A.; Regis, M.; Hattori, A.; Tanaka, H.; Choi, K.-S.; ten Elshof, J. “ $\text{MoS}_2$  nanocube structures as catalysts for electrochemical  $\text{H}_2$  evolution from acidic aqueous solutions” *ACS Appl. Mater. Interfaces*, **2014**, 6, 2003 – 2010.
10. Park, Y.; Kang, D. H.; Choi, K.-S. “Marked Enhancement in Electron-Hole Separation Achieved in the Low Bias Region by Electrochemically Prepared Mo-Doped  $\text{BiVO}_4$  Photoanodes” *Phys. Chem. Chem. Phys.*, **2014**, 16, 1238 – 1246.
11. Kim T. W.; Regis, M.; Cha, H.; Choi, K.-S. “Electrochemical Synthesis of Inorganic Electrodes” *Accounts Chem. Res.* To be submitted, **2014** (Invited).
12. Kang, D. H.; Choi, K.-S. “Electrochemical Preparation of p-type  $\text{CuBi}_2\text{O}_4$  for Solar Hydrogen Production” To be submitted, **2014**.

## Design, Discovery and Evaluation of Semiconductors for Visible Light Harvesting

Polina Burmistrova, Huafeng Huang, Bingfei Cao, Limin Wang, James Ciston, Yimei Zhu, Qixi Mi, Nathan Lewis, John Lofaro, Michael White, Mark Hybertsen, and Peter Khalifah

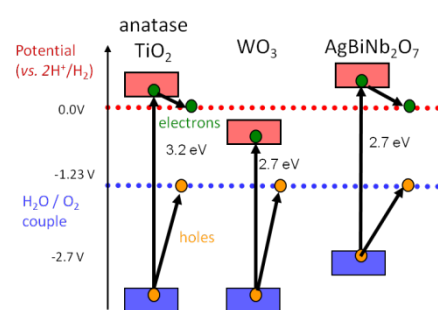
Department of Chemistry

Stony Brook University (joint appointment w/ Brookhaven National Laboratory)

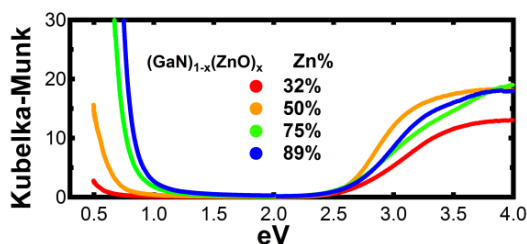
Stony Brook, NY 11794-3400

One of the two primary barriers currently preventing the realization of technologically relevant photoelectrochemical water splitting is the lack of a medium band gap photoanode that can effectively harvest light and efficiently use the photogenerated carriers to drive water oxidation. Our recent efforts to understand, design, and optimize both oxide and oxynitride visible light absorbing semiconductors will be described, with an emphasis on the latter class of compounds.

The oxide semiconductor  $\text{InTaO}_4$  was the first visible light absorbing oxide reported to be capable of driving overall water splitting (*Nature*, 2001) with an intrinsic band gap of 2.6 eV and a reduced band gap of 2.3 eV upon Ni-doping. We have shown that this system has a much larger band gap of  $\sim 4.0$  eV when impurities are eliminated, and that this combination of  $d^{10}/d^0$  metals is therefore not an effective design strategy. A more promising approach is the  $d^{10}/d^0/s^2$  combination of energy levels, which resulted in our discovery that the semiconductor  $\text{AgBiNb}_2\text{O}_7$  has a direct band gap of 2.7 eV and has both band edges suitably positioned for driving overall water splitting, unlike  $\text{WO}_3$ . Next generation oxide pyrochlores have also been found with band gaps as small as 2.4 eV.



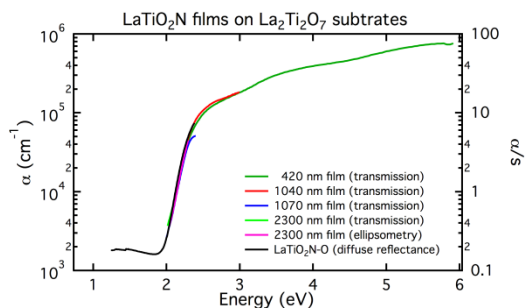
Due to the reduced electronegativity of nitrogen relative to oxygen, it has been observed that oxynitride semiconductors typically have band gaps about 0.5 - 1 eV smaller than their oxide equivalents, an effect primarily derived from their raised valence bands. While these materials have band gaps and band edge energies which are exceptionally well suited for water splitting applications, the fundamental properties of these systems are generally not well understood and there is extra complexity in their crystal structures due to the possibility of O and N being disordered on average but still exhibiting order on a local scale.



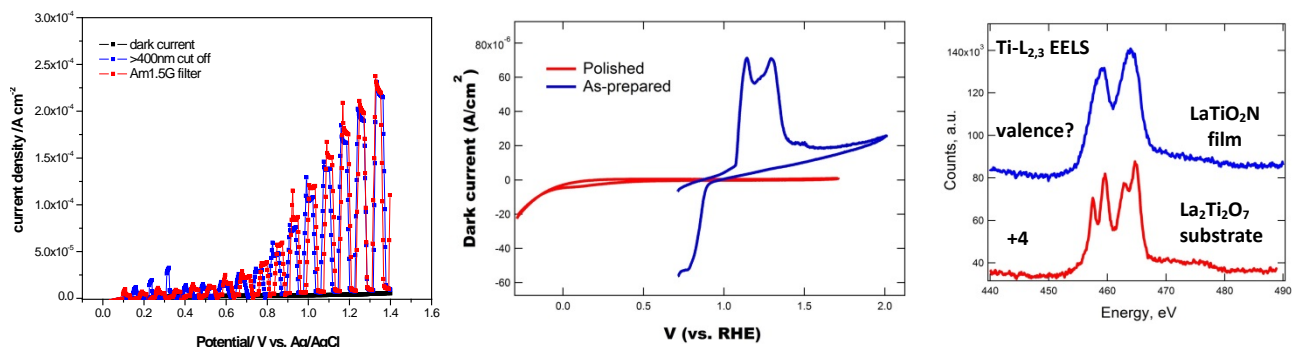
The  $(\text{GaN})_{1-x}(\text{ZnO})_x$  solid solution is one of the smallest band gap systems reported to be able to driving overall water splitting. We have developed bulk synthesis methods for samples spanning the entire range of the  $(\text{GaN})_{1-x}(\text{ZnO})_x$  solid solution. Although the diffraction peaks exhibited by these compounds can all be indexed using the hexagonal wurtzite structure, these samples almost invariably contain a hidden cubic zinc blende type intergrowth that does not produce additional diffraction peaks, and whose abundance is measured to be 10 mole % or more using bulk diffraction analysis techniques we have developed. The mid gap optical absorption of the  $(\text{GaN})_{1-x}(\text{ZnO})_x$  system is found to be sensitive to the free carrier and defect concentrations, providing a new window for monitoring the

concentrations of free carrier and/or defects, and following their concentration dependence on synthesis and post-annealing conditions.

LaTiO<sub>2</sub>N has previously been reported to have a visible light absorbing band gap (2.25 eV) and band levels appropriately positioned for driving overall water splitting. LaTiO<sub>2</sub>N samples have been studied as powders and as epitaxial thin films on both optically transparent and electronically conducting custom single crystal substrates grown in our laboratory. We have found that this system can support non-stoichiometry that is able to reduce the band gap by about 0.1 eV. The absolute optical coefficients of LaTiO<sub>2</sub>N have been studied by spectral ellipsometry, and it is found that this compound absorbs visible light as intensely as the classic direct band gap semiconductor GaAs ( $\alpha \sim 10^5 \text{ cm}^{-1}$  at 2.45 eV). It is believed that this exceptionally strong visible light absorption should be common to mixed anion semiconductors, and collaborative DFT studies are being pursued to better understand the role of the mixed anion TiO<sub>4</sub>N<sub>2</sub> octahedral environment, to determine whether ordered anion lattices may lead to further improvements in visible light absorption, and to understand bonding in these complex solids.



Photoelectrochemical measurements of water oxidation currents of epitaxial LaTiO<sub>2</sub>N films prepared on top of conductive La<sub>5</sub>Ti<sub>5</sub>O<sub>17</sub> substrates confirm that visible light photons are able to efficiently drive water oxidation under applied bias. Unlike traditional oxide systems, the photoelectrochemical activity is reduced by only about 10% when a 400 nm filter is introduced to remove uv light, demonstrating that visible light photons are effectively utilized by this system. Efforts have been focused on understanding the surface chemistry of this system, especially on tools for detecting and eliminating a redox-active surface amorphous layer that can be easily formed during syntheses. The complex mixed anion nature of this surface falls outside of the well-defined parameter space for oxide analogues, and theoretical studies are being pursued to interpret the unusual XPS and EELS spectra from this system. The smaller band gap of LaTiO<sub>2</sub>N (~2.25 eV) relative to that of BiVO<sub>4</sub> ( $E_g \sim 2.45 \text{ eV}$ ) results in a substantially larger fraction of solar energy being absorbed, and present efforts are aimed at raising the quantum efficiency of LaTiO<sub>2</sub>N to levels very recently achieved for BiVO<sub>4</sub> (> 50%).



## DOE Sponsored Publications 2011-2014

1. A. C. Malingowski, P. W. Stephens, A. Huq, Q. Huang, S. Khalid, and P. Khalifah, "Substitutional mechanism of Ni into the wide band gap semiconductor InTaO<sub>4</sub> and its implications for water splitting activity in the wolframite structure type", *Inorg. Chem.*, **51**, 6096-6103 (2012). *Cover article*
2. Q. Mi, Y. Ping, Y. Li, B. Cao, B. S. Brunschwig, P. Khalifah, G. A. Galli, H. B. Gray, and N. S. Lewis, "Thermally stable N<sub>2</sub>-intercalated WO<sub>3</sub> photoanodes for water oxidation", *JACS*, **134**, 18318-18324 (2012).
3. A. A. Reinert, C. Payne, L. Wang, J. Ciston, Y. Zhu, and P. Khalifah, "Synthesis and Characterization of Visible Light Absorbing (GaN)<sub>1-x</sub>(ZnO)<sub>x</sub> semiconductors nanorods", *Inorg. Chem.*, **52**, 8389-8398 (2013).
4. L. Wang, B. Cao, W. Kang, M. Hybertsen, K. Maeda, K. Domen, and P. Khalifah, "Design of medium band gap Ag-Bi-Nb-O and Ag-Bi-Ta-O semiconductors for driving direct water splitting with visible light", *Inorg. Chem.*, **52**, 9192-9205 (2013).
5. Bingfei Cao, Gabriel Veith, Joerg Neuefeind, Radoslav Adzic, and Peter Khalifah, "Mixed close packed cobalt molybdenum nitrides as non-noble metal electrocatalysts for the hydrogen evolution reaction", *JACS*, **135**, 19186-192 (2013).
6. Polina Burmistrova, John Lofaro, Andrew Malingowski, Limin Wang, Dmitri Zakharov, Michael White, and Peter Khalifah, "LaTiO<sub>2</sub>N films on La<sub>2</sub>Ti<sub>2</sub>O<sub>7</sub> and La<sub>5</sub>Ti<sub>5</sub>O<sub>17</sub> substrates: synthesis, surface chemistry, and photoelectrochemical activity", *in preparation*
7. Andrew Malingowski, Limin Wang, Polina Burmistrova, Wei Kang, Bruce Ravel, Mark Hybertsen, Peter Khalifah "Light harvesting properties of LaTiO<sub>2</sub>N semiconductor films on La<sub>2</sub>Ti<sub>2</sub>O<sub>7</sub> and La<sub>5</sub>Ti<sub>5</sub>O<sub>17</sub> single crystal substrates", *in preparation*
8. Huafeng Huang, Alexandra Reinert, Elizabeth Sklute, Timothy Glotch, and Peter Khalifah, "Band gap and mid-gap optical properties of an extended range of (GaN)<sub>1-x</sub>(ZnO)<sub>x</sub> semiconductors for visible light harvesting", *in preparation*
9. Limin Wang, Peichuan Shen, Qixi Mi, Weidong Si, Alexander Orlov, Nathan S. Lewis, Peter Khalifah, "Substituted AgBiNb<sub>2</sub>O<sub>7</sub> semiconductors for enhanced direct water splitting with visible light", *in preparation*
10. Bingfei Cao, Daniel Weinstein, Kazuhiko Maeda, Kazunari Domen, Peter Khalifah, "Pyrochlore semiconductors for visible light harvesting", *in preparation*

## Functionalization and Modification of Transition Metal Dichalcogenide, GaP, and WO<sub>3</sub> Photoelectrodes

Joshua D. Wiensch, Victoria Dix, James McKone, Craig Wiggernhorn, and Nathan S. Lewis  
Department of Chemistry and Chemical Engineering  
California Institute of Technology  
Pasadena, CA 91125

Semiconductor photoelectrochemistry offers the potential to efficiently capture and convert the energy of sunlight into chemical fuels and oxygen. Efficient light absorbers that are stable under conditions that allow the fuel-forming and oxygen-evolution reactions to occur are critical to the development of a photoelectrochemical solar-fuels device. Functionalization and modification of semiconductor surfaces offer ways to probe the reactivity at surface sites, stabilize surfaces against corrosion, and to improve the performance of photoelectrodes. This paper presents progress towards functionalization and modification of Group VI dichalcogenide, GaP, and WO<sub>3</sub> photoelectrodes.

### Group VI Dichalcogenides

Group VI dichalcogenides, such as WSe<sub>2</sub> and MoS<sub>2</sub>, are efficient light absorbers and are also catalysts of the hydrogen-evolution reaction. The materials have a chemically interesting layered crystal structure that presents different reactivity at edge and terrace sites. We have used a chemical-vapor transport (CVT) method to grow single crystals of p-WSe<sub>2</sub>, n-WSe<sub>2</sub>, and n-MoSe<sub>2</sub> and have demonstrated that p-WSe<sub>2</sub> photocathodes decorated with Pt achieved energy-conversion efficiencies of >7% for the hydrogen-evolution reaction under mildly acidic conditions, and were stable under cathodic conditions for at least 2 h in acidic as well as in alkaline electrolytes.

In order to explore the differential reactivity of edge and terrace sites on the surface, we are employing a bidentate coordinating ligand, 1,2-benzenedithiol (1,2-BDT), to bind selectively to edge sites. X-ray photoelectron spectroscopy (XPS) studies of n-MoSe<sub>2</sub> following solution-phase treatment with 1,2-BDT showed sulfur on the entire crystal surface, suggesting successful ligand binding, while monodentate sulfur-based ligands failed to bind tightly enough to be observed spectroscopically in high vacuum environments. Raman studies of treated and untreated crystals indicated selective binding of 1,2-BDT at the edge sites of the single-crystal samples (Figure 1). These findings are consistent with the hypothesis of coordinatively unsaturated metal centers as the primary termination mode at edge sites. The coordination sphere of molybdenum accepts a bidentate ligand to fill the coordination sites.

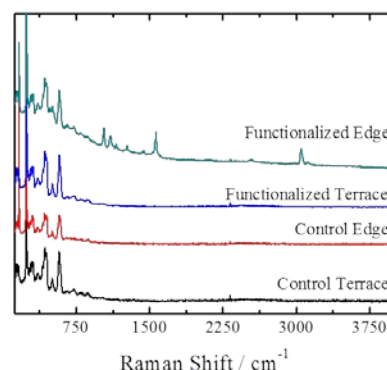


**Figure 1.** Raman studies of functionalized and unfunctionalized MoSe<sub>2</sub> edges and terraces with a 1 micron laser spot size.

## Modification of GaP Surfaces

Functionalization of semiconductor surfaces, via chlorination and subsequent reaction with alkyl Grignard reagents, has provided means of controlling the reactivity of surfaces, either by protecting the surface against corrosion or by providing a chemical handle for desired surface reactions. In order to extend this chemical utility to GaP, we must first obtain surfaces on the gallium-rich (111)A and phosphorus-rich (111)B faces with the correct element specificity of surface terminal atoms.

Figure 2 shows atomic force microscopy (AFM) images of terraces obtained on the GaP (111)A surfaces following treatment with concentrated HF. The terraces were maintained after chlorination of the surface using  $\text{PCl}_5$ . XPS data indicate less than a monolayer of oxides on the etched surfaces, and 80% coverage of the surface by Cl atoms after chlorination.

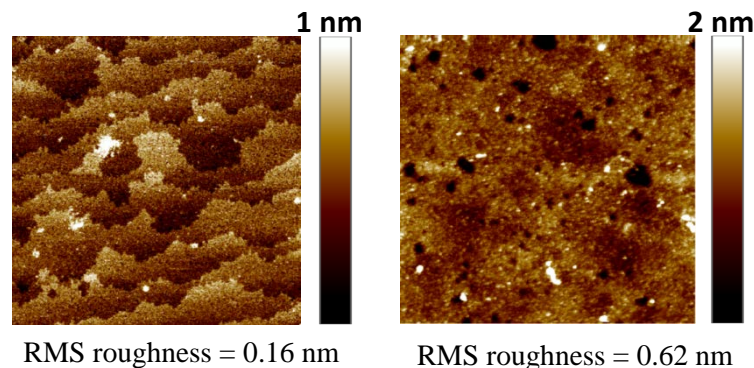


**Figure 2.** 1  $\mu\text{m}$  AFM images of the (111)A surface of GaP after (a) HF-based etching treatment and (b) chlorination.

A fluoride-based etching treatment did not yield single-element terraces on the (111)B face, and treatment with  $\text{PCl}_5$  did not produce chlorine-terminated surfaces. The (111)B surfaces were reacted with fluorine-tagged benzyl bromides to elucidate the chemical state of the terminal phosphorus atoms after etching. XPS data showed binding of the benzyl group to the (111)B surfaces and the presence of fluoride ions on these surface, consistent with lone-pair termination of the phosphorus atoms.

## $\text{WO}_3$ Photoanodes for Water Oxidation

Wide band-gap metal oxides are stable, non-toxic, inexpensive candidates for photoanodes to drive the oxygen-evolution half-reaction for water splitting. Since the compact morphology of the materials is often impractical for solar applications we investigated whether structuring  $\text{WO}_3$  could improve the ability of charge-carriers to efficiently reach the water-oxidation interface.

Nanoporous  $\text{WO}_3$  layers were fabricated by potentiostatic anodization of tungsten foils in fluoride electrolytes. The porous  $\text{WO}_3$  electrodes were stable under aqueous conditions, and produced open-circuit voltages  $> 800$  mV and significantly higher photocurrent densities and external quantum yields than compact  $\text{WO}_3$  electrodes (Figure 3).

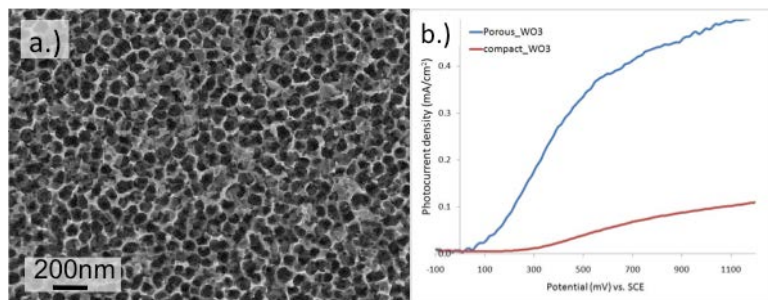


**Figure 3.** Porous  $\text{WO}_3$ . a.) SEM image of porous  $\text{WO}_3$ . b.) Comparison of compact and porous  $\text{WO}_3$  photoanodes in pH 4 buffered solution under  $100 \text{ mW cm}^{-2}$  illumination.

## DOE Sponsored Publications 2011-2014

1. McKone, J. R.; Pieterick, A. P.; Gray, H. B.; Lewis, N. S., Hydrogen Evolution from Pt/Ru-Coated p-Type WSe<sub>2</sub> Photocathodes. *J. Am. Chem. Soc.* **2013**, *135* (1), 223-231.
2. Mi, Q. X.; Coridan, R. H.; Brunnschwig, B. S.; Gray, H. B.; Lewis, N. S., Photoelectrochemical oxidation of anions by WO<sub>3</sub> in aqueous and nonaqueous electrolytes. *Energy Environ. Sci.* **2013**, *6* (9), 2646-2653.
3. Reyes-Gil, K. R.; Wiggernhorn, C.; Brunnschwig, B. S.; Lewis, N. S., Comparison between the Quantum Yields of Compact and Porous WO<sub>3</sub> Photoanodes. *J. Phys. Chem. C* **2013**, *117* (29), 14947-14957.
4. Bosco, J. P.; Scanlon, D. O.; Watson, G. W.; Lewis, N. S.; Atwater, H. A., Energy-band alignment of II-VI/Zn<sub>3</sub>P<sub>2</sub> heterojunctions from x-ray photoemission spectroscopy. *J. Appl. Phys.* **2013**, *113* (20), 8.
5. Fitch, A.; Strandwitz, N. C.; Brunnschwig, B. S.; Lewis, N. S., A Comparison of the Behavior of Single Crystalline and Nanowire Array ZnO Photoanodes. *J. Phys. Chem. C* **2013**, *117* (5), 2008-2015.
6. Kimball, G. M.; Bosco, J. P.; Muller, A. M.; Tajdar, S. F.; Brunnschwig, B. S.; Atwater, H. A.; Lewis, N. S., Passivation of Zn<sub>3</sub>P<sub>2</sub> substrates by aqueous chemical etching and air oxidation. *J. Appl. Phys.* **2012**, *112* (10).
7. Bosco, J. P.; Demers, S. B.; Kimball, G. M.; Lewis, N. S.; Atwater, H. A., Band alignment of epitaxial ZnS/Zn<sub>3</sub>P<sub>2</sub> heterojunctions. *J. Appl. Phys.* **2012**, *112* (9).
8. Mi, Q. X.; Ping, Y.; Li, Y.; Cao, B. F.; Brunnschwig, B. S.; Khalifah, P. G.; Galli, G. A.; Gray, H. B.; Lewis, N. S., Thermally Stable N-2-Intercalated WO<sub>3</sub> Photoanodes for Water Oxidation. *J. Am. Chem. Soc.* **2012**, *134* (44), 18318-18324.
9. Mi, Q. X.; Zhanaidarova, A.; Brunnschwig, B. S.; Gray, H. B.; Lewis, N. S., A quantitative assessment of the competition between water and anion oxidation at WO<sub>3</sub> photoanodes in acidic aqueous electrolytes. *Energy Environ. Sci.* **2012**, *5* (2), 5694-5700.
10. Knapp, D.; Brunnschwig, B. S.; Lewis, N. S., Transmission Infrared Spectra of CH<sub>3</sub><sup>-</sup>, CD<sub>3</sub><sup>-</sup>, and C<sub>10</sub>H<sub>21</sub>-Ge(111) Surfaces. *J. Phys. Chem. C* **2011**, *115* (33), 16389-16397.
11. Xiang, C. X.; Kimball, G. M.; Grimm, R. L.; Brunnschwig, B. S.; Atwater, H. A.; Lewis, N. S., 820 mV open-circuit voltages from Cu<sub>2</sub>O/CH<sub>3</sub>CN junctions. *Energy Environ. Sci.* **2011**, *4* (4), 1311-1318.

## *Session III*

### *Homogeneous Catalysis*



## Mixed-Metal Supramolecular Complexes as Photocatalysts for Hydrogen Production: Light Capture, Charge Separation, Electron Collection and Catalysis in Single Molecules

Rongwei Zhou, Hannah Mallalieu, Gerald Manbeck, Skye King, Karen J. Brewer

Department of Chemistry

Virginia Tech

Blacksburg, VA 24061-0212 (kbrewer@vt.edu)

Large molecular systems composed of smaller molecular building blocks are assembled into supramolecules where each sub-unit carries out a task to provide complex function to these light activated photochemical molecular devices. The function carried out by the title complexes is the capture of solar light, the generation of charge separation on a molecular scale, the multielectron reduction of a metal center and the catalysis of water reduction to produce hydrogen fuel. The systems of current interest couple Ru metal to ligand charge transfer (MLCT) light absorbers to Rh based catalysts that also function as electron collectors in these motifs. A number of related systems with sub-unit variation are employed to provide for an understanding of the perturbation of sub-unit properties upon assembly into molecular devices as well as to allow for a better understanding of the mechanism of function of these photocatalysts. The photocatalyst  $[\{(Ph_2phen)_2Ru(dpp)\}_2RhBr_2]^{5+}$  provides for an overall quantum yield of 8% for hydrogen production with high turnover.

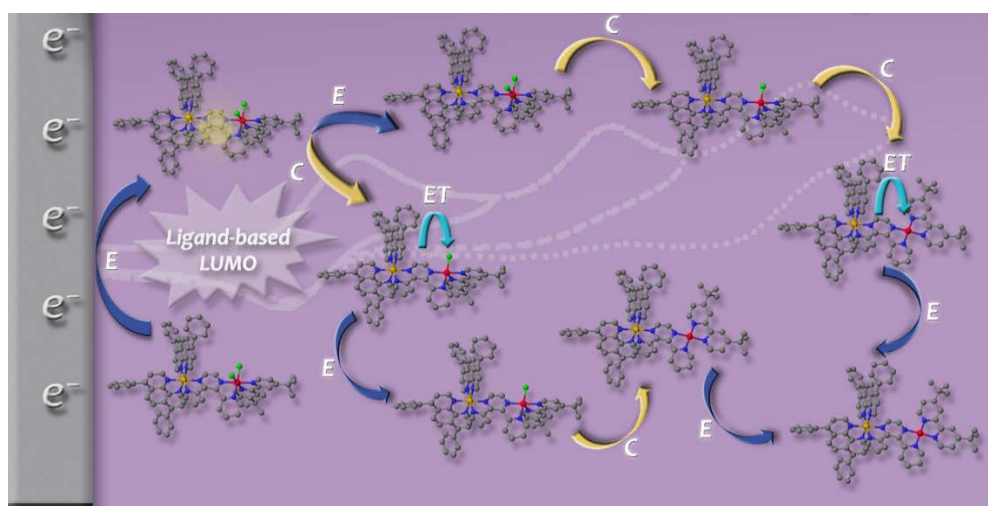


Figure 1. Electrochemistry of  $[(Ph_2phen)_2Ru(dpp)RhCl_2(tBu_2bpy)]^{3+}$ .

The study of a series of Ru,Rh bimetallic complexes have uncovered new electrochemical mechanisms for Rh complexes as well as highlighting the design constraints for production of active water reduction photocatalysts. Figure 1 illustrates the complexity of the electrochemical mechanism for a single member of this series of  $[(TL)_2Ru(dpp)RhCl_2(TL')]^{3+}$  series. In contrast to the electrochemistry of the entire series of RuRhRu trimetallics and related  $[Rh(NN)_2X_2]^+$  monometallics all the RuRh bimetallics display complex redox chemistry following a minimum of two electrochemical pathways for a single molecule that compete due to enhanced stability of the Rh(II) redox state in this motif. RuRh complexes have been prepared with the same motif  $[(Ph_2phen)_2Ru(dpp)RhCl_2(TL')]^{3+}$  only varying the TL' bound to Rh that display PEC and

function as photocatalysts for water reduction, display PEC but are not photocatalysts and are not prone to PEC and also do not function as photocatalysts for water reduction. This highlights the careful balance of steric and electronic factors needed to provide for functioning photocatalysts for water reduction.

New RuRuPt complexes have been studied as model two Ru light absorbers that allow for the extension of the  $^3\text{MLCT}$  excited state lifetime moving the localization of the lowest lying  $^3\text{MLCT}$  excited state away from the reactive metal providing for a dramatic enhancement in the excited state lifetime. In addition, these systems possess low lying  $^3\text{CS}$  excited states with the hole localized on the terminal Ru and the electron localized on the bridging ligand bound to the reactive metal. Time resolved emission studies demonstrated that these complexes violate Kasha's rule and do not populate the lowest lying  $^3\text{MLCT}$  excited state with unit efficiency. This was recently confirmed with transient absorbance spectroscopy which also allowed study of the excited state lifetime of the non-emissive  $^3\text{CS}$  excited state, Figure 2.

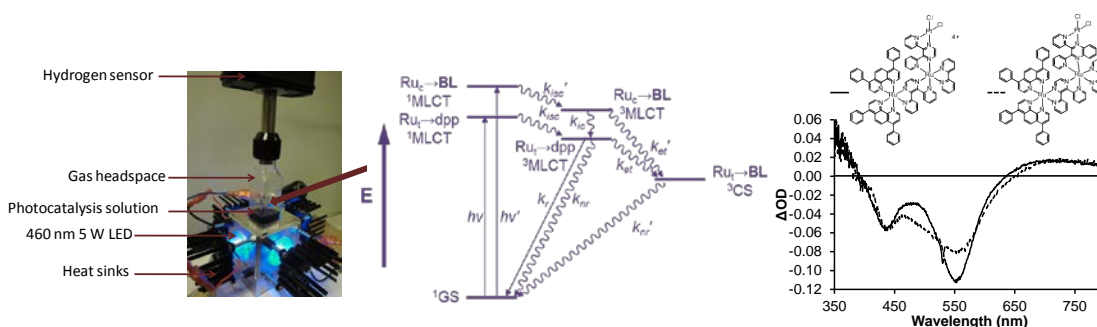
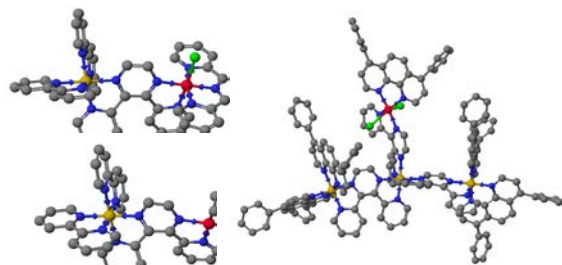


Figure 2. Photocatalysis apparatus for 4-LED excitation and excited state diagram and transient spectroscopy for two RuRuPt complexes.

New structural motifs have been prepared to help elucidate the mechanism of photocatalysis for these single component photocatalysts. These include Ru chromophores coupled to Rh(I) centers which displayed rather unexpected equilibria in solution in the presence of coordinating solvents. New RuRh complexes have been prepared that replace the normal  $\text{Rh}^{\text{III}}(\text{NN})_2\text{X}_2$  sub-units with either  $\text{Rh}^{\text{III}}(\text{NN})(\text{NNN})\text{X}$  or  $\text{Rh}^{\text{III}}(\text{NN})_2(\text{OH})_2$  structures. The systems with a single Rh halide bond are designed to test the need for two labile halides to provide for active catalysts and to assist in the determination of the mechanistic steps involved in the final steps of catalysis,  $\text{H}_2$  generation. The systems with Rh bound hydroxide are prepared to explore the role of these species as possible photogenerated Rh(III) intermediates as the Rh center cycles from six coordinate Rh(III) to four coordinate Rh(I) and back to Rh(III) in the photocatalytic cycle. These hydroxide complexes will also allow the determination of the acidity of a Rh(III) bound water as well as the study of the pH dependence of these aqua and hydroxide complexes.

Figure 3. Structural motifs explored to provide insight into the mechanism of photocatalysis of water reduction by RuRhRu, RuRuRh and RuRh motifs.



## DOE Sponsored Publications 2011-2014

1. “New Structural Motif for Electrocatalytic H<sub>2</sub> Production Elucidating Mechanistic Details of Ru(II),Rh(III),Ru(II) Water Reduction Photocatalysts: Importance of Reduced Speciation and Ligands as Electron Reservoirs,” Manbeck, Gerald F.; Canterbury, Theodore; Zhou, Rongwei; King, Skye; Nam, Geewoo; Brewer, Karen J. **2014**, submitted for publication.
2. “Mechanistic Insight into the Electronic Influences Imposed by Substituent Variation in Polyazine-Bridged Ru(II),Rh(III) Supramolecules,” White, Travis A.; Mallalieu, Hannah E.; Wang, Jing; Brewer, Karen J. *Eur. J. Chem.* **2014**, in press, featured on cover.
3. “Polyatomic Bridging Ligands,” *Elsevier Reference Module in Chemistry, Molecular Sciences and Chemical Engineering*, Editor-in-Chief, Jan Reedijk, **2013**, in press. Invited chapter.
4. “New Supramolecular Structural Motif Coupling a Ruthenium(II) Polyazine Light Absorber to a Rhodium(I) Center,” Zhou, Rongwei; Sedai, Baburam; Manbeck, Gerald F.; Brewer, Karen J. *Inorg. Chem.* **2013**, 52(23), 13314-13324.
5. “Subunit Variation to Uncover Properties of Polyazine-Bridged Ru(II), Pt(II) Supramolecules with Low Lying Charge Separated States Providing Insight into the Functioning as H<sub>2</sub>O Reduction Photocatalysts to Produce H<sub>2</sub>.” Knoll, Jessica D.; Higgins, S. L. H.; White, T. A.; Brewer, K. J. *Inorg. Chem.* **2013**, 52, 9749-9760.
6. “Water reduction in Nafion membranes with Ru-Rh-Ru mixed-metal complexes.” Naughton, Elise M.; Moore, Robert B.; Brewer, Karen J. *From Preprints – American Chemical Society, Division of Energy and Fuels*, **2013**, 58(1), 472.
7. “Photoinitiated electron collection in polyazine chromophores couple to water reduction catalysts for solar H<sub>2</sub> production.” Manbeck, G. F.; Brewer, K. J. *Coord. Chem. Rev.* **2013**, 257, 1660-1675.
8. “Supramolecular Complexes as Photochemical Molecular Devices for Solar Energy Conversion via Water Reduction to Produce Hydrogen Fuel,” Brewer, Karen J.; White, Travis; Arachchige, Shamindri; Tsui, Hei-Man; Knoll, Jessica; Gardner, Paige; Shaw, Ryan *ASES National Solar Conference*, 40th, Raleigh, NC, United States, May 17-20, 2011 **2012**, 538-545.
9. “Supramolecular complexes as photochemical molecular devices for solar energy conversion via water reduction to produce hydrogen.” White, Travis A.; Manbeck, Gerald; Whitaker, Brittany; Quinn, Kevan; Zhou, Rongwei; Dent, Evan; Knoll, Jessica; Wang, Jing; Higgins, Samantha; Arachchige, Shamindri; Brewer, Karen J. *From Preprints of Symposia – American Chemical Society, Division of Fuel Chemistry*, **2012**, 57(1), 581–582.
10. “Hydrogen via Direct Solar Production,” Arachchige, Shamindri; Brewer, Karen J., Edited by Robert A. Meyers, *Encyclopedia of Sustainability Science and Technology*, Springer Reference, Springer-Verlag Berlin Heidelberg, **2013**. Invited chapter.
11. “A series of supramolecular complexes for solar energy conversion via water reduction to produce hydrogen: an excited state kinetic analysis of Ru(II),Rh(III),Ru(II) photoinitiated electron collectors.” White, Travis A.; Knoll, Jessica D.; Arachchige, Shamindri M.; Brewer, Karen J. *Materials* **2012**, 5, 27-46. Invited Paper.
12. “Supramolecular Complex Design and Function for Photodynamic Therapy and Solar Energy Conversion via Hydrogen Production. Common Requirements for Molecular Architectures for Varied Light-Activated Processes,” Jing Wang, Shamindri Arachchige, Karen J, Brewer, Edited by Schneider, Hans-Joerg *From Applications of Supramolecular Chemistry* CRC Press, Boca Raton, Fla **2012**, 255-300, ISBN: 978-1-4398-4014-6, Invited Chapter.

13. "Efficient photocatalytic hydrogen production in a single-component system using Ru,Rh,Ru supramolecules containing 4,7-diphenyl-1,10-phenanthroline," White, Travis A.; Higgins, Samantha L. H.; Arachchige, Shamindri M.; Brewer, Karen J. *Angew. Chem., Int. Ed.* **2011**, *50*(51), 12209-12213.
14. "Discovering the Balance of Steric and Electronic Factors Needed To Provide a New Structural Motif for Photocatalytic Hydrogen Production from Water," White, Travis A.; Whitaker, Brittany N.; Brewer, Karen J. *J. Am. Chem. Soc.* **2011**, *133*(39), 15332-15334.
15. "Electrochemical, spectroscopic, and photophysical properties of structurally diverse polyazine-bridged Ru(II),Pt(II) and Os(II),Ru(II),Pt(II) supramolecular motifs," Knoll Jessica D; Arachchige Shamindri M; Wang Guangbin; Rangan Krishnan; Miao Ran; Higgins Samantha L H; Okyere Benjamin; Zhao Meihua; Croasdale Paul; Magruder Katherine; Brewer, Karen J. *Inorg. Chem.* **2011**, *50*(18), 8850-8860.
16. "A Structurally Diverse Ru(II),Pt(II) Tetrametallic Motif for Photoinitiated Electron Collection and Photocatalytic Hydrogen Production," Knoll Jessica D; Arachchige Shamindri M; Brewer Karen J., *ChemSusChem* **2011**, *4*, 252-261.
17. "High Turnover in a Photocatalytic System for Water Reduction to Produce Hydrogen Using a Ru,Rh,Ru Photoinitiated Electron Collector," Shamindri M. Arachchige, Ryan Shaw, Travis A. White, Vimal Shenoy, Hei-Man Tsui, and Karen J. Brewer *ChemSusChem* **2011**, *4*, 514-518.
18. "A New Structural Motif for Photoinitiated Electron Collection: Ru,Rh Bimetallics Providing Insight into H<sub>2</sub> Production via Photocatalysis of Water Reduction by Ru,Rh,Ru Supramolecules," Travis A. White, Jing Wang, Shamindri M. Arachchige, Karen J. Brewer *Chem. Comm.* **2011**, *47*, 4451-4453.

# A Concerted Synthetic, Spectroscopic, and Computational Approach towards Water Splitting by Heterometallic Complexes

Cláudio N. Verani, John F. Endicott, H. Bernhard Schlegel

Department of Chemistry  
Wayne State University  
Detroit, Michigan 48202

**Overview:** Our research is focused on the requirements for integrating active center, antennae, and acceptor modules into a single molecule. The current emphasis is on obtaining a better understanding of the electronic and redox properties of monometallic modules and multimetallic assemblies for water splitting in-bulk and on surfaces. The Verani/Endicott/Schlegel collaborative uses synthetic, electrochemical, photophysical, and computational tools in this approach. The research encompasses the design and synthesis of new catalytic species for water oxidation and proton reduction and the characterization of their ground state redox, electronic, and electrocatalytic behavior, as well as the photochemical and photophysical investigation of antennae modules to facilitate the design of new ruthenium-based photosensitizers which includes the characterization of excited state structures, energetics and reactivities. This experimental research is synergistically coupled with computational studies to help interpret the observations and to obtain greater insight into the chemical and photophysical processes.

## Trends in cobalt and cobalt-ruthenium catalysts for proton reduction:

The Verani and Schlegel groups are studying the design and development of architectures based on earth-abundant transition metals such as manganese, iron, and cobalt, along with ruthenium coordinated with new robust

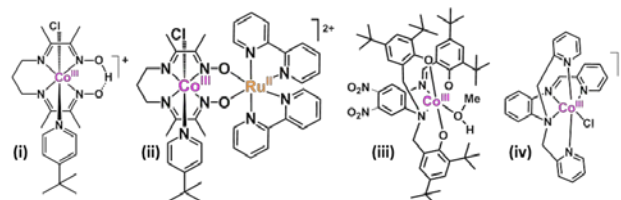


Figure 1. Cobalt complexes for proton reduction.

ligands. In this talk we will focus on the current efforts on the species summarized in **Figure 1** aiming at proton-reduction: (i) investigation of the energetics of axial ligand dissociation in cobalt oximes where we reexamine the order of redox vs. chemical events leading to the formation of the catalytic Co(I) species, (ii) preliminary results on the synthesis and electronic characterization of modular heterobinuclear systems that incorporate cobalt active centers and a ruthenium antenna, (iii) work on the effect of ligand substitution on the overpotential of cobalt complexes with electroactive phenolate-rich  $[N_2O_3]$  donor type ligands where appropriate substituents on phenylenediamine or phenolate moieties decrease the Co-based potentials, and (iv) results on the chemical conversions ( $=O$  and  $-OH$  insertion) of a cobalt complex with a new pendant-arm polypyridyl  $[(N_{am})_2(N_{py})_3]$  ligand where we observe that amines yield imines and amides unless a methyl protective group is used. Species (i) to (iv) show some degree of catalytic activity in acidic media such as p-toluenesulfonic, trifluoroacetic (TFA), triethylamine hydrochloride and acetic acids. The cobalt oxime (i) displays an overpotential of  $0.35 V_{Ag/AgCl}$  in presence of TFA with  $TON = 7.3$ , while the amide version of (iv) shows overpotential =  $0.73V$  and yielded a  $TON$  of  $4.2$  in the same acid. In parallel with experimental methods for studying these catalytic complexes, extensive use has been made of density functional theory (DFT) calculations to characterize the oxidation and spin states of intermediates, and to examine their structures, properties and reactivities. DFT calculations are valuable in determining the sites of

oxidation, the orbitals involved and the energetics of the various catalytic and redox steps. We will discuss calculations of the redox steps in cobalt oxime catalysis of hydrogen evolution (**Figure 2**).

### Trends in the <sup>3</sup>MLCT excited state properties of ruthenium complexes.

The Endicott and Schlegel groups are studying the properties of transition metal excited states that may mediate the conversion of solar to electrical energy or fuel. This requires knowledge of the energies, structures and efficiency of formation of reactive excited states. To this end we have been using spectroscopic probes and computational modeling of the lowest energy triplet excited state manifolds of several series of Ru(II)-pyridyl and polypyridyl complexes. DFT-based assignments indicate that the energies, orbital compositions and electronic distributions in the Franck-Condon (FC) excited states and the reactive triplet excited states do not always correlate in simple complexes (see publications 6, 7 & 10). The calculated emission spectra (energies and vibronic bandshapes) are in very good agreement with the 77 K spectra and indicate that increases in higher energies in vibronic sideband amplitudes results from the “tuning” of the <sup>3</sup>MLCT excited state energies with respect to the energy of the bpy ligand ππ-ππ\* energy gap and the different mixings of bpy and <sup>3</sup>MLCT orbitals (publ. 7). We are also investigating other near in energy states in the triplet manifold and how they affect the <sup>3</sup>MLCT excited state properties. Important among these states are the metal centered (<sup>3</sup>MC or <sup>3</sup>dd) states. The MC states have often been assumed to provide an efficient <sup>3</sup>MLCT deactivation pathway if E(<sup>3</sup>MC) ≤ E(<sup>3</sup>MLCT). We have examined this issue for (i) [Ru(L)<sub>6-n</sub>(MDA)<sub>n</sub>]<sup>2+</sup> complexes (publ. 10); MDA = pyrazine or X-pyridine; X = OAc, phenyl (**Figure 3a**); and (ii) [Ru(NCCH<sub>3</sub>)<sub>4</sub>bpy]<sup>2+</sup> and [Ru([14]aneS<sub>4</sub>)bpy]<sup>2+</sup> ([14]aneS<sub>4</sub>)bpy = a cyclic tetrathiaether ligand; publ. 13). The [Ru(L)<sub>6-n</sub>(MDA)<sub>n</sub>]<sup>2+</sup> complexes emit weakly at 77 K (φ<sub>emis</sub> ≈ 10<sup>-4</sup>-10<sup>-2</sup>), but with typical lifetimes (τ = 1/k<sub>obsd</sub>) for their excited state energies (publ. 5). The calculated <sup>3</sup>MC and <sup>3</sup>MLCT excited state energies are comparable, implying that the small emission yields result from competing FC relaxation pathways, not from <sup>3</sup>MLCT-to-<sup>3</sup>MC state crossing. In contrast, [Ru(NCCH<sub>3</sub>)<sub>4</sub>bpy]<sup>2+</sup> and [Ru([14]aneS<sub>4</sub>)bpy]<sup>2+</sup> have very similar higher energy absorption and emission spectra, but the former emits strongly at 77 K (φ<sub>emis</sub> ≈ 0.47) with τ ≈ 6.5 μs and the latter emits very weakly (φ<sub>emis</sub> < ~ 10<sup>-3</sup>; publ. 13). The DFT calculations for these two complexes indicate that for both {E(<sup>3</sup>MLCT) – E(<sup>3</sup>MC)} ≈ 5 kcal/mol (**Figure 3b**) and the difference in emission properties arises because some Ru-ancillary ligand bonds are much more distorted in the lowest energy <sup>3</sup>MC state of the (NCCH<sub>3</sub>)<sub>4</sub> than of the [14]aneS<sub>4</sub> complex resulting in a much larger kinetic barrier for intersystem crossing in the former than in the latter. These large differences in distortion coordinates allow the transient trapping of the excitation energy in an upper excited state.

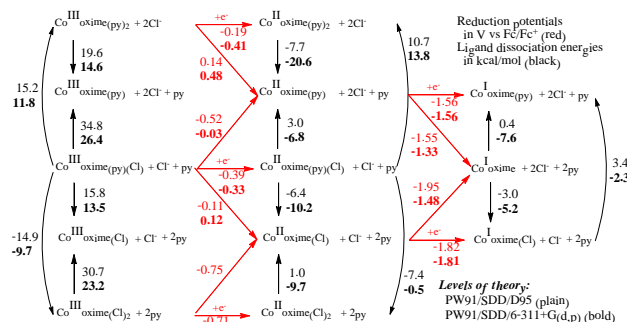


**Figure 2.** DFT results for Co(III) to Co(I) conversion.

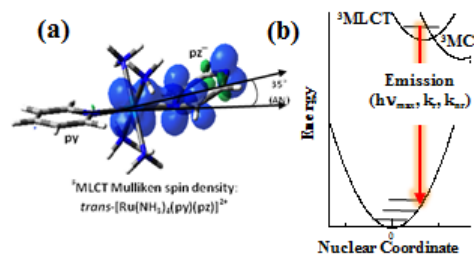


**Figure 3.** Structure and PE diagram for triplet excited states of Ru-MDA (a) and Ru-bpy (b) chromophores.

## DOE Sponsored Publications 2011-2014

1. Lesh, Allard, Shanmugam, Hryhorczuk, Endicott, Schlegel & Verani "Investigation of the Electronic, Photosubstitution, Redox, and Surface Properties of New Ruthenium(II)-Containing Amphiphiles" *Inorganic Chemistry* **2011**, *50*, 969-977 (listed among the top-read articles in January).
2. Lin, Tsai, Huang, Endicott, Chen & Chen: "Nearest- and Next-Nearest-Neighbor Ru(II)/Ru(III) Electronic Coupling in Cyanide-Bridged Ruthenium Square Complexes" *Inorganic Chemistry* **2011**, *50*, 8274–8280.
3. Tsai, Allard, Lord, Luo, Chen, Schlegel, Endicott "Characterization of Low Energy Charge Transfer Transitions in (terpyridine)(bipyridine)Ruthenium(II) Complexes and their Cyanide-Bridged Bi- and Tri-Metallic Analogues" *Inorganic Chemistry*, **2011**, *50*, 11965–11977.
4. Lesh, Lord, Heeg, Schlegel & Verani "Unexpected Formation of a Cobalt(III) Phenoxazinylate Electron Reservoir" *European Journal of Inorganic Chemistry* **2012**, 463–466 (invited contribution).
5. Allard, Sonk, Heeg, McGarvey, Schlegel & Verani "Bioinspired Five-Coordinate Iron(III) Complexes for Stabilization of Phenoxyl Radicals" *Angewandte Chemie Int. Ed.* **2012**, *51*, 3178-3182.
6. Allard, Heeg, Schlegel & Verani "Sequential Phenolate Oxidations in Octahedral Cobalt(III) Complexes with [N<sub>2</sub>O<sub>3</sub>] Ligands" *European Journal of Inorganic Chemistry* **2012**, 4622–4631 (Invited article for the cluster issue 'Modern coordination chemistry and its impact for meeting global challenges').
7. Lord, Allard, Thomas, Odongo, Schlegel, Chen & Endicott "Computational Modeling of the Triplet Metal-to-Ligand Charge-Transfer Excited-State Structures of Mono-Bipyridine–Ruthenium(II) Complexes and Comparisons to their 77 K Emission Band Shapes" *Inorganic Chemistry*, **2013**, *52*, 1185–1198.
8. Shanmugam, Xavier, Heeg, Verani "Electronic and interfacial behavior of bimetallic surfactants with copper(II)/pseudohalide cascade cores" *Dalton Transactions* **2013**, *42*, 15296–15306 (selected to provide the cover art).
9. Endicott, Chen, , "Electronic Coupling between Metal Ions in Cyanide-Bridged Ground State and Excited State Mixed Valence Complexes" *Coordination Chemistry Reviews* **2013**, *257*, 1676.
10. Tsai, Tian, Shi, Lord, Luo, Schlegel, Endicott, Chen, "Charge-Transfer Excited States with (Rutheniumammine)-(Mono-dentate Aromatic Ligand) Chromophores: Emission Spectra, DFT Modeling and Mixed-Valence Excited States," *Inorganic Chemistry* **2013**, *52*, 9774.
11. Endicott, (2013) Molecular Electron Transfer. In: Reedijk, J. (Ed.) Elsevier Reference Module in Chemistry, Molecular Sciences and Chemical Engineering. Waltham, MA: Elsevier. 21-Mar-2014 doi:10.1016/B978-0-12-409547-2.10974-6.
12. Wanniarachchi, Heeg & Verani "Effect of Substituents on the Water Oxidation Activity of [Ru<sup>II</sup>(terpy)(phen)Cl]<sup>+</sup> Procatalysts" *Inorganic Chemistry – ASAP* DOI: 10.1021/ic402118u.

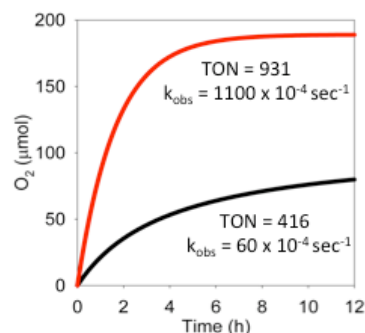
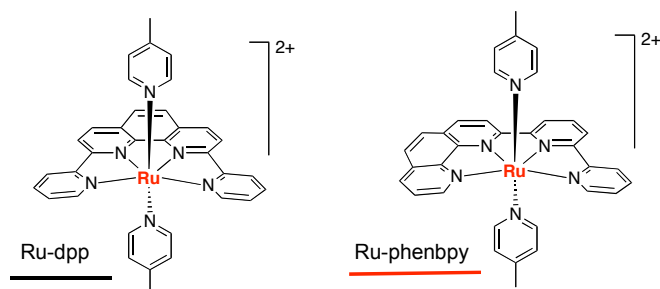
13. Mazumder, Thomas, Lord, Schlegel, Endicott, “A DFT and Spectroscopic study of Intramolecular Electron-Transfer in some mono-Bipyridine Ruthenium(II) Complexes” *Canadian Journal of Chemistry* **2014**, *submitted* (invited paper).
14. Basu, Allard, Xavier, Heeg, Staples, Schlegel & Verani “Modulation of Electronic and Redox Properties of Phenolate-rich [Cobalt<sup>III</sup>(L<sup>N2O3</sup>)MeOH] Complexes toward Proton Reduction” *to be submitted to Chemistry – A European Journal*.
15. Tsai, Thomas, Mazumder, Lord, Van Camp, Lu, Schlegel, Endicott, and Chen, “Patterns of Radiative Charge Transfer, Excited State Emission Yields and Lifetimes in Ruthenium(II) Bipyridine Complexes” *to be submitted to Journal of Physical Chemistry*.

## A Systematic Approach to a Molecular Light-driven Water Splitting Catalyst

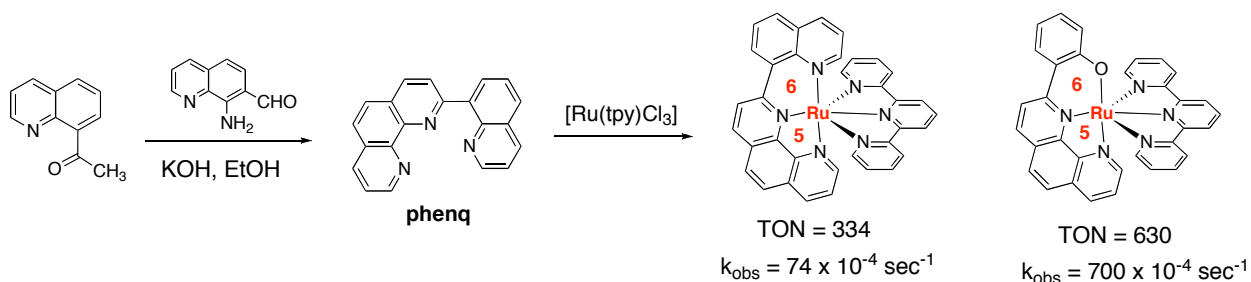
Nattawut Kaveevivitchai, Lars Kohler, Ruifa Zong,  
Lianpeng Tong, and Randolph P. Thummel

Department of Chemistry, 112 Fleming Building, University of Houston,  
Houston, TX 77204-5003

Our recent work has focused on the use of light-driven redox catalysts to promote the decomposition of water into its elements, sometimes also known as artificial photosynthesis. We have noticed that dinuclear and, somewhat surprisingly, mononuclear Ru(II) complexes can be active in this regard. Even more surprising, the coordinatively saturated tetradentate complex **1** is particularly active although ligand dissociation does not appear to occur readily in aqueous solution. We have suggested that upon two electron oxidation, water attacks the more electrophilic Ru(IV) center expanding the coordination sphere to seven. We find that the phen-bpy ligand, that is closely related to dpp (dipyridyl-1,10-phen) provides a tetradentate complex that is even more reactive in water oxidation.

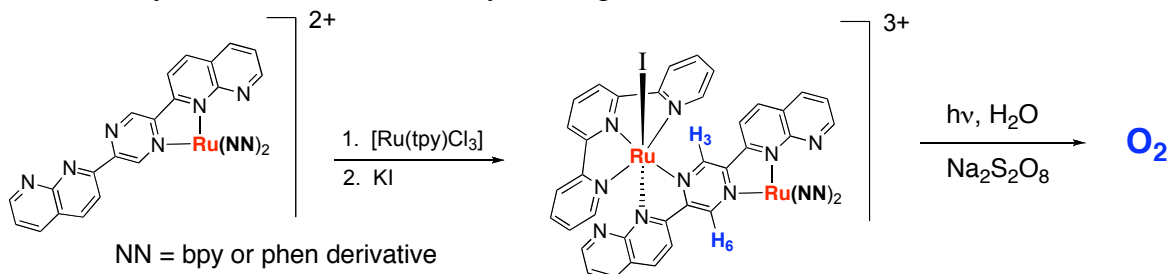


Since a certain level of strain appears to promote reactivity in water oxidation by Ru(II) polypyridine complexes, we decided to look more carefully at the lack of activity exhibited by  $[\text{Ru}(\text{tpy})_2]^{2+}$ . This shortcoming might be partially attributed to the inability of this complex to attain the pentagonal bipyramid geometry required for heptacoordination. We were able to overcome this limitation through the synthesis of the tridentate ligand phenq which forms both a six and five-membered chelate ring upon tridentate coordination. The coordinatively saturated complex  $[\text{Ru}(\text{phenq})(\text{tpy})]^{2+}$  upon exposure to Ce(IV), produced oxygen with a TON = 334. An analogous complex using the anionic ligand 2-(2'-phenoxy)-1,10-phenanthroline produces oxygen with TON = 630 and at a rate almost 10x as fast as the phenq complex.

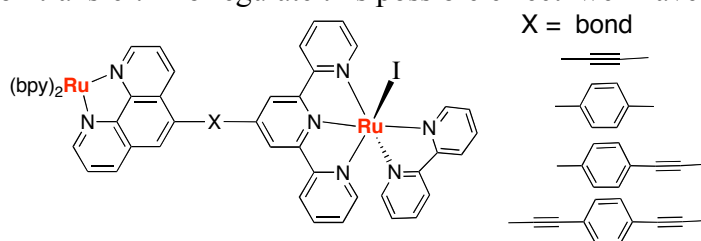


In place of using Ce(IV) as a sacrificial oxidant, we often use photoexcited  $[\text{Ru}(\text{NN})_3]\text{Cl}_2$  (NN = bpy, phen, or a subst. derivative) in the presence of excess sodium persulfate as a sacrificial

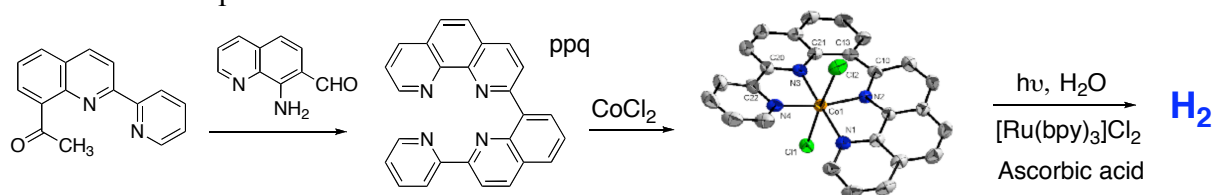
electron acceptor. We use a simple LED light strip to photoactivate the system. Going one step further, we have incorporated the photosensitizer into a dyad assembly along with the water oxidation catalyst to create a molecular system capable of water oxidation.



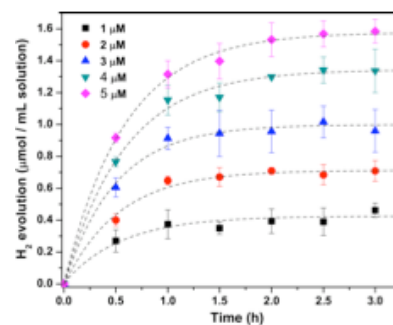
In collaboration with Prof. Sebastiano Campagna, our initial efforts to measure electron transfer rates in the dyad assemblies were thwarted by what appear to be very fast rates. This observation raised the concern about rapid back electron transfer. To regulate this possible effect we have designed and prepared a new series of dyads having alkynyl and phenylene linkers. When the system experiences some orthogonality due to the linker we would expect slower electron transfer rates and the overall effect on oxygen production is being assessed.



In order to decompose water with light in a truly catalytic process, without the need for sacrificial reagents, one needs to make both oxygen and hydrogen simultaneously. A number of different catalysts have been reported for proton reduction and many of these are based on earth-abundant metals such as Co(II) and Ni(II). Thus we decided to examine Co(II) complexes of some of our tetradentate ligands as possible water reduction catalysts. Due to the large size of the binding pocket, the reaction of dpp with Co(II) gave a 2:1 complex with a peripheral pyridine on each dpp uncoordinated. With ppq, having a smaller binding pocket, a well organized tetradentate complex was formed.



The [Co(ppq)Cl<sub>2</sub>] complex showed clear redox behavior in DMF at 100 mV/s. The Co<sup>II/III</sup> oxidation wave appeared at +0.45 V and three reversible reduction waves were observed at -0.55, -0.80, and -1.12 V. It is likely that the ppq ligand is involved in one of these reduction events. We measured hydrogen evolution by GC at 30 min intervals to provide the illustrated set of curves. A plot of initial rate of H<sub>2</sub> evolution vs. Co-ppq concentration indicated good first order behavior. The TOF was > 300 s<sup>-1</sup>.



## DOE Sponsored Publications 2011-2014

1. "Water Oxidation by a Mononuclear Ruthenium Catalyst: Characterization of the Intermediates," Polyansky, D. E.; Muckerman, J. T.; Rochford, J.; Zong, R.; Thummel, R. P.; Fujita, E. *J. Am. Chem. Soc.* **2011**, *133*, 14649-14665.
2. "Effects of a Proximal Base on Water Oxidation and Proton Reduction Catalyzed by Geometric Isomers of  $[\text{Ru}(\text{tpy})(\text{pynap})(\text{OH}_2)]^{2+}$ ," Boyer, J. L.; Polyansky, D. E.; Szalda, D. J.; Zong, R.; Thummel, R. P.; Fujita, E. *Angew. Chem. Int. Ed.* **2011**, *50*, 12600-12604.
3. "Ruthenium(II)-Cored Polythiophene Dendrimers," Deng, S.; Krueger, G.; Taranekar, P.; Sriwichai, S.; Zong, R.; Thummel, R. P.; Advincula R. C. *Chem Mater.* **2011**, *23*, 3302-3311.
4. "Polydentate Analogs of 8-Hydroxyquinoline and their Complexes with Ruthenium," El Ojaimi, M.; Thummel, R. P. *Inorg. Chem.* **2011**, *50*, 10966-10973.
5. "Steric Effect for Proton, Hydrogen-atom, and Hydride Transfer Reactions with Geometric Isomers of NADH-model Ruthenium Complexes," Cohen, B. W.; Polyansky, D. E.; Achord, P.; Cabelli, D.; Muckerman, J. T.; Tanaka, K.; Thummel, R. P.; Zong, R.; Fujita, E. *Faraday Discuss.* **2012**, *155*, 129-144.
6. "Further Observations on Water Oxidation Catalyzed by Mononuclear Ru(II) Complexes," Kaveevivitchai, N.; Zong, R.; Tseng, H.-W.; Chitta, R.; Thummel, R. P. *Inorg. Chem.* **2012**, *51*, 2930-2939.
7. "*Trans*- $[\text{Ru}^{\text{II}}(\text{dpp})\text{Cl}_2]$ : A Convenient Reagent for the Preparation of Heteroleptic Ru(dpp) Complexes where dpp is 2,9-Di-(pyrid-2'-yl)-1,10-phenanthroline," Zong, R.; Wang, B.; Thummel, R. P. *Inorg. Chem.* **2012**, *51*, 3179-3185.
8. "A Molecular Light-driven Water Oxidation Catalyst," Kaveevivitchai, N.; Chitta, R.; Zong, R.; El Ojaimi, M.; Thummel, R. P. *J. Am. Chem. Soc.* **2012**, *134*, 10721-10724.
9. "Water Oxidation with Mononuclear Ruthenium (II) Polypyridine Complexes Involving a Direct  $\text{Ru}^{\text{IV}}=\text{O}$  Pathway in Neutral and Alkaline Media," Badieli, Y.; Polyansky, D. E.; Muckerman, J. T.; Szalda, D. J.; Haberdar, R.; Zong, R.; Thummel, R. P.; Fujita, E. *Inorg. Chem.* **2013**, *52*, 8845-8850.
10. "Enabling Light-Driven Water Oxidation via a Low-Energy  $\text{Ru}^{\text{IV}}=\text{O}$  Intermediate," Lewandowska-Andralojc, A.; Polyansky, D. E.; Zong, R.; Thummel, R. P.; Fujita, E. *Phys. Chem. Chem. Phys.* **2013**, *15*, 14058-14068.
11. "A Ru(II) Bis-terpyridine-like Complex that Catalyzes Water Oxidation: the influence of Steric Strain," Kaveevivitchai, N.; Kohler, L.; Zong, R.; El Ojaimi, M.; Mehta, N.; Thummel, R. P. *Inorg. Chem.* **2013**, *52*, 10615-10622.
12. "Component Analysis of Dyads Designed for Light-Driven Water Oxidation," Kohler, L.; Kaveevivitchai, N.; Zong, R.; Thummel, R. P. *Inorg. Chem.* **2014**, *53*, 912-921.
13. "Visible Light-driven Hydrogen Evolution from Water Catalyzed by A Molecular Cobalt Complex," Tong, L.; Zong, R.; Thummel, R. P. *J. Am. Chem. Soc.* **2014**, *ASAP*, dx.doi.org/10.1021/ja501257d.



*Session IV*

*Heterogeneous Catalysis*



# CO<sub>2</sub> Reduction to Organics in an Aqueous Photoelectrochemical Environment

Jing Gu, Yong Yan, Amanda J. Morris, Elizabeth L. Zeitler, Yuan Hu, and Andrew B. Bocarsly  
Department of Chemistry  
Frick Laboratory  
Princeton University  
Princeton, New Jersey 08544

The use of sunlight to drive the conversion of CO<sub>2</sub> and water to alcohols and related oxidized organic products provides a strategy for both mitigating our dependence on fossil fuels and ameliorating the dumping the CO<sub>2</sub> into our atmosphere. Although it has previously been proposed that the transformations of interest can be carried out photoelectrochemically, exceptionally high cathode overpotentials and limited electrode stability have made the goal of electrogenerated liquid solar fuels difficult to achieve. We previously demonstrated that the kinetic limitations associated with the multielectron/multiproton reduction of CO<sub>2</sub> can be overcome by employing aqueous pyridinium as an electrocatalysts at an illuminated p-GaP photocathode. At pH = 5.2 and using the (100) face of GaP, methanol has been observed with 96% faradaic efficiency at a ~300mV underpotential.

This observation leads to our current studies aimed at understanding the mechanism of catalysis along with an expansion of the chemistry to other photoelectrode materials and other co-catalysts. To this end, we have found that both p-GaAs and p-GaInP<sub>2</sub> efficiently reduce CO<sub>2</sub> in the presence of pyridinium and ring substituted pyridiniums. Interestingly, in these latter two systems, we observe the formation of carbon-carbon bonded products (isopropanol and butanol) in addition to C<sub>1</sub> products (methanol and formic acid). We have also launched an investigation of p-type metal oxides as potential photocathodes, focusing on delafossite-structured materials. This class of semiconductors represents a relatively overlooked materials regime when it comes to photoelectrochemistry.

Over the past year, we have continued our mechanistic studies on the p-GaP/pyridinium system. Recent work shows a strong dependence on crystal face employed, and we are refining our mechanistic models in light of this finding. We have also modeled the pyridinium reaction using metal electrodes and a series of ring substituted pyridines. This work points to the pK<sub>a</sub> of the pyridine as a key parameter, which has led us to consider the role of pyridine as a proton transfer reagent.

Separately, we have synthesized and characterized the p-type delafossite, p-CuFeO<sub>2</sub> and evaluated it as a photocathode for the reduction of CO<sub>2</sub> in aqueous electrolyte near neutral pH. This layered material, as shown in Figure 1, consists of Fe(III) centers octahedrally coordinated to oxygens to form one layer, with Cu(I) oxide layers alternating with the iron based layers. We obtain a measured band gap of 1.36eV with a conduction band edge at ~ -1.1 V vs. SCE for this material.

One important finding here is that Mg doping can be used to control the p-type behavior of this system. We find that this

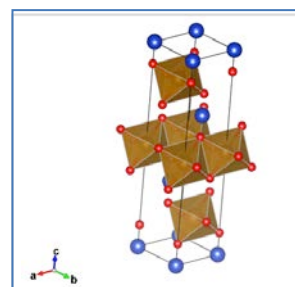


Figure 1: Powder x-ray determined structure of p-CuFeO<sub>2</sub> containing alternating planes of Cu (blue) and O<sub>h</sub> FeO<sub>2</sub> units (brown). Mg doping involves substitution at Fe site.

material selectively reduces CO<sub>2</sub> to formate without the need for a dissolved cocatalyst. The photo and dark response for this system is provided in Figure 2. Under the conditions employed the CO<sub>2</sub>/formate redox potential resides at ~ -0.8 V vs. SCE. Thus, the system develops ~800 mV of underpotential.

Based on this system we synthesized the analogous delafossite, CuRhO<sub>2</sub>, which was found to be p-type as grown. We determined a band gap of 1.9 eV with a conduction band edge at -1.5 V vs. SCE (valence band edge = 0.4 V vs. SCE) at neutral pH for this material. Thus, the band edge energetics of CuRhO<sub>2</sub> are well suited for the direct reduction of CO<sub>2</sub>. However, this material is inept at undertaking this reaction. Rather, it efficiently splits water. Notice that the band edges nicely straddle the water oxidation and reduction redox potentials. Experimentally, we find that that material splits water under zero bias! However, the material is unstable at neutral (and acidic) pH, decomposing via a route that forms Cu(0). This instability can be overcome (with zero bias water splitting remaining intact) by operating at basic pH in the presence of air. Under these conditions, dissolved oxygen re-oxides the photoreduced copper providing a stable CuRhO<sub>2</sub> interface. Faradaic efficiencies for H<sub>2</sub> production reach 80%, even in the presence of O<sub>2</sub>.

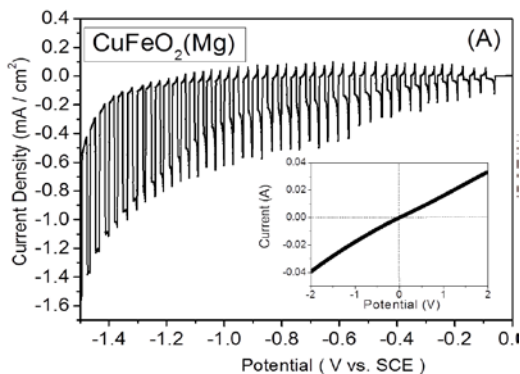


Figure 2: Chopped illumination (450nm) response of a 3 electrode cell employing a p-CuFeO<sub>2</sub> photocathode (0.5% Mg doping), a Pt counterelectrode and CO<sub>2</sub> saturated aqueous electrolyte. The inset demonstrates ohmic contact using gold.

### Future Plans

We find the observation that delafossite oxides can be doped p-type and provide relatively stable photocathodes intriguing. We also find the kinetic preference of these materials (reduction of CO<sub>2</sub> vs. reduction of H<sub>2</sub>O) to provide a useful tool for probing interfacial charge transfer processes. We therefore plan to continue our synthesis, materials characterization and photoelectrochemical analysis of the CuMO<sub>2</sub> and M'RhO<sub>2</sub> systems. In these studies we do not limit our interests to CO<sub>2</sub> reduction, but also consider water splitting. The finding that photoinduced reductive damage in the CuRhO<sub>2</sub> system can be healed by having small quantities of O<sub>2</sub> present presents a new scheme for stabilizing p-type oxides that we will continue to investigate. The relative ease of band edge engineering in these systems presents an essential handle for controlling both the kinetics and energetics of interfacial charge transfer in these systems as observed for the zero bias splitting of water in the p-CuRhO<sub>2</sub> system.

We also will continue our analysis of the interaction of pyridinium with III-V based photoelectrodes. In addition to considering the detailed interactions of pyridinium with the electrode surface, we will seek systems that reproducibly generate carbon-carbon bonded products.

### **DOE Sponsored Publications**

- (1) Keets, K.; Morris, A.; Zeitler, E.; Lakkaraju, P.; Bocarsly, A. Catalytic Conversion of Carbon Dioxide to Methanol and Higher Order Alcohols at a Photoelectrochemical Interface. In *Proceedings of SPIE*, San Diego, CA, **2010**; p. 77700.

- (2) Morris, A. J.; McGibbon, R. T.; Bocarsly, A. B. Electrocatalytic Carbon Dioxide Activation: The Rate-Determining Step of Pyridinium-Catalyzed CO<sub>2</sub> Reduction. *Chemsuschem* **2011**, *4*, 191-196.
- (3) Gu, Jing; Wuttig, Anna; Krizan, Jason W.; Hu, Yuan; Detweiler, Zachary M.; Cava, Robert J.; Bocarsly, Andrew B. Mg-Doped CuFeO<sub>2</sub> Photocathodes for Photoelectrochemical Reduction of Carbon Dioxide. *J. Phys. Chem. C* **2013**, *117*, 12415-12422.
- (4) Appel, A. M.; Bercaw, J. E.; Bocarsly, A. B.; Dobbek, H.; DuBois, D. L.; Dupuis, M.; Ferry, J. G.; Fujita, E.; Hille, R.; Kenis, P. J. A.; Kerfeld, C. A.; Morris, R. H.; Peden, C. H. F.; Portis, A. R.; Ragsdale, S. W.; Rauchfuss, T. B.; Reek, J. N. H.; Seefeldt, L. C.; Thauer, R. K.; Waldrop, G. L. Frontiers, Opportunities, and Challenges in Biochemical and Chemical Catalysis of CO<sub>2</sub> Fixation. *Chem. Rev.* **2013**, *113*, 6621-6658.
- (5) Gu, J.; Yan, Y.; Krizan, J. W.; Gibson, Q. D.; Detweiler, Z. M.; Cava, R. J.; Bocarsly, A. B. p-type CuRhO<sub>2</sub> as a self-healing photoelectrode for water reduction under visible light. *J. Am. Chem. Soc.* **2014**, *136*, 830-833.
- (6) Yan, Yong; Gu, Jing; Zeitler, Elizabeth L.; Bocarsly, Andrew B., Photoelectrocatalytic Reduction of Carbon Dioxide, In *Carbon Dioxide Utilization*; Strying, P., Ed.; Elsevier: UK, in press (**2014**).

## Oxomanganese Catalysts for Solar Fuel Production

Gary W. Brudvig, Charles A. Schmuttenmaer, Robert H. Crabtree and Victor S. Batista  
*Department of Chemistry, Yale University, New Haven, CT 06520-8107*

The goal of this project is to construct solar-driven water-splitting photocatalytic cells, based on our own water-oxidation catalysts and sensitized metal oxide nanoparticles (NPs). Four research groups in the Chemistry Department at Yale University are working together to synthesize metal oxide NPs and anchor-linker-catalyst conjugates, develop new methods for surface attachment of catalysts using oxidation-resistant anchors and linkers that are stable in water, develop and apply computational methods to analyze interfacial electron transfer and characterize catalytic water-oxidation complexes, and use spectroscopic methods to characterize the photochemistry. See also posters by Crabtree and Batista.

### Modular assembly of photoanodes.

By using a modular assembly method, we have constructed T-shaped assemblies that combine an anchoring group attached to pyridine axially bound to a high-potential zinc porphyrin (Fig. 1). The photoexcited electron injection dynamics of these assemblies bound to  $\text{TiO}_2$  and  $\text{SnO}_2$  nanoparticle surfaces have been investigated by using time resolved THz spectroscopy, and recombination dynamics on a  $\mu\text{s}$  time scale have been monitored with transient absorption (TA) spectroscopy.

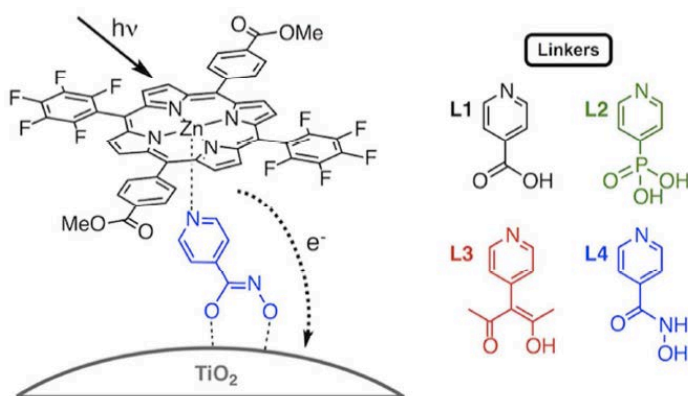


**Figure 1.** Modular assembly of high-potential photoanodes.

**Hole harvesting on high-potential photoanodes.** In water-splitting photoelectrochemical cells, multiple oxidizing equivalents must be delivered to the catalyst in competition with undesired recombination processes. We have designed a porphyrin-based model system to examine the use of lateral intermolecular charge transfer as an efficient means to increase charge flow to a catalyst (Fig. 2). The hole-hopping kinetics have been investigated by using TA spectroscopy.

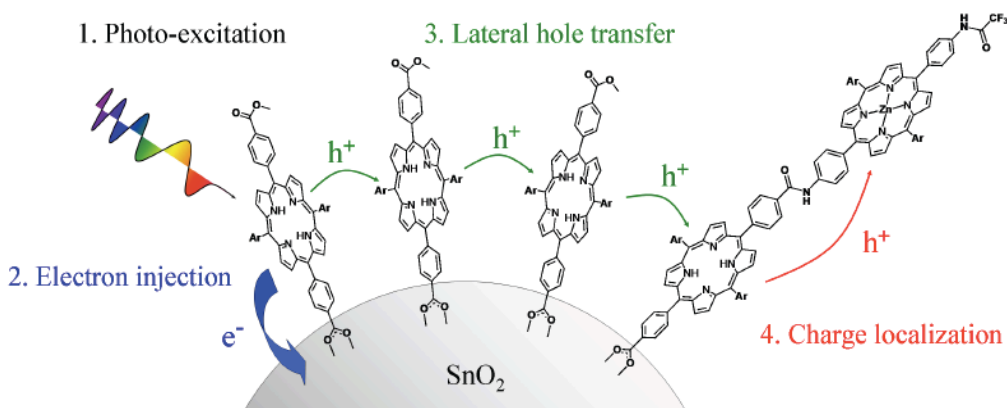


**Figure 2.** Hole-hopping antenna.

**Photocatalysis.** A Mn complex attached to a TiO<sub>2</sub> electrode via a light-absorbing organic linker (**L1**) has been used for photooxidation of a non-fluorescent substrate (2',7'-dihydrodichloro-fluorescein, H<sub>2</sub>DCF) to yield

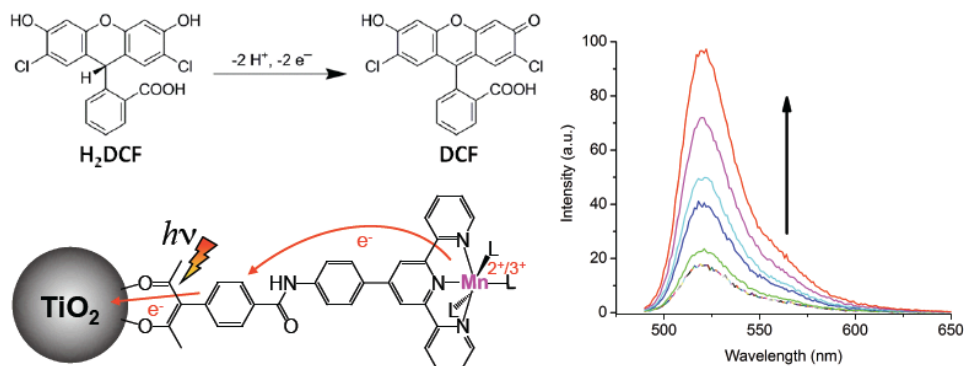


**Figure 3.** top: Oxidation of H<sub>2</sub>DCF yields DCF; bottom: Mn<sup>II</sup> catalyst attached to a TiO<sub>2</sub> surface via a terpy-acac ligand (**L1**); right: light-induced fluorescence.

the fluorescent compound, 2',7'-dichlorofluorescein (DCF) (Fig. 3). Sustained photocurrent is observed upon visible-light illumination of the anode in the presence of the substrate. The high fluorescence quantum yield of DCF allows for nanomolar sensitivity and real-time monitoring of substrate oxidation. Additionally, illumination of the sensitized electrode in a 1% solution of 2-propanol results in similar sustained photocurrents, indicating that the Mn<sup>II</sup>-**L1**-TiO<sub>2</sub> electrode is competent for the photoelectrochemical oxidation of 2-propanol to acetone.

**Molecular rectification.** Steady-state illumination of Mn<sup>II</sup>-**L1**-TiO<sub>2</sub> leads to reversible photooxidation of Mn(II) to Mn(III) as measured by EPR spectroscopy (Fig. 4). However, steady-state illumination of the complex with the opposite orientation of the amide linkage (Mn<sup>II</sup>-**L2**-TiO<sub>2</sub>) does not lead to a long-lived charge separation, although charge injection is equivalent for the two complexes (Fig. 4). Thus, the appropriate choice of the orientation of the amide linkage yields directionality of interfacial electron transfer, essential to enhance electron injection and slow back-electron transfer.

**Plans.** Ongoing work is exploring the application of hole-hopping antenna and molecular rectifiers in the design of TiO<sub>2</sub> photoanodes functionalized with water-oxidation catalysts and high-potential porphyrin dyes for light-driven water oxidation.

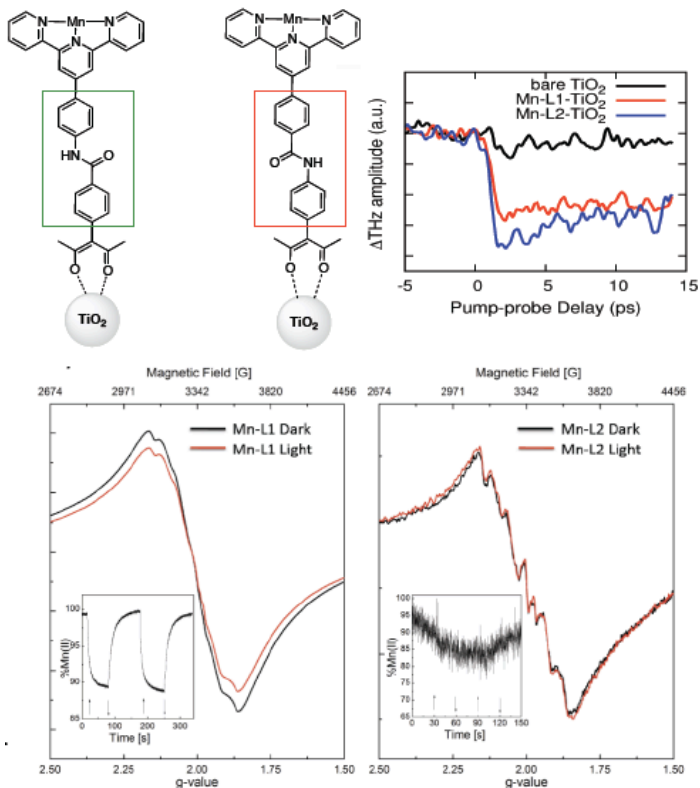


**Figure 4.** Charge injection (top right) and steady-state Mn photooxidation (bottom) of Mn<sup>II</sup>-**L1**-TiO<sub>2</sub> (top left) and Mn<sup>II</sup>-**L2**-TiO<sub>2</sub> (top center).

## DOE Sponsored Solar Photochemistry Publications 2011-2014

1. “Multifunctional Ligands in Transition Metal Catalysis”, Robert H. Crabtree (2011) *New J. Chem.* **35**, 18-23.
2. “Tunneling Under Control by Sequences of Unitary Pulses”, Rajdeep Saha and Victor S. Batista (2011) *J. Phys. Chem. C* **115**, 5234-5242.
3. “Energy Conversion in Photosynthesis: A Paradigm for Solar Fuel Production”, Gary F. Moore and Gary W. Brudvig (2011) *Annu. Rev. Condensed Matter Phys.* **2**, 303–327.
4. “Comparing Photosynthetic and Photovoltaic Efficiencies and Recognizing the Potential for Improvement”, Robert E. Blankenship, David M. Tiede, James Barber, Gary W. Brudvig, Graham Fleming, Maria Ghirardi, M. R. Gunner, Wolfgang Junge, David M. Kramer, Anastasios Melis, Thomas A. Moore, Christopher C. Moser, Daniel G. Nocera, Arthur J. Nozik, Donald R. Ort, William W. Parson, Roger C. Prince and Richard T. Sayre (2011) *Science* **332**, 805–809.
5. “A Visible Light Water-Splitting Cell with a Photoanode formed by Codeposition of a High-Potential Porphyrin and an Iridium Water-Oxidation Catalyst”, Gary F. Moore, James D. Blakemore, Rebecca L. Milot, Jonathan F. Hull, Hee-eun Song, Lawrence Cai, Charles A. Schmuttenmaer, Robert H. Crabtree and Gary W. Brudvig (2011) *Energy Environ. Science* **4**, 2389–2392.
6. “Photocatalytic Water Oxidation Using Manganese Compounds Immobilized in Nafion Polymer Membranes”, Karin J. Young, Yunlong Gao and Gary W. Brudvig (2011) *Australian J. Chem.* **64**, 1219–1226.
7. “Fluctuation-Induced Tunneling Conductivity in Nanoporous TiO<sub>2</sub> Films”, Steven J. Konezny, Christiaan Richter, Robert C. Snoberger III, Alexander R. Parent, Gary W. Brudvig, Charles A. Schmuttenmaer and Victor S. Batista (2011) *J. Phys. Chem. Lett.* **2**, 1931–1936.
8. “Wilkinson’s Iridium Acetate Trimer as a Water-Oxidation Catalyst”, Alexander R. Parent, James D. Blakemore, Gary W. Brudvig and Robert H. Crabtree (2011) *Chem. Comm.* **47**, 11745–11747.
9. “An Organometallic Future in Green and Energy Chemistry?”, Robert H. Crabtree (2011) *Organometallics* **30**, 17-19.
10. “AC Conductivity of Nanoporous Metal-Oxide Photoanodes for Solar Energy Conversion”, Steven J. Konezny, Diyar Talbayev, Ismail El Beggari, Charles A. Schmuttenmaer and Victor S. Batista (2011) *Proc. SPIE* 8098, 809804.
11. “Covalent Attachment of a Rhenium CO<sub>2</sub>-Reduction Catalyst to Rutile TiO<sub>2</sub>”, Chantelle L. Anfuso, Robert Snoberger III, Allen M. Ricks, Weimin Liu, Dequan Xiao, Victor S. Batista and Tianquan Lian (2011) *J. Am. Chem. Soc.* **133**, 6922–6925.
12. “Resolving Heterogeneity Problems and Impurity Artifacts in Operationally Homogeneous Transition Metal Catalyst”, Robert H. Crabtree (2012) *Chem. Rev.* **112**, 1536–1554.
13. “Cp\* Iridium Precatalysts for Selective C-H Oxidation via Direct Oxygen Insertion. A Joint Experimental/Computational Study”, Meng Zhou, David Balcells, Alexander R. Parent, Robert H. Crabtree and Odile Eisenstein (2012) *ACS Catalysis* **2**, 208–218.
14. “Tuning Redox Potentials of Bis(imino)pyridine Cobalt Complexes: An Experimental and Theoretical Study Involving Solvent and Ligand Effects”, C. Moyses Araujo, Mark D. Doherty, Steven J. Konezny, Oana R. Luca, Alex Usyatinsky, Hans Grade, Emil Lobkovsky, Grigori L. Soloveichik, Robert H. Crabtree and Victor S. Batista (2012) *Dalton Trans.*

- 41**, 3562-3573.
15. “Bioinspired High-Potential Porphyrin Photoanodes”, Gary F. Moore, Steven J. Konezny, Hee-eun Song, Rebecca L. Milot, James D. Blakemore, Minjoo L. Lee, Victor S. Batista, Charles A. Schmuttenmaer, Robert H. Crabtree and Gary W. Brudvig (2012) *J. Phys. Chem. C* **116**, 4892-4902.
  16. “Water Oxidation Catalyzed by a Tetranuclear Mn Cluster:  $[\text{Mn}^{\text{IV}}_4\text{O}_5(\text{terpy})_4(\text{H}_2\text{O})_2](\text{ClO}_4)_6$  (terpy = 2,2':6,2''-Terpyridine)”, Yunlong Gao, Robert H. Crabtree and Gary W. Brudvig (2012) *Inorg. Chem.* **51**, 4043–4050.
  17. “Synthesis and Computational Studies of Mg Complexes Supported by 2,2':6,2''-Terpyridine Ligands”, Louise M. Guard, Julio L. Palma, William P. Stratton Laura J. Allen, Gary W. Brudvig, Robert H. Crabtree, Victor S. Batista and Nilay Hazari, (2012) *Dalton Trans.* **41**, 8098-8110.
  18. “Oxomanganese Complexes for Natural and Artificial Photosynthesis”, Ivan Rivalta, Gary W. Brudvig, Victor S. Batista (2012) *Curr. Opinion Chem. Biol.* **16**, 11-18.
  19. “Light-driven Water Oxidation for Solar Fuel Production”, Karin J. Young, Lauren A. Martini, Rebecca L. Milot, Robert C. Snoeberger III, Victor S. Batista, Charles A. Schmuttenmaer, Robert H. Crabtree and Gary W. Brudvig (2012) *Coord. Chem. Rev.* **256**, 2503-2520.
  20. “Interfacial Electron Transfer into Functionalized Crystalline Polyoxotitanate Nanoclusters”, Robert C. Snoeberger III, Karin J. Young, Jiji Tang, Laura J. Allen, Robert H. Crabtree, Gary W. Brudvig, Philip Coppens, Victor S. Batista and Jason B. Benedict (2012) *J. Am. Chem. Soc.* **134**, 8911-8917.
  21. “Orientation of a Series of CO<sub>2</sub> Reduction Catalysts on Single TiO<sub>2</sub> using Phase Sensitive Vibrational Sum Frequency Generation Spectroscopy (PS-VSFGS)”, Chantelle L. Anfuso, Dequan Xiao, Allen M. Ricks, Christian F. A. Negre, Victor S. Batista and Tianquan Lian (2012) *J. Phys. Chem. C* **116**, 24107-24114.
  22. “Cp\* Iridium Precatalysts for Selective C–H Oxidation with Sodium Periodate as the Terminal Oxidant”, Meng Zhou, Ulrich Hintermair, Brian G. Hashiguchi, Alexander R. Parent, Sara M. Hashmi, Menachem Elimelech, Roy A. Periana, Gary W. Brudvig and Robert H. Crabtree (2013) *Organometallics* **32**, 957-965.
  23. “Comparison of Primary Oxidants for Water-Oxidation Catalysis”, Alexander R. Parent, Robert H. Crabtree and Gary W. Brudvig (2013) *Chem. Soc. Rev.* **42**, 2247-2252.
  24. “Artificial Photosynthesis as a Frontier Technology for Energy Sustainability”, Thomas Faunce, Stenbjörn Styring, Michael R. Wasielewski, Gary W. Brudvig, A. William Rutherford, Johannes Messinger, Adam F. Lee, Craig L. Hill, Huub deGroot, Marc Fontecave, Douglas R. MacFarlane, Ben Hankamer, Daniel G. Nocera, David M. Tiede, Holger Dau, Warwick Hillier, Lianzhou Wang and Rose Amal (2013) *Energy & Environ. Science* **6**, 1074-1076.
  25. “Computational Studies of Natural and Artificial Photosynthesis”, Ivan Rivalta, Gary W. Brudvig and Victor S. Batista (2013) *ACS Sym. Ser.* **1133**, 203-215.
  26. “Hydroxamate Anchors for Improved Photoconversion in Dye-Sensitized Solar Cells”, Timothy P. Brewster, Steven J. Konezny, Stafford W. Sheehan, Lauren A. Martini, Charles A. Schmuttenmaer, Victor S. Batista, and Robert H. Crabtree (2013) *Inorg. Chem.* **52**, 6752–6764.
  27. “An Anionic N-donor Ligand Promotes Manganese-catalyzed Water Oxidation”, Karin J.

- Young, Michael K. Takase and Gary W. Brudvig (2013) *Inorg. Chem.* **52**, 7615-7622.
28. “Modular assembly of high-potential Zn-porphyrin photosensitizers attached to TiO<sub>2</sub> with a series of anchoring groups”, Lauren A. Martini, Gary F. Moore, Rebecca L. Milot, Lawrence Z. Cai, Stafford W. Sheehan, Charles A. Schmittenmaer, Gary W. Brudvig, and Robert H. Crabtree (2013) *J. Phys. Chem. C* **117**, 14526–14533.
  29. “Precursor Transformation during Molecular Oxidation Catalysis with Organometallic Iridium Complexes”, Ulrich Hintermair, Stafford W. Sheehan, Alexander R. Parent, Daniel H. Ess, David T. Richens, Patrick H. Vaccaro, Gary W. Brudvig and Robert H. Crabtree (2013) *J. Am. Chem. Soc.* **135**, 10837-10851.
  30. “Electron Injection Dynamics from Photoexcited Porphyrin Dyes into SnO<sub>2</sub> and TiO<sub>2</sub> Nanoparticles”, Rebecca L. Milot, Gary F. Moore, Robert H. Crabtree, Gary W. Brudvig, and Charles A. Schmittenmaer (2013) *J. Phys. Chem. C* **117**, 21662-21670.
  31. “Efficiency of Interfacial Electron Transfer from Zn-Porphyrin Dyes into TiO<sub>2</sub> Correlated to the Linker Single Molecule Conductance”, Christian F. A. Negre, Rebecca L. Milot, Lauren A. Martini, Wendu Ding, Robert H. Crabtree, Charles A. Schmittenmaer, and Victor S. Batista (2013) *J. Phys. Chem. C* **117**, 24462-24470.
  32. “Photoelectrochemical Oxidation of a Turn-On Fluorescent Probe Mediated by a Surface Mn<sup>II</sup> Catalyst Covalently Attached to TiO<sub>2</sub> Nanoparticles”, Alec C. Durrell, Gonghu Li, Matthieu Koepf, Karin J. Young, Christian F. A. Negre, Laura J. Allen, William R. McNamara, Hee-eun Song, Victor S. Batista, Robert H. Crabtree and Gary W. Brudvig (2014) *J. Catal.* **310**, 37-44.
  33. “Ultrafast Carrier Dynamics in Nanostructures for Solar Fuels”, Jason B. Baxter, Christiaan Richter, and Charles A. Schmittenmaer (2014) *Ann. Rev. Phys. Chem.* **65**, 423-447.
  34. “Linker Rectifiers for Covalent Attachment of Transition Metal Catalysts to Metal-Oxide Surfaces”, Wendu Ding, Christian F. A. Negre, Julio L. Palma, Alec C. Durrell, Laura J. Allen, Karin J. Young, Rebecca L. Milot, Charles A. Schmittenmaer, Gary W. Brudvig, Robert H. Crabtree and Victor S. Batista (2014) *ChemPhysChem* **15**, in press.
  35. “High Conductance Conformers in Histograms of Single-Molecule Current-Voltage Characteristics”, Wendu Ding, Christian Negre, Leslie Vogt and Victor S. Batista (2014) *J. Phys. Chem. C* **118**, in press.

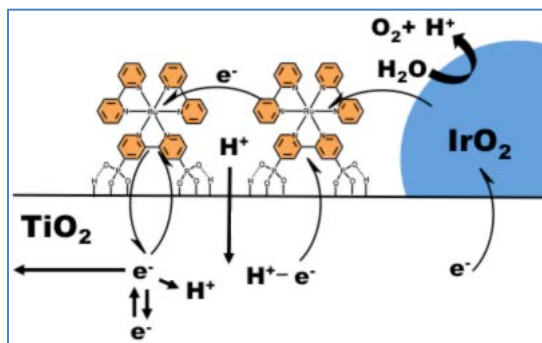
## Nanostructured Photocatalytic Water Splitting Systems

John R. Swierk, Nicholas S. McCool, Nella M. Vargas-Barbosa, Timothy Saunders, Dongdong Qin, Greg D. Barber, Christopher Gray, Jennifer Dysart, Pengtao Xu, and Thomas E. Mallouk  
Department of Chemistry, The Pennsylvania State University, University Park, PA 16802

Dalvin D. Mendez-Hernandez, Ana L. Moore, Thomas A. Moore, and Devens Gust  
Department of Chemistry and Biochemistry, Arizona State University, Tempe AZ 85281

Our DOE-supported work investigates the assembly and electron transfer reactions in water splitting dye-sensitized photoelectrochemical cells. So far the project has focused predominantly on understanding and improving the photoanode, a nanoporous  $\text{TiO}_2$  electrode that contains a ruthenium polypyridyl or porphyrin sensitizer and a colloidal  $\text{IrO}_x \cdot n\text{H}_2\text{O}$  water oxidation catalyst. Although the anode assembly is similar to that of a dye-sensitized solar cell (DSSC), the kinetics are more complicated because water oxidation is slow and occurs only at the catalyst sites. Different groups have reported varying results with different sensitizers and catalysts. Typically the incident photon current efficiency is low (1-15%) and the photoanode polarizes over a period of seconds. We are now using a combination of spectroscopic and electrochemical methods to understand the kinetics that govern these effects. To extend this concept to unassisted overall water splitting, we are also assembling and studying molecular photocathodes for light-driven water reduction. The photocathodes are donor-acceptor-catalyst assemblies grown layer-by-layer on high surface area transparent conductor substrates. Electrochemical and transient spectroscopic techniques are used to study the kinetics of the individual components and donor-acceptor diads, as well more complex systems assembled from them.

In previous studies of the photoanode, we used phosphonate linkers to position the sensitizer molecules between the  $\text{TiO}_2$  surface and the catalytic  $\text{IrO}_x \cdot n\text{H}_2\text{O}$  particles. We later found that catalyst particles linked directly to the  $\text{TiO}_2$  surface gave similar results, and also that the activity of the catalyst was sensitive to the linker chemistry. We have now made nanoporous  $\text{TiO}_2$  electrodes in which rutile  $\text{IrO}_2$  nanoparticles are directly deposited from colloidal citrate-capped  $\text{IrO}_x \cdot n\text{H}_2\text{O}$  and sintered at  $450^\circ\text{C}$ . These particles have reproducible, high catalytic activity and enable a more detailed and reliable study of the electron transfer kinetics of the photoanode.

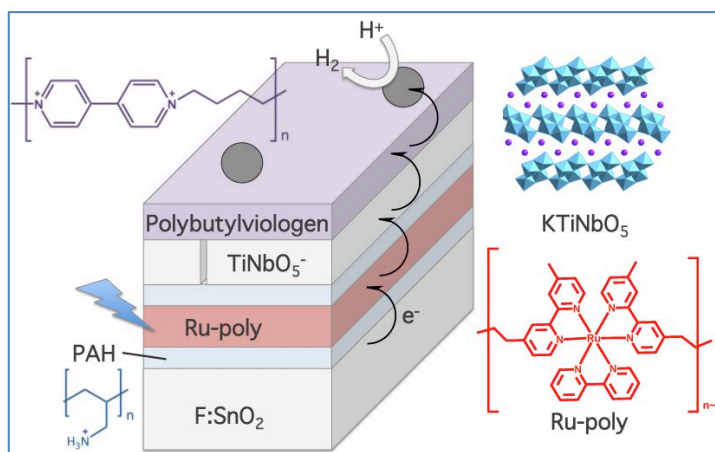


Transient photovoltage, photocurrent measurements, and electrochemical impedance spectroscopy reveal the importance of electron traps in  $\text{TiO}_2$ , and their stabilization by proton intercalation, in the kinetics of the dye sensitized photoanode. As shown schematically at the left, photoinjected electrons reach the photoanode back contact by diffusion through electron traps below the valence band edge. Protonation of these traps increases the probability of back electron transfer to the dye. Thus, the water

splitting cell has dramatically lower photocurrent when the dye is adsorbed from acidic aqueous electrolytes, despite the fact that lateral hole transport is faster under these conditions. Protonation of trap states also contributes to the long-term degradation of the photocurrent.

Lateral hole diffusion along the surface of  $\text{TiO}_2$  (i.e., electron self-exchange between neighboring oxidized and reduced sensitizer molecules) is a key step in photochemical water oxidation. This process competes with back electron transfer and also with scavenging of photoinjected electrons by  $\text{IrO}_2$  nanoparticles at the  $\text{TiO}_2$  surface. A kinetic model incorporating these terms accurately fits the experimental photocurrent-time behavior and shows that electron trapping is responsible for the polarization of the photoanode. These results suggest ideas for re-designing the photoanode for higher efficiency. We are currently experimenting with strategies to block the electron scavenging pathway and increase the density of sensitizer molecules for more rapid hole diffusion. Kinetic modeling also suggests that high aspect ratio  $\text{TiO}_2$  electrodes, which have not conferred much advantage to conventional DSSCs because of rapid sensitizer regeneration by  $\text{I}^-$ , could significantly improve the efficiency of the water-splitting photoanode. Towards this end we have developed some new hydrothermal methods for making “bed of nails” rutile and anatase nanowire array electrodes.

We are also exploring photoredox assemblies for hydrogen evolution using lamellar assemblies of rectifying oxide nanosheets, such as  $\text{HTiNbO}_5$ , with cationic polyelectrolytes and donor and acceptor molecules. Together with the photoanodes described above these photocathodes could make a tandem molecular cell for overall water-splitting. Transient absorbance spectra collected in attenuated total reflectance (ATR) geometry indicate a charge transfer cascade from the sensitizer



through the oxide nanosheet to the polyviologen acceptor. The excited state triplet lifetime of metalloporphyrin sensitizers is quite sensitive to the polyelectrolyte matrix, which complicates analysis of the transient data. We are currently investigating polymeric ruthenium(polypyridyl) sensitizers as alternatives. An efficient electron transfer cascade requires the conduction band edge potential of the oxide layer to be intermediate between the donor and acceptor redox levels. The pH dependence of the band edge potentials in 2-D oxides has not yet been measured and has direct implications on the kinetics of charge transfer. We have measured the pH dependence by combining spectroelectrochemical and luminescence quenching measurements. Initial results indicate that the band shift ca.  $-60 \text{ mV/pH}$  as is typically observed with bulk transition metal oxide semiconductors.

The operation of water splitting cells near neutral pH raises the question of whether buffer/membrane combinations can be found to complete the circuit without adding fatal polarization, resistance, and crossover losses. We measured the polarization and resistance of anion- and cation-exchange membranes and found that substantial pH gradients develop because of electromigration of buffer anions. Recently, we have studied this effect using bipolar anion/cation exchange membranes. In reverse bias, bipolar membranes do not develop a pH gradient but they require a driving voltage of several hundred mV at current densities in the range of  $10 \text{ mA/cm}^2$ .

## DOE Sponsored Publications 2011-2014

1. N. I. Kovtyukhova and T. E. Mallouk, "Conductive indium-tin oxide nanowire and nanotube arrays made by electrochemically assisted deposition in template membranes: switching between wire and tube growth modes by surface chemical modification of the template," *Nanoscale* 3, 1541-1552 (2011).
2. Y. Zhao, E. A. Hernandez-Pagan, N. M. Vargas, J. L. Dysart, and T. E. Mallouk, "A High Yield Synthesis of Ligand-Free Iridium Oxide Nanoparticles with High Electrocatalytic Activity," *J. Phys. Chem. Lett.*, 2, 402-406 (2011).
3. E. A. Hernandez-Pagan, W. Wang, and T. E. Mallouk, "Template Electrodeposition of Single-Phase p- and n-Type Copper Indium Diselenide (CuInSe<sub>2</sub>) Nanowire Arrays," *ACS Nano* 5, 3237-3241 (2011).
4. B. D. Sherman, S. Pillai, G. Kodis, J. Bergkamp, T. E. Mallouk, D. Gust, T. A. Moore, and A. L. Moore, "A porphyrin-stabilized water oxidation catalyst," *Can. J. Chem.* 89, 152-157 (2011).
5. Y. Zhao, N. M. Vargas-Barbosa, E. A. Hernandez-Pagan, and T. E. Mallouk, "Anodic Deposition of Colloidal Iridium Oxide Thin Films from Hexahydroxyiridate(IV) Solutions," *Small*, 7, 2087-2093 (2011).
6. S.-H. A. Lee, Y. Zhao, E. A. Hernandez-Pagan, L. Blasdel, W. J. Youngblood, and T. E. Mallouk, "Electron transfer kinetics in water splitting dye-sensitized solar cells based on core-shell oxide electrodes," *Faraday Discussions*, 155, 165-176 (2011).
7. Y. Zhao, J. R. Swierk, J. D. Megiatto, Jr., B. Sherman, W. J. Youngblood, D. D. Qin, D. M. Lentz, A. L. Moore, T. A. Moore, D. Gust, and T. E. Mallouk, "Improving the efficiency of water splitting in dye-sensitized solar cells by using a biomimetic electron transfer mediator," *PNAS*, 109, 15612-15616 (2012).
8. E. A. Hernandez-Pagan, N. M. Vargas-Barbosa, T.-H. Wang, Y. Zhao, E. S. Smotkin, and T. E. Mallouk, "Resistance and polarization losses in aqueous buffer-membrane electrolytes for water-splitting photoelectrochemical cells," *Energy Environ. Sci.*, 5, 7582-7589 (2012).
9. J. R. Swierk and T. E. Mallouk, "Design and development of photoanodes for water-splitting dye-sensitized photoelectrochemical cells," *Chem. Soc. Rev.*, 42, 2357-87 (2013).
10. T. E. Mallouk, "Water electrolysis: divide and conquer," *Nature Chem.*, 5, 362-363 (2013).
11. A. S. Hall, A. Kondo, K. Maeda, and T. E. Mallouk, "Microporous brookite-phase titania made by replication of a metal-organic framework" *J. Am. Chem. Soc.*, 135, 16276-16279 (2013).
12. A. R. Hess, G. D. Barber, C. Chen, T. E. Mallouk, and H. R. Allcock, "Organophosphates as solvents for electrolytes in electrochemical devices," *ACS Adv. Mater. Interf.*, 5, 13029-13034 (2013).
13. D.-D. Qin, Y. Bi, X. Feng, W. Wang, G. D. Barber, T. Wang, Y. Song, and T. E. Mallouk, "Highly oriented, crystalline anatase TiO<sub>2</sub> nanorods grown on transparent conducting substrates for efficient photoelectrochemical oxidation of water," submitted to *Angew. Chem. Int. Ed.*

14. J. R. Swierk, N. S. McCool, T. P. Saunders, G. D. Barber, M. E. Strayer, N. M. Vargas-Barbosa, and T. E. Mallouk, "Photovoltage effects of sintered IrO<sub>2</sub> nanoparticle catalysts in water-splitting dye-sensitized photoelectrochemical cells," *J. Phys. Chem. C.*, in press.
15. J. R. Swierk, N. S. McCool, T. P. Saunders, and T. E. Mallouk, "Effects of electron trapping and protonation on the efficiency of water-splitting dye-sensitized solar cells," submitted to *J. Am. Chem. Soc.*

*Session V*

*Nanostructured Subsystems*



## Nanotechnological and Biological Systems for Light-Driven Hydrogen Evolution

Kara L. Bren, Richard Eisenberg, Todd D. Krauss

Department of Chemistry

University of Rochester

Rochester, NY and 14627-0216

The conversion of solar energy into chemically stored energy is a crucial component of the effort to develop solar energy resources in the U.S. This project focuses on developing systems for light-driven production of the clean energy carrier hydrogen ( $H_2$ ) from water. Our multidisciplinary project employs synthetic chemistry, nanotechnology, and biochemistry to engineer novel catalysts for aqueous proton reduction and robust photosensitizers for these catalysts. By drawing on expertise in multiple fields, we take advantage of the particular benefits offered by each.

During the current grant period, efforts to discover new molecular catalysts for  $H_2$  formation proved successful. Several specific classes of complexes were examined including bis-dithiolene complexes of Co and Ni and related derivatives. These complexes possess redox-active ligands that appear valuable for assembling two protons and two electrons into  $H_2$  at the catalyst center. Another series of active catalysts discovered in 2011 and examined in the past year were Ni pyridylthiolate and pyrimidinethiolate complexes that function by proton transfer through an unchelated ligand donor to a metal-bound hydride ligand for heterocoupling to form  $H_2$ , as has been proposed in different [Fe,Fe] and [Fe,Ni] hydrogenases. Based on experimental data and a computational study, a similar heterocoupling mechanism of a metal-bound hydride combining with a ligand-bound proton also exists for Co bis(dithiolene) complexes exemplified by  $Co(bdt)_2^-$  (bdt = benzene-1,2-dithiolate).

A major leap forward in the light-driven generation of  $H_2$  from aqueous protons was taken with the construction of a system in which the light absorber or photosensitizer consists of water-solubilized CdSe quantum dots or nanocrystals and the catalyst is an in situ formed Ni complex. Both activity and robustness are impressive with turnover numbers (TONs) approaching  $10^6$ , activity maintained over 15 days, and a quantum yield for  $H_2$  of 36% with 520-nm light. The water solubilizing agent dihydrolipoic acid (DHLA) was also found to dissociate from the QD surface to a minor but significant extent so that a Ni(DHLA) complex capable of catalyzing the  $H_2$ -forming reaction is generated. Synthesis of new water-solubilizing  $S_3$ -capping agents with a tridentate architecture that proved inert to dissociation from the QD surface was performed. In this manner, sets of different catalysts have been assessed in terms of activity. Efforts are now in progress to eliminate the need for ascorbic acid or another chemical sources of electrons and use instead electrochemically supplied electrons at a potential insufficient for  $H_2$  production without light. The photocathode in these photoelectrochemical cells, which in ongoing work has yielded positive results, is based on  $S_3$ -capped CdSe QDs attached to NiO on a conductive substrate.

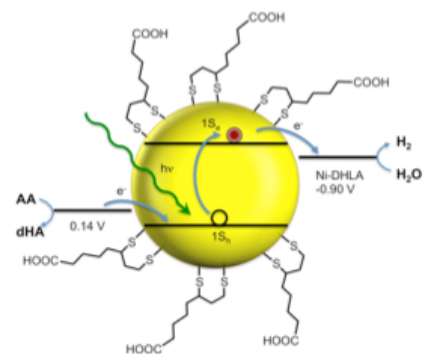


**Figure 1.** CdSe-Ni system for photocatalytic  $H_2$  generation

Nature provides highly efficient catalysts and light-harvesting systems for the conversion of solar energy into chemical energy that offer the significant advantage of functioning in an aqueous environment under mild conditions. Protein-based assemblies provide complex scaffolds that encapsulate and protect active sites, provide second-sphere interactions such as hydrogen bonding that enhance efficiency, and control substrate (proton and water) access to the active site through the arrangement of water channels. We are engineering artificial hydrogenases through new biosynthetic routes to porphyrin-peptide assemblies and by engineering robust protein scaffolds. We recently reported electrocatalytic H<sub>2</sub> evolution by a water-soluble cobalt porphyrin peptide, CoMP11-Ac (Fig. 2, top), with a turnover number of over 20,000 at nearly quantitative Faradaic yield, at pH 7.0, in the presence of air. In initial photochemical studies, we have demonstrated that CoMP11-Ac can be activated by the photosensitizer [Ru(bpy)<sub>3</sub>]<sup>2+</sup> in the presence of a sacrificial electron donor to yield H<sub>2</sub> with a turnover number of 450. While these initial results are promising, the catalyst has disadvantages including requiring a high overpotential and showing degradation under electrocatalytic conditions. To produce a more robust catalyst, we prepared the axial ligand M61A mutant of thermostable *H. thermophilus* cytochrome *c*-552 and substituted the heme iron with cobalt. Co-M61A stays active at least 3 times longer than CoMP11-Ac to yield over 100,000 turnovers of H<sub>2</sub> per mole of Co-M61A. Furthermore, Co-M61A remains highly active in seawater, in which activity of CoMP11-Ac drops significantly. We are taking advantage of the fact that Co-M61A contains the cobalt porphyrin catalytic site within a protein scaffold in ongoing efforts to introduce a water channel to enhance activity and to engineer hydrogen bonding groups near the cobalt to lower overpotential.

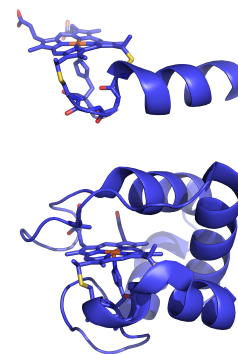


**Figure 2.** Top: CoMP11-Ac. Bottom: Co-HtM61A.

Many potential uses exist for a membrane that can simultaneously transport protons and electrons under aqueous conditions for development of solar fuel technologies, i.e., the generation of hydrogen gas by photocatalyzed water splitting during artificial photosynthesis. Among the many technical requirements of such a system as presently conceived is a membrane capable of transporting both photogenerated electrons and the ionic components of the desired chemical fuel, i.e. protons. We have synthesized freestanding, vertically aligned carbon nanotube (VANT) membranes, characterized their electron conductivity and proton transport properties, and demonstrated their successful use in an integrated system with colloidal CdSe quantum dots to generate photocurrents. By synthesizing long NTs in a vertically aligned array, their excellent electron transport properties can direct electrons over micron distances in a macroscopically directional manner. Vertical alignment also facilitates proton transport over long distances through the bore. Although the bulk electronic and proton transport properties of VANT membranes have been previously explored in separate applications, it is extremely rare to have them both integrated into the same system. Furthermore the membranes described here provide for and allow the demonstration of the attachment of photoreceptive systems that make it particularly compelling in solar energy applications.

## DOE Sponsored Publications 2011-2014

1. The Impact of Ligand Exchange in Hydrogen Production from Cobaloxime-Fluorescein Photocatalytic Assemblies, McCormick, T. M.; Han, Z.; Weinberg, D. J.; Holland, P. L.; Eisenberg, R., *Inorg. Chem.* **2011**, *50*, 10660-10666.
2. A Cobalt-Dithiolene Complex for the Photocatalytic and Electrocatalytic Reduction of Protons, McNamara, W. R.; Han, Z.; Alperin, P. J.; Brennessel, W. W.; Holland, P. L.; Eisenberg, R., *J. Am. Chem. Soc.* **2011**, *133*, 15368-15371.
3. Cytochrome *c* Heme Lyase Can Mature a Fusion Peptide Composed of the Amino-terminal Residues of Horse Cytochrome *c*, Asher, W. B.; Bren, K. L. *Chem. Comm.* **2012**, *48*, 8344-8346.
4. A Nickel Thiolate Catalyst for the Long-Lived Photocatalytic Production of Hydrogen in a Noble-Metal-Free System, Han, Z.; McNamara, W. R.; Eum, M.-S.; Holland, P. L.; Eisenberg, R., *Angew. Chem. Int. Ed.* **2012**, *51*, 1667-1670.
5. Catalysts Made of Earth-Abundant Elements (Co, Ni, Fe) for Water Splitting: Recent Progress and Future Challenges, Du, P.; Eisenberg, R., *Energy Environ. Sci.* **2012**, *5*, 6012-6021.
6. Cobalt-Dithiolene Complexes for the Photocatalytic and Electrocatalytic Reduction of Protons in Aqueous Solutions, McNamara, W. R.; Han, Z.; Yin, C.-J.; Brennessel, W. W.; Holland, P. L.; Eisenberg, R., *Proc. Nat. Acad. Sci.* **2012**, *109*, 15594-15599.
7. Molecular Systems for Light Driven Hydrogen Production, Eckenhoff, W. T.; Eisenberg, R., *Dalton Trans.* **2012**, *41*, 13004-13021.
8. Robust Photogeneration of H<sub>2</sub> in Water Using Semiconductor Nanocrystals and a Nickel Catalyst, Han, Z.; Qiu, F.; Eisenberg, R.; Holland, P. L.; Krauss, T. D. *Science* **2012**, 1321-1324.
9. Cobalt Complexes as Artificial Hydrogenases for the Reductive Side of Water Splitting, Eckenhoff, W. T.; McNamara, W. R.; Du, P.; Eisenberg, R., *Biochimica Biophysica Acta - Bioenergetics*, **2013**, *1827*, 958-973.
10. Nickel Pyridylthiolate Complexes for the Photocatalytic Production of Hydrogen from Aqueous Solutions in Noble-Metal-Free Systems, Han, Z.; Shen, L.; Holland, P. L.; Brennessel, W. W.; Holland, P. L.; Eisenberg, R. *J. Am. Chem. Soc.* **2013**, *135*, 14659-14669.
11. Photogeneration of Hydrogen from Water Using CdSe Nanocrystals: The Importance of Surface Exchange, Das, A.; Han, Z.; Haghghi, M. G.; Eisenberg, R., *Proc. Nat. Acad. Sci.*, **2013**, *110*, 16716-16723.
12. Hydrogen Evolution from Neutral Water Under Aerobic Conditions Catalyzed by Cobalt Microperoxidase-11, Kleingardner, J. G.; Kandemir, B.; Bren, K. L. *J. Am. Chem. Soc.* **2014**, *136*, 4-7.
13. Electron Conductive and Proton Permeable Vertically Aligned Carbon Nanotube Membranes, Pilgrim, G. A.; Leadbetter, J. W.; Qiu, F.; Siitonen, A. J.; Pilgrim, S. M.; Krauss, T. D. *Nano Lett.* **2014**, ASAP; DOI: 10.1021/nl403696y
14. Fuel from Water: The Photochemical Generation of Hydrogen from Water, Han, Z.; Eisenberg, R. *Accounts Chem. Res.*, **2014**, submitted.

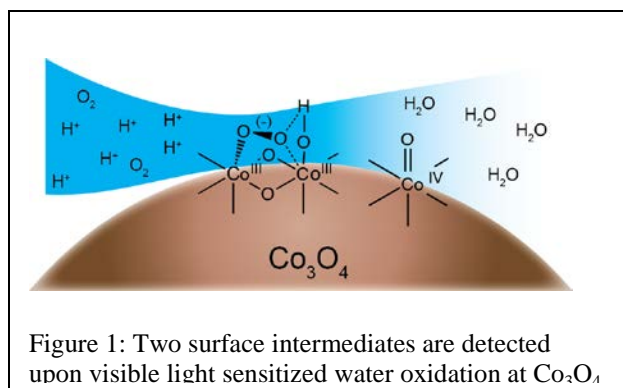
## Inorganic Assemblies for Closing the Photosynthetic Cycle on the Nanoscale

Heinz Frei

Physical Biosciences Division  
Lawrence Berkeley National Laboratory  
Berkeley, CA 94720

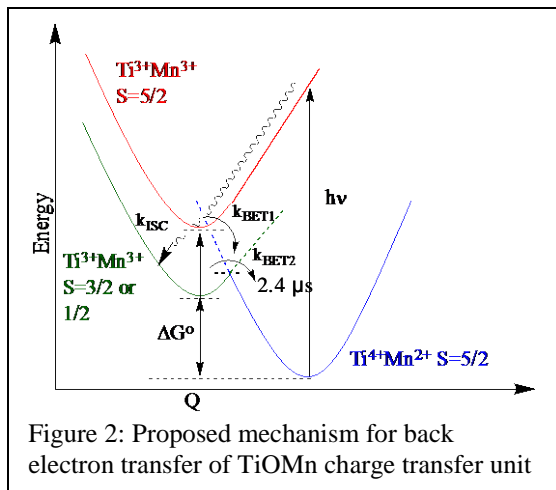
The long term goal of our research is the direct conversion of carbon dioxide and water with visible light to a liquid fuel on the nanoscale under product separation. We are developing a robust assembly featuring all-inorganic heterobinuclear light absorbers and metal oxide catalysts for water oxidation. The latter are used in the form of a nanotube surrounded by a nanometer thin silica shell that functions as proton transmitting, gas impermeable membrane for separating the water oxidation catalysis from the light absorber and the carbon dioxide reduction chemistry. Efficiency improvements are guided by insights from monitoring of the processes of the various components by dynamic optical and vibrational spectroscopy, both isolated and when coupled in subsystems, and from TEAM imaging.

*Mechanism of water oxidation at  $\text{Co}_3\text{O}_4$  nanoparticle surfaces:* Using time-resolved FT-IR spectroscopy in the ATR configuration, intermediates of visible light sensitized water oxidation at the liquid-solid interface of  $\text{Co}_3\text{O}_4$  nanocrystals were identified and the catalytic role established on the basis of the temporal behavior. Following a 300 ms visible light excitation pulse for injecting holes from the sensitizer  $[(\text{Ru}(\text{bpy})_3)^{3+}]$  into the catalyst particles, a surface superoxide at  $1013\text{ cm}^{-1}$  interacting with two Co centers was detected and its structure established by  $^{18}\text{O}$  isotope shifts (Figure 1). Mass



spectrometric analysis of the evolving  $\text{O}_2$  gas showed the same  $^{18}\text{O}$  isotopic composition as the superoxide species, which confirmed the kinetic relevancy of this 3-electron transfer intermediate. At the same time, a band observed at  $840\text{ cm}^{-1}$  is attributed to an oxo  $\text{Co}(\text{IV})$  site (one electron oxidation intermediate). The spontaneous decay of the  $\text{Co}(\text{IV})=\text{O}$  species ( $t_{1/2}=0.99\text{ s}$ ) assigned to  $\text{OO}$  bond formation by nucleophilic attack of  $\text{H}_2\text{O}$  is much slower than the rise of the superoxide intermediate, which grows mainly during the 300 ms light pulse. Therefore, the two intermediates belong to different catalytic sites exhibiting substantially different rates, with the fast site exhibiting a turnover frequency of  $\geq 3\text{ s}^{-1}$ . The structure for the fast site is proposed to consist of two adjacent (di- $\mu$ -oxo bridged) octahedral  $\text{Co}^{\text{III}}\text{-OH}$  groups, while the slow site is attributed to a  $\text{Co}^{\text{III}}\text{-OH}$  group that is not coupled to another  $\text{Co}^{\text{III}}\text{-OH}$  group. This is the first observation of surface intermediates of an Earth abundant metal oxide catalyst for water oxidation under reaction conditions.

*Origin of the long lifetime of all inorganic heterobinuclear light absorbers:* For the precise tuning of the optical and redox properties of light absorbers, we have developed oxo-bridged heterobinuclear light absorbing units covalently anchored on a silica surface. A dozen different units utilizing mostly first and second row transition metal centers such as  $\text{TiOMn}^{2+}$  have been synthesized and characterized in the past few years. The units are anchored on the pore surfaces of mesoporous silica, or on the convex surface of silica nanoparticles. They possess a visible light absorbing metal-to-metal charge transfer transition (MMCT, e.g.  $\text{Ti}^{4+}\text{OMn}^{2+} \rightarrow \text{Ti}^{3+}\text{OMn}^{3+}$ ) suitable for driving a multi-electron catalyst for water oxidation coupled to the donor center, or  $\text{CO}_2$  reduction at the acceptor metal if it is a Zr center. Transient absorption spectroscopy of the  $\text{TiOMn}$  unit on silica nanoparticles, which provided



optically transparent (non-scattering) wafers allowed us to detect the Ti and Mn ligand field transitions upon visible light excitation of the MMCT transition. The temperature dependence of the excited MMCT lifetime of  $2.43 \pm 0.20 \mu\text{s}$  at 295 K in vacuum revealed a moderate activation energy and a small pre-exponential factor, indicating that the slow back electron transfer kinetics are due to weak coupling between the excited state and ground state potential energy surfaces (electronic coupling constant of less than  $1 \text{ cm}^{-1}$ ). Comparison with the large optical coupling constant ( $4200 \text{ cm}^{-1}$  by Hush analysis) indicates ultrafast spin flip following initial MMCT excitation, resulting in slow, spin forbidden transition back to the high spin  $\text{Ti}^{4+}\text{O}\text{Mn}^{2+}$  ground state (Figure 2).

*Light driven carbon dioxide reduction by water at ZrOCo unit coupled to IrO<sub>2</sub> nanocluster catalyst:* We have demonstrated the closing of the photosynthetic cycle of CO<sub>2</sub> reduction by H<sub>2</sub>O upon photoexcitation of the MMCT transition of a ZrOCo<sup>2+</sup> unit coupled to an Ir oxide nanocluster (2 nm) for water oxidation. The hierarchical structure of the assembly was achieved by positioning the IrO<sub>x</sub> cluster adjacent to the Co donor center by MMCT-driven photodeposition of an Ir precursor. Evolution of CO and O<sub>2</sub> was detected by FT-IR and mass spectroscopy. Photo products were only observed in the presence of H<sub>2</sub>O and when preparing Ir oxide catalyst particles by the spatially directing photodeposition step.

*Co<sub>3</sub>O<sub>4</sub>-SiO<sub>2</sub> core shell nanoparticles and nanotubes for closing the photosynthetic cycle under product separation:* The geometry of our assembly for closing the cycle of CO<sub>2</sub> reduction by H<sub>2</sub>O is a Co<sub>3</sub>O<sub>4</sub> nanotube that functions as an efficient water oxidation catalyst, surrounded by a few nanometer thick, dense SiO<sub>2</sub> shell acting as proton conducting, gas impermeable membrane. We have developed the materials chemistry for embedding molecular wires of type oligo(paraphenylenevinylene) (OPPV) into the silica shell for controlled hole transport from a visible light sensitizer on the outside, to the Co<sub>3</sub>O<sub>4</sub> catalyst core on the inside. The wire molecules are covalently attached in the Co oxide surface and cast into silica by a solvothermal method. Transient optical absorption spectroscopy revealed efficient hole injection into the embedded OPPV (3 aryl units) molecules followed by fast (microsecond or less) transfer to the Co oxide particle, demonstrating efficient and tightly controlled charge transport across the silica membrane. Electrochemical measurements using SiO<sub>2</sub>/Pt as working electrode allowed us to demonstrate and quantify proton transport through nanometer thin dense silica layers, which at the same time block crossover of O<sub>2</sub>. Plasma-enhanced ALD was used to prepare silica films of precise variable thickness on a Pt electrode. Proton transmission through the silica layer in aqueous solution was observed by the H<sup>+</sup> reduction wave (to yield PtH) during cathodic sweeps. For thicknesses greater than 3 nm, O<sub>2</sub> permeation was completely blocked, and an overvoltage increase of  $25 \text{ mV nm}^{-1}$  SiO<sub>2</sub> observed. Hence, the wire-embedded silica membrane affords transmission of protons at acceptable overpotentials.

*Future work:* We will explore photo driven CO<sub>2</sub> reduction by H<sub>2</sub>O at the Co<sub>3</sub>O<sub>4</sub>/SiO<sub>2</sub> core shell nanotubes with visible light, first using isolated nanotubes, then nanotube arrays. Effort will focus on the detailed understanding of charge flow across the silica membrane and initiation of catalytic transformation at the core, the coupling of two heterobinuclear units for implementing a 2-photon light absorber system, and the coupling of the reductive heterobinuclear unit with a multi electron transfer catalyst to achieve 4 or 6 electron reduction of CO<sub>2</sub>.

## DOE Sponsored Solar Photochemistry Publications 2011-2014

1. H.S. Soo, M.L. Macnaughtan, W.W. Weare, J. Yano, and H. Frei. EXAFS Spectroscopic Analysis of Heterobinuclear TiOMn Charge-Transfer Chromophore in Mesoporous Silica. *J. Phys. Chem. C* **115**, 24893-24905 (2011).
2. N. Sivasankar, W.W. Weare, and H. Frei. Direct Observation of a Hydroperoxide Surface Intermediate upon Visible Light Sensitized Water Oxidation at Ir Oxide Nanocluster Catalyst by Rapid-Scan FT-IR Spectroscopy. *J. Am. Chem. Soc.* **133**, 12976-12979 (2011).
3. H.S. Soo, A. Agiral, A. Bachmeier, and H. Frei. Visible Light-Induced Hole Injection into Rectifying Molecular Wires Anchored on Co<sub>3</sub>O<sub>4</sub> and SiO<sub>2</sub> Nanoparticles. *J. Am. Chem. Soc.* **134**, 17104-17116 (2012).
4. D. Behar, H. Frei, M. MacNaughtan, and J. Rabani. Determination of the Redox Potential of Immobilized Oxo-Bridged Metals in Porous Supports. The Ti-O-Mn SBA-15 System. *J. Phys. Chem. C* **116**, 23477-23484 (2012).
5. C.C. Yang, T.M. Eggenhuisen, M. Wolters, A. Agiral, H. Frei, P. E. de Jongh, K. P. de Jong, and G. Mul. Effects of Support, Particle Size, and Process Parameters on Co<sub>3</sub>O<sub>4</sub> Catalyzed H<sub>2</sub>O Oxidation Mediated by the [Ru(bpy)<sub>3</sub>]<sup>2+</sup> Persulfate System. *ChemCatChem* **5**, 550-556 (2013).
6. A. Agiral, H.S. Soo, and H. Frei. Visible Light Induced Hole Transport from Sensitizer to Co<sub>3</sub>O<sub>4</sub> Water Oxidation Catalyst across Nanoscale Silica Barrier with Embedded Molecular Wires. *Chem. Mater.* **25**, 2264-2273 (2013).
7. F. Jiao and H. Frei. Nanostructured Transition Metal Oxides Useful for Water Oxidation Catalysis. *U.S. Patent* No. 8,613,900 (2013).
8. M. Zhang, M. de Respinis, and H. Frei. Time Resolved Observation of Water Oxidation Intermediates on Cobalt Oxide Nanoparticle Catalyst in Aqueous Solution. *Nature Chem.* **6**, 362-367 (2014).
9. M.L. Macnaughtan, H.S. Soo, and H. Frei. Binuclear ZrOCo Metal-to-Metal Charge-Transfer Unit in Mesoporous Silica for Light-Driven CO<sub>2</sub> Reduction to CO and Formate. *J. Phys. Chem. C* **118** (2014) ASAP (DOI: 10.1021/jp5014994)
10. Kisielowski, C.; Helveg, S.; Yuan, G.; Frei, H. Atom Dynamics at the Gas-Catalyst Interface with Atomic Resolution. *Micron*, accepted.
11. B.A. McClure and H. Frei. Excited State Electron Transfer of All-Inorganic Heterobinuclear TiOMn<sup>2+</sup> Chromophore Anchored on Silica Nanoparticle Surface. *J. Phys. Chem. C.*, submitted
12. W.Y. Kim, G. Yuan, B.A. McClure, and H. Frei. Light-Driven Carbon Dioxide Reduction by Water at Binuclear ZrOCo<sup>2+</sup> Unit Coupled to Ir oxide Nanocluster Catalyst. *J. Am. Chem. Soc.*, submitted.
13. G. Yuan, B. A. McClure, W. Y. Kim, M. Zhang, and H. Frei. Inorganic Core-Shell Assemblies for Closing the Photosynthetic Cycle. *Faraday Disc.*, submitted.

# Solar Energy-Driven Multi-Electron-Transfer Catalysts for Water Splitting: Robust and Carbon-Free Nano-Triads

Craig L. Hill, Tianquan Lian, and Djamaladdin G. Musaev

Department of Chemistry  
Emory University  
Atlanta, Georgia 30322

Our integrated experimental-computational project aims to elucidate the success-limiting factors in realizing more efficient and stable visible-light-driven water splitting systems by targeting the synthetic, photophysical and photochemical properties of water oxidation dyads and triads using our carbon-free, stable, soluble and fast polyoxometalate (POM)-based water oxidation catalysts (WOCs). The specific technical achievements of the last year, but also the projected work of the next grant period are in the following areas:

**Reactivity and stability of POM-based water oxidation catalysts (WOCs).** Since our publication of the first POM WOCs, there have been scores of papers on this class of catalysts. Many groups have successfully used our first all-earth-abundant-element WOC,  $[\text{Co}_4(\text{H}_2\text{O})_2(\text{PW}_9\text{O}_{34})_2]^{10-}$  (**Co<sub>4</sub>P<sub>2</sub>**) (*Science*, **2010**; *JACS*, **2011**, etc) but Stracke and Finke (SF) implied that this POM was just a precursor of cobalt oxide which was the actual catalyst. However, theirs was a very different experiment under very different conditions. Three other research groups (Dau, Limberg and Galan-Mascaros) in 2013 and 2014 arrived at our original conclusion: **Co<sub>4</sub>P<sub>2</sub>** is the dominant WOC under homogeneous conditions. Ultimately so did SF (2014). However, a comprehensive study (pH, buffer, buffer concentration) of **Co<sub>4</sub>P<sub>2</sub>**, and by extension other POM WOCs of their speciation and reactivity was needed, so we just published such a study which includes new experiments, in addition to the 7 in the original *Science* paper, for distinguishing catalysis by POMs vs. catalysis by metal oxide. We have also developed several new POM WOCs, including one that is by far the fastest synthetic molecular WOC,  $[\text{Co}_4(\text{H}_2\text{O})_2(\text{VW}_9\text{O}_{34})_2]^{10-}$  (TOF > 1000 sec<sup>-1</sup>), and we are starting to investigate the mechanisms of water oxidation by the Co POMs as we did in 2009 and 2010 for the first POM WOC,  $[\text{Ru}_4(\mu\text{-O})_4(\mu\text{-OH})_2(\text{H}_2\text{O})_4(\gamma\text{-SiW}_{10}\text{O}_{36})_2]^{10-}$ .

**Charge Separation Dynamics in Covalently Linked Sensitizer-POM Dyads.**

Effective capture and conversion of visible light into chemical energy requires the combination of a photosensitizer, a charge separator and a catalyst. Here, nanoporous TiO<sub>2</sub> films were modified with the novel (5-crown-phen)<sub>2</sub>Ru(4,4'-(PO<sub>3</sub>H<sub>2</sub>)bpy)]<sup>2+</sup> where phen = 1,10-phenanthroline and bpy = 2,2'-bipyridine, and  $[\{\text{Ru}_4\text{O}_4(\text{OH})_2(\text{H}_2\text{O})_4\}\gamma\text{-SiW}_{10}\text{O}_{36}]^{10-}$  to create triadic photoanodes for water oxidation. Their photochemical water oxidation activity and long-term hydrolytic stability were compared for pH 5.8 NaSiF<sub>6</sub>/HCO<sub>3</sub><sup>-</sup> buffer and pH 7.2, 2,6-lutidine buffer. A Faradaic efficiency of 60% for photoelectrochemical water oxidation in pH 5.8 NaSiF<sub>6</sub>/HCO<sub>3</sub><sup>-</sup> buffer was obtained and confirmed through detection and quantification of O<sub>2</sub> by amperometry.

**Molecular Metal-to-Metal (MMCT) and Metal-to-Polyoxometalate (MPCT) Chromophores.** We have investigated the viability of transition-metal-substituted polyoxometalates (POMs) as molecular inorganic chromophores. Previous reports have documented extended visible light absorption due to MPCT, but the excited state lifetimes have been too short for viable electron-transfer applications. To better understand the photophysics of POM-based systems, we studied the electronic structure and excited state dynamics of a series of cobalt-containing Keggin POMs with the goal of establishing a relationship between the metal oxidation state, coordination environment and excited state lifetime. Our study found that  $[\text{Co}^{\text{II}}\text{W}_{12}\text{O}_{40}]^{6-}$ , containing a tetrahedrally-coordinated cobalt atom, has the longest lived charge

transfer excited state so far observed in a non-derivatized POM ( $\tau = 420$  ps in H<sub>2</sub>O;  $\tau = 1700$  ps in MeCN), tentatively assigned to a localized intermediate MPCT state. In contrast, [SiCo<sup>II</sup>(H<sub>2</sub>O)W<sub>12</sub>O<sub>40</sub>]<sup>6-</sup>, in which the cobalt atom is in a pseudo-octahedral position, exhibits a far shorter excited state lifetime ( $\tau = 1.3$  ps). The greatly extended excited state lifetime is ascribed to a structural change allowed by the more flexible central site of the POM and putative transient valence trapping of the excited electron in the tungsten framework. Additional studies on a series of transition-metal-substituted POMs, [Co<sup>II</sup>Z<sup>n+</sup>(H<sub>2</sub>O)W<sub>12</sub>O<sub>40</sub>]<sup>(10-n)-</sup> (Z = V<sup>4+</sup>, Cr<sup>3+</sup>, Mn<sup>2+</sup>, Fe<sup>3+</sup>, Co<sup>2+</sup>, Ni<sup>2+</sup>, Cu<sup>2+</sup>, and Zn<sup>2+</sup>) verify that the previously studied Co→W MPCT transition is still accessible. Transient absorption spectroscopy reveals that the excited state lifetimes of the new series are all shorter than [Co<sup>II</sup>W<sub>12</sub>O<sub>40</sub>]<sup>6-</sup>, likely due to additional non-radiative decay pathways and the presence of a labile aqua ligand. Our computational (TD-DFT and DFT) studies further address the nature of these transitions.

**Hydrophobic immobilization of POMs on electrodes.** We have developed new methods to immobilize POM WOCs on electrodes. One such method utilizes the hydrophobic alkylammonium salts of POM WOCs that are soluble in organic solvents but totally insoluble in water. These salts spontaneously immobilize themselves on a range of electrode surfaces, remarkably stabilize the POM to hydrolysis even at pH 13.6, and increase the photocurrent when immobilized on irradiated semiconductor electrodes, consistent with water oxidation activity.

**In search of new computational approaches to study interfacial electron transfer dynamics.**

To study exciton wavefunctions in quantum confinement it is absolutely necessary to include an effective mass  $m^*$  of electron (and hole) in the equation which is allowed to change depending on position. To bypass the shortcomings of the existing and widely used approaches, we have developed and extensively tested an alternative approach based on an infinite order (IO) DVR theory. The attractive features of (IO)DVR are: (1) calculations depend only on one parameter, the grid spacing  $\Delta x$ , which is related to the de Broglie wavelength ( $\lambda$ ) of the particle and can be determined naturally; (2) the matrix elements of the (IO)DVR Hamiltonian are remarkably simple and no integral evaluation is required; (3) the resulting (IO)DVR matrix is sparse, which is particularly important for very large calculations where the matrix can be easily evaluated on-the-fly in lieu of being stored in memory; and (4) an efficient grid contraction scheme from the infinite limit, defined only by the shape of the structure, also guarantees that the wavefunction has an analytic representation, which is crucial for evaluating overlaps with external electron or hole states (neighboring quantum dots, adsorbed ligand molecules, etc). We validated this new method for the previously reported experiments on a Type I CdSe/ZnS core/shell QD and functionalized anthraquinone (AQ) molecule. This new method can be used to treat electron transfer dynamics. In our ongoing work we consider numerical calculations of the electron transfer rate between exciton states of a QD and virtual molecular orbitals (MOs) of an electron acceptor using a hybrid approach. At present, we are working on numerical tests to treat non spherically-shaped QDs. In particular, we are interested in two-dimensional dots, or nanorods and nanowires, and the effect of electron-hole interaction in such systems.

### Publications (2011-2014)

1. Kaledin, A. L.; Lian, T.; Hill, C. L.; Musaev, D. G.; “An infinite order discrete variable representation of an effective mass Hamiltonian” *J. Comp. Theor. Chem.* **2014**, *in revision*.
2. Glass, E. N.; Fielden, J.; Kaledin, A. L.; Musaev, D. G.; Lian, T.; Hill, C. L. “Extending Metal-to-Polyoxometalate Charge Transfer Lifetimes: The Effect of Heterometal Location” *Chem.-A Eur. Journal*, **2014**, *20* (15), 4297-4307.
3. Zhao, C.; Glass, E. N.; Musaev, D. G.; Bacsa, J.; Zhu, G.; Hill, C. L. “Towards High Nuclear Tin(II) Polyoxometalate Frameworks: A Structural and Theoretical Investigation”, *J. Am. Chem. Soc.* **2014**, *in revision*
4. Sumliner, J. M.; Vickers, J. W.; Lv, H.; Geletii, Y. V.; Hill, C. L. “Polyoxometalate Water Oxidation

- Catalytic Systems” In “Molecular Water Oxidation Catalysts”, Chapter 11, Llobet, A. Ed.; Wiley: New York, 2014, in press.
5. Sumliner, J. M.; Lv, H.; Fielden, J.; Geletii, Y. V.; Hill, C. L. “Polyoxometalate multi-electron transfer catalytic systems for water splitting”, *Eur. J. Inorg. Chem.* **2014**, Published online 17 Jan 2014 (Invited review). 10.1002/ejic.201301573
  6. Kaledin, A. L.; Zhu, H.; Lian, T.; Hill, C. L.; Musaev, D. G. “A Study of electron transfer and recombination rates between Type I CdSe/ZnS quantum dots and anthraquinone”, *J. Phys. Chem. C*, **2014**, *submitted*
  7. Zhao, C.; Rodríguez-Córdoba, W.; Kaledin, A. L.; Yang, Y.; Geletii, Y. V.; Lian, T.; Musaev, D. G.; Hill, C. L. “An Inorganic Chromophore Based on a Molecular Oxide Supported Metal Carbonyl Cluster:  $[P_2W_{17}O_{61}\{Re(CO)_3\}_3\{ORb(H_2O)\}(\mu_3-OH)]^{9-}$ ”, *Inorg. Chem.* **2013**, *52* (23), 13490–13495
  8. Lv, H.; Rudd, J. A.; Zhuk, P. F.; Lee, J. Y.; Constable, E. C.; Housecroft, C. E.; Hill, C. L.; Musaev, D. G.; Geletii, Y. V. “Bis(4'-(4-pyridyl)-2,2':6',2"-terpyridine) ruthenium(II) complexes and their N-alkylated derivatives in catalytic light-driven water oxidation“ *RSC ADVANCES*, **2013**, *3* (43), 20647-20654
  9. Vickers, J. W.; Lv, H.; Sumliner, J. M.; Fielden, J.; Zhu, G.; Luo, Z.; Musaev, D. G.; Geletii, Y. V.; Hill, C. L. “Hydrolytic stability studies of  $[Co_4(H_2O)_2(\alpha-PW_9O_{34})_2]^{10-}$ . Additional evidence that transition-metal substituted polyoxometalates are molecular water oxidation catalysts.“ *J. Am. Chem. Soc.*, **2013**, *135* (38), 14110–14118
  10. Lv, H.; Song, J.; Zhu, H.; Geletii, Y. V.; Bacsa, J.; Zhao, C.; Lian, T.; Musaev, D. G.; Hill, C. L. “Visible-Light-Driven Hydrogen Evolution from Water Using a Noble-Metal-Free Polyoxometalate Catalyst“, *J. Catalysis*, **2013**, *307*, 48-54
  11. Zhao, C.; Kambara, C. S.; Yang, Y.; Kaledin, A. L.; Musaev, D. G.; Lian, T.; Hill, C. L. “Synthesis, Structures, and Photochemistry of Tricarbonyl Metal Polyoxoanion Complexes,  $[X_2W_{20}O_{70}\{M(CO)_3\}_2]^{12-}$  (X = Sb, Bi and M = Re, Mn)“, *Inorg. Chem.*, **2013**, *52*, 671–678
  12. Xiang, X.; Fielden, J.; Rodríguez-Córdoba, W.; Huang, Z.; Zhang, N.; Luo, Z.; Musaev, D. G.; Lian, T.; Hill, C. L. “Electron Transfer Dynamics in Semiconductor–Chromophore–Polyoxometalate Catalyst Photoanodes” *J. Phys. Chem. C*, **2013**, *117*, 918–926
  13. Matt, B.; Xiang, X.; Kaledin, A. L.; Han, N.; Moussa, J.; Amouri, H.; Alves, S.; Hill, C. L.; Lian, T.; Musaev, D. G.; Izzet, G.; Proust, A. “Long lived charge separation in iridium(III)-photosensitized polyoxometalates: synthesis, photophysical and computational studies of organometallic–redox tunable oxide assemblies”, *Chem. Sci.*, **2013**, *4*, 1737-1745
  14. Kaledin, Adri C. T. van Duin, Craig L. Hill, Djamaladdin G. Musaev, “Parameterization of Reactive Force Field: Dynamics of the  $[H_xNb_6O_{19}]^{(8-x)}$  Lindqvist Polyoxoanion in Bulk Water“, *J. Phys. Chem. A*, **2013**, *117*, 6967-6974
  15. Zhu, G.; Song, J.; Geletii, Y. V.; Zhao, C.; Hill, C. L. “Di- and Tri-Cobalt Silicotungstates: Synthesis, Characterization, and Stability Studies” *Inorg. Chem.*, **2013**, *52* (2), 1018–1024. DOI: 10.1021/ic302279m
  16. Anfuso, C. L.; Xiao, D.; Ricks, A. M.; Negre, C. F. A.; Batista, V. S.; Lian, T. Orientation of a Series of CO<sub>2</sub> Reduction Catalysts on Single Crystal TiO<sub>2</sub> Probed by Phase-Sensitive Vibrational Sum Frequency Generation Spectroscopy (PS-VSFG). *J. Phys. Chem. C* **2012**, *116*(45), 24107-24114
  17. Anfuso, C. L.; Ricks, A. M.; Rodriguez-Cordoba, W.; Lian, T. Ultrafast Vibrational Relaxation Dynamics of a Rhenium Bipyridyl CO<sub>2</sub>-Reduction Catalyst at a Au Electrode Surface Probed by

- Time-Resolved Vibrational Sum Frequency Generation Spectroscopy. *J. Phys. Chem. C* **2012**, *116*, 26377-26384
18. Wu, K.; Zhu, H.; Liu, Z.; Rodriguez-Cordoba, W.; Lian, T. Ultrafast Charge Separation and Long-Lived Charge Separated State in Photocatalytic CdS-Pt Nanorod Heterostructures. *J. Am. Chem. Soc.* **2012**, *134*, 10337-10340
  19. Kaledin, A. L.; Lian, T.; Hill, C. L.; Musaev, D. G. "Structural Modification of TiO<sub>2</sub> Surfaces in Bulk Water and Binding Motifs of a Functionalized C<sub>60</sub> on TiO<sub>2</sub> Anatase and Rutile Surfaces in Vacuo and in Water: Molecular Dynamics Studies", *J. Phys. Chem. C*, **2012**, *116*, 20937-20948
  20. Lv, H.; Geletii, Y. V.; Zhao, C.; Vickers, J. W.; Zhu, G.; Luo, Z.; Song, J.; Lian, T.; Musaev, D. G.; Hill, C. L. "Polyoxometalate water oxidation catalysts and the production of green fuel," *Chem. Soc. Rev.*, **2012**, *41*, 7572-7589
  21. Huang, Z.; Lin, Y.; Xiang, X.; Rodríguez-Córdoba, W.; McDonald, K. J.; Hagen, K. S.; Choi, K.-S.; Brunschwig, B. S.; Musaev, D. G.; Hill, C. L.; Wang, D.; Lian, T. "In situ probe of photocarrier dynamics in water-splitting hematite (alpha-Fe<sub>2</sub>O<sub>3</sub>) electrodes" *Energy & Environmental Science*, **2012**, *5*, 8923-8926
  22. Huang, Z.; Geletii, Y. V.; Musaev, D. G.; Hill, C. L.; Lian, L. "Spectroscopic Studies of Light-driven Water Oxidation Catalyzed by Polyoxometalates", *Industrial & Engineering Chemistry Research*, **2012**, *51*, 11850-11859
  23. Zhu, G.; Glass, E. N.; Zhao, C.; Lv, H.; Vickers, J. W.; Geletii, Y. V.; Musaev, D. G.; Hill, C. L. "A soluble and stable Ni-based water oxidation catalyst for solar fuel production", *Dalton Trans*, **2012**, *41*, 13043 - 13049
  24. Zhu, G.; Glass, E. N.; Zhao, C.; Geletii, Y. V.; Musaev, D. G.; Hill, C. L. "A Novel Dodecanuclear Zn<sup>II</sup> Cluster Sandwiched by Polyoxometalate Ligands", *Dalton Trans*, **2012**, *41*, 9908-9913
  25. Zhu, G.; Geletii, Y. V.; Koegerler, P.; Schilder, H.; Song, J.; Lense, S.; Zhao, C.; Hardcastle, K. I.; Musaev, D. G.; Hill, C. L. "Water oxidation catalyzed by a new tetracobalt-substituted polyoxometalate complex: [{Co<sub>4</sub>(μ-OH)(H<sub>2</sub>O)<sub>3</sub>}(Si<sub>2</sub>W<sub>19</sub>O<sub>70</sub>)]<sup>11-</sup>" *Dalton Trans*, **2012**, *41*, 2084-2090
  26. Zhao, C.; Huang, Z.; Rodríguez-Córdoba, W.; Kambara, C. S.; O'Halloran, K. P.; Hardcastle, K. I.; Musaev, D. G.; Lian, T.; Hill, C. L., "Synthesis and Characterization of a Metal-to-Polyoxometalate Charge Transfer Molecular Chromophore" *J. Am. Chem. Soc.* **2011**, *133*, 20134-20137
  27. Huang, Z.; Luo, Z.; Geletii, Y. V.; Vickers, J.; Yin, Q.; Wu, D.; Hou, Y.; Ding, Y.; Song, J.; Musaev, D. G.; Hill, C. L.; Lian, T., "Efficient Light-Driven Carbon-Free Cobalt-Based Molecular Catalyst for Water Oxidation" *J. Am. Chem. Soc.* **2011**, *133*, 2068-2071.
  28. Zhu, G.; Lv, H.; Vickers, J. W.; Geletii, Y. V.; Luo, Z.; Song, J.; Huang, Z.; Musaev, D. G.; Hill, C. L. In "Structural and mechanistic studies of tunable, stable, fast multi-cobalt water oxidation catalysts", *Proceedings of SPIE*, **2011**, 8109 (Solar Hydrogen and Nanotechnology VI), San Diego, CA., San Diego, CA., 2011; pp 81090A-81090A-6
  29. Anfuso, C. L.; Robert C. Snoeberger, I.; Ricks, A. M.; Liu, W.; Xiao, D.; Batista, V. S.; Lian, T., Covalent Attachment of a Rhenium Bipyridyl CO<sub>2</sub> Reduction Catalyst to Rutile TiO<sub>2</sub>. *J. Am. Chem. Soc.* **2011**, *133*, 6922-6925
  30. Huang, Z.; Geletii, Y. V.; Wu, D.; Anfuso, C. L.; Musaev, D. G.; Hill, C. L.; Lian, T. In Interfacial charge transfer dynamics in TiO<sub>2</sub>-Sensitizer-Ru<sub>4</sub>POM photocatalytic systems for water oxidation, *SPIE proceedings*, **2011**, 8109 (Solar Hydrogen and Nanotechnology VI), San Diego, CA., San Diego, CA., 2011; pp 810903-810903-10

*Session VI*

*Catalysis Fundamental Research*



## Mechanochemistry and Fuel-Forming Mechano-Electrocatalysis on Spring Electrodes

Drazenka Svedruzic, Suzanne Ferrere and Brian A. Gregg  
National Renewable Energy Laboratory  
15013 Denver West Pkwy., Golden, CO 80401

Mechanochemistry: causing or promoting chemical reactions by the application of mechanical force or, conversely, employing chemical energy to generate a mechanical force. Some of the best known examples are found in living systems: hearing, touch, muscle contraction, cell motility, etc. It is strongly suspected that mechanochemistry plays a role in the catalytic ability of some important redox enzymes (the entatic state hypothesis). Man-made catalysts, however, are almost always in or near their equilibrium structure because small molecules, metal clusters and such tend to relax to their structural ground state and there is no mechanism to leverage them into less energetically favorable, but possibly more useful, structures. Thus a large effort is devoted to synthesizing molecules, ligands and complexes with strained bonds in the search for improved catalytic ability. Also, growing strained lattices in semiconductor systems is a known method of adjusting their electronic properties. We are attempting to strain bonds dynamically.

If it is possible to physically deform a material—altering its bond lengths and angles—its electronic structure will adjust to the applied stress. We explore the hypothesis that a single material possesses a continuum of electronic and electrocatalytic properties that can be *reversibly* tuned over its elastic range. We focus on two types of experimental systems. One consists of mechanophores such as porphyrins or transition metal bipyridine complexes covalently bound

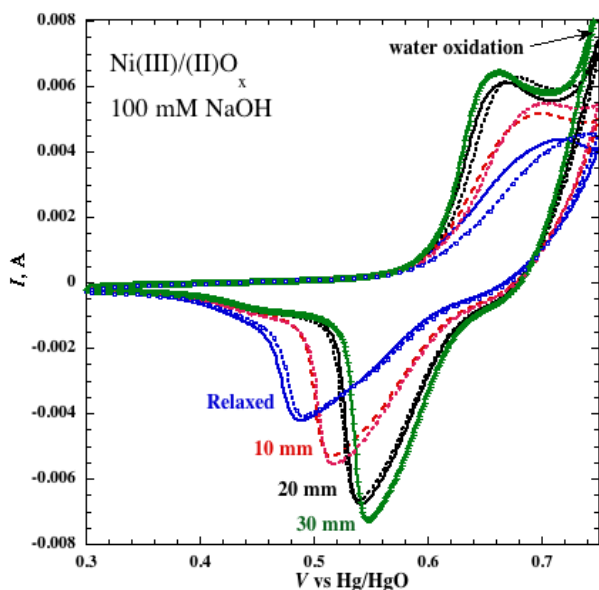


**Figure 1.** CVs vs strain of NiO<sub>x</sub>/Ni-plated stainless steel spring electrodes in 0.1 M NaOH. Solid lines during stretching, dashed lines relaxing. The spring's elastic limit  $E_{lim} = 36$  mm,  $v = 100$  mV/s.

through at least two bonds to an elastomeric polymer network. As the elastomer is stretched, force is applied to either buckle the porphyrin from its planar to its saddle-shaped form or to stretch the metal-bipyridine bond of the complex. In both cases we measure absorption and emission spectra as a function of strain. So far this approach has not been successful, probably because we can strain only a small fraction of the molecules before the films rupture. But the yield strengths of our mechanophore-elastomers are steadily increasing and we expect to soon have a photosystem in which we can measure the changes in optical properties with applied strain.

The other experimental system involves electrocatalytic fuel-forming reactions on stretchable electrodes. As an initial test system we employ stainless steel extension springs and nickel-plated springs as electrodes. Stretching the springs expands crystallite grain boundaries as well as the average interatomic spacing.

However, although stainless steel can be strained by ~20% and still return to its original shape, most of this is inelastic (or plastic) strain, only 1% or less is elastic strain. So stretching a spring to its reversible limit expands the interatomic spacing by only ~0.1%. Thus we are still near the bottom of the Morse-like interatomic potential curve and do not expect to observe substantial changes in catalytic behavior. We have not yet observed reversible changes in overpotential for the electrocatalytic processes. Presumably that would require substantially more than a ~0.1% change in atomic spacing. Nevertheless, this modest strain reversibly doubles the heterogeneous rate constant for electron transfer to a redox species in solution,  $\text{Ru}(\text{NH}_3)_6\text{Cl}_3$ , while the charge transfer rate through a surface film of Ni(II/III) oxy-hydroxide increases ~4 fold (Figure 1). This latter process is usually written



Strained at 84% of its elastic limit, the hydrogen evolution current increases by ~50% on a stainless steel spring while the oxygen evolution current increases by ~300% (Figure 2). We have shown by stretching springs beyond their elastic limit that the observed changes are caused by the elastic strain, not the inelastic strain. Thus even the modest elastic strain that can be applied by stretching a spring leads to significant and reversible increases in the rates of: 1) electron transfer to a redox couple in solution, 2) charge transport through a surface film, and 3) electrocatalysis.

We have recently learned of a "superelastic" material, nitinol, consisting of Ni and Ti almost 1:1. This intermetallic complex (not alloy) can be elastically stretched 7% with almost no inelasticity. It is commonly employed in its superelastic state in eyeglass frames, structural supports, etc. and in its shape memory state in medical applications such as expandable stents. We are initiating studies of NiTi electrochemistry and electrocatalysis vs strain in preparation for studying thin catalytic films either electroplated on, or covalently bound to, its surface.

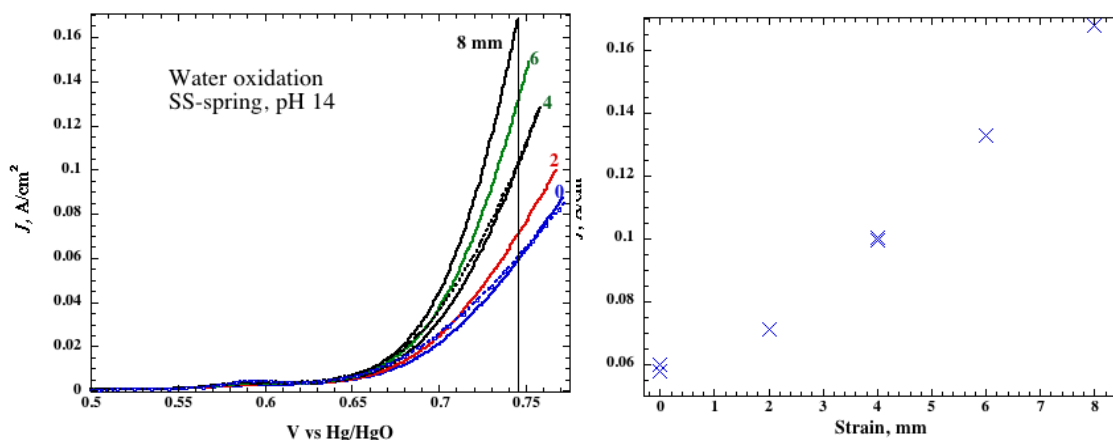


**Figure 2.** a) Oxygen evolution reaction at pH 14 on a 2-coil stainless steel spring as it is stretched to 84% of  $E_{\text{lim}}$  and relaxed again. Currents are corrected for  $2 \Omega$  solution resistance. b) OER current at 0.745 V vs strain.

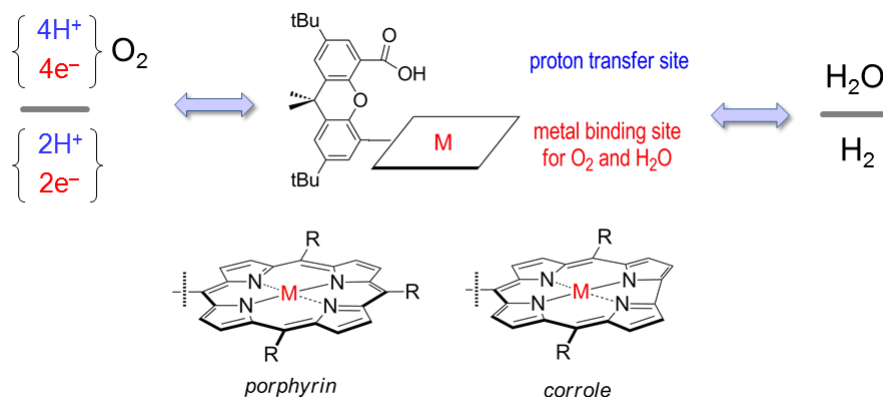
## DOE Sponsored Publications 2011-2014

1. Liang, Z., Cormier, R. A., Nardes, A. M. and Gregg, B. A., "Developing Perylene Diimide Based Acceptor Polymers for Organic Photovoltaics", *Synth. Met.* **2011**, *161*, 1014-1021.
2. Liang, Z., Reese, M. and Gregg, B. A., "Chemically Treating Poly(3-hexylthiophene) Defects to Improve Bulk Heterojunction Photovoltaics" *ACS Appl. Mater. Interfaces*, **2011**, *3*, 2042-2050.
3. Li, J. V., Nardes, A., Liang, Z., Shaheen, S. E., Gregg, B. A., Levi, D. H., "Simultaneous Measurement of Carrier Density and Mobility of Organic Semiconductors Using Capacitance Techniques", *Org. Electronics*, **2011**, *12*, 1879 - 1885.
4. Hains, A. W., Chen, H.-Y., Reilly, T. H., Gregg, B. A., "Crosslinked Perylene Diimide-Based n-Type Interfacial Layer for Inverted Organic Photovoltaic Devices", *ACS Appl. Mater. Interfaces*, **2011**, *3*, 4381 - 4387.
5. Gregg, B. A., "Entropy of Charge Separation in Organic Photovoltaic Cells: The Benefit of Higher Dimensionality", *J. Phys. Chem. Lett.*, **2011**, *2*, 3013 - 3015.
6. Reilly, T. H., Hains, A. W., Chen, H.-Y., Gregg, B. A., "A Self-Doping, Air-Stable, n-Type Interfacial Layer for Organic Electronics", *Adv. Energy Mater.* **2012**, *2*, 455-460.
7. Liang, Z., Nardes, A. M., von de Lagemaat, J., Gregg, B. A., "Activation Energy Spectra: Insights into Transport Limitations of Organic Semiconductors and Photovoltaic Cells", *Adv. Funct. Mater.* **2012**, *22*, 1087-1091
8. Liang, Z., Gregg, B. A., "Compensating Poly(3-hexylthiophene) Reveals Its Doping Density and Its Strong Exciton Quenching by Free Carriers", *Adv. Mater.* **2012**, *24*, 3258-3262.
9. Gregg, B. A., van de Lagemaat, J. "Folding Photons", *Nat. Photonics*, **2012**, *6*, 278-280.
10. Cormier, R. A., Gregg, B. A., "Bis-Dithiano Perylene Diimide: Synthesis and Characterization of a Novel Ring System", *RSC Advances*, **2014**, *4* (5), 2368-2373.
11. Kirner, J., Stracke, J., Gregg, B. A., Finke, R., "Visible-light assisted photoelectrochemical water oxidation by a phosphonate-functionalized perylene diimide plus a CoO<sub>x</sub> cocatalyst", *ACS Appl. Mater. Interfaces*, **2014**, in press.

## Hangman Catalysis for the Activation of Small Molecules

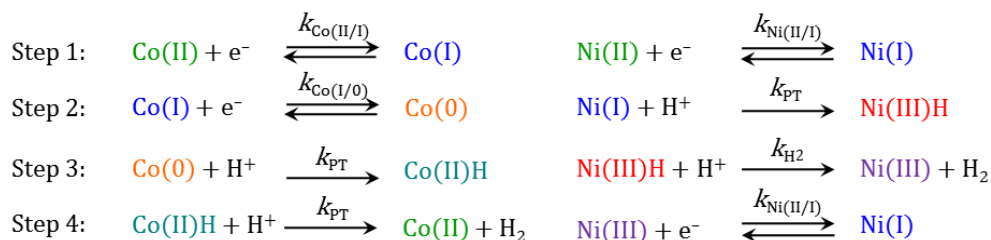
Dilek K. Dogutan, Daniel Graham, Manolis Roupelakis and Daniel G. Nocera  
 Department of Chemistry and Chemical Biology  
 Harvard University  
 Cambridge, MA 02138

The focus of this DOE program is solar fuel catalysis – specifically the chemistry of the hydrogen evolution reaction (HER), oxygen evolution reaction (OER) and the oxygen reduction reaction (ORR). We have sought to define the proton-coupled electron transfer (PCET) chemistry of these small molecule reactions by photochemical and electrochemical means. We have developed the Hangman approach in this program because the scaffold allows us to precisely control the delivery of a proton to a substrate bound at a redox active metal platform. In this construct, an acid-base functionality is poised over a redox active metal platform. These



“hangman” ligands utilize the acid-base functionality to form a secondary coordination sphere that can assist proton movement and facilitate substrate assembly and activation within the molecular cleft. Thus, the coupling of the proton and electron is ensured. An emphasis of our studies is to unify electrokinetic mechanistic rate models of the type developed by Saveant with photochemical kinetics models of the PCET reactions of hangman catalysts. To do so, we have embarked on electrochemical studies that afford us rate laws, which we can then utilize in the interpretation of photoinitiated processes.

Cobalt and nickel hangman porphyrins with a xanthen backbone and a carboxylic acid hanging group have been shown to promote HER. The hangman group is observed to facilitate HER by mediating a PCET pathway that leads to a hydridic  $Co(II)H$  and  $Ni(III)H$  species. These react with protons in an ensuing PT step, leading directly to  $H_2$  generation. The two mechanisms have been interrogated by electrokinetic analysis according to the following steps:

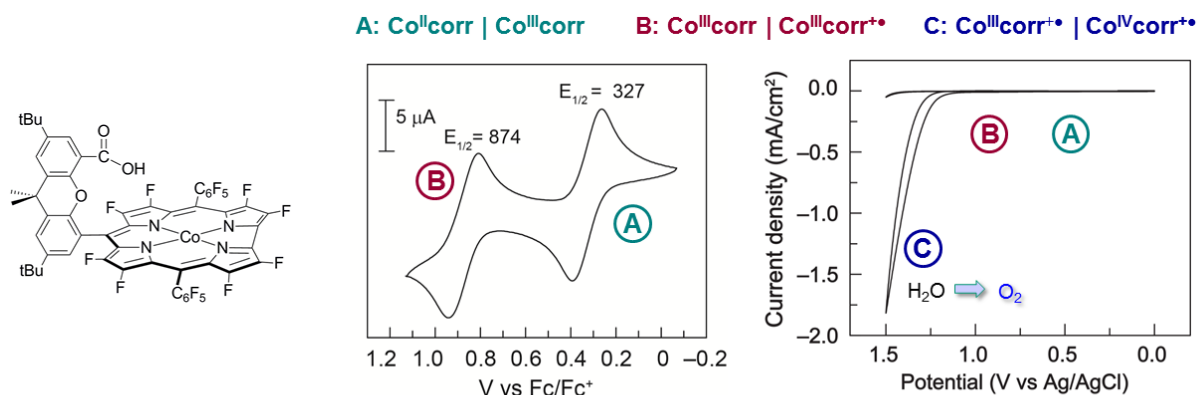


We have analyzed these mechanisms with “trumpet” plots derived from the following analytical expression for rate determining ET (left) and rate determining PT (right),

$$E_p = E^0 - 1.56 \frac{RT}{F} + 2 \frac{RT}{F} \ln \left( k_{Co(II/I)}^0 \sqrt{\frac{2RT}{FvD}} \right) \quad E_p = E^0 - 0.78 \frac{RT}{F} + \frac{RT}{2F} \ln \left( \frac{RT}{F} \frac{k_{PT}}{v} \right)$$

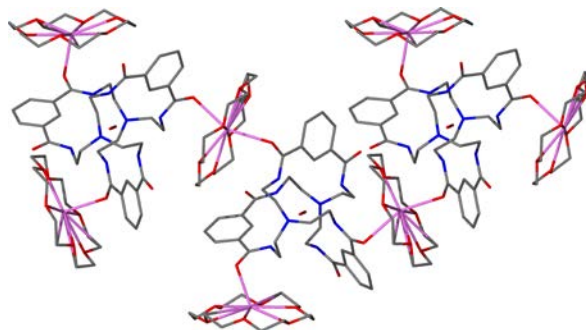
to assess quantitatively the hanging group effect. Importantly our results are general and can be used to assess the effect of proton relays in the second coordination sphere of a variety of HER catalysts.

On the OER front, the  $\beta$ -octafluorinated hangman metalloporphyrin deposited as Nafion supported film is an active OER catalyst. The four-electron four-proton catalytic production of oxygen from water in aqueous solution can be achieved at the single cobalt center of the hangman platform. Electrokinetic measurements show that the O–O bond formation occurs at the third hole of the PCET reaction. This finding is crucial to the design of a photocatalyst that will enable us to observe O–O bond formation in real time.



◆ PCET at 3<sup>rd</sup> hole equivalent key to H<sub>2</sub>O splitting

Finally, we have developed a completely new hangman platform based on the hexacarboxamide cryptand mBDCA–5t–H6. The ligand provides two cofacial trigonal platforms to present two metals or a metal and a hydrogen bonding second coordination sphere. Small molecules may be encapsulated in this cleft, including O<sub>2</sub> and CO<sub>2</sub>. This new ligand platform provides a method to study the basic redox properties of these molecules in an isolated environment, with significant implication to technologies including reversible metal-air batteries. These results will be presented, including a model that unifies Butler-Volmer and Marcus kinetics for ORR.



A view of crystal structure of [K(18-crown-6)]<sub>2</sub>[(O<sub>2</sub>)c-mBDCA-5t-H6] depicting the 1D coordination polymer formed in the solid state. Solvents of crystallization, t-butyl groups, and H atoms are omitted for clarity. C: gray, N: blue, O: red, K: pink.

## DOE Sponsored Publications 2011-2014

1. “Hangman Corroles: Efficient Synthesis and Oxygen Reaction Chemistry”; Dilek K. Dogutan, Sebastian A. Stoian, Robert McGuire Jr., Matthias Schwalbe, Thomas S. Teets and Daniel G. Nocera, *J. Am. Chem. Soc.* **2011**, *133*, 131–40.
2. “Xanthene–Modified and Hangman Iron Corroles”; Matthias Schwalbe, Dilek K. Dogutan, Sebastian A. Stoian, Thomas S. Teets, and Daniel G. Nocera, *Inorg. Chem.* **2011**, *50*, 1368–77.
3. “Electrocatalytic Water Oxidation by Cobalt(III) Hangman  $\beta$ -Octafluoro Corroles”; Dilek K. Dogutan, Robert McGuire Jr. and Daniel G. Nocera, *J. Am. Chem. Soc.* **2011**, *133*, 9178–80.
4. “Hydrogen Generation by Hangman Metalloporphyrins”; Chang Hoon Lee, Dilek K. Dogutan and Daniel G. Nocera, *J. Am. Chem. Soc.* **2011**, *133*, 8775–7.
5. “Porphyrin and Corrole Platforms for Water Oxidation, Oxygen Reduction and Peroxide Dismutation”; Christopher M. Lemon, Dilek K. Dogutan and Daniel G. Nocera, In *Handbook of Porphyrin Chemistry*; Kadish, K. M., Smith, K. M., Guilard, R., Eds; Academic Press: Amsterdam, **2012**, Vol. 21, Ch. 99, pp 144.
6. “Proton–Coupled Electron Transfer Kinetics for the Hydrogen Evolution Reaction of Hangman Porphyrins”; Manolis M. Roubelakis, D. Kwabena Bediako, Dilek K. Dogutan and Daniel G. Nocera, *Energy Environ. Sci.* **2012**, *5*, 7737–40.
7. “Hangman Effect on Hydrogen Peroxide Dismutation by Fe(III) Corroles”; Daniel J. Graham, Dilek K. Dogutan and Daniel G. Nocera, *Chem. Commun.* **2012**, *48*, 4175–7.
8. “Terpyridine–Porphyrin Hetero-Pacman Compounds”; Matthias Schwalbe, Ramona Metzinger, Thomas S. Teets and Daniel G. Nocera, *Chem. Eur. J.* **2012**, *48*, 15449–58..
9. “The Nature of Lithium-Battery Materials Under Oxygen Evolution Reaction Conditions”; Seung Woo Lee, Christopher Carlton, Marcel Risch, Yogesh Surendranath, Shuo Chen, Sho Furutsuki, Atsuo Yamada, Daniel G. Nocera and Yang Shao–Horn, *J. Am. Chem. Soc.* **2012**, *134*, 16959–62.
10. “Pacman and Hangman Cobalt Tetraazamacrocycles”; Chang Hoon Lee, Dino Villagrán, Timothy R. Cook, Jonas C. Peters and Daniel G. Nocera, *ChemSusChem* **2013**, *6*, 1541–4.
11. “Post-synthetic Modification of Hangman Porphyrins on the Gram Scale.” Daniel J. Graham, Shao-Liang Zheng and Daniel G. Nocera, *ChemSusChem* **2014**, submitted for publication.
12. “Electrocatalytic H<sub>2</sub> Evolution through Proton Gating by Hangman Iron Porphyrins.” Daniel J. Graham and Daniel G. Nocera, *Organometallics* **2014**, accepted for publication.
13. “Electron Transfer Studies of Peroxide Dianion.” Andrew M. Ullman, Xianru Sun, Daniel J. Graham, Nazario Lopez, Matthew Nava, Rebecca De Las Cuevas, Peter Müller, Elena V. Rybak-Akimova, Christopher C. Cummins and Daniel G. Nocera, *Inorg Chem.* **2014**, ASAP: April 28, 2014, DOI: 10.1021/ic500759g.
14. “Methods and Compositions Comprising Macrocycles: Including Halogenated Macrocycles”, Daniel G. Nocera and Dilek Kiper Dogutan. U.S. Pat. Appl. US 20110144324 A1 20110616, Publ 2011.

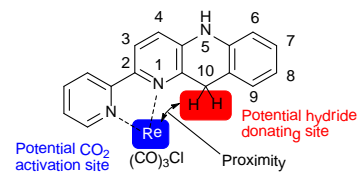
## Artificial Photosynthesis for Photogeneration of Fuels

Etsuko Fujita, Dmitry E. Polyansky, David C. Grills, and James T. Muckerman  
Chemistry Department  
Brookhaven National Laboratory  
Upton, NY 11973

The goal of our research is to gain a fundamental understanding of processes involved in the chemical conversion of solar energy. Specifically, we are carrying out fundamental research involving coordinated experimental and theoretical studies of the factors that must be considered simultaneously in designing artificial photosynthetic systems for the photogeneration of fuels. Among the factors to be considered are: (A) searching for visible-light absorbers, e.g., transition-metal photosensitizers and semiconductors, and efficiently coupling them with electron transfer and/or catalytic processes for solar fuels production; (B) avoiding high-energy intermediates through multi-electron, multi-proton processes; (C) using inexpensive and earth-abundant metals, or metal complexes that have bio-inspired or non-innocent ligands to achieve low-energy pathways via 2<sup>nd</sup>-coordination sphere interaction or redox leveling; (D) adopting water as the target solvent and the source of protons and electrons for fuel-generating reactions; and (E) immobilizing catalysts on electrode or semiconductor surfaces for the highest possible reaction rates and slowest unwanted side reactions.

As seen from our publications on reductive half-reactions for fuel generation since 2011, the BNL Artificial Photosynthesis group has been involved intensively in mechanistic studies of (1) proton, hydrogen-atom, and hydride transfer reactions; (2) reversible interconversion of CO<sub>2</sub> and formic acid; (3) electrochemical CO<sub>2</sub> reduction in water, organic solvents, or room-temperature ionic liquids; (4) photochemical CO<sub>2</sub> reduction in DMF/scCO<sub>2</sub>; (5) thermodynamics and kinetics of small molecule binding and activation; and (6) nano-structured non-precious metal carbides and nitrides for hydrogen production. At this meeting, we will focus on photo- and electrochemical CO<sub>2</sub> reduction and their alternative process of CO<sub>2</sub> hydrogenation together with our discovery of efficient earth-abundant Mo and W catalysts for H<sub>2</sub> evolution reaction (HER).

*Photo- and Electrochemical CO<sub>2</sub> Reduction:* Tricarbonyl rhenium complexes with  $\alpha$ -diimine ligands are known as efficient photo- and electrochemical catalysts for producing CO selectively from CO<sub>2</sub>. Therefore, the rhenium complex shown at the right is a potential candidate for CO<sub>2</sub> reduction, having both a CO<sub>2</sub> activation site and a

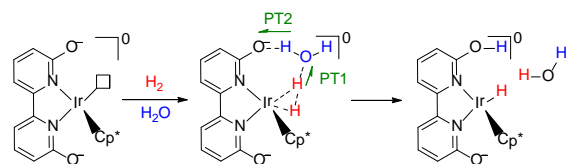
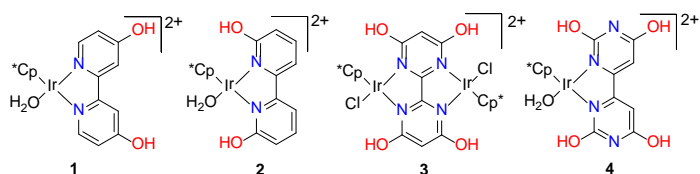


hydride donating site in the same coordination sphere, allowing for an examination of the reactivity of the dihydro form, an NADH-like ligand, toward CO<sub>2</sub> reduction. While this complex can be produced from the corresponding NAD<sup>+</sup>-like form via a mechanism involving H-atom abstraction by photoproducted Et<sub>3</sub>N<sup>•+</sup>, it is a rather weak hydride donor (84 <  $\Delta G_{H^-}$  << 99 kcal/mol). However, both Re complexes catalyze electrochemical CO<sub>2</sub> reduction to CO. We also investigated a series of molecular complexes that are structurally similar to the Ni<sup>II</sup> macrocycle [Ni(cyclam)]<sup>2+</sup> (cyclam = 1,4,8,11-tetraazacyclotetradecane) as electrocatalysts for the reduction of CO<sub>2</sub> at a mercury pool working electrode in aqueous solution. We found that at least two of the complexes investigated are better electrocatalysts than [Ni(cyclam)]<sup>2+</sup>, probably due to: (i) geometries that are suitable for adsorption on the mercury electrode surface, and (ii) electronic

effects of methyl groups or cyclohexane rings on the cyclam backbone. Mechanistic studies by pulse radiolysis show evidence of Ni(CO<sub>2</sub>) adducts for two of the catalysts, with  $K_{\text{CO}_2} \sim 10 \text{ M}^{-1}$  for the reaction of Ni<sup>I</sup> with CO<sub>2</sub> in aqueous solution. Measured pK<sub>a</sub>s (~2) of the Ni-H species are consistent with the selective formation of CO without H<sub>2</sub> or formate.

**CO<sub>2</sub> Hydrogenation and Formic Acid Decomposition:** Based on Himeda's work on Ir complex **1**, we have shown reversible H<sub>2</sub> storage near room temperature and pressure with pH as the

'switch' for controlling the direction of the reaction using complex **3** as a catalyst. H<sub>2</sub> is stored as formate through hydrogenation of CO<sub>2</sub> under slightly basic conditions, or released by decomposition of formic acid under slightly acidic conditions. We have prepared several bio-inspired 'proton-responsive' mononuclear Ir(III) catalysts for CO<sub>2</sub> hydrogenation (**2** and **4** in the figure above are among those studied), and gained mechanistic insight through investigation of the factors that control the effective generation of formate. These factors include: (i) kinetic isotope effects by water, hydrogen, and bicarbonate; (ii) position and number of hydroxyl groups on bpy-type ligands; and (iii) mono- vs di-nuclear iridium complexes. We have, for the first time, obtained clear evidence from kinetic isotope effects and computational studies of the involvement of a water molecule in the rate-determining step, and accelerated proton transfer by formation of a water-bridged intermediate in CO<sub>2</sub> hydrogenation catalyzed by bio-inspired complexes bearing a pendent base (see figure at right). Furthermore, contrary to expectations, a more significant enhancement of the catalytic activity was observed from electron donation by the ligand than on the number of the active metal centers.



**Earth-Abundant HER Catalysts:** The electrolysis of water presents an environmentally responsible alternative for hydrogen generation when electricity is produced by renewable energy. However, carrying out the hydrogen evolution reaction (HER,  $2\text{H}^+ + 2\text{e}^- \rightarrow \text{H}_2$ ) requires alternatives to noble metal catalysts. To address this challenge, the material must (i) be catalytically active for the HER, (ii) be stable under harsh conditions, (iii) have a low electrochemical overpotential, and (iv) be easy to produce on a large scale. We synthesized graphene-supported molybdenum and tungsten carbide-nitride nanocomposites by using soybeans and aniline, respectively, as the source of nitrogen to produce active, durable electrocatalysts with very low overpotentials for the HER in acidic environments.

**Future Plans:** We will continue to pursue the generation of fuels from light (or solar-produced electricity), water and carbon dioxide. Our goal is to carry out fundamental research involving coordinated experimental and theoretical studies aimed at designing artificial photosynthetic systems. The target fuels such as H<sub>2</sub>, CO, syngas, and ultimately methanol and higher alcohols will be prepared via new catalysis for photoinduced electron-, atom- and hydride-ion transfer reactions, and bond formation and breaking. We will also focus on photocatalytic reactions with immobilized catalysts.

We thank Dr. Yuichiro Himeda (AIST), Prof. Koji Tanaka (Kyoto U.) and Dr. Kotaro Sasaki (BNL).

## DOE Sponsored Publication (2011-2014) excluding ones from the HFI Water Oxidation Project

1. Small, Y. A.; DuBois, D. L.; Fujita, E.; Muckerman, J. T. "Proton Management as a Design Principle for Hydrogenase-Inspired Catalysts," *Energy Environ. Sci.* **2011**, 4, 3008-3020.
2. Fujita, E.; Muckerman, J. T.; Domen, K. "A Current Perspective on Photocatalysis," *ChemSusChem.* **2011**, 4, 155-157.
3. Muckerman, J. T.; Fujita, E. "Theoretical Studies of the Mechanism of Catalytic Hydrogen Production by a Cobaloxime," *Chem. Commun.* **2011**, 47, 12456-12458.
4. Cohen, B. W.; Polyansky, D. E.; Achord, A.; Cabelli, D.; Muckerman, J. T.; Tanaka, K.; Thummel, R. P.; Zong, R.; Fujita, E. "Steric Effect for Proton, Hydrogen-Atom, and Hydride Transfer Reactions with Geometric Isomers of NADH-Model Ruthenium Complexes," *Faraday Discuss.* **2012**, 155, 129-144.
5. Schneider, J.; Jia, H.; Muckerman, J. T.; Fujita, E. "Thermodynamics and Kinetics of CO<sub>2</sub>, CO and H<sup>+</sup> Binding to a Metal Centre of CO<sub>2</sub> Reduction Catalysts," *Chem. Soc. Rev.* **2012**, 41, 2036-2051.
6. Hull, J. F.; Himeda, Y.; Wang, W.-H.; Hashiguchi, B.; Periana, R.; Szalda, D. J.; Muckerman, J. T.; Fujita, E. "Reversible Hydrogen Storage using CO<sub>2</sub> and a Proton-Switchable Iridium Catalyst in Aqueous Media under Mild Temperatures and Pressures," *Nat. Chem.* **2012**, 4, 383-388.
7. Agarwal, J.; Fujita, E.; Schaefer, H. F. III; Muckerman, J. T. "Mechanisms for CO Production from CO<sub>2</sub> Using Reduced Rhenium Tricarbonyl Catalysts," *J. Am. Chem. Soc.* **2012**, 134, 5180-5186.
8. Al-Mahboob, A.; Muller, E.; Karim, A.; Muckerman, J. T.; Ciobanu, C. V.; Sutter, P. "Site-Dependent Activity of Atomic Ti Catalysts in Al-Based Hydrogen Storage Materials," *J. Am. Chem. Soc.* **2012**, 134, 10381-10384.
9. Agarwal, J.; Sanders, B. C.; Fujita, E.; Schaefer III, H. F.; Harrop, T. C.; Muckerman, J. T. "Exploring the Intermediates of Photochemical CO<sub>2</sub> Reduction: Reaction of Re(dmb)(CO)<sub>3</sub>COOH with CO<sub>2</sub>," *Chem. Commun.* **2012**, 48, 6797-6799.
10. Wang, W.-H.; Hull, J. F.; Muckerman, J. T.; Fujita, E.; Hirose, T.; Himeda, Y. "Highly Efficient D<sub>2</sub> Generation by Dehydrogenation of Formic Acid in D<sub>2</sub>O via H<sup>+</sup>/D<sup>+</sup> Exchange on Iridium Catalyst. Application to Synthesis of Deuterated Compounds by Transfer Deuterogenation," *Chem. Eur. J.* **2012**, 18, 9397-9404.
11. Wang, W.-H.; Hull, J. F.; Muckerman, J. T.; Fujita, E.; Himeda, Y. "Combined Ligand Effects Enhance Iridium(III)-Catalyzed Homogeneous Hydrogenation of Carbon Dioxide in Water near Ambient Temperature and Pressure," *Energy Environ. Sci.* **2012**, 5, 7923-7926.
12. Chen, W.-F.; Sasaki, K.; Ma, C.; Frenkel, A. I.; Marinkovic, N.; Muckerman, J. T.; Zhu, Y.; Adzic, R. R. "Hydrogen-Evolution Catalysts Based on Non-Noble Metal NiMo Nitride Nanosheets" *Angew. Chem. Int. Ed.* **2012**, 51, 6131-6135.
13. Lacina, D.; Yang, L.; Chopra, I.; Muckerman, J. T.; Chabal, Y.; Graetz, J. "Investigation of LiAlH<sub>4</sub>-THF formation by direct hydrogenation of catalyzed Al and LiH," *Phys. Chem.*

- Chem. Phys.* **2012**, *14*, 6569-6576.
14. Muckerman, J. T.; Achord, P.; Creutz, C. A.; Polyansky, D. E.; Fujita, E. "Calculation of Thermodynamic Hydricities and the Design of Hydride Donors for CO<sub>2</sub> Reduction," *Proc. Nat. Acad. Sci. USA* **2012**, *109*, 15657-15662.
  15. Matsubara, Y.; Fujita, E.; Doherty, M. D.; Muckerman, J. T.; Creutz, C. "Thermodynamic and Kinetic Hydricity of Ruthenium(II) Hydride Complexes," *J. Am. Chem. Soc.* **2012**, *134*, 15743-15757.
  16. Schneider, J.; Jia, H.; Kobihiro, K.; Cabelli, D.; Muckerman, J. T.; Fujita, E. "Nickel(II) Macrocycles: Highly Efficient Electrocatalysts for the Selective Reduction of CO<sub>2</sub> to CO," *Energy Environ. Sci.* **2012**, *5*, 9502-9510.
  17. Polyansky, D. E. "Electrocatalysts for Carbon Dioxide Reduction, " in *Encyclopedia of Applied Electrochemistry*, Eds. R. Adzic and N. Marinkovic, Springer, in press.
  18. Zhao, H. C.; Mello, M.; Fu, B.-L.; Chowdury, H.; Szalda, D. J.; Tsai, M.-K.; Grills, D. C.; Rochford, J. "Investigation of Monomeric versus Dimeric *fac*-Rhenium(I) Tricarbonyl Systems Containing the Noninnocent 8-Oxyquinolate Ligand", *Organometallics*, **2013**, *32*, 1832-1841.
  19. Doherty, M. D.; Grills, D. C.; Huang, K.-W.; Muckerman, J. T.; Polyansky, D.; Fujita, E. "Kinetics and Thermodynamics of Small Molecule Binding to Pincer-PCP Rhodium(I) Complexes," *Inorg. Chem.*, **2013**, *52*, 4160-4172.
  20. Hayashi, Y.; Szalda, D. J.; Grills, D. C.; Hanson, J.; Huang, K. -W.; Muckerman, J. T.; Fujita, E. "Isolation and X-ray Structures of Four Rh(PCP) Complexes Including a Rh(I) Dioxygen Complex with a Short O–O Bond," *Polyhedron* (Michelle Millar Special Issue), **2013**, *58*, 106-114.
  21. Chen, W.-F.; Wang, C.-H.; Sasaki, K.; Marinkovic, N.; Xu, W.; Muckerman, J. T.; Zhu, Y.; Adzic, R. R. "Highly Active and Durable Nanostructured Molybdenum Carbide Electrocatalysts for Hydrogen Production," *Energy Environ. Sci.*, **2013**, *6*, 943-951.
  22. Muckerman, J. T.; Skone, J. H.; Ning, M.; Wasada-Tsutsui, Y. "Toward the Accurate Calculation of pK<sub>a</sub> Values in Water and Acetonitrile," *Biochim. Biophys. Acta - Bioenergetics*, **2013**, *1827*, 882-891.
  23. Fujita, E.; Muckerman, J. T.; Himeda, Y. "Interconversion of CO<sub>2</sub> and Formic Acid by Bio-Inspired Ir Complexes with Pendent Bases," *Biochim. Biophys. Acta - Bioenergetics*, **2013**, *1827*, 1031-1038.
  24. Ni, C.; Yang, L.; Muckerman, J. T.; Graetz, J. "N-Alkylpyrrolidine-Alane Compounds for Energy Applications," *J. Phys. Chem. C* **2013**, *117*, 2628-2634.
  25. Yang, L.; Karim, A.; Muckerman, J. T. "Density Functional Kinetic Monte Carlo Simulation of Water-Gas Shift Reaction on Cu/ZnO," *J. Phys. Chem. C* **2013**, *117*, 3414-3425.
  26. Appel, A. M.; Bocarsly, A. B.; Bercaw, J. E.; Dobbek, H.; Dupuis, M.; DuBois, D. L.; Ferry, J. G.; Fujita, E.; Hille, R.; Kenis, P. J. A.; Kerfeld, C. A.; Morris, R. H.; Peden, C.;

- Portis, A.; Ragsdale, S.; Rauchfuss, T. B.; Reek, J. N. H.; Seefeldt, L. C.; Spitler, M.; Stack, R. J.; Thauer, R. K.; Waldrop, G. L. "Frontiers, Opportunities, and Challenges in Biochemical and Chemical Catalysis of CO<sub>2</sub>," *Chem. Rev.* **2013**, *113*, 6621–6658.
27. Wang, W.-H.; Hull, J. F.; Muckerman, J. T.; Fujita, E.; Himeda, Y. "Hydroxy-Substituted Aromatic N-heterocycles: Versatile Ligands in Organometallic Catalysis," *New J. Chem.*, **2013**, *37*, 1860-1866.
28. Wang, W.-H.; Muckerman, J. T.; Fujita, E.; Himeda, Y. "Mechanistic Insight through Factors Controlling Effective Hydrogenation of CO<sub>2</sub> Catalyzed by Bio-inspired Proton-responsive Iridium(III) Complexes," *ACS Catal.*, **2013**, *3*, 856-860.
29. Chen, W.-F.; Iyer, S.; Iyer, S.; Sasaki, K., Wang, C. -H.; Zhu, Y.; Muckerman, J. T.; Fujita, E. "Biomass-Derived Electrocatalytic Composites for Hydrogen Evolution," *Energy Environ. Sci.*, **2013**, *6*, 1818-1826.
30. Schneider, J.; Fujita, E. "Carbon Dioxide Capture and Activation," in *Comprehensive Inorganic Chemistry II*, Vol. 8, Eds. Reedijk, J.; Poeppelemeier K.; Elsevier, Oxford, England, 2013, pp 475-504.
31. Wang, W.-H.; Suna, Y.; Himeda, Y.; Muckerman, J. T.; Fujita, E. "Functionalized Cyclopentadienyl Rhodium(III) Bipyridine Complexes: Synthesis, Characterization, and Catalytic Application in Hydrogenation of Ketones," *Dalton Trans.* **2013**, *42*, 9628-9636.
32. Kawanami, H.; Grills, D. C.; Ishizaka, T.; Chatterjee, M.; Suzuki, A. "Photocatalytic Reduction of CO<sub>2</sub> under Supercritical CO<sub>2</sub> Conditions: Effect of Pressure, Temperature, and Solvent on Catalytic Efficiency," *J. CO<sub>2</sub> Util.* **2013**, *3-4*, 93-97.
33. Chen, W.-F.; Muckerman, J. T.; Fujita, E. "Recent Developments in Transition Metal Carbides and Nitrides as Hydrogen Evolution Electrocatalysts," *Chem. Commun.* **2013**, *49*, 8896-8909.
34. Zamadar, M.; Asaoka, S.; Grills, D. C.; Miller, J. R. "Giant Infrared Absorption Bands of Electrons and Holes in Conjugated Molecules," *Nature Commun.* **2013**, *4*, 2818.
35. Badiei, Y. M.; Wang, W.-H.; Hull, J. F.; Szalda, D. J.; Muckerman, J. T.; Himeda, Y.; Fujita, E. "Cp\*Co(III) Catalysts with Proton-Responsive Ligands for Carbon Dioxide Hydrogenation in Aqueous Media," *Inorg. Chem.* **2013**, *52*, 12576-12586.
36. Wang, W.-H.; Himeda, Y.; Muckerman, J. T.; Fujita, E. "Interconversion of CO<sub>2</sub>/H<sub>2</sub> and Formic Acid under Mild Conditions in Water: Ligand Design for Effective Catalysis," *Advances in Inorganic Chemistry*, Vol. 66, CO<sub>2</sub> Chemistry, Eds. Van Eldik, R.; Aresta, M. Burlington, Elsevier, 2014, pp 190-220.
37. Matsubara, Y.; Hightower, S. H.; Chen, J.; Grills, D. C.; Polyansky, D. E.; Muckerman, J. T.; Tanaka, K.; Fujita, E. "Reactivity of a *fac*-ReCl( $\alpha$ -diimine)(CO)<sub>3</sub> Complex with an NAD<sup>+</sup> Model Ligand toward CO<sub>2</sub> Reduction," *Chem. Commun.* **2014**, *50*, 728-730.
38. Manaka, Y.; Wang, W.-H.; Suna, Y.; Kambayashi, H.; Muckerman, J. T.; Fujita, E.; Himeda, Y. "Efficient H<sub>2</sub> Generation from Formic Acid Using Azole Complexes in Water," *Catal. Sci. Technol.* **2014**, *4*, 34-37.

39. Lewandowska-Andralojc, A.; Grills, D. C.; Zhang, J.; Bullock, R. M.; Miyazawa, A.; Kawanishi, Y.; Fujita, E. "Kinetic and Mechanistic Studies of Carbon-to-Metal Hydrogen Atom Transfer Involving Os-Centered Radicals: Evidence for Tunneling," *J. Am. Chem. Soc.* **2014**, ASAP, DOI: 10.1021/ja4123076.
40. Wang, W.-H.; Xu, S.; Manaka, Y.; Suna, Y.; Kambayashi, H.; Muckerman, J. T.; Fujita, E.; Himeda, Y. "Highly Efficient Formic Acid Dehydrogenation Using Bio-Inspired Ir Complexes: A Deuterium Kinetic Isotope Effect Study and Mechanistic Insight," *ChemSusChem* **2014**, accepted, DOI: 10.1002/cssc.201301414.
41. Grills, D. C.; Farrington, J. A.; Layne, B. H.; Lyman, S. V.; Mello, B. A.; Preses, J. M.; Wishart, J. F. "Mechanism of the Formation of a Mn-Based CO<sub>2</sub> Reduction Catalyst Revealed by Pulse Radiolysis with Time-Resolved Infrared Detection," *J. Am. Chem. Soc.* **2014**, ASAP, DOI: 10.1021/ja501051s.
42. Chen, W.-F.; Schneider, J. M.; Sasaki, S.; Wang, C.-H.; Schneider, S.; Iyer, S.; Iyer, S.; Chu, Y.; Muckerman, J. T.; Fujita, E. "Tungsten Carbide-Nitride on Graphene Nanoplatelets as a Durable Hydrogen Evolution Electrocatalyst," *Angew. Chem. Int. Ed.* submitted.
43. Grills, D. C.; Matsubara, Y.; Gollisz, S. R.; Kurtz, D. A.; Kuwahara, Y.; Mello, B. A. "Electrocatalytic CO<sub>2</sub> Reduction with a Homogeneous Catalyst in Ionic Liquid: High Catalytic Activity at Low Overpotential" *J. Am. Chem. Soc.*, submitted

*Session VII*

*Theoretical and Experimental Techniques*



# Semiconductor-Electrocatalyst Contacts: Theory, Experiment, and Applications to Solar Water Photoelectrolysis

Shannon W. Boettcher, Fuding Lin, Thomas J. Mills  
 Department of Chemistry and the Materials Science Institute  
 University of Oregon  
 Eugene, OR 97403

**Project Scope:** High-efficiency photoelectrochemical water-splitting devices require integrating electrocatalysts (ECs) onto light-absorbing semiconductors (SCs), but the energetics and charge transfer processes at SC|EC interfaces are poorly understood. The common picture for the operation of such semiconductor/catalyst/solution (SCS) systems is that the semiconductor absorbs light and separates charge while the catalyst increases the rate of the hydrogen- or oxygen-evolution reaction (HER or OER, respectively). Experiments, however, show that after deposition of OER catalysts onto n-type semiconductors the photoelectrode characteristics, e.g. the photovoltage, photocurrent, and fill-factor, change in a manner not always consistent with this simple model. Competing hypotheses have attributed this behavior to changes in surface recombination, band-bending, interface charge-trapping, optical effects, or kinetics. The goal of this work is to develop a complete microscopic picture of electron transfer to describe SCS systems. To achieve this goal we combine theory and simulation with new types of photoelectrochemical experiments.

**Recent Results:** In order to understand ECs on semiconductor photoelectrodes, we fabricated model EC-coated single-crystal TiO<sub>2</sub> electrodes and directly probed

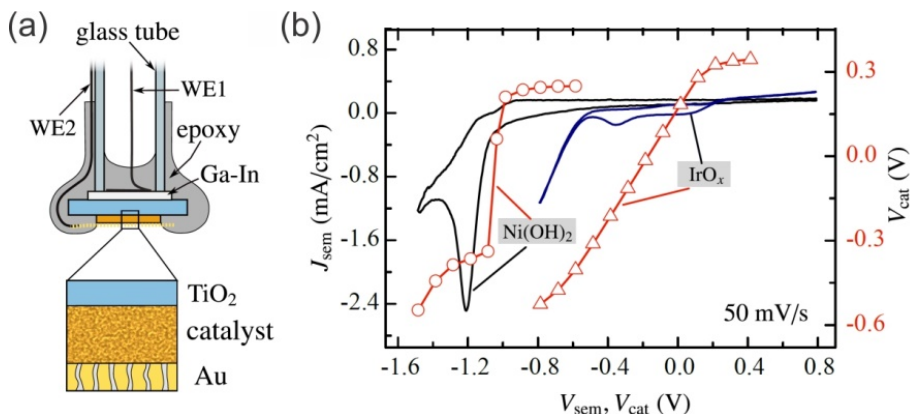


**Fig 1.** (a) Schematic of dual-electrode photoelectrochemical cell. (b) Data showing how catalyst potential  $V_{\text{cat}}$  changes as the electrode potential  $V_{\text{sem}}$  is swept using a potentiostat under illumination.

SC|EC interfaces *in situ* using a new dual-electrode photoelectrochemistry technique that we developed to independently monitor and control the potential/current at both the SC and the EC.<sup>1</sup> We discovered that redox-active ion-permeable ECs such as Ni(OH)<sub>2</sub>/NiOOH yield “adaptive” SC|EC junctions where the effective Schottky barrier height changes *in situ* with the oxidation level of the EC. In contrast, dense, ion-impermeable IrO<sub>x</sub> ECs yield constant-barrier-height “buried” junctions. Conversion of dense, thermally deposited NiO<sub>x</sub> on TiO<sub>2</sub> into ion-permeable Ni(OH)<sub>2</sub>/NiOOH correlated with increased apparent photovoltage and fill-factor. Understanding such interfaces is important because redox-active Co, Ni, and Fe-based ion-permeable catalysts have the highest-known oxygen evolution activities in neutral to basic solutions. An example of data collected is shown in **Fig. 1**, where we observed that as the semiconductor potential  $V_{\text{sem}}$  is

swept during a typical photoelectrochemical current-potential experiment, the catalyst potential  $V_{\text{cat}}$  for ion-permeable  $\text{Ni}(\text{OH})_2/\text{NiOOH}$  changes abruptly while that of the ion-impermeable  $\text{IrO}_x$  changes nearly linearly with the applied voltage.

To better understand this data and the results of related experiments we developed the first theory of SCS devices that accounts for ion-permeability and faradaic charging of the catalyst layer and applied it via numerical simulation.<sup>2</sup> The simulations agree well with the experimental data. **Fig. 2a** shows simulated steady-state band diagrams for illuminated SC|EC interfaces as function of the catalyst activity (indicated by the color of the hole quasi Fermi level  $E_{F,p}$  curves) where the catalyst is ion-porous. Under operative conditions the catalyst Fermi level  $E_{\text{cat}}$  moves down as it charges such that the current is continuous across the SC|EC and EC|solution interfaces. This leads to larger effective barrier heights  $\phi_{\text{b,eff}}$  for slower catalysts. **Figs. 2b** and **2c** compare the simulated dependence of the catalyst potential  $V_{\text{cat}}$  as the semiconductor potential is swept under illumination with the measured response. The agreement for both ion-permeable and dense catalysts is remarkable.

Collectively these new dual-electrode photoelectrochemical and simulation results demonstrate quantitatively the role of ion-permeability and catalyst charging on the interface properties and measured photoelectrode response. The resulting adaptive junction idea implies that ion-porosity is useful for optimizing SC|EC junctions and explains why the best-performing oxide photoanodes reported in the literature appear to utilize catalysts deposited using “soft” conditions (e.g. electrodeposition) where the catalyst is likely to remain ion-porous.

**Future Plans:** Our immediate efforts are in expanding the scope of the new experimental techniques and theory we have developed. In the experimental thrust we are now studying a wide range of ion-porous and dense catalysts on well-defined  $\text{TiO}_2$  electrodes. Preliminary results suggest that, as expected based on our microscopic picture of the interface, the type and activity of ion-porous catalyst used has little effect on the measured current-potential behavior when  $\text{TiO}_2$  is used as the semiconductor. We are beginning studies of catalyst-modified visible-light-absorbing oxides such as  $\text{BiVO}_4$  as well as catalyst-modified hydrogen-evolving photocathodes to further test predications. We are further expanding the theoretical aspects of our work to account for different electronic densities of states of the catalyst as well as non-uniform catalyst coverage.

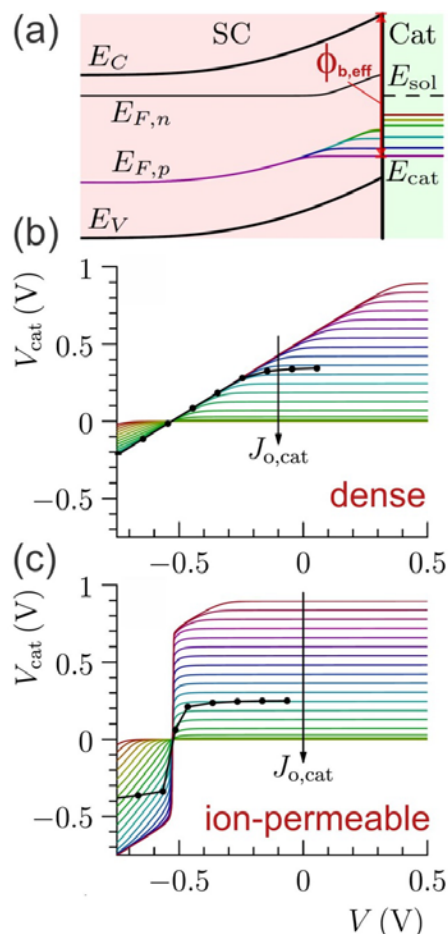


**Fig 2.** (a) Simulations of SC|EC interface showing steady state electron, hole, and catalyst quasi Fermi levels under illumination as a function of the catalyst activity. (b) and (c) Comparison of experimental (points) and simulated (curves)  $V_{\text{cat}}$  data.

### **DOE Sponsored Publications 2011-2014**

1. Lin, F.; Boettcher, S. W. Adaptive semiconductor-electrocatalyst junctions in water splitting photoanodes. *Nat. Mater.* **2014**, 13, 81-86.
2. Mills, T. J.; Boettcher, S. W. Theory and simulations of electrocatalyst-coated semiconductor electrodes for solar water splitting. **In press.** *Phys. Rev. Lett.* **2014**.
3. Trotochaud, L.; Mills, T. J.; Boettcher, S. W. An photocatalytic model for semiconductor-catalyst water-splitting photoelectrodes based on in situ optical measurements on operational catalysts. *J. Phys. Chem. Lett.* **2013**, 4, 931-935.

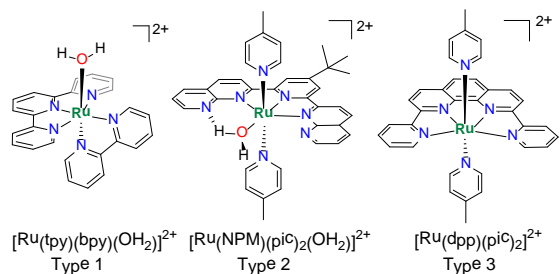
**Note: Grant started 7/15/12**

## Photo- and Electrochemical Water Oxidation: New Water Oxidation Chemistry of Ruthenium Complexes with Polypyridyl Ligands

James T. Muckerman, Javier J. Concepcion, Dmitry Polyansky, and Etsuko Fujita  
 Chemistry Department  
 Brookhaven National Laboratory  
 Upton, NY 11973-5000

We are carrying out coordinated experimental and theoretical studies to address the scientific challenge of visible-light-driven water oxidation as a critical element of an efficient, direct solar water-splitting system. Visible light absorption and the water oxidation reaction currently limit the overall efficiency of solar H<sub>2</sub> production from water. The goal of our project is to develop efficient and durable water oxidation catalysts (WOC) *via* detailed mechanistic investigations, to improve band-gap-narrowed semiconductors (BGNSCs) for use as photoanodes and to couple the photo-generated holes of BGNSCs (or the positive charges generated at electrodes) to catalysts that promote the four-electron oxidation of water to O<sub>2</sub>.

As seen from our publications on water oxidation since 2011, the BNL Artificial Photosynthesis group has been involved intensively in mechanistic studies of water oxidation by homogeneous WOC (pubs. 1,3,5,12,16-20,22) or immobilized molecular WOC (pubs. 9,11) in aqueous solution and heterogeneous reactions at the semiconductor–aqueous solution interface (pubs. 2,14,21). Our coworkers have also characterized improved BGNSCs (pubs. 6,10,13,15) and semiconductor/catalyst interfaces (pubs. 4,7,8). We will focus here on three types of mononuclear polypyridyl ruthenium complexes (shown at right) as WOC: (1) those that have water as an axial ligand, *e.g.*, [Ru<sup>II</sup>(tpy)(bpy)(OH<sub>2</sub>)]<sup>2+</sup>; (2) those that have water as an equatorial ligand, *e.g.*, [Ru<sup>II</sup>(NPM)(pic)<sub>2</sub>(OH<sub>2</sub>)]<sup>2+</sup>; and (3) those that have no aqua ligand in their primary coordination shell, *e.g.*, [Ru<sup>II</sup>(dpp)(pic)<sub>2</sub>]<sup>2+</sup>, where dpp is a tetradentate equatorial ligand.



For the “Type 1” catalysts, as previously reported by Meyer et al. (UNC), the major pathway proceeds through a [Ru<sup>V</sup>=O]<sup>3+</sup> species, which is a key intermediate produced by a non-PCET reaction from [Ru<sup>IV</sup>=O]<sup>2+</sup>, that reacts to produce an O–O bond via nucleophilic attack by a water molecule. The Ru<sup>V</sup>=O/Ru<sup>IV</sup>=O standard potentials of the Ru centers of these WOC are quite high (1.6 – 1.89 V vs. NHE), close to the thermodynamic limit of oxidation by the Ce<sup>IV</sup>/Ce<sup>III</sup> couple with a standard potential of 1.61 V vs. NHE in 1.0 M HNO<sub>3</sub>. As the solution pH is increased, the potential of the PCET precursor reactions decreases but the potential for the pH-independent oxidation of Ru<sup>IV</sup>=O to Ru<sup>V</sup>=O remains constant and the overpotential increases with pH.

However, our experimental and theoretical results show that the pH-dependent onset catalytic potentials of “Type 2” catalysts are indicative of a PCET driven low-energy pathway for the formation of products with an O–O bond (such as [Ru<sup>III</sup>–OOH]<sup>2+</sup> and [Ru<sup>IV</sup>–OO]<sup>2+</sup>) at an applied potential below the Ru<sup>V</sup>=O/Ru<sup>IV</sup>=O couple (pubs. 3,6). Because the aqua ligand is in the equatorial plane, and can interact with both the d<sub>π</sub> orbitals of the Ru center and the π\* orbitals of the NPM-type ligand in a *trans* effect, the oxidation potentials of the metal center are shifted.

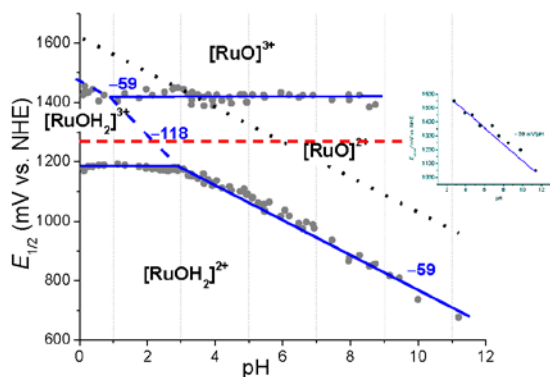


**Fig. 1.** Pourbaix diagram of  $[\text{Ru}(\text{NPM})(\text{pic})_2(\text{OH}_2)]^{2+}$ : The black dotted line corresponds to the calculated potential for  $[\text{Ru}^{\text{IV}}(\text{O})]^{2+} + \text{H}_2\text{O} \rightarrow [\text{Ru}^{\text{III}}(\text{OOH})]^{2+} + \text{e}^- + \text{H}$ , and the red dash line indicates the  $\text{Ru}(\text{bpy})_3^{3+}/\text{Ru}(\text{bpy})_3^{2+}$  potential. Insert: pH dependent onset potential for water oxidation.

Ce(IV) such as photogenerated  $[\text{Ru}(\text{bpy})_3]^{3+}$  (1.26 V vs. NHE, see red dashed line in Fig. 1) to drive water oxidation. The overall quantum yield of 9%, TOF of  $0.12 \text{ s}^{-1}$  and TON of 103 (limited solely by a drop in pH below 3) were obtained, rendering it one of the most active mononuclear ruthenium-based catalysts for light-driven water oxidation in a homogeneous system (pub. 12).

Turning to “Type 3” catalysts,  $[\text{Ru}^{\text{II}}(\text{dpp})(\text{pic})_2]^{2+}$  is representative of several that we are currently studying. This complex has an 18-electron metal center and picoline axial ligands that are non-labile in aqueous solution. It must detach a coordination site of the tetradentate equatorial ligand or be oxidized twice in order to bind a water molecule to the metal center. Our studies indicate PCET pathways. At low pH the pathway involves a  $2\text{e}^-/2\text{H}^+$  oxidation of the  $1\text{e}^-$  oxidized  $[\text{Ru}^{\text{III}}]^{3+}$  and a water molecule to produce the seven-coordinate  $[\text{Ru}^{\text{V}}(\text{O})]^{3+}$  species. At neutral and high pH, the pathway involves the  $2\text{e}^-/2\text{H}^+$  PCET oxidation of  $[\text{Ru}^{\text{II}}]^{2+}$  and a water molecule to produce a  $[\text{Ru}^{\text{IV}}(\text{O})]^{2+}$  species. These oxo complexes participate in subsequent PCET steps upon attack by another water molecule resulting in the formation of an O–O bond. After the first cycle, it is likely that all steps in subsequent catalytic cycles proceed through an unprecedented sequence of seven-coordinate intermediates. This mechanism reveals an entirely “new chemistry” for Type 3 polypyridyl ruthenium WOC (pub. 22).

Our future WOC work will pursue a more complete understanding of Type 3 polypyridyl ruthenium complexes that will allow us to tune their free-energy profiles along the water oxidation pathway at a specific pH. The replacement of the two pyridines on dpp by other groups capable of PCET chemistry (e.g.,  $-\text{P}(\text{O})(\text{OH})_2$ ,  $-\text{B}(\text{OH})_2$ ) will introduce additional pH dependence allowing control of electron density at the metal,  $\text{p}K_{\text{a}}$ s and overall charge of the complex. In addition, these groups will introduce pendent bases in close proximity to the catalytically active site. We also plan to attach them to conductor and semiconductor metal oxide electrodes through phosphonate linkers. Other thrusts will be to understand the role of Ce(IV) as a sacrificial oxidant by measuring association constants,  $\text{p}K_{\text{a}}$ s and electron transfer rates in different acids; using Resonance Raman, XAFS, XRD and PDF spectra under applied potential to obtain spectral signatures of reactive intermediates in *in-situ* studies of metal oxide water

While the standard potential of the  $[\text{Ru}^{\text{IV}}=\text{O}]^{2+} + \text{H}_2\text{O} \rightarrow [\text{Ru}^{\text{III}}(\text{OOH})] + \text{H}^+ + \text{e}^-$  reaction is higher than that for the  $1\text{e}^-$  oxidation of  $\text{Ru}^{\text{IV}}=\text{O}$ , it is proton coupled so that the PCET reaction becomes more favorable than the  $1\text{e}^-$  oxidation above pH 3 (see Fig. 1, dotted black line). We further investigated the  $[\text{Ru}^{\text{II}}(\text{NPM})(\text{pic})_2(\text{OH}_2)]^{2+}$  complex as a catalyst for visible-light-driven water oxidation in a three-component homogeneous system containing  $[\text{Ru}(\text{bpy})_3]^{2+}$  as a photosensitizer, persulfate as a sacrificial electron acceptor and the catalyst. In agreement with our earlier electrochemical and theoretical results, we demonstrated that the low-energy pathway incorporating the proton-coupled “direct reaction” step takes place with the use of a milder oxidant than

oxidation systems containing Co and Ir metals; and theoretical water oxidation studies at the GaN/ZnO aqueous interface using highly realistic model systems.

We thank R. P. Thummel at the University of Houston for providing us with ruthenium complexes, and thank our other collaborators J. A. Rodriguez, M. S. Hybertsen, S. Lyamar, O. V. Prezhdo and P. G. Khalifah.

### DOE Sponsored Publications 2011-2014 for HFI Water Oxidation Project (AP Subtask 2)

1. Wada, T.; Muckerman, J. T.; Fujita, E.; Tanaka, K. "Substituents Dependent Capability of Bis(ruthenium-dioxolene-terpyridine) Complexes Toward Water Oxidation," *Dalton Trans.* **2011**, *40*, 2225-2233.
2. Li, L.; Muckerman, J. T.; Hybertsen, M. S.; Allen, P. B. "Phase Diagram, Structure and Electronic Properties of  $(\text{Ga}_{1-x}\text{Zn}_x)(\text{N}_{1-x}\text{O}_x)$  Solid Solution from DFT-Based Simulations," *Phys. Rev. B* **2011**, *83*, 134202.
3. Polyansky, D. E.; Muckerman, J. T.; Rochford, J.; Zong, R.; Thummel, R. P.; Fujita, E. "Water Oxidation by a Mononuclear Ruthenium Catalyst: Characterization of the Intermediates," *J. Am. Chem. Soc.* **2011**, *133*, 14649-14665.
4. Yang, F.; Kundu, S.; Vidal, A.B.; Graciani, J.; Ramírez, P.J.; Senanayake, S.D.; Stacchiola, D.; Evans, J.; Liu, P.; Fdez Sanz, J.; Rodriguez, J.A. "Determining the Behaviour of  $\text{RuO}_x$  Nanoparticles in Mixed-Metal Oxides: Structural and Catalytic Properties of  $\text{RuO}_2/\text{TiO}_2(110)$  Surfaces," *Angew. Chem. Int. Ed.* **2011**, *50*, 10198-10202.
5. Boyer, J. L.; Polyansky, D. E.; Szalda, D. J.; Zong, R.; Thummel, R. P.; Fujita, E. "Effects of a Proximal Base on Water Oxidation and Proton Reduction Catalyzed by Geometric Isomers of  $[\text{Ru}(\text{tpy})(\text{pynap})(\text{OH}_2)]^{2+}$ ," *Angew. Chem. Int. Ed.* **2011**, *50*, 12600-12604.
6. Malingowski, A. C.; Stephens, P. W.; Huq, A.; Huang, Q.; Khalid, S.; Khalifah, P. G. "Substitutional Mechanism of Ni into the Wide Band Gap Semiconductor  $\text{InTaO}_4$  and its Implications for Water Splitting Activity in the Wolframite Structure Type," *Inorg. Chem.* **2012**, *51*, 6096-6103.
7. Kundu, S.; Vidal, A.B.; Yang, F.; Ramírez, P.J.; Senanayake, S.D.; Stacchiola, D.; Evans, J.; Liu, P.; Rodriguez, J.A. "Special Chemical Properties of  $\text{RuO}_x$  Nanowires in  $\text{RuO}_x/\text{TiO}_2(110)$ : Dissociation of Water and Hydrogen Production," *J. Phys. Chem. C* **2012**, *116*, 4767-4773.
8. Kundu, S.; Ciston, J.; Senanayake, S. D.; Arena, D.; Fujita, E.; Stacchiola, D.; Rodriguez, J. A. "Exploring the Structural and Electronic Properties of Pt/Ceria-Modified  $\text{TiO}_2$  and its Photo-Catalytic Activity for Water Splitting under Visible Light," *J. Phys. Chem. C* **2012**, *116*, 14062-14070.
9. Zidki, T.; Zhang, L.; Shafirovich, V.; Lyamar, S. V. "Water Oxidation Catalyzed by Cobalt(II) Adsorbed on Silica Nanoparticles," *J. Am. Chem. Soc.* **2012**, *134*, 14275-14278.
10. Mi, Q.; Ping, Y.; Li, Y.; Cao, B. F.; Brunschwig, B. S.; Khalifah, P. G.; Galli, G. A.; Gray, H. B.; Lewis N. S., "Thermally Stable  $\text{N}_2$  Intercalated  $\text{WO}_3$  Photoanodes for Water Oxidation," *J. Am. Chem. Soc.*, **2012**, *134*, 18318-18324.

11. Zhong, D. K.; Zhao, S.; Polyansky, D. E.; Fujita, E. "Photoisomerization of Active Ruthenium Water Oxidation Catalyst Inhibited by Immobilization onto Metal Oxide Electrodes," *J. Catal.* **2013**, *307*, 140-147.
12. Lewandowska-Andralojc, A.; Polyansky, D. E.; Zong, R.; Thummel, R. P.; Fujita, E. "Enabling Light-Driven Water Oxidation via a Low Energy Ru<sup>IV</sup>=O Intermediate," *Phys. Chem. Chem. Phys.* **2013**, *15*, 14058-14068.
13. Reinert, A. A.; Payne, C.; Wang, L.; Ciston, J.; Zhu, Y.; Khalifah, P. "Synthesis and Characterization of Visible Light Absorbing (GaN)<sub>1-x</sub>(ZnO)<sub>x</sub> Semiconductor Nanorods," *Inorg. Chem.* **2013**, *52*, 8389-8398.
14. Akimov, A. V.; Muckerman, J. T.; Prezhdo, O. V. "Non-Adiabatic Dynamics of Positive Charge during Photocatalytic Water Splitting on GaN(10-10) Surface: Charge Localization Governs Splitting Efficiency," *J. Am. Chem. Soc.* **2013**, *135*, 8682-8691.
15. Wang, L.; Kang, W.; Hybertsen, M.; Maeda, K.; Domen, K.; Khalifah, P. "Design of Medium Band Gap Ag-Bi-Nb-O and Ag-Bi-Ta-O Semiconductors for Driving Direct Water Splitting with Visible Light," *Inorg. Chem.* **2013**, *52*, 9192-9205.
16. Badiei, Y. M.; Polyansky, D. E.; Muckerman, J. T.; Szalda, D. J.; Haberdar, R.; Zong, R.; Thummel, R. P.; Fujita, E. "Water Oxidation with Mononuclear Ruthenium (II) Polypyridine Complexes Involving a Direct Ru<sup>IV</sup>=O Pathway in Neutral and Alkaline Media," *Inorg. Chem.* **2013**, *52*, 8845-8850.
17. Lewandowska-Andralojc, A.; Polyansky, D. E. "Mechanism of the Quenching of the Tris(bipyridine)ruthenium(II) Emission by Persulfate: Implications for Photo-Induced Oxidation Reactions," *J. Phys Chem. A* **2013**, *117*, 10311-10319.
18. Polyansky, D. E.; Hurst, J. K.; Lyman, S. V. "Application of Pulse Radiolysis to Mechanistic Investigation of Water Oxidation Catalysis," *Eur. J. Inorg. Chem.* **2014**, 619-634.
19. Wada, T.; Tanaka, K.; Muckerman, J. T.; Fujita, E. "Water Oxidation by Ruthenium Catalysts Having Non-innocent Ligands," in *Molecular Water Oxidation Catalysis* (edited by A. Llobet), Wiley, 2014, pp 77-111.
20. Lewandowska-Andralojc, A.; Polyansky, D. E.; Wang, C.-H.; Wang, W.-H.; Himeda, Y.; Fujita, E. "Efficient Water Oxidation with Organometallic Iridium Complexes as Precatalysts at Neutral pH," *Phys. Chem. Chem. Phys.* **2014**, Advance Article, DOI: 10.1039/C3CP55101F.
21. Kharche, N.; Hybertsen, M. S.; Muckerman, J. T. "Computational Investigation of Structural and Electronic Properties of Aqueous Interfaces of GaN, ZnO, and GaN/ZnO Alloy," *Phys. Chem. Chem. Phys.* **2014**, Advance Article, DOI:10.1039/C4CP00486H.
22. Muckerman, J. T.; Kowalczyk, M.; Badiei, Y. M.; Polyansky, D. E.; Yang, Y.; Concepcion, J. J.; Zong, R.; Thummel, R. P.; Fujita, E. "New Water Oxidation Chemistry of a Seven-Coordinate Ruthenium Complex with a Tetradentate Polypyridyl Ligand," *Inorg. Chem.* **2014**, submitted.

# Pulse Radiolysis as a Tool for Unraveling Mechanistic Details of Redox Processes Relevant to Solar Energy Conversion

David C. Grills, Dmitry E. Polyansky, and Etsuko Fujita  
Chemistry Department  
Brookhaven National Laboratory  
Upton, NY 11973-5000

The overarching goal of our research is to gain a fundamental understanding of the processes involved in the capture and chemical conversion of solar energy, typically using transition metal complexes as catalysts. These processes involve multiple redox states, many of which are transient in nature. Pulse radiolysis (PR) can be used for the rapid production of radical ions, and is thus a powerful technique for directly preparing catalytically-relevant, unstable redox-active species that can be subsequently probed by UV/visible transient absorption (TA) spectroscopy. Gaining a detailed mechanistic knowledge of catalytic processes is crucial for understanding and developing more efficient photoconversion systems. To this end, we have recently developed a unique nanosecond time-resolved infrared (TRIR) detection capability for PR, targeting improved characterization of transient intermediates due to the structural specificity of mid-IR spectroscopy. The processes we have investigated with TA and/or TRIR detection include catalytic water oxidation, CO<sub>2</sub> reduction, and organic hydride formation. In addition, we have begun to use PR-TRIR to investigate the radiation-induced fragmentation of room-temperature ionic liquids (RTILs).

*Mechanism of Formation of a Mn-Based CO<sub>2</sub> Reduction Catalyst:* Using PR-TRIR, we have unraveled the mechanism of formation of a Mn-based CO<sub>2</sub> reduction catalyst, **Mn–Mn** (**Mn** = Mn(<sup>t</sup>Bu<sub>2</sub>-bpy)(CO)<sub>3</sub>; <sup>t</sup>Bu<sub>2</sub>-bpy = 4,4'-<sup>t</sup>Bu<sub>2</sub>-2,2'-bipyridine) from a new Mn-formate precatalyst, *fac*-**Mn**–(OCHO) (pub. 8). There is currently growing interest in the use of Mn-based precatalysts for the electrocatalytic reduction of CO<sub>2</sub> to CO because they contain an earth-abundant metal and facilitate CO<sub>2</sub> reduction at ~0.3 V lower overpotential than their Re-based counterparts. However, little is known about the mechanistic details of their reactivity. Due to the photosensitive nature of Mn complexes, PR is the ideal method for generating the short-lived one-electron reduced precatalyst, which is the first step in the catalytic CO<sub>2</sub> reduction cycle. Using TRIR detection, we have identified, for the first time, all of the subsequent intermediates involved in the formation of the dinuclear catalyst, **Mn–Mn** in acetonitrile (Fig. 1). This has revealed that formate dissociation is extremely rapid following one-electron reduction ( $\tau = 77$  ns). The large rate constant for dimerization of the resulting Mn radicals,  $2k_{\text{dim}} = 1.3 \times 10^9 \text{ M}^{-1} \text{ s}^{-1}$ , compared with Re-based systems ( $2k_{\text{dim}} \sim 1 \times 10^2 \text{ M}^{-1} \text{ s}^{-1}$ ), reveals that they exist as five-coordinate species, with no binding of a solvent molecule at the vacant coordination site, prior to dimerization.

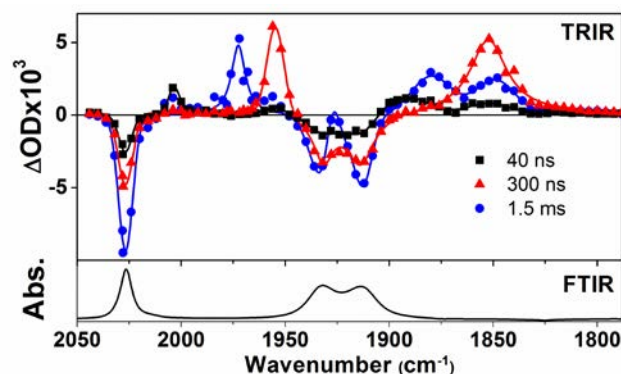
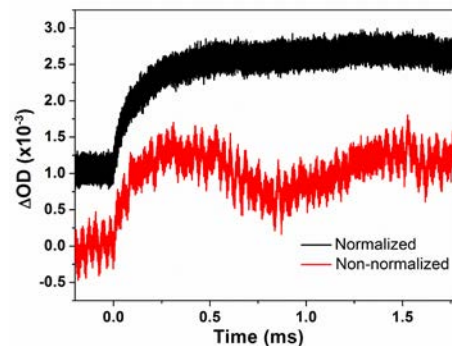


Fig. 1. IR spectrum of a 1.5 mM solution of *fac*-**Mn**–(OCHO) in CH<sub>3</sub>CN containing 50 mM [<sup>t</sup>Bu<sub>4</sub>N][OCHO] (bottom), and TRIR spectra recorded 40 ns, 300 ns and 1.5 ms after pulse radiolysis of this argon-purged solution (top). Black transient bands are due to [**Mn**–(OCHO)]<sup>•</sup>, red bands are due to **Mn**<sup>•</sup>, and blue bands are due to **Mn–Mn**.

*Recent Developments in TRIR Detection for Pulse Radiolysis:* Recent technical developments (pub. 9) include: (A) the development of a thiocyanate-based dosimetry standard for PR-TRIR studies based on monitoring the recovery of the very strong  $\nu(\text{CN})$  stretch of the  $\text{SCN}^-$  anion at  $\sim 2050\text{ cm}^{-1}$  following PR of a thiocyanate solution.; (B) the implementation of dual-beam probe/reference normalization TRIR detection. This detection technique allows IR laser-induced signal fluctuations to be normalized out, and has resulted in a large improvement in signal-to-noise ratios, particularly for longer timescale measurements (see Fig. 2).



**Fig. 2:** Kinetic traces (offset for clarity) recorded at  $1976\text{ cm}^{-1}$  after pulse radiolysis of a solution of a Mn-carbonyl complex in  $\text{CH}_3\text{CN}$ , with (black) and without (red) dual-beam probe/ref. normalized detection.

*Water Oxidation:* We have successfully employed PR in mechanistic investigations of catalyzed water oxidation reactions (pub. 7). The ability of the PR technique to produce strongly oxidizing radicals, such as  $\text{CO}_3^{\bullet-}$  (1.55 V) or  $\text{SO}_4^{\bullet-}$  (2.43 V) in a wide pH range, in addition to nanosecond time resolution, makes this method more suitable for mechanistic studies of oxidative reactions compared to the use of traditional sacrificial oxidants, such as Ce(IV) (pub. 7). Recently, we studied a family of Ru polypyridyl water oxidation catalysts such as  $[\text{Ru}(\text{NPM})(\text{pic})_2]^{2+}$  (NPM = 4-*t*-butyl-2,6-di-1',8'-(naphthyrid-2'-yl)-pyridine, pic = 4-picoline), in which the formation of the O–O bond can proceed through a Ru(IV)=O intermediate (pubs. 1,5). Using PR we have been able to produce and characterize two unstable intermediates involved in the catalytic cycle – Ru(III)–OH and Ru(IV)=O. The observed disproportionation of Ru(III)–OH provided key experimental support for rationalizing the Pourbaix diagram of  $[\text{Ru}(\text{NPM})(\text{pic})_2]^{2+}$ .

*Other CO<sub>2</sub> Reduction and Organic Hydride Studies:* A series of Ni(II) complexes with cyclam-related ligands (cyclam = 1,4,8,11-tetraazacyclotetradecane) was prepared and investigated for electrocatalytic CO<sub>2</sub> reduction activity in water. Using PR, spectra of the Ni(I), Ni(III)–H and Ni–CO<sub>2</sub> species were determined, together with the  $\text{p}K_a$  of Ni–H and the CO<sub>2</sub> binding equilibrium constants to Ni(I). These data are useful to design effective catalysts for CO<sub>2</sub> reduction (pubs. 3,4). Another method for reducing CO<sub>2</sub> might be the use of renewable hydride donors such as photochemically produced metal hydrides or C–H hydrides (i.e., NADH-model complexes). Our PR investigation of NAD<sup>+</sup>-model complexes showed that the  $2e^-/2\text{H}^+$  process to produce the corresponding hydride donors takes place via a disproportionation reaction of the corresponding protonated one-electron-reduced species (pub. 2).

*Future Plans:* The unique capability of the PR method to selectively generate oxidizing or reducing conditions in aqueous or organic solution has allowed us to study a variety of redox-active transient species involved in catalytic transformations relevant to solar energy conversion. Such studies will continue with new catalysts as they are developed. Furthermore, the wealth of structural information available from TRIR detection enables us to understand the changes in bonding that accompany many fast chemical reactions. Therefore, we will continue to use PR-TRIR as a complementary technique to photochemical methods for studying the catalytic reduction of CO<sub>2</sub>, transformations of NO, and atom transfer reactions of metal carbonyl complexes.

We thank our collaborators, R. P. Thummel (U. Houston), K. Tanaka (Kyoto U.), K. Kobihiro (Kochi U. T.), H. Jia (Toyota Res. Inst. N. Am.), J. K. Hurst (Washington State U.), and our BNL coworkers, J. T. Muckerman, J. F. Wishart, S. V. Lyamar, D. Cabelli, J. M. Preses, and J. R. Miller.

### **DOE Sponsored Publications (2011-2014) that include, or are related to, pulse radiolysis investigations**

1. Polyansky, D. E.; Muckerman, J. T.; Rochford, J.; Zong, R.; Thummel, R. P.; Fujita, E. "Water Oxidation by a Mononuclear Ruthenium Catalyst: Characterization of the Intermediates" *J. Am. Chem. Soc.* **2011**, *133*, 14649-14665.
2. Cohen, B. W.; Polyansky, D. E.; Achord, A.; Cabelli, D.; Muckerman, J. T.; Tanaka, K.; Thummel, R. P.; Zong, R.; Fujita, E. "Steric Effect for Proton, Hydrogen-Atom, and Hydride Transfer Reactions with Geometric Isomers of NADH-Model Ruthenium Complexes" *Faraday Discuss.* **2012**, *155*, 129-144.
3. Schneider, J.; Jia, H.; Muckerman, J. T.; Fujita, E. "Thermodynamics and Kinetics of CO<sub>2</sub>, CO and H<sup>+</sup> Binding to a Metal Centre of CO<sub>2</sub> Reduction Catalysts" *Chem. Soc. Rev.* **2012**, *41*, 2036-2051.
4. Schneider, J.; Jia, H.; Kobihiro, K.; Cabelli, D.; Muckerman, J. T.; Fujita, E. "Nickel(II) Macrocycles: Highly Efficient Electrocatalysts for the Selective Reduction of CO<sub>2</sub> to CO" *Energy Environ. Sci.* **2012**, *5*, 9502-9510.
5. Badiei, Y. M.; Polyansky, D. E.; Muckerman, J. T.; Szalda, D. J.; Haberdar, R.; Zong, R.; Thummel, R. P.; Fujita, E. "Water Oxidation with Mononuclear Ruthenium (II) Polypyridine Complexes Involving a Direct Ru<sup>IV</sup>=O Pathway in Neutral and Alkaline Media" *Inorg. Chem.* **2013**, *52*, 8845-8850.
6. Zamadar, M.; Asaoka, S.; Grills, D. C.; Miller, J. R. "Giant Infrared Absorption Bands of Electrons and Holes in Conjugated Molecules" *Nature Commun.* **2013**, *4*:2818.
7. Polyansky, D. E.; Hurst, J. K.; Lyamar, S. V. "Application of Pulse Radiolysis to Mechanistic Investigation of Water Oxidation Catalysis" *Eur. J. Inorg. Chem.* **2014**, 619-634.
8. Grills, D. C.; Farrington, J. A.; Layne, B. H.; Lyamar, S. V.; Mello, B. A.; Preses, J. M.; Wishart, J. F. "Mechanism of the Formation of a Mn-Based CO<sub>2</sub> Reduction Catalyst Revealed by Pulse Radiolysis with Time-Resolved Infrared Detection" *J. Am. Chem. Soc.* **2014**, ASAP, <http://dx.doi.org/10.1021/ja501051s>
9. Grills, D. C.; Farrington, J. A.; Layne, B. H.; Preses, J. M.; Wishart, J. F. "Development of Nanosecond Time-Resolved Infrared Detection at a Pulse Radiolysis Facility" *Rev. Sci. Instrum.*, submitted.

## Visible Light Photoactivity of a Mixed $\alpha$ -(Fe,Cr) $_2$ O $_3$ (0001) Surface

M.A. Henderson, S.E. Chamberlin, Y. Wang, T.C. Kaspar, P.V. Sushko and S.A. Chambers  
Fundamental and Computational Sciences Directorate  
Pacific Northwest National Laboratory  
Richland, WA 99352

### Introduction

The growing need for alternative energy sources has motivated researchers to find new materials that promote production of fuels using solar radiation. The majority of research in heterogeneous photocatalysis over the last four decades has been concentrated on study of TiO $_2$ , despite the fact that this material shows little utility as a ‘stand-alone’ solar photocatalyst. Pursuit of new solar photocatalytic materials has refocused effort toward more complex semiconducting oxides with ternary (and beyond) compositions. For example, Parkinson group’s<sup>1</sup> combinatorial searches for viable heterogeneous photoelectrocatalysts has revealed that various Fe-based mixed oxide compositions show promise as potential visible light photoelectrocatalysts. This project is dedicated to preparing well-characterized mixed Fe-containing oxide films and studying their photochemical properties under similar well-controlled conditions using ultrahigh vacuum (UHV) methodologies.

### Results

We have successfully coupled single crystal film growth synthesis, detailed UHV surface photochemical measurements and DFT theory to characterize the photochemical activity of mixed  $\alpha$ -(Fe,Cr) $_2$ O $_3$ (0001) thin films. In concept, hematite ( $\alpha$ -Fe $_2$ O $_3$ ) is a potential solar photocatalyst (bandgap of  $\sim$ 2.1 eV), but its performance is limited poor carrier dynamics. Groups have attempted to improve the photocatalytic properties of hematite through nanotexturing, doping or alloying the oxide. For example, mixing Cr into  $\alpha$ -Fe $_2$ O $_3$  decreases its bandgap and improves charge transport properties.<sup>2-5</sup> Wang et al.<sup>5</sup> calculated

the optical absorption spectra of  $\alpha$ -Fe $_2$ O $_3$ ,  $\alpha$ -FeCrO $_3$  and  $\alpha$ -Cr $_2$ O $_3$  using time dependent DFT (Figure 1). Our results conclude that mixing of Cr $^{3+}$  and Fe $^{3+}$  in the corundum structure contributed to the bandgap narrowing both through decoupling of the metal spin states resulting in significant spin polarization of the O 2p and Cr 3d valence band states and orbital broadening, and by generating new excitation pathways between occupied Cr 3d states (mixed with O 2p states) at the top of the mixed oxide’s valence band to unoccupied Fe 3d states.

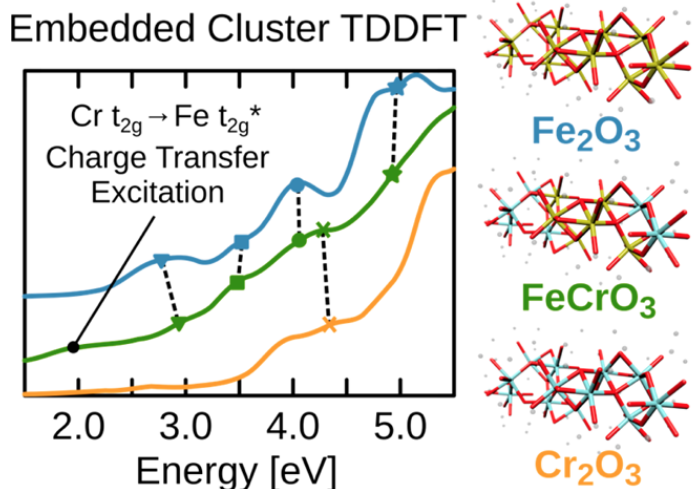


Figure 1: Calculated optical absorption spectra for  $\alpha$ -Fe $_2$ O $_3$ ,  $\alpha$ -FeCrO $_3$  and  $\alpha$ -Cr $_2$ O $_3$ .

Mixed oxide films of Fe and Cr oxide were grown by molecular beam epitaxy (MBE) on latticed matched  $\alpha$ - $\text{Al}_2\text{O}_3(0001)$ . The resulting films retained the corundum structure across the composition extremes (from  $\alpha$ - $\text{Fe}_2\text{O}_3$  to  $\alpha$ - $\text{Cr}_2\text{O}_3$ ) with no evidence for phase separation based on TEM. Chamberlin et al.<sup>2</sup> measured the

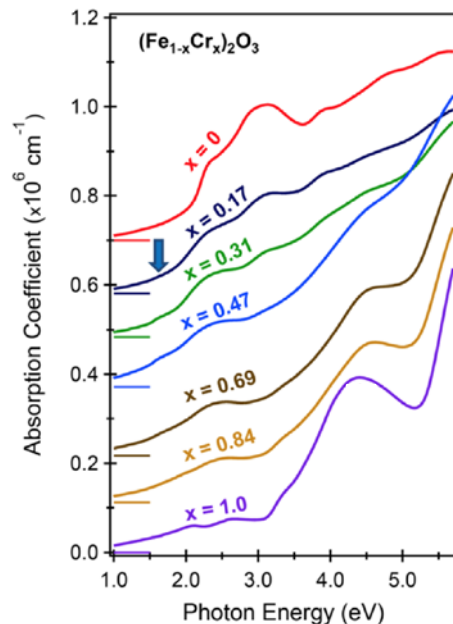


Figure 2: Optical absorption spectra of mixed  $\alpha$ - $(\text{Fe,Cr})_2\text{O}_3(0001)$  films grown on  $\alpha$ - $\text{Al}_2\text{O}_3(0001)$ .

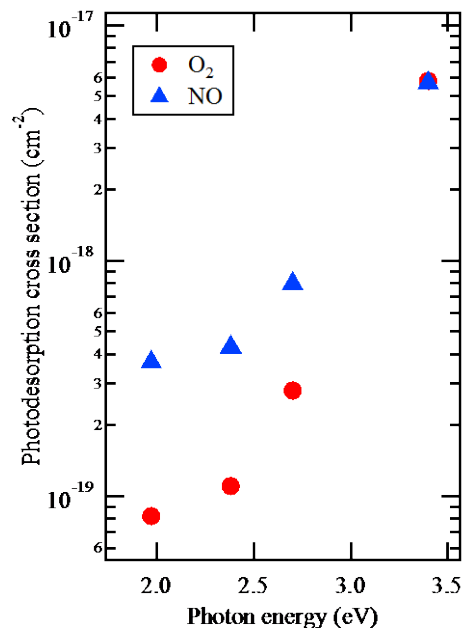


Figure 3: Photodesorption cross sections as a function of wavelength for  $\text{O}_2$  and  $\text{NO}$  adsorbed on a  $\alpha$ - $(\text{Fe,Cr})_2\text{O}_3(0001)$  film.

optical absorption spectra within the composition limits (Figure 2). Our photoabsorption data shows a redshift in the threshold to below 2 eV when Cr was incorporated in  $\alpha$ - $\text{Fe}_2\text{O}_3$ , in agreement with our theory.

$\text{NO}$  and  $\text{O}_2$  were used as probe molecules of the photochemical properties of a mixed  $\alpha$ - $(\text{Fe,Cr})_2\text{O}_3(0001)$  film containing a Fe:Cr ratio of  $\sim 1:0.3$ .<sup>6</sup> Light emitting diodes (LED) sources with wavelengths at 365, 460, 520 and 630 nm were employed. The trend in photodesorption cross sections for  $\text{O}_2$  (circles in Figure 3) matched what one would expect based on the photoabsorption spectrum for such a film (Figure 2). In particular, the  $\text{O}_2$  photodesorption cross section dropped significantly as the photon energy approached the bandgap energy. In contrast, the  $\text{NO}$  photodesorption cross section (triangles) decreased when the photon energy was decreased from the UV to the visible, but did not significantly change as the photon energy was decreased from above to below bandgap energy of  $\alpha$ - $\text{Fe}_2\text{O}_3$ . The photoactivities of  $\text{O}_2$  and  $\text{NO}$  near the bandgap energy validates the theoretical proposal that optical transitions between Cr and Fe provide new avenues for photochemistry not seen on  $\alpha$ - $\text{Fe}_2\text{O}_3$ . The greater activity for  $\text{NO}$  versus  $\text{O}_2$  at the bandgap energy suggests that specific surface configurations of these molecules are important in describing their photochemical activities.

### Future studies

- Photochemical studies of mixed  $\alpha$ - $(\text{Fe,Cr})_2\text{O}_3(0001)$  films grown on Pt(111).
- Growth and characterization of V-doped pure and mixed corundum oxides.
- Theory and experiment on the incorporation of  $\text{Fe}^{2+}$  in mixed  $\alpha$ - $(\text{Fe,Cr})_2\text{O}_3(0001)$  films.

## Acknowledgements

This work was supported by the U.S. Department of Energy's (DOE) Office of Basic Energy Sciences, Division of Chemical Sciences, Biosciences, and Geosciences, and was performed in part using the Molecular Science Computing Facility (MSCF) in the William R. Wiley Environmental Molecular Sciences Laboratory, a DOE national scientific user facility sponsored by the Department of Energy's Office of Biological and Environmental Research and located at the Pacific Northwest National Laboratory (PNNL). PNNL is operated by Battelle for DOE.

## References

1. (a) M. Woodhouse, G.S. Herman, B.A. Parkinson, *Chemistry of Materials* 17 (2005) 4318; (b) M. Woodhouse, B.A. Parkinson, *Chemical Society Reviews* 38 (2009) 197; (c) M. Woodhouse, B.A. Parkinson, *Chemistry of Materials* 20 (2008) 2495.
2. S.E. Chamberlin, Y. Wang, K. Lopata, T.C. Kaspar, A.W. Cohn, D.R. Gamelin, N. Govind, P.V. Sushko, S.A. Chambers, *Journal of Physics: Condensed Matter* 25 (2013) 392002.
3. E.A. Moore, *Physical Review B* 76 (2007) 195107.
4. C.S. Cheng, H. Gomi, H. Sakata, *Physica Status Solidi A* 155 (1996) 417.
5. Y. Wang, K. Lopata, S.A. Chambers, N. Govind, P.V. Sushko, *Journal of Physical Chemistry C* 117 (2013) 25504.
6. M.A. Henderson, *Journal of Physical Chemistry C*, to be submitted.

## DOE Sponsored Publications 2011-2014

1. Chambers, S.A., L. Qiao, T.C. Droubay, T.C. Kaspar, B.W. Arey and P.V. Sushko (2011). "Band Alignment, Built-In Potential, and the Absence of Conductivity at the LaCrO<sub>3</sub>/SrTiO<sub>3</sub>(001) Heterojunction." *Physical Review Letters* 107(20): 206802.
2. Henderson, M.A. (2011). "A surface science perspective on TiO<sub>2</sub> photocatalysis." *Surface Science Reports* 66(6-7): 185.
3. Mangham, A.N., N. Govind, M.E. Bowden, V. Shutthanandan, A.G. Joly, M.A. Henderson and S.A. Chambers (2011). "Photochemical Properties, Composition, and Structure in Molecular Beam Epitaxy Grown Fe-Doped and (Fe,N)-Codoped Rutile TiO<sub>2</sub>(110)." *Journal of Physical Chemistry C* 115(31): 15416.
4. Govind, N., K.A. Lopata, R.J. Rousseau, A. Andersen and K. Kowalski. (2011). "Visible Light Absorption of N-Doped TiO<sub>2</sub> Rutile Using (LR/RT)-TDDFT and Active Space EOMCCSD Calculations." *Journal of Physical Chemistry Letters* 2(21): 2696.
5. Du, Y., D.J. Kim, T.C. Kaspar, S.E. Chamberlin, I. Lyubinetsky and S.A. Chambers (2012). "In-situ imaging of the nucleation and growth of epitaxial anatase TiO<sub>2</sub>(001) films on SrTiO<sub>3</sub>(001)." *Surface Science* 606(17-18): 1443.
6. Franking, R., H. Kim, S.A. Chambers, A.N. Mangham and R.J. Hamers (2012). "Photochemical Grafting of Organic Alkenes to Single-Crystal TiO<sub>2</sub> Surfaces: A Mechanistic Study." *Langmuir* 28(33): 12085.
7. Henderson, M.A. (2012). "Visible light induced photodesorption of NO from the  $\alpha$ -Cr<sub>2</sub>O<sub>3</sub>(0001) surface." *Surface Science* 606(3-4): 505. (Corrigendum: *Surface Science*

606(17-18): 1467)

8. Kaspar, T.C., A. Ney, A.N. Mangham, S.M. Heald, Y. Joly, V. Ney, F. Wilhelm, A. Rogalev, F. Yakou and S.A. Chambers (2012). "Structure of epitaxial (Fe,N) codoped rutile  $\text{TiO}_2$  thin films by x-ray absorption." *Physical Review B* 86(3): 035322.
9. Qiao, L., H.L. Zhang, M.E. Bowden, V. Shutthanandan, R. Colby, Y. Du, B. Kabius, P. V. Sushko and S.A. Chambers (2013). "The impacts of cation stoichiometry and substrate surface quality on nucleation, structure, defect formation and intermixing in complex oxide heteroepitaxy –  $\text{LaCrO}_3$  on  $\text{SrTiO}_3(001)$ ." *Advanced Functional Materials* 23(23): 2953.
10. Sushko, P.V., L. Qiao, M. Bowden, T. Varga, G.J. Exarhos, F.K. Urban, D. Barton and S.A. Chambers (2013). "Multiband Optical Absorption Controlled by Lattice Strain in Thin-Film  $\text{LaCrO}_3$ ." *Physical Review Letters* 110(7): 077401.
11. Henderson, M.A. and I. Lyubinetzky (2013). "Molecular-Level Insights into Photocatalysis from Scanning Probe Microscopy Studies on  $\text{TiO}_2(110)$ ." *Chemical Reviews* 113(6): 4428.
12. Wang, Y., K.A. Lopata, S.A. Chambers, N. Govind and P.V. Sushko (2013). "Optical absorption and band gap reduction in  $(\text{Fe}_{1-x}\text{Cr}_x)_2\text{O}_3$  solid solutions: A first-principles study." *Journal of Physical Chemistry C* 117(48): 25504.
13. Qiao, L., H.Y. Xiao, S.M. Heald, M.E. Bowden, T. Varga, G.J. Exarhos, M.D. Biegalski, I.N. Ivanov, W.J. Weber, T. Droubay and S.A. Chambers (2013). "The impact of crystal symmetry on the electronic structure and functional properties of complex lanthanum chromium oxides." *Journal of Materials Chemistry C* 1(30): 4527.
14. Chamberlin, S.E., Y. Wang, K.A. Lopata, T.C. Kaspar, A. Cohn, D.R. Gamelin, N. Govind, Sushko, P.V. and S.A. Chambers (2013). "Optical Absorption and Spectral Photoconductivity in  $\alpha$ - $(\text{Fe}_{1-x}\text{Cr}_x)_2\text{O}_3$  Solid-Solution Thin Films." *Journal of Physics: Condensed Matter* 25(39): 392002.
15. Kaspar, T.C., S.E. Chamberlin and S.A. Chambers (2013). "Surface structure of  $\alpha$ - $\text{Cr}_2\text{O}_3(0001)$  after activated oxygen exposure." *Surface Science* 618: 159.
16. Kaspar, T.C., S.E. Chamberlin, M.E. Bowden, R.J. Colby, V. Shutthanandan, S. Manandhar, Y. Wang, P.V. Sushko and S.A. Chambers (2014). "Impact of lattice mismatch and stoichiometry on the structure and bandgap of  $(\text{Fe,Cr})_2\text{O}_3$  epitaxial thin films." *Journal of Physics: Condensed Matter*, in press.
17. Henderson, M.A. and M.E. Engelhard (2014). "Adsorption of Probe Molecules on the Mixed  $\alpha$ - $(\text{Fe,Cr})_2\text{O}_3(0001)$  Surface." *Journal of Physical Chemistry C*, submitted. (Invited, special issue in honor of Prof. John Hemminger's 65<sup>th</sup> birthday.)

# Structural Control and Dynamics of Excited State Cu(I) Diimine Complexes for Interfacial Photoinduced Charge Transfer and Other Solar Energy Conversion Systems

L. X. Chen,<sup>1,2</sup> J. Huang,<sup>1</sup> M. W. Mara,<sup>1,2</sup> M. R. Harpham,<sup>1</sup> N. M. Dimitrijevic,<sup>1</sup> K. Fransted,<sup>1</sup> in Collaboration with Groups of R. Thummel,<sup>3</sup> E. Jakubikova,<sup>4</sup> Jean-Pierre Sauvage<sup>5</sup> and Fraser Stoddart<sup>2</sup>

<sup>1</sup>Chemical Sciences and Engineering Division, Argonne National Laboratory, Lemont, IL 60439

<sup>2</sup>Department of Chemistry, Northwestern University, Evanston, IL, 60208

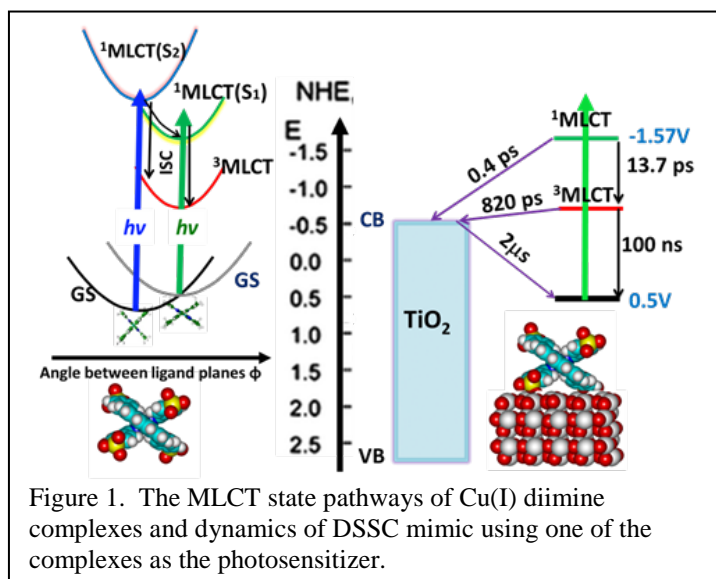
<sup>3</sup>Department of Chemistry, University of Houston, Houston, Texas 77204

<sup>4</sup>Department of Chemistry, North Carolina State University, Raleigh, NC 27695

<sup>5</sup>Institut de Chimie, Université de Strasbourg, 67000 Strasbourg (France)

Photophysical and photochemical properties of Cu(I) diimine complexes have been studied by both optical and X-ray transient absorption spectroscopies, from which the correlations of the ground and excited state structures with the excited metal-to-ligand-charge-transfer (MLCT) state properties have been established with two main structural factors: 1) the solvent accessibility to the copper center in the MLCT state and 2) the angle between the two aromatic conjugated ligand planes  $\phi$  based on studying a series of Cu(I) bis-phenanthroline complexes with systematically changing steric hindrance at the 2, 9 positions. The first factor affects the <sup>3</sup>MLCT state lifetime from a few ps for a fully exposed copper center to  $> 1\mu\text{s}$  for a completely shielded copper center. The second factor affect the intersystem crossing (ISC) time that is faster in the pseudotetrahedral conformation than in the flattened geometry. Based on these findings, we extended our studies to other types of Cu(I) complexes in collaboration with Randy Thummel and started a project that will investigate the role of structural dynamics in dye sensitized solar cell (DSSC) mimics in collaboration with Profs. Sauvage and Stoddart. Meanwhile, we also collaborate with Prof. Jakubikova to calculate the effects of the linkers in terms of electronic coupling between the Cu(I) complexes with TiO<sub>2</sub> nanoparticles.

Photoinduced electron transfer (ET) from transition metal complexes into semiconductor nanoparticles (NPs) has been studied extensively in recent decades on account of its relevance to photocatalysis, solar fuel generation and DSSCs most commonly using Ru polypyridyl complex-sensitized TiO<sub>2</sub> NP electrodes, which provide a relatively high light-to-electron energy conversion efficiency (~11%). The high cost and low abundance of Ru, however, inhibit large scale applications of such DSSCs. Therefore, dye sensitizers of abundant first-row metal complexes have long



been sought, such as metalloporphyrin sensitizer-based DSSCs. Polypyridyl Cu(I) diimine complexes are considered as a replacement for Ru polypyridyl complex sensitizers due to their striking similarities in absorption spectra and photophysics. In contrast with Ru<sup>II</sup> polypyridyl complexes, the MLCT states of Cu<sup>I</sup>-diimine complexes undergo a “pseudo Jahn-Teller” distortion with significant structural re-organizations and exhibit solvent-dependent lifetimes. More importantly, the ISC rate/yield and hence the <sup>1</sup>MLCT state lifetime can be influenced by the coordination geometry of the copper center as well as solvent accessibility (Figure 1). Utilizing the information from our studies on the MLCT state dynamics, we are able to select the Cu(I) diimine complexes with long lived <sup>3</sup>MLCT state lifetime due to the blockage of the solvent access to the copper center, and with relatively long-lived <sup>1</sup>MLCT state rate to gain extra driving force, so that the electron injection to TiO<sub>2</sub> can be efficient because of the higher driving force. Thus, there will be two possible routes to transfer an electron from the photoexcited Cu<sup>I</sup> polypyridyl complex to the TiO<sub>2</sub> NPs: 1) from the <sup>1</sup>MLCT state with a higher energy and ET driving force but very short excited-state lifetime (i.e. ~10 ps or shorter), and 2) from the <sup>3</sup>MLCT state with a lower energy and ET driving force but much longer excited-state lifetime (a few ns to a few hundred ns). [Cu<sup>I</sup>(dppS)<sub>2</sub>]<sup>+</sup> has been selected in our studies using both dynamics and structural methods, and parallel studies are also performed on two other complexes with different linkers (not shown).

A highly efficient and ultrafast interfacial electron injection from the <sup>1</sup>MLCT state of surface bound [Cu<sup>I</sup>(dppS)<sub>2</sub>]<sup>+</sup> to TiO<sub>2</sub> NPs has been observed in EPR, TA and XTA studies with the charge separation and recombination dynamics correlated with the ground and excited state structures. The studies confirmed the formation of [Cu<sup>II</sup>(dppS)<sub>2</sub>]<sup>2+</sup>, resulting from an efficient charge transfer process in [Cu<sup>I</sup>(dppS)<sub>2</sub>]<sup>+</sup>/TiO<sub>2</sub> where electrons are injected into TiO<sub>2</sub> NPs. The flattened tetrahedral geometry of the ground state [Cu<sup>I</sup>(dppS)<sub>2</sub>]<sup>+</sup> in the hybrid system as detected by the XTA effectively prolongs the ISC time to enable ET from the <sup>1</sup>MLCT state with a rate constant of 0.4 ps. In comparison, the electron injection rate from <sup>3</sup>MLCT state is longer than several hundred ps. Two other similar Cu(I) diimine complexes with polyethyloxy loops to stabilize the Cu(II) ligation in the MLCT state as well as different linkers have been investigated by both experimental and computational methods in collaboration with Prof. Jakubikova. Studies in tuning the HOMO-LUMO levels of these complexes by structural constraints will be conducted in the future. This research not only demonstrates the structural control necessary for effective ET processes, but also shows the potential of using low cost copper complexes for the dye sensitized solar cells in the future.

In the second part of the presentation, the progress made on X-ray transient absorption spectroscopy will be briefly shown featuring the following aspects: 1) the excited state dynamics of transition metal complexes for solar thermal energy conversion where a transient structure of the intermediate from photoexcitation has been shown to differ from that of DFT calculations based on thermal equilibrium, 2) the environment effect of CO dissociation with heme proteins and iron porphyrins mimicking catalytic reactions, where the feasibility of XTA on protein samples have been demonstrated, and 3) highlights of instrumentation improvements with much higher data quality and the ease of experiments, as well as a variety of sample environments, such as low temperature environment and thin film samples. We expect that the XTA method will be much more commonly used in solar energy research, especially for solar fuel catalytic reactions. However, the new experimental detection schemes will need to be developed.

## DOE Sponsored Publications 2011-2014 (Acknowledge this grant)

1. Interplays of Excited State Structures and Dynamics in Copper(I) Diimine Complexes: Implications and Perspectives, M. W. Mara, K. A. Fransted, L.X. Chen, (Invited) *Coord. Chem. Rev.*, submitted (2014).
2. New Insight into Metalloporphyrin Excited State Structures and Axial Ligand Binding from X-ray Transient Absorption Spectroscopic Studies, M. W. Mara, M. L. Shelby, L. X. Chen, (Invited) *Coord. Chem. Rev.*, submitted (2014).
3. Recent Advances of Ultrafast X-ray Spectroscopy in Chemical Sciences, L. X. Chen, X. Zhang, M. L. Shelby, (Invited Review) *Chem. Sci.* submitted, (2014).
4. Effects of Intramolecular Exciton Dynamics in Charge-Transfer Polymer Organic Photovoltaic Devices, B. S. Rolczynski, J. M. Szarko, H. J. Son, Y. Liang, L. Yu, L. X. Chen, *J. Phys. Chem. Lett.* submitted (2014).
5. Photovoltaic Functions of Intramolecular Charge Transfer Copolymers: Exciton and Charge Transfer Dynamics Studies of PTB7, Jodi M. Szarko, Brian S. Rolczynski, Sylvia J. Lou, Tao Xu, Luping Yu, Lin X. Chen, *Adv. Func. Mater.*, 24, 10-26 (2014).
6. Photochemical Processes Revealed by X-ray Transient Absorption Spectroscopy, L. X. Chen, X. Zhang, (Invited Perspective) *J. Phys. Chem. Lett.* 4, 4000–4013 (2013)
7. Electronic and Nuclear Structural Snapshots in Ligand Dissociation and Recombination Processes of Iron Porphyrin in Solution: A Combined Optical/X-ray Approach, M. W. Mara, A. B. Stickrath, M. L. Shelby, M. R. Harpham, J. Huang, X. Zhang, L. X. Chen *J. Phys. Chem. B* 117, 14089–14098 (2013).
8. Detection of a charge-separated catalyst precursor state in a linked photosensitizer-catalyst assembly, A. Mukherjee, O. Kokhan, J. Huang, J. Niklas, L. X. Chen, D. M. Tiede, K. L. Mulfort, *Phys.Chem.Chem.Phys.*, 15, 21070-21076, (2013).
9. X-ray transient absorption structural characterization of the <sup>3</sup>MLCT triplet excited state of cis-[Ru(bpy)<sub>2</sub>(py)<sub>2</sub>]<sup>2+</sup>, E. Borfecchia, C. Garino, L. Salassa, T. Ruiu, D. Gianolio, X. Zhang, K. Attenkofer, L. X. Chen, R. Gobetto, P. J. Sadler, C. Lamberti, *Dalton Trans.* 42, 6564-6571 (2013).
10. Interrogating Photogenerated Higher Valence States of a Water Oxidation Catalyst in an Acceptor-Chromophore-Catalyst Triad, M. T. Vagnini, M. W. Mara, M. R. Harpham, J. Huang, M. L. Shelby, L. X. Chen, M. R. Wasielewski, *Chem. Sci.* 4, 3863-3873 (2013).
11. Photodissociation Structural Dynamics of Triruthenium Dodecacarbonyl Investigated by X-Ray Transient Absorption Spectroscopy, M. R. Harpham, A. B. Stickrath, X. Zhang, J. Huang, M. W. Mara, L. X. Chen, D.-J. Liu, *J. Phys. Chem. A.* (Invited) 117, 9807–9813 (2013).
12. Femtosecond X-ray Absorption Spectroscopy at a Hard X-ray Free Electron Laser: Application to Spin Crossover Dynamics, H. T. Lemke, C. Bressler, L. X. Chen, D. M. Fritz, K. J. Gaffney, A. Galler, W. Gawelda, K. Haldrup, R. W. Hartsock, H. Ihee, J. Kim, J. H. Lee, M. M. Nielsen, A. B. Stickrath, W. Zhang, D. Zhu, M. Cammarata, *J. Phys. Chem. A*, 117, 735–740 (2013).

13. Characterization and modeling of an amorphous iridium oxide water-oxidation catalyst with a carbon admixture, J. D. Blakemore, M. W. Mara, M. N. Kushner-Lenhoff, N. D. Schley, S. J. Konezny, I. Rivalta, C. F. A. Negre, R. C. Snoeberger, J. Huang, A. Stickrath, M. L. Parr, L. X. Chen, D. M. Tiede, V. S. Batista, G. W. Brudvig, R. H. Crabtree, *Inorg. Chem.* 52, 1860-1871 (2013).
14. Ultrafast Structural Dynamics of bis(2,9-di-phenyl-1,10-phenanthroline)copper(I) Using X-ray Transient Absorption Spectroscopy, M. W. Mara, N. E. Jackson, J. Huang, A. B. Stickrath, M. R. Harpham, K. M. Haldrup, N. A. Gothard, L. X. Chen, *J. Phys. Chem. B.* 117, 1921–1931 (2013).
15. Chapter 12. X-ray Transient Absorption Spectroscopy for Solar Energy Research, Lin X. Chen (Invited book chapter) in “Dynamics of interfacial electron and excitation transfer in solar energy conversion: theory and experiment”, in “Solar Energy Conversion: Dynamics of Interfacial Electron and Excitation Transfer” P. Piotrowiak, Ed., Royal Chemical Society, Cambridge, England (2013), pp. 337-370.
16. Detailed Transient Heme Structures of Mb-CO in Solution after CO Dissociation: An X-ray Transient Absorption Spectroscopic Study, A. B. Stickrath, M. W. Mara, J. V. Lockard, M. R. Harpham, X. Zhang, K. Attenkofer, L. X. Chen, *J. Phys. Chem. A.* (Invited) 117, 4705-4712 (2013).
17. Highly Efficient Ultrafast Electron Injection from the Singlet MLCT Excited State of Cu(I)-Diimine Complexes to TiO<sub>2</sub> Nanoparticles, J. Huang, O. Buyukcakir, M. W. Mara, A. Coskun, N. M. Dimitrijevic, G. Barin, O. Kokhan, A. B. Stickrath, R. Ruppert, D. M. Tiede, J. F. Stoddart, J.-P. Sauvage, L. X. Chen, *Angew. Chem. Intl. Ed.* 51, 12711–12715 (2012).
18. Photodriven Charge Separation Dynamics in CdSe/ZnS Core/ Shell Quantum Dot/Cobaloxime Hybrid for Efficient Hydrogen Production, J. Huang, K. L. Mulfort, P. Du, L. X. Chen, *J. Am. Chem. Soc.* 134, 16472–16475 (2012).
19. Structure and Activity of Photochemically Deposited “CoPi” Oxygen Evolving Catalyst on Titania, R. S. Khnayzer, M. W. Mara, J. Huang, L. X. Chen, F. N. Castellano, *ACS Catalysis*, 2, 2150–2160 (2012).
20. X-ray Transient Absorption and Picosecond IR Spectroscopy of Fulvalene(tetracarbonyl)diruthenium on Photoexcitation, M. R. Harpham, S. C. Nguyen, Z. Hou, J. C. Grossman, C. B. Harris, M. W. Mara, A. B. Stickrath, Y. Kanai, A. M. Kolpak, D. Lee, D.-J. Liu, J. P. Lomont, K. Moth-Poulsen, N. Vinokurov, L. X. Chen, K. P. C. Vollhardt, *Angew. Chem. Intl. Ed.* 51, 7692–7696 (2012).
21. Ground-State and Excited-State Structures of Tungsten–Benzylidyne Complexes, B. M. Lovaasen, J. V. Lockard, B. W. Cohen, S. Yang, X. Zhang, C. K. Simpson, L. X. Chen, M. D. Hopkins, *Inorg. Chem.* 51, 5660 – 5670 (2012).
22. Ultrafast Intramolecular Exciton Splitting Dynamics in Isolated Low Bandgap Polymers and Their Implications in Photovoltaic Materials Design, B. S. Rolczynski, J. M. Szarko, H. J. Son, Y. Liang, L. Yu, L. X. Chen, *J. Am. Chem. Soc.* 134, 4142–4152 (2012).

23. Strong Steric Hindrance Effect on Excited State Structural Dynamics of Cu(I) Diimine Complexes, N. A. Gothard, M. W. Mara, J. Huang, J. M. Szarko, B. S. Rolczynski, L. X. Chen, *J. Phys. Chem. A.* 116, 1984–1992 (2012).
24. Examining the Effect of the Dipole Moment on Charge Delocalization in Donor-Acceptor Polymers for Organic Photovoltaic Applications, Bridget Carsten, J. M. Szarko, H. Jung Son, W. Wang, B. S. Rolczynski, S. J. Lou, L. X. Chen, L. Yu, *J. Am. Chem. Soc.* 133, 20468–20475 (2011).
25. Effects of Additives on the Morphology of Solution Phase Aggregates Formed by Active Layer Components of High-Efficiency Organic Solar Cells, S. J. Lou, J. M. Szarko, T. Xu, L. Yu, T. J. Marks, L. X. Chen, *J. Am. Chem. Soc.* 133, 20661–20663 (2011).
26. Development of high-repetition-rate laser pump/x-ray probe methodologies for synchrotron facilities, A. M. March, A. B. Stickrath, G. Doumy, E. P. Kanter, B. Krässig, S. H. Southworth, K. Attenkofer, C. A. Kurtz, L. X. Chen, L. Young, *Rev. Sci. Instr.* 82, 073110 (2011).
27. Nanoscale Structure, Dynamics and Power Conversion Efficiency Correlations in Multiblock Oligomer and Polymer Based Solar Cell, J. M. Szarko, B. S. Rolczynski, J. Guo, L. X. Chen, *Nano Reviews*, 2, 7249 (2011).
28. Current trends in the optimization of low bandgap polymers used in photovoltaic devices, J. M. Szarko, J. Guo, B. S. Rolczynski, L. X. Chen, *J. Mat. Chem.* (Invited Highlight) 21, 7849–7857 (2011).
29. Local structure of photoexcited bimetallic complexes refined by quantitative XANES analysis, G. Smolentsev, S. E. Canton, J. V. Lockard, V. Sundström and L. X. Chen, *J. Elec. Spec. Rel. Phenom.*, 184, 125–128 (2011).
30. Coherence in Metal-Metal-to-Ligand-Charge-Transfer Transitions of a Dimetallic Complex Revealed by Ultrafast Transient Absorption Anisotropy, S. Cho, M. W. Mara, X. Wang, J. V. Lockard, A. A. Rachford, F. N. Castellano, L. X. Chen, *J. Phys. Chem. A.*, 115, 3990–3996 (2011).
31. Length-Dependent Self-Assembly of Oligothiophene Derivatives in Thin Films: Implications in Photovoltaic Material Fabrications, B. S. Rolczynski, J. M. Szarko, B. Lee, J. Strzalka, J. Guo, Y. Liang, L. Yu, L. X. Chen, *J. Mat. Chem.* 26, 296–305 (2011).
32. Visualizing interfacial charge transfer in dye sensitized nanoparticles using X-ray transient absorption spectroscopy, X. Zhang, G. Smolentsev, J. Guo, K. Attenkofer, C. Kurtz, G. Jennings, J. V. Lockard, A. B. Stickrath, L. X. Chen, *J. Phys. Chem. Lett.* 2, 628 – 632 (2011).



## *Posters*



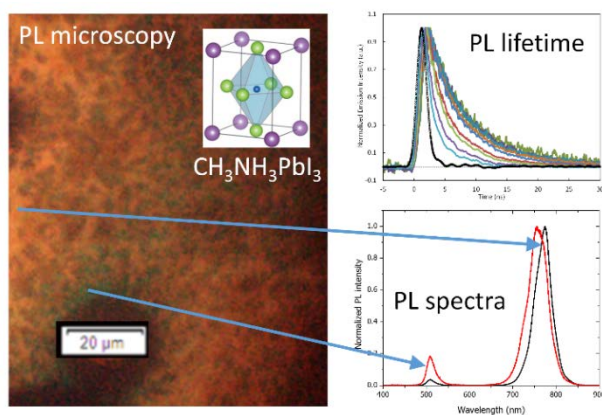
## Molecular Origins of Electronic Structure in Inorganic Systems for Solar Photoconversion

Robert J. Stewart, Christopher Grieco, Adam D. Rimshaw, and John B. Asbury  
Department of Chemistry  
The Pennsylvania State University  
University Park, PA 16802

The influences that molecular species have on the electronic structure and charge recombination mechanisms of inorganic semiconducting heterostructures are investigated using time-resolved infrared spectroscopy in conjunction with electronic spectroscopy and microscopy. Two chemical systems of interest for solar photoconversion are investigated in parallel.

In the first example, organic-inorganic interactions are examined in ligand exchanged lead sulfide nanocrystals by probing the molecular species on nanocrystal surfaces that are associated with the formation of long-lived transient electronic states following optical excitation of their bandgap transitions. The influence of quantum confinement on the electronic states is investigated through temperature and size-dependent studies of ligand exchanged lead sulfide nanocrystals densely packed into solid films. Optical absorption and photoluminescence spectra of the corresponding films are used to provide complementary information about the near-edge electronic structure of the nanocrystals. Together, these studies provide a comprehensive view of the molecular origins of electronic states in the nanocrystal assemblies that are principally responsible for charge transport and mediation of charge recombination following bandgap excitation.

In the second example, nanostructured organohalide lead perovskites are examined in an effort to elucidate fundamental mechanisms of photoconversion in these systems that exhibit surprisingly high photoluminescence quantum yields. The high quantum yields suggest that the perovskites may function close to the radiative recombination limit when used for solar photoconversion. A study was undertaken to examine the hypothesis that organohalide perovskite materials exhibit high radiative quantum yields because the ionic nature of the components discourages the formation of dangling covalent bonds and corresponding mid-gap states that serve as recombination centers in other inorganic chemical systems. Furthermore, it was hypothesized that impurities give rise to electronic species with bandgaps wider than the organohalide perovskites and therefore contribute scattering centers rather than charge recombination centers. The compositions of organohalide perovskite films were intentionally varied and the corresponding transient electronic and vibrational spectra were compared to photoluminescence microscopy results, indicating that perovskite materials can exhibit remarkably clean band-edge electronic structures despite containing a significant fraction of lead halide impurities.



Transient absorption, photoluminescence and microscopy are used to examine the influence that inorganic impurities have on the band edge electronic structure of organohalide perovskites.

## Linker Rectifiers for Covalent Attachment of Catalysts to Semiconductor Surfaces

Wendu Ding, Christian Negre, Laura J. Allen, Rebecca L. Milot,  
Gary W. Brudvig, Charles A. Schmuttenmaer, Robert H. Crabtree and Victor S. Batista  
Energy Sciences Institute and Department of Chemistry  
Yale University, New Haven, CT 06520-8107

Linkers that favor rectification of interfacial electron transfer are likely to be required for efficient photo-driven catalysis of multi-electron reactions at electrode surfaces. Design principles are discussed, together with the synthesis and characterization of a specific pair of molecular linkers, related by inversion of the direction of an amide bond at the heart of the molecule. The linkers have a terpyridyl group that can covalently bind Mn as in a well-known water oxidation catalyst and an acetylacetonate group that allows attachment to TiO<sub>2</sub> surfaces. The

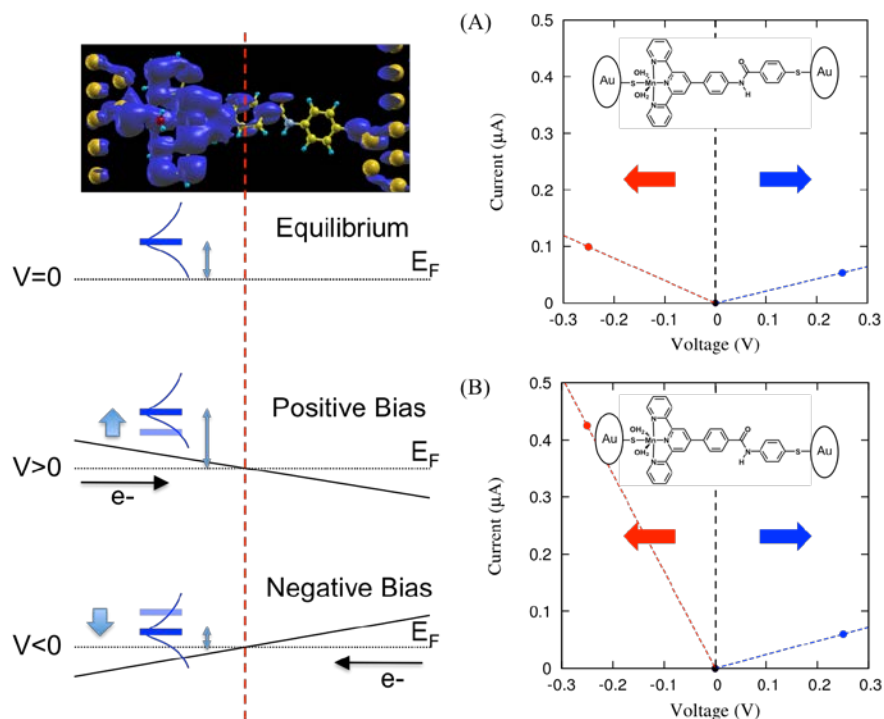


**Figure 1:** (Left) Schematic representation of the state responsible for electron transport (LUMO) and alignment relative to the Fermi level under equilibrium ( $V=0$ ), positive ( $V>0$ ) and negative ( $V<0$ ) bias. (Right) Calculated I-V curves for Mn-terpy-L1 (A) and Mn-terpy-L2 (B). The red and blue lines represent the current under negative and positive bias, respectively. Mn-terpy-L2 shows significant rectification.

appropriate choice of the sense of the amide linkage yields directionality of interfacial electron transfer, essential to enhance electron injection and slow back-electron transfer. Support comes from electron paramagnetic resonance and terahertz spectroscopic measurements, as well as computational modeling characterizing the asymmetry of electron transfer properties.

1. *J. Phys. Chem. C* (2014) in press. High Conductance Conformers in Histograms of Single-Molecule Current-Voltage Characteristics. W. Ding, C.F.A. Negre, L. Vogt and V.S. Batista.
2. *ChemPhysChem* (2014) in press. Linker Rectifiers for Covalent Attachment of Transition Metal Catalysts to Metal-Oxide Surfaces. W. Ding, C.F.A. Negre, J.L. Palma, A.C. Durrell, L.J. Allen, K.J. Young, R.L. Milot, C.A. Schmuttenmaer, G.W. Brudvig, R.H. Crabtree and V.S. Batista.
3. *J. Chem. Theory Comput.* (2014) submitted. Single Molecule Rectification Induced by the Asymmetry of a Single Frontier Orbital. W. Ding, C.F.A. Negre, L. Vogt, and V.S. Batista.

## Photo-Induced Electron Transfer and Electrons in Ionic Liquids

Edward W. Castner, Jr., Min Liang, Boning Wu, Luiz Felipe O'Faria, and Sufia Khatun

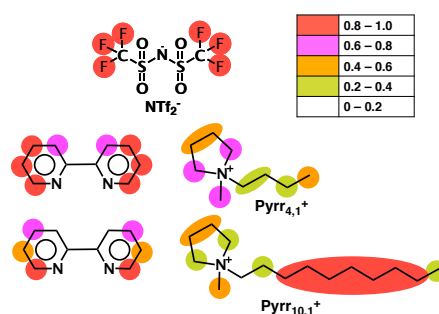
Department of Chemistry and Chemical Biology

Rutgers, The State University of New Jersey

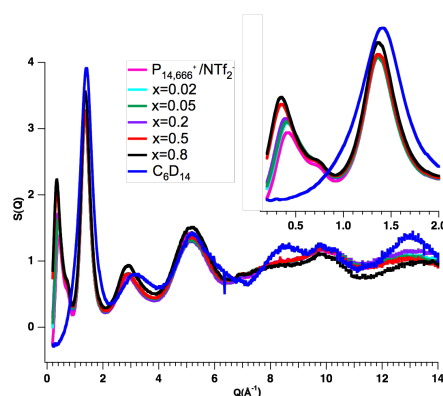
Piscataway, NJ 08854

Productive collaborations continue between the DOE-funded SISGR research groups (Blank; Minnesota; Castner; Rutgers; Margulis, Iowa; Maroncelli, Penn State; and Wishart, Brookhaven). Research focuses on how the unique solvation and structural properties of ionic liquids (ILs) affect photo-induced electron-transfer reaction rates and mechanisms. The Blank, Margulis and Wishart groups are comparing experiments and theory for electrons in ionic liquids generated photochemically and radiolytically.

The Castner group continues to study solvation properties using nuclear Overhauser effect spectroscopy (HOESY and ROESY) to study the interactions between the  $^1\text{H}$  atoms of the  $\text{Ru}^{2+}(\text{bpy})_3$  photosensitizer with the cationic  $^1\text{H}$  atoms and the  $^{19}\text{F}$  atoms of the  $\text{NTf}_2^-$  anion, as shown in the figure at right. The color scale indicates the strength of interactions between the  $\text{NTf}_2^-$  anion and both the bpy ligand protons and those on the 1-alkyl-1-methylpyrrolidinium cations. Note the significant difference between the weak butyl vs. strong decyl interactions with the anion.



Tetradecyltrihexylphosphonium is one of the most hydrophobic of the common IL cations; this leads to broad miscibility alkanes. The liquid structure from high energy X-ray scattering reveals the typical pattern of three intermolecular scattering peaks in the  $q$ -range  $< 2.0 \text{ \AA}^{-1}$ , with the peak at  $0.37 \text{ \AA}^{-1}$  indicating intermediate range order on the 15-20  $\text{\AA}$  scale. The nearest neighbor and next-neighbor peaks are virtually unaffected by dilution with hexane up to 80% mole fraction while the intermediate order peak indicates hydrophobic domain expansion to 25  $\text{\AA}$ .

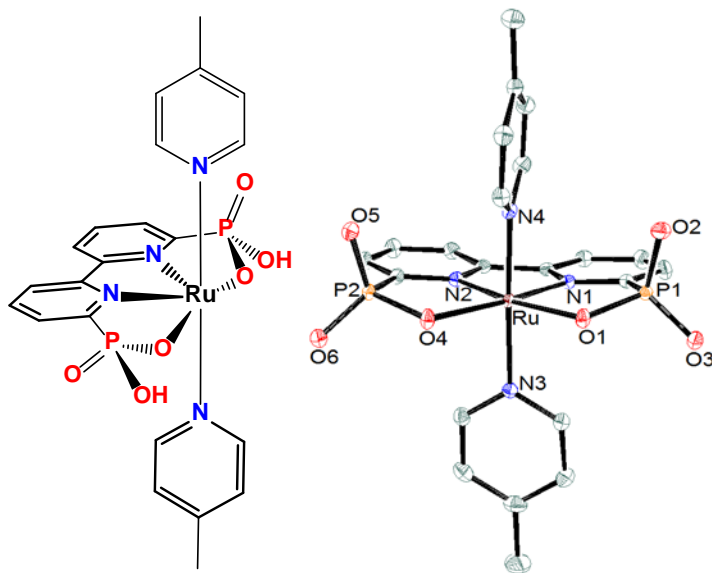


Collaborations between the Castner, Margulis, Maroncelli and Wishart groups show that photo-excited states are reductively quenched by ILs where the electron donors are either cyanate anions such as  $\text{SeCN}^-$ ,  $\text{SCN}^-$  and  $^-\text{C}(\text{CN})_3$  or  $\text{N}$ -alkyl- $\text{N}'$ , $\text{N}'$ -dimethylaminopyridinium cations. We are studying bimolecular photo-induced from both the anionic and cationic donors to a range of substituted anthracene species to vary the free energy for electron-transfer through the normal, barrierless and inverted regimes. We are reconciling evidence for polar vs. non-polar domains observed in the bulk IL structures with observed bimolecular electron-transfer reaction dynamics.

## Molecular Water Oxidation Catalysis: Homogeneous vs Heterogeneous

Javier J. Concepcion, Etsuko Fujita, and James T. Muckerman  
Chemistry Department  
Brookhaven National Laboratory  
Upton, NY 11973

Water oxidation to oxygen is an oxidative half reaction in natural photosynthesis that created the source of most of the energy we use today. It is also anticipated to be (and it has to be) the source of most of the energy we use in the future through artificial photosynthesis. For the latter, one of the main challenges is the development of efficient and robust water oxidation catalysts. In this presentation, water oxidation catalysis by ruthenium complexes with two types of tetradentate ligands (2,2'-bipyridine-6,6'-dicarboxylic acid, bda and 2,2'-bipyridine-6,6'-diphosphonic acid, bpa) will be discussed. Water oxidation catalysts of the type  $[\text{Ru}(\text{bda})(\text{L})_2]$  (L is 4-picoline (pic), or isoquinoline (isq)), as well as their mechanism for water oxidation, have been reported by Sun and coworkers. Nevertheless, unlikely 20- and 19-electron intermediates were proposed in the catalytic cycle. Here we revisit the mechanism for water oxidation by these catalysts based on electrochemistry, X-ray crystallography and well established inorganic and organometallic chemistry principles. We find that these catalysts become seven coordinate species after oxidation to the Ru(IV) level and oxidize water. In addition, a comparison between the two types of systems in solution and bound to metal-oxide electrodes is made with respect to catalytic performance. This comparison sheds light on the mechanism by which these complexes oxidize water in a true solar cell configuration.



# Relating Structure and Photoelectrochemical Properties: Electron Injection by Structurally and Theoretically Characterized Transition-Metal-Doped Polyoxotitanate Nanoparticles

Philip Coppens, Yang Chen, Katarzyna N. Jarzemska, and Elzbieta Trzop  
Chemistry Department, University at Buffalo, State University of New York  
Buffalo, NY, 14260-3000

Although a large number of sensitized polyoxotitanate clusters have been reported, detailed information on the electrochemical properties of fully structurally defined nanoparticles have not yet been reported. Bridging of the gap between structure and electrochemical properties would allow a systematic analysis of the relation between the interfacial geometry, electronic structure and electron injection into the nanoparticles. We have synthesized a series of transition-metal doped polyoxotitanate nanoparticles, determined their structure and calculated their electronic

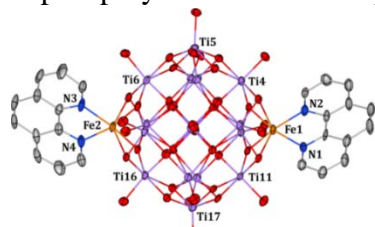


**Fig. 1. Molecular structure of (1) hydrogen atoms and (O<sup>i</sup>)Pr groups are omitted for clarity; 50% probability ellipsoids).**

properties. They include manganese-doped  $\text{Ti}_{28}\text{MnO}_{38}(\text{OEt})_{40}\text{H}_2$ ,  $\text{Ti}_{14}\text{MnO}_{16}(\text{OEt})_{28}\text{H}_2$ ,  $(\text{Ti}_{13}\text{Mn}_4\text{O}_{16}[\text{MeC}(\text{CH}_2\text{O})_3]_4(\text{OEt})_{12}\text{Br}_4)_\infty$ , a series of  $\text{Ti}_{11}$  cluster of composition  $\text{Ti}_{11}(\text{XY})\text{O}_{14}(\text{O}^i\text{Pr})_{17}$  with X= Co, Mn and Fe, and Y= Cl, Br and I. Especially for the Mn and Fe complexes a significant reduction of the bandgap is observed, leading to absorption in the visible region.

Of particle interest are a series on nano particles of which  $\text{Ti}_{17}\text{O}_{28}(\text{O}^i\text{Pr})_{16}[\text{Fe-phen}]_2$  (phen-phenanthroline) (1) (Fig. 1) and  $\text{Ti}_{11}(\text{FeBr})\text{O}_{14}(\text{O}^i\text{Pr})_{17}$ (2) are the prototypes. (1) is a member of a doubly-doped series of nanoclusters in which the phenanthroline is attached to the surface-located transition metal atom. Its visible spectrum in dichloromethane solution shows a series of absorption bands in the 400-900 nm region. Theoretical calculations show the bands of (1) in increasing wavelength order to correspond to metal-to-core charge transfer (MCCT), metal-to-ligand charge transfer (MLCT) and *d-d* metal-atom transitions. Exposure of a thin layer of the sample to light in a photoelectrochemical cell produces an anodic electric current in the 400~640 nm region. The calculations confirm the MCCT nature of the transition in this region. Complex (2) similarly produces an anodic current (Fig. 2). (1) and (2) have occupied Fe *d*-  $\beta$  orbitals located within the main bandgap

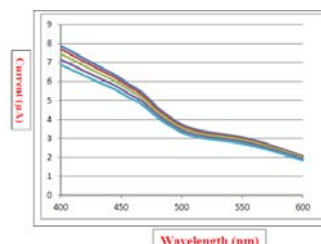


**Fig. 2 Current ( $\mu\text{A}$ ) vs. wavelength (nm) of (2). (Dark current not subtracted.)**

(Fig. 3), leading to Fe-Ti injection in the visible region. Other complexes will be discussed. We would like to thank Prof. D.F. Watson and J.N. Nasca of our Department for assistance with the electrochemical measurements.

## References.

- (1) Chen, Y.; Sokolow, J.; Trzop, E.; Chen, Y.-S.; Coppens, P. *J. Chin. Chem. Soc.* **2013**, *60*, 887.
- (2) Chen, Y.; Trzop, E.; Makal, A. M.; Chen, Y.-S.; Coppens, P. *Dalton Trans.* **2014**, 3839
- (3) Chen, Y.; Trzop, E.; Sokolow, J. D.; Coppens, P. *Chem. Eur. J.* **2013**, 16651.
- (4) Jarzemska, K. N.; Chen, Y.; Nasca, J. N.; Trzop, E.; Watson, D. F.; Coppens, P. *Submitted* **2014**.
- (5) Coppens, P., Chen, Y., Trzop, E. *Chem. Rev.* **2014**. In press

properties. They include manganese-doped  $\text{Ti}_{28}\text{MnO}_{38}(\text{OEt})_{40}\text{H}_2$ ,  $\text{Ti}_{14}\text{MnO}_{16}(\text{OEt})_{28}\text{H}_2$ ,  $(\text{Ti}_{13}\text{Mn}_4\text{O}_{16}[\text{MeC}(\text{CH}_2\text{O})_3]_4(\text{OEt})_{12}\text{Br}_4)_\infty$ , a series of  $\text{Ti}_{11}$  cluster of composition  $\text{Ti}_{11}(\text{XY})\text{O}_{14}(\text{O}^i\text{Pr})_{17}$  with X= Co, Mn and Fe, and Y= Cl, Br and I. Especially for the Mn and Fe complexes a significant reduction of the bandgap is observed, leading to absorption in the visible region.

Of particle interest are a series on nano particles of which  $\text{Ti}_{17}\text{O}_{28}(\text{O}^i\text{Pr})_{16}[\text{Fe-phen}]_2$  (phen-phenanthroline) (1) (Fig. 1) and  $\text{Ti}_{11}(\text{FeBr})\text{O}_{14}(\text{O}^i\text{Pr})_{17}$ (2) are the prototypes. (1) is a member of a doubly-doped series of nanoclusters in which the phenanthroline is attached to the surface-located transition

metal atom. Its visible spectrum in dichloromethane solution shows a series of absorption bands in the 400-900 nm region. Theoretical calculations show the bands of (1) in increasing wavelength order to correspond to metal-to-core charge transfer (MCCT), metal-to-ligand charge transfer (MLCT) and *d-d* metal-atom transitions. Exposure of a thin layer of the sample to light in a photoelectrochemical cell produces an anodic electric current in the 400~640 nm region. The calculations confirm the MCCT nature of the transition in this region. Complex (2) similarly produces an anodic current (Fig. 2). (1) and (2) have occupied Fe *d*-  $\beta$  orbitals located within the main bandgap

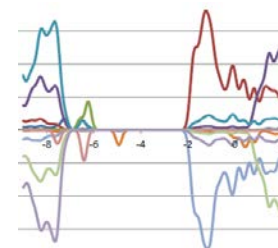


**Fig. 3. Band structure of (2).  $\beta$  orbitals negative. Blue/orange Fe, Brown/light-blue Ti.**

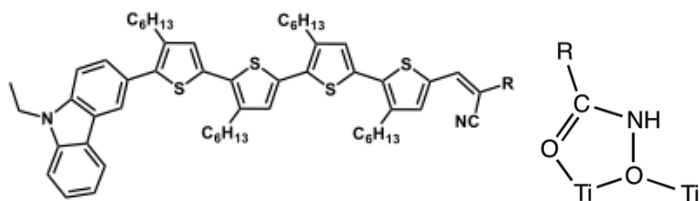
## Hydroxamates as Enhanced Stability Anchors in Solar Cells

Christopher Koenigsmann, Bradley J. Brennan, Christian F.A. Negre, Matthieu Koepf, Alec C. Durrell, Rebecca L. Milot, Victor S. Batista, Gary W. Brudvig, Robert H. Crabtree, Charles A. Schmuttenmaer, Teresa S. Ripolles, Jose A. Torre, and Juan Bisquert  
Department of Chemistry and Energy Sciences Institute, Yale University, New Haven, CT 06520  
and  
Photovoltaic and Optoelectronic Devices Group, Department of Physics, University Jaume I,  
12071 Castellon, Spain

The hydroxamate functional group has been unjustifiably ignored, with very little work being reported outside the biological literature, where hydroxamates are well-known anchors for Fe(III) in some siderophores. We now find that it acts as a suitable anchor for solar cell applications in that it supports electron injection. More importantly, it is more stable to humidity than the classic carboxylate anchor and can easily be introduced by reaction of the carboxylate ester with hydroxylamine.

We took the organic solar dye, MK2, with its carboxylate anchor and converted it to the hydroxamic acid. With this in hand, we compared the efficiency of dye-sensitized solar cells with N-719 carboxylate, MK2 carboxylate (R=COOH) and MK2 hydroxamate (R= CONHOH). All the cells gave closely comparable performance, but the remarkable feature of the MK2 hydroxamate cell was that, unlike the other cases, it performed *better* with 10% water in the acetonitrile solvent and even with 20% water it performed better than in the anhydrous case.

The significance of this result is that in artificial photosynthetic water splitting cells, water is by definition present. In such a case, we need dyes and anchors that tolerate water. Our work, therefore, suggests that hydroxamate should receive greater consideration for applications in this area. This work has been submitted for publication and so is not yet widely available, but prior work on hydroxamates has appeared from our group.<sup>1-3</sup>



*MK-2 structure and proposed hydroxamate binding mode.*

1. McNamara WR, Snoeberger III RC, Li G, Richter C, Allen LJ, Milot RL, Schmuttenmaer CA, Crabtree RH, Brudvig GW, Batista VS, Hydroxamate Anchors for Water-Stable Attachment to TiO<sub>2</sub> Nanoparticles, *Energy Environ Sci*, 2009, 2, 1173-1175.
2. McNamara WR, Milot RL, Song, H, Snoeberger III RC, Batista, VS, Schmuttenmaer CA, Brudvig GW, Crabtree RH, Water-stable, hydroxamate anchors for functionalization of TiO<sub>2</sub> surfaces with ultrafast interfacial electron transfer, *Energy Environ Sci*, 2010, 3, 917-923.
3. Brewster, TP, Konezny, SJ, Sheehan, SW, Martini, LA, Schmuttenmaer, CA, Batista, VS, Crabtree, RH, Hydroxamate Anchors for Improved Photoconversion in Dye-Sensitized Solar Cells, *Inorg. Chem.*, 2013, 52, 6752-6764.

## A Cobalt Perfluoropinacolate Complex for WOC

Laleh Tahsini,<sup>1</sup> Sarah E. Specht,<sup>1</sup> Mehmed Z. Ertem,<sup>2,3</sup> Victor S. Batista,<sup>2</sup> and Linda H. Doerrer<sup>1</sup>

<sup>1</sup>Department of Chemistry, Boston University, Boston, MA 02215

<sup>2</sup>Department of Chemistry, Yale University, P.O. Box 208107, New Haven, Connecticut

<sup>3</sup>Chemistry Department, Brookhaven National Laboratory, Upton, New York 11973

Cobalt-based complexes for homogeneous water oxidation catalysis are under intense investigation because of the efficacy of heterogeneous Co-oxide species in water oxidation, and the desire to model what happens in those systems under more controlled conditions. Our group has developed a mononuclear Co-based complex with all O-donor ligands that catalyzes water oxidation. Using the perfluorinated pinacolate group, pin<sup>F</sup>, as both the ligand for Co *and* the solution buffer, we have developed an important new WOC system. Simple [M(pin<sup>F</sup>)<sub>2</sub>]<sup>2-</sup> complexes had been previously reported in the literature but with incomplete characterization. We have fully characterized the series [M(pin<sup>F</sup>)<sub>2</sub>]<sup>2-</sup> for M = Fe, Co, Ni, Cu, and Zn including aqueous and non-aqueous preparations, and electrochemical studies in CH<sub>3</sub>CN.<sup>1</sup> Oxidation studies of the Co complex in the pH range ~9.5 – 11.5 with NaNO<sub>3</sub> electrolyte exhibit a quasi-reversible, pH-independent Co(III)/Co(II) couple at E<sub>1/2</sub> = 770 mV (vs NHE) and large, irreversible currents from catalytic water oxidation starting at 1.10 V. A Faradaic efficiency of 60% was determined by fluorescence probe quantification of O<sub>2</sub>. Not coincidentally this pH range is that in which the (Hpin<sup>F</sup>)/(pin<sup>F</sup>)<sup>2-</sup> (pK<sub>a2</sub> = 10.66±0.04) system is an effective buffer. This *dual-function buffer-ligand* system also prevents loss of Co(II) under catalytic conditions.<sup>2</sup>

Several pieces of evidence support the homogeneous nature of the catalyst. Oxygen evolution is immediate and largely constant once a potential is applied. The imperfect Faradaic efficiency with the absence of loss of chromophore suggests that some oxidizing equivalents are not entirely being converted to O<sub>2</sub>. As demonstrated by Craig Hill and colleagues (*JACS*, **2013**, *135*, 14110), if an anionic molecular species is responsible for catalytic turnover, it can be extracted under cationic exchange conditions into an organic solvent, thereby removing the active species. Our system passes this test and kinetic studies determined a turnover frequency of 42 s<sup>-1</sup>, which is consistent with and better than many other homogenous WOC systems.<sup>2</sup>

Computational investigations<sup>2</sup> have revealed thermodynamic parameters consistent with experimental results, as well as set mechanistic boundaries for possible intermediates. The proposed mechanism corroborates the two-electron, one-proton 2 e<sup>-</sup>/1 H<sup>+</sup> dependence as found in the system Pourbaix diagrams. Conversion of the [Co(III)(OH)(pin<sup>F</sup>)<sub>2</sub>]<sup>2-</sup> species to a Co(IV)-oxyl species that forms the crucial O-O bond upon water nucleophilic attack (WNA) is proposed. This mechanism provides several targets for isolation and further characterization, particularly [Co(III)(OH)(pin<sup>F</sup>)<sub>2</sub>]<sup>2-</sup>, efforts toward which will be presented.

(1) Tahsini, L.; Specht, S. E.; Lum, J. S.; Nelson, J. J. M.; Long, A. F.; Golen, J. A.; Rheingold, A. L.; Doerrer, L. H. *Inorg. Chem.* **2013**, *52*, 14050.

(2) Tahsini, L.; Carbery, W.; Cantalupo, S. A.; Golen, J. A.; Rheingold, A. L.; Ertem, M. Z.; Batista, V. S.; Doerrer, L. H. *submitted* **2014**.

## Dirhodium Complexes for H<sub>2</sub> Production Using Visible Light Irradiation

Zhanyong Li, Jarett Martin, Nicholas Leed, Suzanne Witt, Kim R. Dunbar and Claudia Turro

Department of Chemistry  
Texas A&M University  
College Station, TX 77840

The generation of H<sub>2</sub> fuel from water by utilizing sunlight represents one of the major directions in the research area of solar energy conversion. The photoactive H<sub>2</sub>O reduction systems studied to date are typically multicomponent with a photosensitizer to harvest the sunlight, a catalyst to reduce H<sup>+</sup>, a redox active electron mediator couple to effect the electron transfer between the two aforementioned components and a sacrificial electron donor as the electron source. The fast charge recombination of the sensitizer as well as the requirement of the electron mediator greatly limits the light conversion efficiency.

Our DOE-funded project focuses on the design of a series of dinuclear metal complexes that can act as a dual photosensitizer and photocatalyst in an effort to eliminate the additional charge transfer process and hence achieve higher efficiencies. Inspired by the principles for designing organic donor-acceptor type dyes, we set out to connect the donor and acceptor ligands through the intermediacy of a dirhodium(II,II) dimetal core. Two families of dirhodium complexes, namely *cis*-[Rh<sub>2</sub>(DTolF)<sub>2</sub>(L)<sub>2</sub>]<sup>2+</sup> and *cis*-[Rh<sub>2</sub>(F-form)<sub>2</sub>(L)<sub>2</sub>]<sup>2+</sup> (DTolF = *p*-ditolylformamidinate, F-Form = *p*-difluorobenzylformamidinate; L = the chelating diimine ligands dpq (dipyrido[3,2-*f*:2',3'-*h*]-quinoxaline), dppz (dipyrido[3,2-*a*:2',3'-*c*]phenazine) and dppn (benzo[*i*]dipyrido[3,2-*a*:2',3'-*h*]quinoxaline) (Fig. 1) were synthesized and characterized by a variety of techniques, including X-ray crystallography and <sup>1</sup>H NMR spectroscopy. Electronic absorption spectroscopic studies indicate that these complexes exhibit absorption features in the visible region, assigned as directional charge transfer from the electron donating formamidinate ligands to the electron accepting diimine ligands (LL'CT transitions). The oxidation of these complexes is facile as evidenced by the electrochemical studies. Preliminary studies indicate that the compound *cis*-[Rh<sub>2</sub>(DTolF)<sub>2</sub>(dpq)<sub>2</sub>]<sup>2+</sup> exhibits potential for catalyzing H<sub>2</sub>O reduction with visible light and without the need for an external photosensitizer. To further probe the mechanism for the H<sub>2</sub> production, electrocatalytic H<sup>+</sup> reduction experiments by these complexes are being conducted.

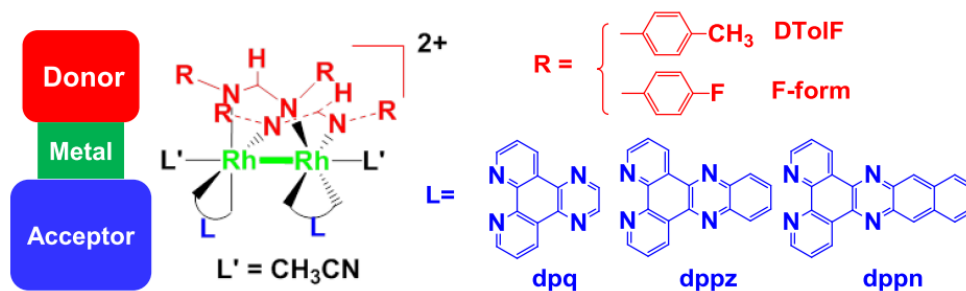


**Fig. 1.** Design strategy and chemical structural representations of the complexes.

Future efforts are directed at developing complexes with increased water solubility, strategies that include the attachment of hydrophilic groups, such as -COOH, -SO<sub>3</sub>H or zwitterions to the scaffold of the formamidinate or diimine ligands.

## **Polymer Mechanochemistry of Metal Bipyridyls**

Suzanne Ferrere, Drazenka Svedruzic, and Brian Gregg

Chemical and Materials Sciences Center  
National Renewable Energy Laboratory  
Golden, CO 80401

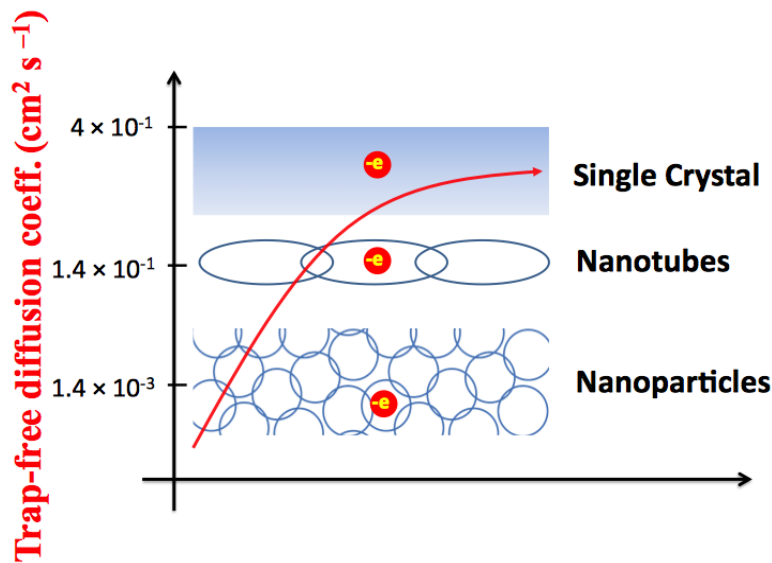
A molecule's electronic structure, and thus its properties, can be altered by strain. The ability to reversibly stretch bonds and monitor the accompanying changes in properties has important implications for catalysis and more generally, for the understanding of structure-function relationships. Furthermore, dynamic control of bonding has the potential to transform a single molecule into a molecular "system" without the cost, patience, and skills required of synthetic modifications. However, reversibly accessing strained states is exceptionally challenging. Our objective is to link a "mechanophore" molecule into an elastic material, such that stretching the material results in translation of the applied forces to the mechanophore bonds.

The approach that will be presented is the use of elastomeric polymers containing covalently incorporated mechanophores. Typically, our systems contain metal bipyridyl mechanophores in either thermoset or thermoplastic polyurethane. Changes in bond length should manifest as changes in electronic spectra and/or infrared spectra. While we have not demonstrated the dynamic stretching of a bond, we do observe effects that indicate stretching provides control over intermolecular interactions. Thus, we are also investigating the use of elastomeric films to manipulate relevant intermolecular (e.g., donor-acceptor) phenomena. Design of mechanophore systems, elastomer synthesis and linkage chemistry, and the effects of stretching on electronic and infrared spectra will be presented.

## Trap-free Transport in Ordered and Disordered TiO<sub>2</sub> Nanostructures

Julio Villanueva-Cab,<sup>†</sup> Song-Rim Jang,<sup>‡</sup> Adam F. Halverson,<sup>§</sup> Kai Zhu, and Arthur J. Frank  
Chemical and Materials Science Center  
National Renewable Energy Laboratory  
Golden, CO 80401

Understanding the influence of different film structures on electron diffusion in nanoporous metal oxide films has been scientifically challenging. Because of the rate-limiting role that traps play in determining the transport properties, the structural effects of different film architectures are largely obscured or reduced. We describe a general approach to probe the impact of structural order and disorder on the charge-carrier dynamics without the interference of transport-limiting traps. As an illustration of this approach, we explore the consequences of trap-free diffusion in vertically aligned nanotube structures and random nanoparticle networks in sensitized titanium dioxide solar cells. Values of the electron diffusion coefficients are considerably larger in the nanotube arrays than in the nanoparticle films, spanning a range of average crystallite sizes, and approaches values of the diffusion coefficient in the single crystal.



Transport measurements together with modeling show that electron scattering at grain boundaries in particle networks limits trap-free diffusion. In presence of traps, transport was  $10^3$ – $10^5$  times slower in nanoparticle films than in the single crystal. Understanding the link between structure and carrier dynamics is important for systematically altering and eventually controlling the electronic properties of nanoscaled materials.

Present Addresses:

<sup>†</sup>Departamento de Física Aplicada, CINVESTAV-IPN, Mérida, Yucatán 97310, México.

<sup>‡</sup>Corporate R&D, LG Chem Research Park, LG Chem, Ltd., #104-1 Munji-dong, Yuseong-gu, Daejeon, 305-380, Korea.

<sup>§</sup>GE Global Research, 1 Research Circle, Niskayuna, New York 12309.

## Quantum chemical calculations on transition metal containing systems: redox potentials, pKa's, and application to modeling electron trapping and transport in the Gratzel cell

Jing Zhang, Steve Jerome, Mike Steigerwald, Louis Brus, and Richard A. Friesner

Department of Chemistry

Columbia University

New York, NY 10025

Our current efforts are focused in two principal directions: (1) develop density functional theory (DFT)-based methods for accurate treatment of transition metal containing systems, particularly redox potentials, pKa's, and other quantities of importance in reactions important for solar energy conversion such as charge separation and water splitting; (2) application of these methods to understand charge separation, trapping, and transport in the Gratzel cell. Progress in both areas is described below.

In previous work, we have shown that a simple, ligand based correction scheme, in the framework of a general approach to improving DFT based on localized orbital corrections (LOCs), reduces the mean unsigned error (MUE) for redox potentials in transition metal complexes from  $\sim 0.4\text{eV}$  to  $\sim 0.1\text{eV}$ . In recent work (submitted for publication to J. Phys. Chem.), we have initiated testing of this approach for the calculation of pKa's in transition metal complexes. The initial calculations have been carried out for hexaquo complexes of first row transition metals. Despite their apparent simplicity, standard DFT calculations using the B3LYP functional yields a MUE of 5.7 pKa units; the error is reduced to 0.9 pKa units when the LOC corrections are utilized. In this calculation, only one adjustable parameter was employed; the raw pKa value was scaled to optimize the fit to experiment. The remaining parameters were all taken from the existing B3LYP-LOC model for transition metals (DBLOC). We are in the process of extending these calculations to pKa calculations on a larger set of transition metal complexes.

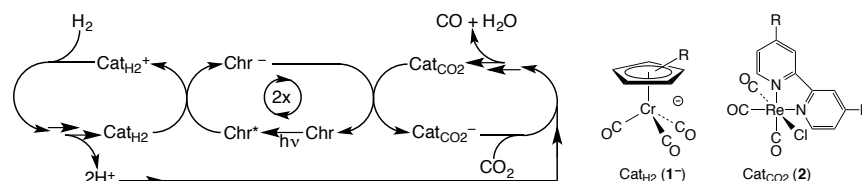
We have also applied the redox corrections from DBLOC to the calculation of the barrier height in the extraction of a hydrogen atom by the heme group of cytochrome P450. Experiment indicates that this rate is very fast, with a barrier less than 10 kcal/mole, but quantum chemical calculations have uniformly predicted a barrier that is too high by 5-10 kcal/mole, even when QM/MM techniques are employed. We hypothesized that the error arises from the fact that the hydrogen abstraction is actually a coupled electron-proton transfer, with the electron from the hydrogen already reducing the heme iron from Fe(IV) to Fe(III) by the time the transition state for the hydrogen is reached. Applications of the DBLOC redox corrections for the heme iron results in a substantial lowering of the barrier, and good agreement with the experimental data

Finally, in previous work, we investigated an ambipolar model for electron transport in the Gratzel cell, achieving good agreement with experiment for various energetic and transport properties, and providing a physical model for the electron trapping site. These calculations used the lithium cation as the ion stabilizing an excess electron in a reduced Ti(III) site. We have now investigated what happens if a proton is used in the model rather than lithium. The calculations show that the proton binds differently to the  $\text{TiO}_2$  than lithium; it forms a covalent bond with an oxygen atom, as opposed to an ion pair. This leads to a greater trap depth and larger activation energy for transport, in good agreement with experimental measurements of these quantities. These results demonstrate the consistency and predictive capabilities of our model.

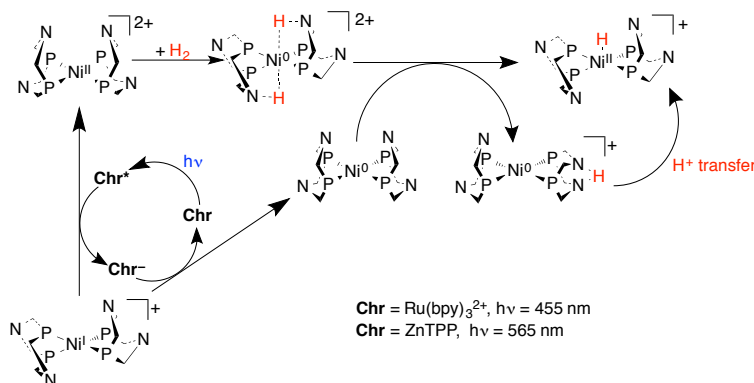
## Homogeneous Approaches to Photochemically Driving the Reverse Water Gas Shift Reaction

Nathan T. La Porte, Mark Westwood, Davis B. Moravec and Michael D. Hopkins  
Department of Chemistry  
The University of Chicago  
Chicago, IL 60637

Energy-storing artificial-photosynthetic systems for CO<sub>2</sub> reduction must derive the reducing equivalents from a renewable source rather than from sacrificial donors. To this end, several homogeneous, integrated chromophore/two-catalyst systems have been investigated that are thermodynamically capable of photochemically driving the energy-storing reverse water-gas shift reaction ( $\text{CO}_2 + \text{H}_2 \rightarrow \text{CO} + \text{H}_2\text{O}$ ,  $\Delta H_f = 41.2 \text{ kJ mol}^{-1}$ ), where the reducing equivalents are provided by renewable H<sub>2</sub>. These systems contain the chromophores ZnTPP or Ru(bpy)<sub>3</sub><sup>2+</sup>, H<sub>2</sub> oxidation catalysts of the form [Cp<sup>R</sup>Cr(CO)<sub>3</sub>]<sup>n-</sup> and Ni(P<sup>Cy</sup><sub>2</sub>N<sup>tBu</sup><sub>2</sub>)<sub>2</sub><sup>n+</sup>, and CO<sub>2</sub> reduction catalysts of the form Re(bpy-4,4'-R<sub>2</sub>)(CO)<sub>3-n</sub>L<sub>n</sub>Cl (L = PR<sub>3</sub>). Using time-resolved spectroscopy, a comprehensive mechanistic and kinetic picture of the photoinitiated reactions of these systems has been developed. For the [Cp<sup>R</sup>Cr(CO)<sub>3</sub>]<sup>n-</sup>/ZnTPP/Re(bpy-4,4'-R<sub>2</sub>)(CO)<sub>3</sub>Cl systems, it has been found that one-photon excitation of sensitizes intercatalyst electron transfer to produce the substrate-active forms of each with a quantum yield of near unity. The catalytically competent state persists with a second-order half-life of ~15 μs, which is of the right magnitude for substrate-trapping of sensitized catalyst intermediates.



Systems containing Ni(P<sup>Cy</sup><sub>2</sub>N<sup>tBu</sup><sub>2</sub>)<sub>2</sub><sup>n+</sup> photocatalytically oxidize H<sub>2</sub> upon electron-transfer sensitization by Ru(bpy)<sub>3</sub><sup>2+</sup> or ZnTPP. These system proceed via reductive quenching of the chromophore by Ni(P<sup>Cy</sup><sub>2</sub>N<sup>tBu</sup><sub>2</sub>)<sub>2</sub><sup>n+</sup> to produce Ni(P<sup>Cy</sup><sub>2</sub>N<sup>tBu</sup><sub>2</sub>)<sub>2</sub><sup>n+</sup>. Critically, this transient is trapped by H<sub>2</sub> prior to back-electron transfer to give Ni(H<sub>2</sub>)(P<sup>Cy</sup><sub>2</sub>N<sup>tBu</sup><sub>2</sub>)<sub>2</sub><sup>n+</sup>. In the absence of CO<sub>2</sub> reduction catalysts, the system achieves turnover by employing Ni(P<sup>Cy</sup><sub>2</sub>N<sup>tBu</sup><sub>2</sub>)<sub>2</sub><sup>n+</sup> as the sacrificial oxidant; the resultant Ni(H<sub>2</sub>)(P<sup>Cy</sup><sub>2</sub>N<sup>tBu</sup><sub>2</sub>)<sub>2</sub><sup>n+</sup> reacts with Ni(H<sub>2</sub>)(P<sup>Cy</sup><sub>2</sub>N<sup>tBu</sup><sub>2</sub>)<sub>2</sub><sup>n+</sup> to provide Ni(H)(P<sup>Cy</sup><sub>2</sub>N<sup>tBu</sup><sub>2</sub>)<sub>2</sub><sup>n+</sup>, which has been isolated and crystallographically characterized.



## Mapping Morphology Dependent Charge Separation Pathways in Conjugated Polymer Blends

Zhi Guo,<sup>1,2</sup> Chris Wong<sup>1</sup>, Doyun Lee,<sup>3</sup> Richard Schaller,<sup>4</sup> Xiaobing Zuo,<sup>5</sup> Byeongdu Lee,<sup>5</sup> Tengfei Luo,<sup>2</sup> Haifeng Gao,<sup>3</sup> and Libai Huang<sup>1</sup>

<sup>1</sup>Radiation Laboratory, <sup>2</sup>Department of Aerospace and Mechanical Engineering, <sup>3</sup>Department of Chemistry and Biochemistry, University of Notre Dame, Notre Dame, IN 46556, USA

<sup>4</sup>Center for Nanoscale Materials, <sup>5</sup>Center for Advanced Photon Source, Argonne National Laboratory, Argonne, IL 60439, USA

We present our recent progress on the roles of crystallinity, interchain interaction, and exciton delocalization on ultrafast charge separation pathways in conjugated polymer blends utilizing ultrafast spectroscopy and microscopy. We characterize the energy levels, excited state structures, and dynamics of the interchain species by combining ultrafast spectroscopy and computational quantum chemistry approaches. The alkyl side chain of a highly efficient donor-acceptor copolymer for solar cell applications, PBDTTT (poly(4,8-bis-alkyloxybenzo[1,2-*b*:4,5-*b'*]dithiophene-2,6-diyl-alt-(alkylthieno[3,4-*b*]thiophene-2-carboxylate)-2,6-diyl), is varied to tune the molecular packing and interchain interaction of the polymers in order to elucidate the charge separation pathways originating from intrachain and interchain excitons. Polymers with linear side chains induce strong interchain interactions that lead to preferential formation of interchain excitons that are delocalized over more than one polymer backbone in the solid state. Our results demonstrate that the formation of the interchain excited state is energetically unfavorable for charge separation in low-bandgap copolymers. Such energetics of the interchain excitons in low-bandgap copolymers calls for optimized solar cell morphologies that are fundamentally different from those based on homopolymers such as P3HT (poly-3-hexylthiophene). A long-range crystalline polymer domain is detrimental rather than beneficial to solar cell performance for a low-bandgap copolymer which stands in direct contrast to the observed behavior in P3HT based devices (Figure 1).

Proof-of-concept transient absorption microscopy (TAM) experiments have been performed on thermally annealed P3HT and [6,6]-phenyl-C<sub>61</sub>-butyric acid methyl ester (PCBM) blends as well as PBDTTT:PCBM blends. By directly comparing spatially resolved charge dynamics to ensemble dynamics, the TAM results demonstrate that the apparent lifetimes obtained by ensemble measurements can be misleading due to averaging over microscopically disparate areas. In these experiments the spatial resolution is ~ 200 nm, much larger than exciton diffusion length. Near-field TAM with sub-diffraction spatial resolution of ~50 nm, approaching the optimal domain size, is highly desirable for further investigations into the morphology-dependent charge generation and recombination. Construction of a near-field TAM apparatus is currently underway.

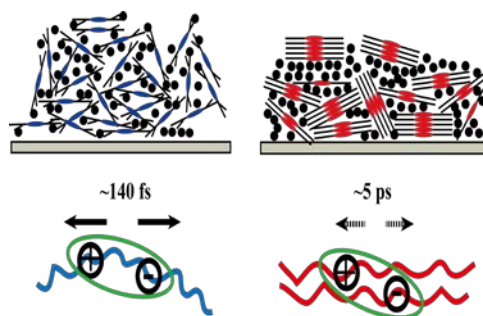


**Figure 1** Schematic representation of the charge separation time scale deriving from intrachain (left) and interchain excitons (right) in low-bandgap copolymers blends.

## Visible Light Induced Electron Transfer with Thiolated Gold Clusters

Yong-Siou Chen, Kevin Stamplecoskie and Prashant V. Kamat  
Radiation Laboratory and Department of Chemistry and Biochemistry  
University of Notre Dame, Notre Dame, Indiana 46556

Glutathione capped metal nanoclusters ( $\text{Au}_x\text{-GSH NCs}$ ) exhibit molecular like properties and their excited state properties can be controlled through numbers of metal atoms and capping ligands. The long lived excited state (lifetime  $\sim 770$  ns) and the reversible reduction ( $E^0 = -0.63$  V vs. RHE) and oxidation ( $E^0 = 0.97$  V and 1.51 V vs. RHE) potentials of these metal nanoclusters make them suitable for driving water splitting reaction [1-3]. These metal nanoclusters which serve as a new class of visible photosensitizers are suitable for designing light harvesting assemblies. When a mesoscopic  $\text{TiO}_2$  film sensitized by  $\text{Au}_x\text{-GSH NCs}$  was used as the photoanode in a photoelectrochemical cell we can generate photocurrent under visible light irradiation with a photoconversion efficiency of 2% (Figure 1). When a mesoscopic  $\text{TiO}_2$  film sensitized by  $\text{Au}_x\text{-GSH NCs}$  was used as a photoanode along with Pt counter electrode in aqueous buffer solution (pH = 7), we observe significant photocurrent activity under visible light excitation. Additionally, sensitizing Pt/ $\text{TiO}_2$  nanoparticles with  $\text{Au}_x\text{-GSH NCs}$  in an aqueous slurry system and irradiating with visible light produced  $\text{H}_2$  at a rate of 0.3 mmole of hydrogen/h/gram of  $\text{Au}_x\text{-GSH NCs}$ . The rate of  $\text{H}_2$  evolution was significantly enhanced ( $\sim 5$  times) when a sacrificial donor, such as EDTA, was introduced into the system. The visible activity of  $\text{Au}_x\text{-GSH NCs}$  lays the foundation for the future exploration of other metal nanoclusters with well controlled numbers of metal atoms and capping ligands.

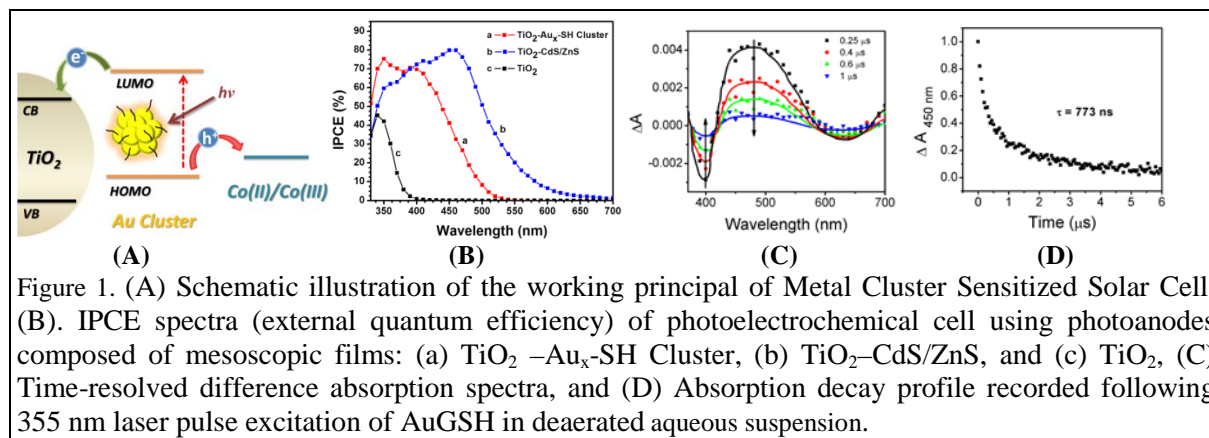


Figure 1. (A) Schematic illustration of the working principal of Metal Cluster Sensitized Solar Cell, (B). IPCE spectra (external quantum efficiency) of photoelectrochemical cell using photoanodes composed of mesoscopic films: (a)  $\text{TiO}_2\text{-Au}_x\text{-SH Cluster}$ , (b)  $\text{TiO}_2\text{-CdS/ZnS}$ , and (c)  $\text{TiO}_2$ , (C) Time-resolved difference absorption spectra, and (D) Absorption decay profile recorded following 355 nm laser pulse excitation of AuGSH in deaerated aqueous suspension.

### References.

1. Chen, Y.-S.; Choi, H.; Kamat, P. V., *Metal Cluster Sensitized Solar Cells. A New Class of Thiolated Gold Sensitizers Delivering Efficiency Greater Than 2%*. J. Am. Chem. Soc., 2013, **135**, 8822–8825.
2. Stamplecoskie, K. G.; Chen, Y.-S.; Kamat, P. V., *Excited-State Behavior of Luminescent Glutathione-Protected Gold Clusters*. The Journal of Physical Chemistry C, 2014, **118**, 1370-1376.
3. Chen, Y.-S.; Kamat, P. V., *Glutathione Capped Gold Nanoclusters as Photosensitizers. Visible Light Induced Hydrogen Generation in Neutral Water*. J. Am. Chem. Soc., 2014, doi: 10.1021/ja5017365.

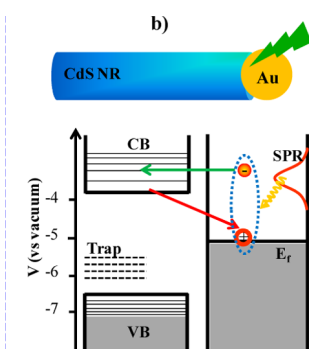
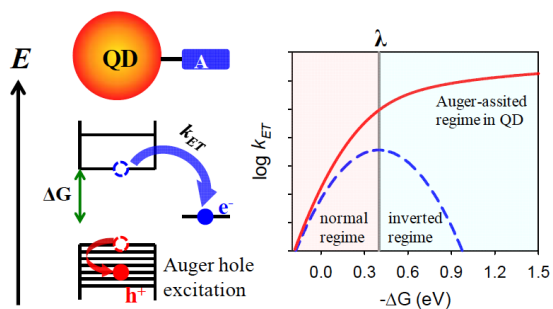


## Auger Assisted Electron Transfer from Quantum Dots and Plasmon Induced Hot Electron Transfer in CdS-Au Nanorods

Haiming Zhu, Ye Yang, Kaifeng Wu, Zheyuan Chen, and Tianquan Lian  
Department of Chemistry  
Emory University  
Atlanta, Georgia 30322

Quantum confined semiconductor nanocrystals are widely investigated as light harvesting and charge separation components in photovoltaic and photocatalytic devices. Although the dissociation of excitons (bound electron-hole pairs) through interfacial charge (electron or hole) transfer to acceptor materials is one of the most fundamental and crucial steps in these devices, it remains poorly understood. In this presentation, we report two recent findings on the mechanisms of exciton dissociation and plasmon-exciton interaction in .

**Auger assisted electron transfer.** (Zhu, Ye, et al. Nano Letters, 2014, 14, 1263) In excitonic nanomaterials, both the electron-hole interaction and electron-phonon interactions fall between those of the bulk semiconductor materials and molecular chromophores and the appropriate models for describing photoinduced charge transfer (or exciton dissociation) remains unclear. In a recent study, we investigated the size dependence of electron transfer (ET) processes from CdS, CdSe and CdTe quantum dots (QDs) to three molecular acceptors. The combination of band edge of bulk materials, size tunable confinement energy, and acceptor redox potential enabled an examination of ET rates over a wide range of driving force (0 ~ 1.3 eV). Our experiment showed that ET rates from QDs to these acceptors increased monotonically with decreasing QD size, regardless of QD compositions and acceptor molecule redox potentials. To account for the experimental observation, which is inconsistent with the inverted regime expected from Marcus ET theory, we propose an Auger-assisted model for ET from QDs. In the Auger-assisted ET process, the excess energy of the electron can be transfer to the hole, which overcomes the unfavorable Franck-Condon overlap in the Marcus inverted regime and facilitates the ET process. We believe that the proposed Auger-assisted ET model is generally applicable to many excitonic nanomaterials.



**Plasmon induced hote electron transfer.** (Wu, K. et al, Nano Lett. 2013, 13, 5255-5263) Using transient absorption spectroscopy, we showed that optical excitation of the plasmon band in the Au tip leads to efficient hot electron injection into the semiconductor nanorod in CdS-Au and CdSe-Au nanorod heterostructures. In the presence of sacrificial electron donors, this plasmon induced hot electron transfer process can be utilized to drive photoreduction reactions under continuous illumination. Ongoing studies are examining how to further improve the plasmon induced hot electron injection efficiency through controlling the size and shape of the plasmonic and excitonic domains.

## Controlled Growth and Transport Properties of Indium Tin Oxide Nanoforest

Timothy Garvey, Byron Farnum, and Rene Lopez

Department of Physics and Astronomy  
University of North Carolina at Chapel Hill  
Chapel Hill, NC, 27713

Efficient absorption of photons and effective carrier extraction are usually antithetical goals in many photovoltaic and photoelectrochemical devices. A typical design for a device of this kind tries to maximize photon capture by increasing the thickness of the absorbing layer. In surface sensitized devices such as traditional dye loaded nanoporous  $\text{TiO}_2$  cells this is detrimental to charge collection since increased transport path lengths lead to larger recombination. To maintain a high dye loading while speeding up the charge transport, a hierarchical scaffold nanostructure of a true conductive material could be highly beneficial.

We have developed a technique to fabricate such structure made of indium doped Tin oxide (ITO) by pulse laser deposition and characterized its morphology and charge transport properties. TEM micrographs show the films are composed of tree-like nanoparticle ( $< 10$  nm) assemblies. The ITO films were found to develop differences in morphology as a function of the deposition conditions, decreasing packing and apparently increasing surface area as gas background pressure was ramped up during growth (fig 1). By measuring its dye loading though, mid pressure films (50 mTorr) loaded  $\sim 2 \times 10^{-8}$  mol  $\text{cm}^{-2}$   $\mu\text{m}^{-1}$  dye molecules, which is twice the loading achieved for high pressure ones (300 mTorr), the result of an extremely open structure with large void areas and overall lower film densities as confirmed by Rutherford backscattering and ellipsometry.

The same structural features led to even marked changes in film sheet resistance, spanning 4 orders of magnitude from 50 to  $3 \times 10^5$   $\Omega/\square$  in film growth from 20 to 300 mTorr. The high resistance along the film plane is not surprising as the individual trees in the forest make progressively less contact with each other. However, the critical factor to judge the potential applicability of the nanoforest would be its conductivity vertically through the individual ITO structures to the substrate. Applying cyclic voltammetry in loaded samples with robust ruthenium dye, we found the dye molecules are near 100% electro-active, indicating the existence of charge transport paths from every point in the individual nanostructures to the substrate.

Pulse laser perturbation transient measurements performed on N719 dye sensitized cells fabricated with ITO films in open and closed circuit conditions, showed transient photocurrents and photovoltages with time decays on the order of 100 ms and 10 s time scales, respectively. No significant transport time differences across film morphologies were observed, a good indication that the ITO nanostructured films will be able to realize the sought after fast carrier transport when employed as scaffold for thin layers of photoactive semiconductors, dyes or quantum dots.

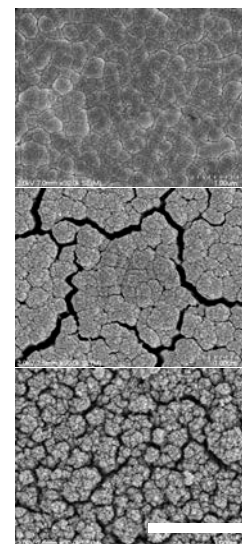


Fig.1 Top view electron cross sectional images of Indium Tin oxide nanoforest films grown on flat substrates by pulse laser deposition. Top to bottom 20 mTorr, 100 mTorr, and 200 mTorr. Scale bar 1 $\mu\text{m}$ .

## Modular Homogeneous and Framework Chromophore-Catalyst Assemblies

Karen L. Mulfort, Anusree Mukherjee, Oleksandr Kokhan, Jens Niklas, Lin X. Chen, Oleg G. Poluektov, and David M. Tiede  
Division of Chemical Sciences and Engineering  
Argonne National Laboratory  
Argonne, IL 60439

This poster will describe our recent efforts to implement biological design principles to develop and discover new photocatalysts towards the goal of artificial photosynthesis. Specifically, new synthesis and targeted, high-resolution physical characterization of photocatalyst architectures which contain identical modules in complementary environments will contribute to our knowledge of how spatial organization impacts the fundamental donor-acceptor photochemistry.

Cobaloximes are among the most promising molecular compounds for H<sub>2</sub> electro- and photocatalysis known, and here we present an entirely new approach to linked cobaloxime-based photocatalysts by Co(II)-templated formation of Ru(II)polypyridyl-decorated macrocycles. The supramolecular assemblies have been probed by high-resolution structural and physical characterization including synchrotron-based X-ray scattering, X-ray absorption spectroscopy, and ultrafast and nanosecond transient optical spectroscopies. Visible excitation of an equatorially-coordinated cobaloxime photocatalyst provides the first example of sub-picosecond photoinduced charge separation to yield the catalytically-active Co(I) oxidation state in cobaloxime-based assemblies. Interestingly, EPR analysis reveals that the ground state Co(II) center is high-spin, a unique aspect among previously described cobaloxime photocatalysts, and likely plays a significant role in the kinetics following excitation.

The homogeneous photocatalyst assemblies will be juxtaposed with studies of heterogeneous metal-organic frameworks (MOFs) which integrate donor-chromophore-acceptor triads and sustain long-lived charge separation following visible excitation. Preliminary work has focused on the development of a core-shell MOF crystallites with Ru(bpy)<sub>3</sub><sup>2+</sup>-based chromophore struts on the shell and diquat cations in the core. Nanosecond transient optical spectroscopy reveals

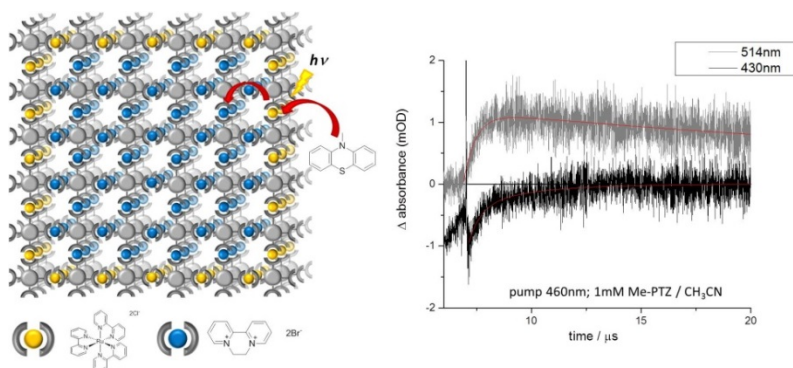


**Figure.** Left: scheme of interfacial electron transfer and charge separation between diquat—Ru(bpy)<sub>3</sub><sup>2+</sup> core-shell MOF based on Al(OH)(dcbpy) parent MOF and methyl phenothiazine (dcbpy = 4,4'-dicarboxylic acid-2,2'-bipyridyl). Right: nanosecond transient optical spectroscopy of core-shell MOF crystallites in CH<sub>3</sub>CN. Kinetic at 514nm follows Me-PTZ cation formation and decay following excitation of the MOF shell.

that interfacial charge separation between the diquat core and an external electron donor (methyl phenothiazine) persists for 35μs, nearly four times longer than the analogous homogeneous system. Ongoing work is aimed at further understanding heterogeneous charge separation in donor-acceptor type MOFs as a function of pore guest and particle size.

# Efficient Solar Photoelectrolysis by Nanoporous Mo:BiVO<sub>4</sub> through Controlled Electron Transport

Jason A. Seabold, Kai Zhu, and Nathan R. Neale  
Chemical and Materials Science Center  
National Renewable Energy Laboratory  
Golden, CO 80401

A detailed understanding of doping level, electron diffusion length and coefficient, as well as light capture and charge separation efficiencies in nanoporous Mo-doped BiVO<sub>4</sub> (Mo:BiVO<sub>4</sub>) photoanodes is obtained using photoelectrochemical techniques. Efficient water oxidation is achieved by doping with 1.8% Mo, resulting in a several-fold enhancement in photooxidation rate versus non-doped BiVO<sub>4</sub>. Two techniques are used to study the effect of Mo doping on the electron transport: (1) an analysis of the front/back illumination ratio of incident photon-to-current efficiency and (2) intensity modulated photocurrent spectroscopy. These techniques show that Mo doping improves the diffusion coefficient four-fold and increases the diffusion length to ca. 300 nm (from 10 nm for the non-doped material), which is also the empirically-determined optimal Mo:BiVO<sub>4</sub> film thickness for photoelectrolysis. As shown in Fig. 1, these films are found to have a 90% charge separation efficiency and an 80% absorbed photon-to-current efficiency, excellent values for metal oxide photoabsorbers. Among the many oxygen evolution catalysts studied, surface modification with iron oxyhydroxide (FeOOH), a simple earth abundant catalyst, dramatically enhances the water oxidation performance of Mo:BiVO<sub>4</sub> to an integrated IPCE of 2.41 mA cm<sup>-2</sup> and a photocurrent density of 2.77 mA cm<sup>-2</sup> in neutral phosphate at 1.23 V vs. RHE. These results are extremely promising for overall solar water splitting using metal oxide photoanodes in low-cost tandem PEC systems, and more generally, this unique understanding and control of charge separation and electron transport provides a methodology for studying other metal oxide photoanodes for solar photoelectrolysis.

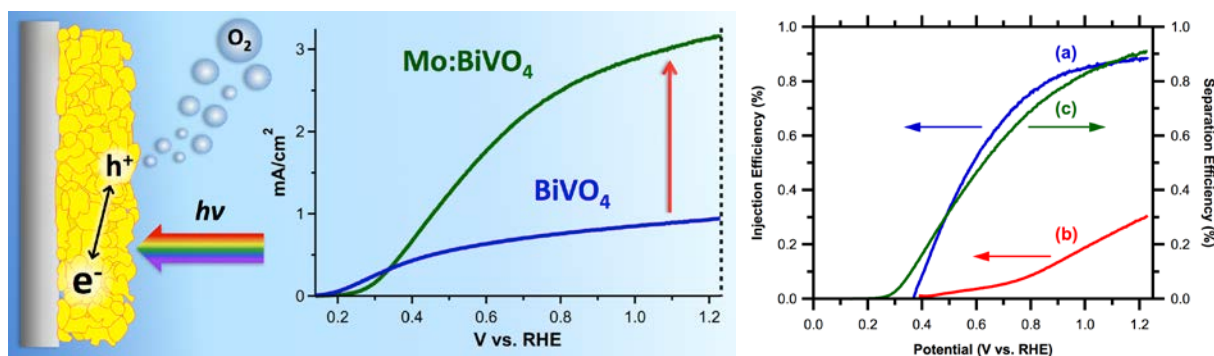


**Figure 1.** Left: Effect of Mo-doping on the  $I$ - $V$  characteristics of nanoporous BiVO<sub>4</sub> photoanodes. Right: Injection efficiency of 300 nm thick Mo:BiVO<sub>4</sub> (a) with FeOOH and (b) without FeOOH. (c) Separation efficiency of 300 nm thick Mo:BiVO<sub>4</sub>.

J.A. Seabold, K. Zhu, and N.R. Neale. "Efficient Solar Photoelectrolysis by Nanoporous Mo:BiVO<sub>4</sub> Through Controlled Electron Transport," *Phys. Chem. Chem. Phys.* **2014**, *16*, 1121-1131. DOI: 10.1039/c3cp54356k (online Nov 19, 2013)

## Formal and Computational Assessment of the ‘States’ Involved in Donor/Acceptor Coupling

Marshall D. Newton  
Chemistry Department  
Brookhaven National Laboratory  
Upton, New York 11973-5000

A key quantity controlling transport of charge (ET) and excitation (EET) between local molecular donor (D) and acceptor (A) sites is the electronic Hamiltonian coupling element linking initial and final states, denoted as HDA, where D and A are the initial and final ‘diabatic’ states (either many-electron or effective 1-particle), in which the charge or excitation is primarily confined, respectively, to local D and A sites. Here we consider the formulation of the D and A states ( $\psi_D$  and  $\psi_A$ ) using physically-motivated criteria (taking account of how the initial state of the system is ‘prepared’), and the resulting coupling (HDA) for a generic linear DBA system, where the D, B, and A sites are assumed to be in contact, either bonded or nonbonded, leading respectively, to intra- and intermolecular DA coupling. Expressions for  $\psi_D$ ,  $\psi_A$ , and HDA may be obtained variationally or via perturbation theory (PT) or other means. The validity of PT in the time-dependent context, based on the magnitude of HDA, is important in distinguishing the nonadiabatic and adiabatic limits of the simple 2-state rate constants for ET and EET. Some of the highlights of our study (with R. Cave) will be presented, focusing on ET, and comparing 2- and 3-state approaches for estimating HDA (here, ‘state’ refers to the electronic state subspace adopted), and also comparing results from the variational Generalized Mulliken Hush (GMH) and those obtained by symmetrical Lowdin orthogonalization of states obtained for isolated D,B, and A moieties (subsequently brought to contact in the DBA system).

It is important to recognize that the diabatic states entailed in HDA *must* be orthogonal, since HDA, which can be cast as an observable, must be independent of the zero of the Hamiltonian. The orthogonality of the effective  $\psi_D$  and  $\psi_A$  may be either implicit or explicit in the various formulations of HDA. The required orthogonality of  $\psi_D$  and  $\psi_A$  complicates the analysis of HDA: since totally localized D,B, and A states would not in general be orthogonal, orthogonalization unavoidably introduces ‘delocalization tails’, over and above those typically invoked in discussing bridge-mediated coupling (either via PT (superexchange) or full green function treatments). The distinct roles of the two types of tails (denoted as ‘orthogonalization’ and ‘covalency’ tails) are found to yield dramatically different results in the cases of ‘hole’ and ‘electron’ transfer through the bridge, as will be illustrated on the basis of model 1-particle DBA calculations. Another consequence of the orthogonalization tails is a blurring of the commonly assumed distinction between through space (TS) and through bond (TB) coupling, as noted also by Paddon-Row and Jordan.

We have found that HDA at the 2-state GMH level is nearly invariant with respect to large ‘off shell’ excursions of the initial and final state vertical energy gaps (*eg*, comparing gaps for optical and thermal ET), thus yielding only minor non condon behavior. By its nature, the nonperturbative GMH coupling does not require identification of an effective tunneling energy ( $E_{\text{tunn}}$ ), and provides an lower bound to coupling magnitudes based on  $E_{\text{tunn}}$  estimates.

## Novel Approaches to Efficient Production of Solar Fuels

Candy Mercado<sup>\*</sup>, Andriy Zakutayev<sup>†</sup>, Kai Zhu<sup>†</sup>, and Arthur J. Nozik<sup>\*,†</sup>

<sup>\*</sup>Department of Chemistry and Biochemistry  
University of Colorado, Boulder  
Boulder, Colorado 80309

and

<sup>†</sup>National Renewable Energy Laboratory  
Golden, Colorado 80401

Production of solar fuels, like hydrogen from sunlight and water, or carbon-based fuels like alcohols and hydrocarbons from sunlight, water and carbon dioxide (a process labeled artificial photosynthesis), at energy costs that are competitive or even less costly than fuels derived from coal, petroleum, or natural gas, has been a goal of solar photoconversion research for over 40 years. It is a daunting challenge and progress has been slow—there is still no commercial solar fuels industry. Solar fuels are generally distinguished from biofuels in that the latter is based on biological photosynthesis, while solar fuels are created using non-biological photoconverters. The maximum experimental power conversion efficiency (PCE) - defined as chemical free energy produced per unit area / solar irradiance of biofuels averaged over a year, is low (a few percent or less depending upon how it is defined and calculated), while the theoretical maximum thermodynamic PCE for solar fuels is quite high, reaching values for ideal systems  $> 30\%$  for 1 photosystem and  $> 40\%$  for 2 photosystems arranged in a tandem Z scheme like biological photosynthesis; the ideal systems are defined as having zero overvoltage and 100% quantum efficiency for collection of the photogenerated carriers that drive the coupled oxidation-reduction reactions that produce the fuel products. Realistic overvoltages required for reasonable reaction kinetics and quantum efficiencies  $< 100\%$  lower the PCEs, but 2 photosystems always outperform 1 photosystem at all overvoltage values. Higher PCEs for solar fuels can also be obtained when solar concentration is utilized in cells where the photosystems exhibit carrier multiplication through either singlet fission in molecular chromophores or multiple exciton generation (MEG) in semiconductor nanocrystals (quantum dots or quantum rods). When the 2 photosystems in the Z scheme for artificial photosynthesis are formed from dye-sensitized nanocrystalline supports (as in Graetzel cells), a good hole-conducting nanocrystalline support is required. The required good electron-conducting supports are already available, such as  $\text{TiO}_2$  and  $\text{ZnO}$ , but a sufficiently good hole-conducting support that can work as a photoelectrode in a Z scheme for solar fuels is not yet available. Here, we present the details of how the PCE for solar fuels can be significantly enhanced using 2 photosystems in a Z scheme with solar concentration, and new results on very promising new hole-conductors that could enable Z scheme architectures.

Acknowledgement: CM and AJN were supported by the UNC Center for Solar Fuels, an Energy Frontier Research Center funded by the U.S. Department of Energy, Office of Science; AZ was supported by the NREL Center for Inverse Design, an Energy Frontier Research Center funded by the U.S. Department of Energy, Office of Science; and KZ was supported by the DOE/BES Solar Photochemistry Program at NREL.

## Photoelectrochemical Studies of Metal Oxide Single Crystals

Lauren King, Meghan Kern, Ted Kraus, Alexander Nepomnyashchii,  
Kevin Watkins, and Bruce Parkinson

Department of Chemistry and School of Energy Resources  
University of Wyoming  
Laramie, WY 82071

Homoepitaxial growth of highly ordered and pure layers of rutile on rutile crystal substrates and anatase on anatase crystal substrates using atomic layer deposition (ALD) is reported. The epilayers grow in a layer-by-layer fashion at low deposition temperatures but are still not well ordered on rutile. Subsequent annealing at higher temperatures produces highly ordered, terraced rutile surfaces that in many cases have fewer electrically active defects than the substrate crystal. The anatase epitaxial layers, grown at 250°C, have much fewer electrically active defects than the rather impure bulk crystals. Annealing the epilayers at higher temperatures increased band gap photocurrents in both anatase and rutile.

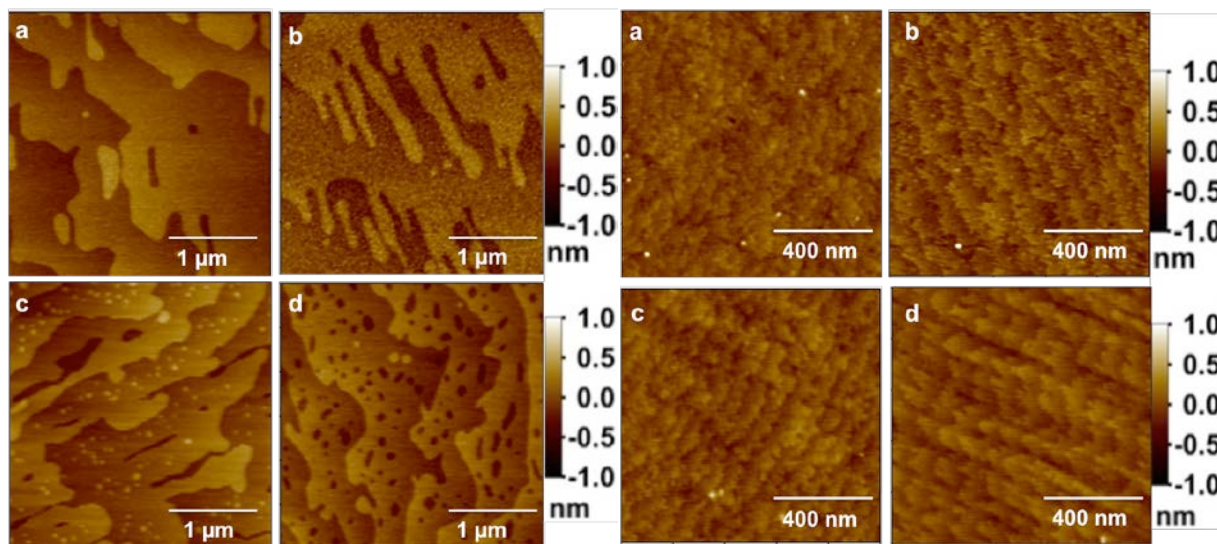


**Figure 1.** (left) AFM images of a rutile  $\text{TiO}_2$  (110) rutile single crystal: a) prior to deposition; b) after 20 nm of  $\text{TiO}_2$  deposition; c) after 1 hour annealing at 600°C; d) after an additional 1 hour at 600°C. (right) AFM images of an anatase  $\text{TiO}_2$  (101) natural crystal: a) as prepared; b) after 5 nm of  $\text{TiO}_2$  deposition; c) after 20 nm of  $\text{TiO}_2$  deposition; d) after annealing of the 20 nm film for 2 hours.

Sensitized photocurrents from the epilayers, as well as substrate crystals of  $\text{TiO}_2$  and  $\text{ZnO}$ , have been studied with various covalently bound sensitizers. The influence of the doping level of the oxide crystals on the magnitude of sensitized photocurrents was also investigated and showed that there is an optimum doping level for the collection of injected carriers. Total internal reflection spectra measured simultaneously with photocurrent spectra provides information about the relative efficiencies of sensitizer absorption, electron injection and photocurrent collection from various sensitizer species such as quantum dots and dye aggregates. Progress on obtaining quantum yields of 2 or greater using quantum dot and quantum rod sensitizers will also be reported.

## CO<sub>2</sub> Capture by Metal Supported Metal-Organic Frameworks

Hrvoje Petek, Min Feng, Hao Sun, and Jin Zhao  
Department of Physics and Astronomy  
University of Pittsburgh  
Pittsburgh, PA 15260

We image at the molecular scale the adsorption and interactions of CO<sub>2</sub> molecules on metal-organic frameworks (MOFs) self-assembled on gold surfaces. MOFs consisting of nearly-equally spaced linear chains of alternating Au adatom and 1, 4-phenylene diisocyanide (PDI) units, [-Au-PDI]<sub>n</sub>, self-assemble on single crystal Au surfaces. By scanning tunneling microscopy (STM) we image Au-PDI chains with an average interchain distance of 1.4 nm before (Figure 1) the adsorption of CO<sub>2</sub> molecules. The adsorption of CO<sub>2</sub> at 77 K introduces attractive interchain forces, leading to nm scale motion of Au-PDI chains over and CO<sub>2</sub> capture in ordered, one-molecule wide serried ranks with interchain separation of 1.0 nm. The chain compression on the (100) surfaces is modulated along the chains, whereas on (111) surface it is uniform leading to exposure of bare gold surface. The distinct chain responses on the (111) and (100) surfaces reflect differences in the Au-PDI chain interaction with the Au substrates. The captured CO<sub>2</sub> molecules can be resolved within the ranks indicating an ordered pattern of three molecules per Au-PDI unit cell, with the strongest interactions at the Au site. At 4.5 K, The adsorbed molecules at Au sites seed CO<sub>2</sub> cluster formation, where individual molecules can be resolved. The real space microscopic characterization of the adsorption and interactions of CO<sub>2</sub> molecules with one-dimensional substrates could be exploited as a platform for molecular design of CO<sub>2</sub> capture and reduction.

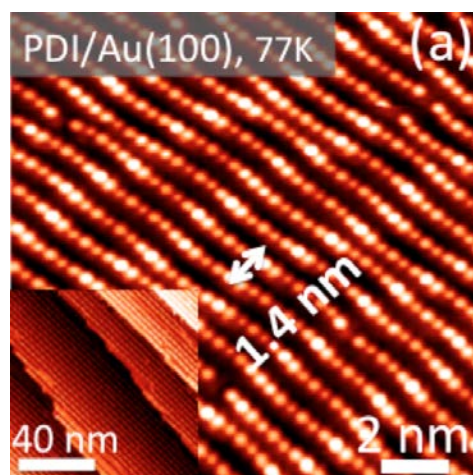


Figure 1. The Au-PDI chains imaged on Au(100) surface before CO<sub>2</sub> adsorption. The alternating bright contrast corresponds to PDI and the dimmer contrast to Au. The nm scale modulation of contrast is due to the reconstruction of the Au(100) substrate.

## Electronic Structure of Molecular Based Co and Ni Catalysts for Solar Fuel Production as Revealed by EPR and DFT

Oleg G. Poluektov, Jens Niklas, Karen L. Mulfort, Lisa M. Utschig, and David M. Tiede  
Chemical Sciences and Engineering Division, Argonne National Laboratory  
Argonne, IL 60439

Michael D. Hopkins, Mark Westwood  
Department of Chemistry, University of Chicago  
Chicago, IL 60637

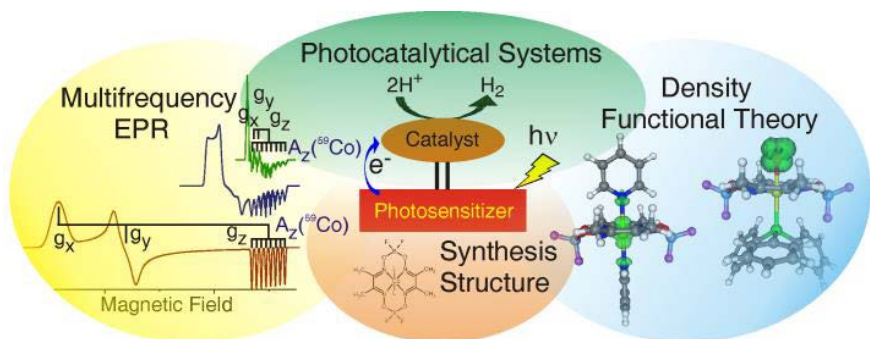
Claudio N. Verani  
Department of Chemistry, Wayne State University  
Detroit, MI 48202

Kristy L. Mardis  
Department of Chemistry & Physics, Chicago State University  
Chicago, IL 60628

Currently, our group is involved in solar fuels research that aims to mimic photosynthesis and devise integrated systems that can capture, convert, and store solar energy in high-energy molecular bonds. The development and improvement of these systems relies on understanding the inherent, fundamental mechanisms for coupling captured photons to fuel generation. One key element of these systems is the molecular catalyst. Our research is focused on two classes of molecular catalysts which are among the most promising first row transition metal complexes for fuel production, namely cobaloximes and bis(diphosphine)nickel complexes. The efficiency of the catalysts depends on the local surroundings, in particular on the direct ligands to the central metal ion but also the next coordination spheres.

We are applying advanced spectroscopic techniques such as multifrequency, pulsed electron paramagnetic resonance (EPR) to elucidate the electronic structure of the molecular catalysts and establish correlations between structure,

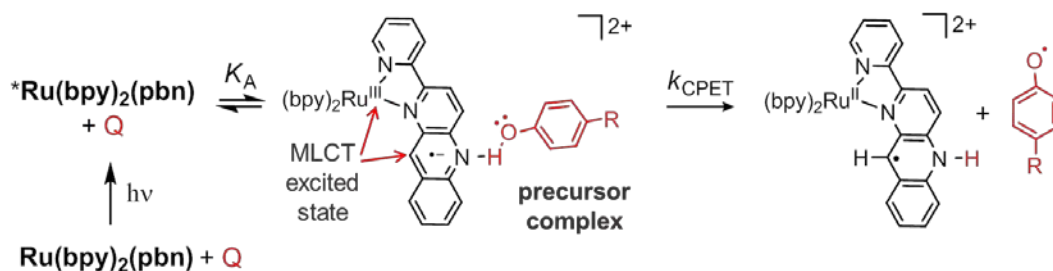
surrounding and their catalytic activity. EPR spectroscopy is applicable only to paramagnetic states of these complexes. Catalysts with a diamagnetic ground state were converted to a paramagnetic state by chemical reduction or oxidation. We also investigated cobalt oxime species containing different axial ligands, such as thiocyanate, pyridine and chloride, in distinct oxidation states obtained via bulk electrolysis. A comprehensive suite of DFT techniques was used to reveal the electronic structure of the catalytic complexes both in their paramagnetic and diamagnetic states. These data play a fundamental role in supporting other experimental techniques to obtain an insight into molecular mechanisms of the catalytic transformations.



## Mechanistic Insights into Concerted Proton-Electron Transfer Reactions in the Excited States of NADH-like Transition Metal Complexes

Dmitry E. Polyansky, Etsuko Fujita, and James T. Muckerman  
 Chemistry Department  
 Brookhaven National Laboratory  
 Upton, NY 11973-5000

Artificial photosynthetic systems exploit a variety of photochemical transformations with the ultimate goal of efficient conversion of the energy of photons into chemical bonds. The efficiency of catalytic reactions, light-induced charge separation and charge transfer strongly depends on how successfully proton-coupled electron-transfer (PCET) processes are implemented. In the Artificial Photosynthesis group we are interested in understanding mechanisms of PCET, including one of its subsets – concerted proton-electron transfer (CPET).



Within the scope of this project we study light-driven CPET reactions between a series of  $\text{NAD}^+$  model compounds, such as  $[\text{Ru}(\text{bpy})_2(\text{pbn})]^{2+}$ ,  $[\text{Ru}(\text{bpy})_2(\text{bpz})]^{2+}$ ,  $[\text{Ru}(\text{bpz})_3]^{2+}$  (bpy = 2,2'-bipyridine, pbn = 2-(2-pyridyl)benzo[*b*]-1,5-naphthyridine, bpz = 2,2'-bipyrazine) and hydrogen atom donors, such as substituted hydroquinones and *para*-substituted phenols. We found that in solvents with high donor numbers (e.g., acetonitrile), the strong hydrogen bonding between phenol donors and solvent molecules results in significant kinetic solvent effects (KSEs). It is necessary to account for these effects if any mechanistic conclusions are based on the rate analysis. The use of low coordinating solvents such as dichloromethane enabled the measurements of CPET rate constants with minimum contribution from KSE. Based on the transient spectra and observation of substantial kinetic isotope effects (KIEs) the quenching of the excited state of all metal complexes by *para*-substituted phenols proceeds through a CPET mechanism except for the  $[\text{Ru}(\text{bpz})_3]^{2+}$  / *para*-nitrophenol pair, which follows an electron-transfer (ET) mechanism. The analysis of activation parameters for CPET is indicative of zero or slightly negative activation energy, with significant negative activation entropies contributing to the overall free energy barrier. On the other hand, in the case of the ET reaction a positive activation energy and virtually zero activation entropy are observed making it distinctly different from CPET. The analysis of kinetic data using Marcus theory provides deeper insight into how the mechanism of CPET compares to ET reactions.

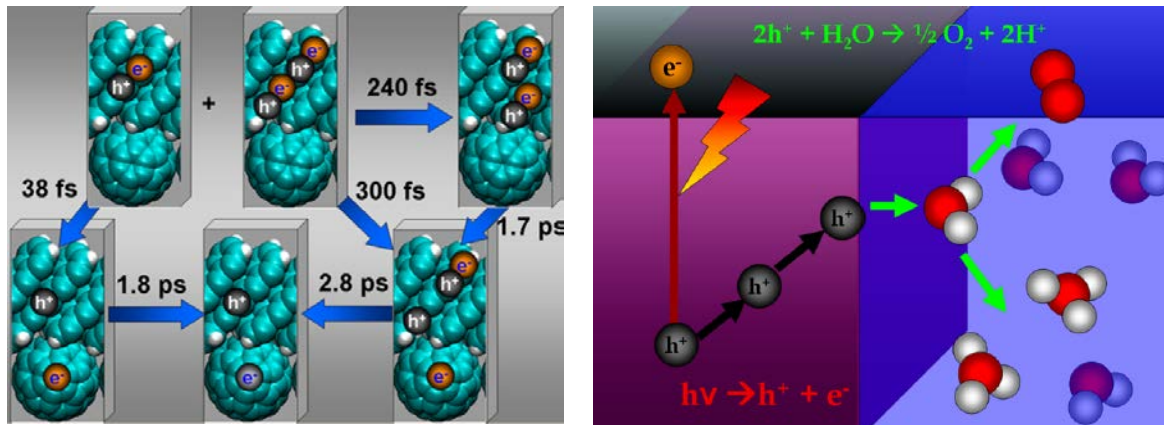
**Acknowledgements:** We thank our coworkers A. Lewandowska-Andralojc, P. Achord, B. W. Cohen and J. Schneider for their assistance, and S. Lyman, D. C. Grills and N. Sutin for helpful discussions. We also thank our collaborators R. P. Thummel and K. Tanaka.

Cohen, B. W.; Achord, P.; Cabelli, D.; Fujita, E.; Muckerman, J. T.; Polyansky, D. E.; Tanaka, K.; Thummel, R. P.; Zong, R. *Faraday Discuss.* **2012**, *155*, 129.

## Photoinduced Dynamics at Interfaces: Time-Domain Ab Initio Studies

Oleg V. Prezhdo  
Department of Chemistry  
University of Rochester  
Rochester, NY 14627

By developing novel approaches combining time-domain density functional theory and non-adiabatic molecular dynamics, we model non-equilibrium processes in novel photovoltaic and photo-catalytic materials. The poster will focus on organic/inorganic interfaces, constituting a challenge due to fundamental differences between organic and inorganic materials, described by chemistry (orbitals, electron correlation, vibrations) or physics (band structure, excitons, phonons). We will show how the asymmetry of electron and hole transfer at a polymer/nanotube interface can be used to optimize solar cell performance [1]; that the mechanism of electron injection from a CdSe nanoparticle depends on TiO<sub>2</sub> dimensionality [2]; that plasmon-driven charge separation on TiO<sub>2</sub> sensitized with plasmonic nanoparticles can occur already during light absorption [3]; that optically dark states govern the rates and yields of singlet fission and charge transfer at a pentacene/C<sub>60</sub> interface [4]; that nanoscale materials exhibit a new type, Auger-assisted electron transfer [5]; that the low efficiency of photo-catalytic water splitting by GaN is due to unfavorable competition of charge relaxation and transfer [6]; that atomic defects can be both detrimental and beneficial for the charge separation [7]; how a long, insulating bridge can accelerate charge separation [8]; why graphene, a metal, can be used as a TiO<sub>2</sub> sensitizer [9]. The software to perform these simulations [10] is available free of charge at <http://gdriv.es/pyxaid>.



1. R. Long, O. V. Prezhdo, *Nano Lett.*, submitted.
2. D. N. Tafen, R. Long, O. V. Prezhdo, *Nano Lett.*, **14**, 1790 (2014)
3. R. Long, O. V. Prezhdo, *J. Am. Chem. Soc.*, **136**, 4343 (2014).
4. A. V. Akimov, O. V. Prezhdo, *J. Am. Chem. Soc.*, **136**, 1599 (2014).
5. H. Zhu, Y. Yang, K. Hyeon-Deuk, M. Califano, N. Song, Y. Wang, W. Zhang, O. V. Prezhdo, T. Lian, *Nano Lett.*, **14**, 1263 (2014)
6. A. V. Akimov, J. T. Muckerman, O. V. Prezhdo, *J. Am. Chem. Soc.*, **135**, 8682 (2013).
7. R. Long, N. J. English, O. V. Prezhdo, *J. Am. Chem. Soc.*, **135**, 18892 (2013).
8. V. V. Chaban, V. V. Prezhdo, O. V. Prezhdo, *J. Chem. Phys. Lett.*, **4**, 1 (2013).
9. R. Long, N. English, O. V. Prezhdo, *J. Am. Chem. Soc.*, **134**, 14238 (2012).
10. A. V. Akimov, O. V. Prezhdo, *J. Chem. Theor. Comp.*, **9**, 4959 (2013); *ibid.* **10**, 789 (2014).

# Catalytic Water Oxidation with Monomeric Ru Complexes: Analysis of Reactive Intermediates

Lifen Yan, Guibo Zhu, and Yulia Pushkar

Department of Physics  
Purdue University  
West Lafayette, Indiana 47907

Modern chemistry's grand challenge is to significantly improve catalysts for water splitting. Further progress requires detailed spectroscopic and computational characterization of catalytic mechanisms.

We analyzed series of monomeric Ru complexes including one of the most studied homogeneous single site Ru catalysts,  $[\text{Ru}^{\text{II}}(\text{bpy})(\text{tpy})\text{H}_2\text{O}]^{2+}$  (where bpy = 2,2'-bipyridine, tpy=2,2':6',2''-terpyridine). Our results reveal that the  $[\text{Ru}^{\text{V}}(\text{bpy})(\text{tpy})=\text{O}]^{3+}$  intermediate, reportedly detected in catalytic mixtures and portrayed as a rate limiting intermediate in water activation<sup>1,2</sup> is not present as such. Using a combination of EPR and X-ray absorption spectroscopy, we demonstrate that 95% of the Ru complex in the catalytic steady state is of the form  $[\text{Ru}^{\text{IV}}(\text{bpy})(\text{tpy})=\text{O}]^{2+}$ .  $[\text{Ru}^{\text{V}}(\text{bpy})(\text{tpy})=\text{O}]^{3+}$  was not observed at any times and according to DFT analysis (Figure 1) might be thermodynamically inaccessible at our experimental condition (0.1 M  $\text{HNO}_3$ ). A reaction product with unique EPR spectrum was detected in reaction mixtures at about 5% and assigned to  $\text{Ru}^{\text{III}}$ -peroxo species with (-OOH or -OO- ligands). We also analyzed the  $[\text{Ru}^{\text{II}}(\text{bpy})(\text{tpy})\text{Cl}]^+$  catalyst precursor and confirmed that this molecule is not a catalyst and its oxidation past  $\text{Ru}^{\text{III}}$  state is impeded by a lack of proton-coupled electron transfer. Ru-Cl exchange with water is required to form active catalysts with the Ru-H<sub>2</sub>O fragment. We show that Cl K-edge spectroscopy serves as sensitive probe for the Ru-Cl interaction.  $[\text{Ru}^{\text{II}}(\text{bpy})(\text{tpy})\text{H}_2\text{O}]^{2+}$  is the simplest representative of a larger class of water oxidation catalysts with neutral, nitrogen containing heterocycles. We expect this class of catalyst to work mechanistically in a similar fashion with  $[\text{Ru}^{\text{IV}}(\text{bpy})(\text{tpy})=\text{O}]^{2+}$  as a key intermediate unless more electronegative (oxygen containing) ligands are introduced in the Ru coordination sphere, allowing the formation of more oxidized  $\text{Ru}^{\text{V}}$  intermediate.  $[\text{Ru}^{\text{IV}}(\text{bpy})(\text{tpy})=\text{O}]^{2+}$  has redox potential permissive to water oxidation (1.4 V at pH=1) and displays radicaloid character similar to the one detected in  $\text{Ru}^{\text{V}}=\text{O}$  complex<sup>3</sup>.

## References:

1. Concepcion, J. J.; Tsai, M. K.; Muckerman, J. T.; Meyer, T. J., *J. Am. Chem. Soc.* **2010**, *132*, (5), 1545-1557.
2. Wasylenko, D.; Ganesamoorthy, C.; Henderson, M.; Berlinguette, C. P., *Inorg. Chem.* **2011**, *50*, (8), 3662-3672.
3. Moonshiram, D.; Alperovich, I.; Concepcion, J. J.; Meyer, T. J.; Pushkar, Y., *Proc. Natl. Acad. Sci. U. S. A.* **2013**, *110*, (10), 3765-3770.

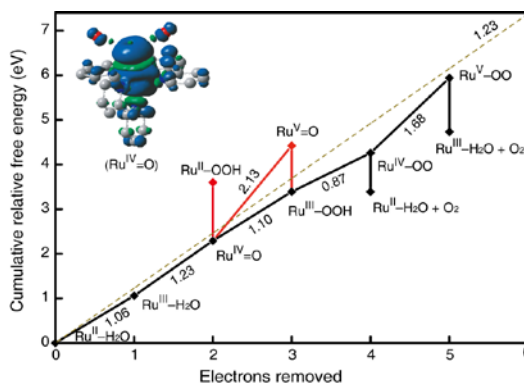


Figure 1. DFT (UB3LYP/DGDZVP) derived Latimer-Frost diagram for oxidation of  $[\text{Ru}^{\text{II}}(\text{bpy})(\text{tpy})\text{H}_2\text{O}]^{2+}$  under standard conditions (pH=0). Main path ( $\blacklozenge$ ) and paths with significant barriers ( $\blacklozenge$ ). Dashed line shows 1.23 eV water oxidation potential at pH=0. Insert: the spin density of  $\text{Ru}^{\text{IV}}=\text{O}$  species.

## Time Resolved X-ray Analysis of Water Splitting in Photosystem II

Katherine Davis, Lifen Yan, and Yulia Pushkar

Department of Physics  
Purdue University  
West Lafayette, IN 47907

The light driven water splitting achieved in the oxygen evolving complex (OEC) of Photosystem II is a critical process that sustains our biosphere. Photosynthetic water splitting is fascinating in its complexity, inspiring due to its practical applications in designing artificial photosynthesis, and not yet understood. At the heart of the water splitting process is the  $\text{Mn}_4\text{Ca}$  cluster embedded in a fine tuned protein environment.

The electronic structure and geometry of this cluster were probed by X-ray spectroscopy at the functional room temperature state.<sup>1,2</sup> Detailed kinetic analysis of the X-ray induced damage was performed and allowed selection of undamaging conditions for experimentation. High-quality extended X-ray absorption fine structure (EXAFS) spectra of the OEC at room temperature will be presented and compared with XRD and DFT derived molecular models of the dark stable  $S_1$  state. The determined Debye-Waller factors, sensitive to dynamic processes, support the rigid structure of the  $\text{Mn}_4\text{Ca}$  cluster at room temperature.

Laser-pump X-ray probe time-resolved X-ray emission measurements (XES) allowed monitoring of changes in the electronic structure of the OEC in real time during the catalysis. Using time-resolved XES we monitored the evolution of the electronic structure of the OEC of Photosystem II during the Kok cycle and in particular for the most critical  $S_3$  to  $S_0$  transition which results in  $\text{O}_2$  evolution. Snapshots of the  $S_3$  to  $S_0$  transition were collected at 50, 200 and 500  $\mu\text{s}$ . Data collected at the shorter two delays were selected to evaluate the proposed 'stable'  $S_4$  intermediate. Preliminary 50 $\mu\text{s}$  emission data appear already reduced. Data obtained after 200 $\mu\text{s}$  show with 98.1% confidence that a reductive shift from  $S_3$  to  $S_4$  is not a random statistical fluctuation. Our data show no oxidation but only a gradual reduction of the Mn centers after excitation of the complex past the  $S_3$  state. These observations allow us to propose a unique O-O bond formation and water splitting mechanism. Combined with DFT modeling, our analysis reveals the mechanism of catalytic water splitting.

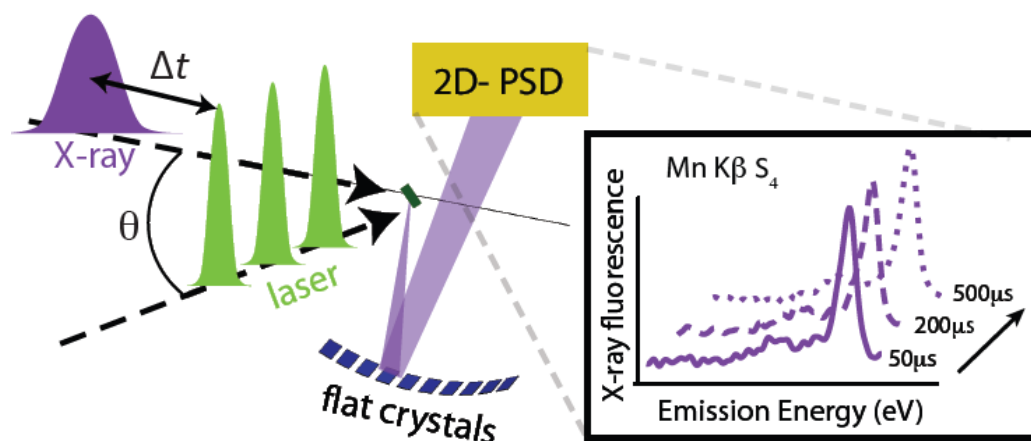


Figure 1. Schematic of experimental setup. Nanosecond laser pulses are incident on the sample at  $\theta < 5^\circ$  to the x-ray beam (not to scale).  $\Delta t$ , the pump/probe delay time, is set to 50 $\mu\text{s}$ , 200 $\mu\text{s}$ , 500 $\mu\text{s}$  or 40ms dependent on the desired S-state. The X-ray probe pulse arrives in a 40 $\mu\text{s}$  bunch and fluorescence from the sample is reflected by 10 flat analyzer crystals onto the 2D-PSD detector. K $\beta$  emission spectra are extracted from these images to form snapshots of the electronic structure in time.

# Photo-Induced Electron Transfer of Silicon-Phthalocyanines Dispersed in a Conjugated Polymer

Garry Rumbles, Adam Brunell, Jaehong Park and Obadiah Reid  
Chemical and Materials Sciences Center  
National Renewable Energy Laboratory  
Golden, Colorado, 80401

We report on a study of photo-induced electron transfer of a series of phthalocyanines (Pcs) dispersed in a conjugated polymer film both with and without the prototypical electron-accepting fullerene, PCBM. External quantum efficiency (EQE) studies of Pcs dispersed in a 1:1 mixture

of p3HT with PCBM show a clear spectroscopic signature of electron transfer from the excited Pc to the PCBM, in addition to electron transfer from the p3HT to the oxidized Pc (Figure 1b). Using time-resolved microwave conductivity (TRMC) we have shown that both these processes occur with high efficacy to yield long-lived, free charges when the phthalocyanine is dispersed in both neat p3HT (Figure 1c) and neat PCBM films.

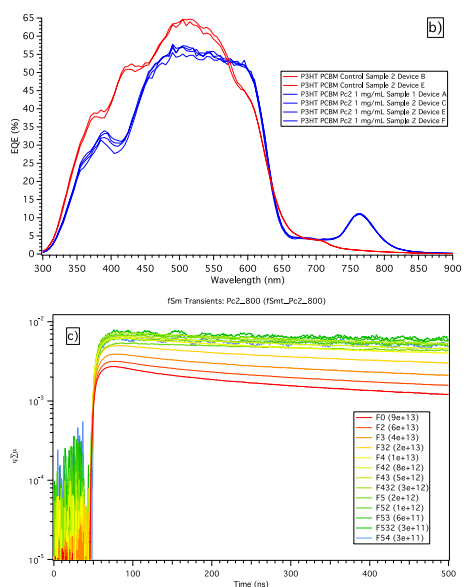
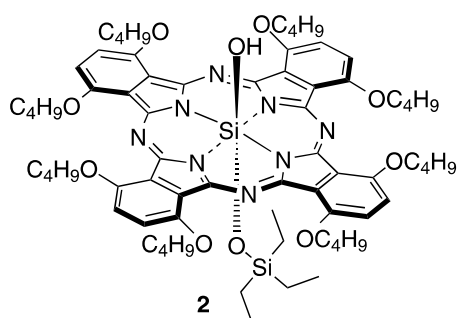


Figure: a) Silicon Phthalocyanine, Pc2 molecular structure; b) EQE spectra of 1:1 blend of p3HT and PCBM without (red) and with a 1 wt% Pc2 dispersion; c) TRMC transients exciting Pc2 in neat p3HT at 800nm at different excitation intensities.

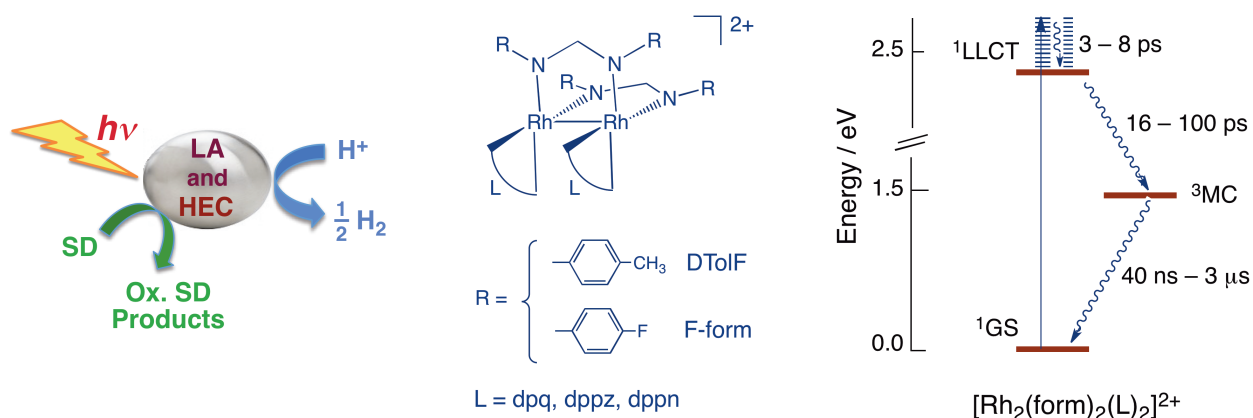
In the case of the Pc in neat p3HT, the TRMC data demonstrate clearly that the excited Pc oxidizes the p3HT to yield a very long-lived ( $> 10$  microseconds) separation of charges, with the electron residing on the Pc, and a mobile hole, which is detected by the microwave experiment, remaining in the p3HT. The Pc is therefore fulfilling exactly the same electron-accepting role as the fullerene derivatives that we have reported previously. To explain the EQE data, we propose a model where the Pc molecule acts as a bridge between a p3HT chain and a PCBM molecule within the amorphous phase of the polymer, where the charges are primarily generated, and not at the boundary between neat p3HT and PCBM phases. This differs from conventional wisdom, which suggests that free charges are only generated at this phase boundary, and the mixed, amorphous phase leads only to geminate recombination. To explain these data, a Marcus formulation is used to distinguish between the generation of free charges instead of bound charge-transfer states in this mixed region.

## Photocatalysts for H<sub>2</sub> Evolution: Combination of the Light Absorbing Unit and Catalytic Center in a Single Molecule

Nicholas Leed, Zhanyong Li, Suzanne Witt, Kim R. Dunbar, and Claudia Turro  
 Department of Chemistry and Biochemistry  
 The Ohio State University  
 Columbus, OH 43210

New bimetallic complexes for the photochemical and electrochemical production of H<sub>2</sub> gas from acidic aqueous solutions will be presented. The approach focuses on combining the light-absorbing (LA) unit with the hydrogen-evolving center (HEC) in the same molecule in order to reduce losses in efficiency due to charge transfer reactions. Moreover, this tactic circumvents the lengthy synthesis and purification procedures required to covalently tether different chromophores in an effective geometry or at a specific distance. Bimetallic complexes with highly reducing excited states and open coordination sites that can act as both the LA and HEC are being explored.

The photophysical properties of Rh<sub>2</sub>(II,II) compounds with formamidinate bridging ligands that are highly electron donating to the metal will be presented. These complexes are easily oxidized, making them strong excited state reducing agents. In addition, the photochemistry of the Rh<sub>2</sub>(form)<sub>4</sub> complexes can be accessed with low energy light since the compounds exhibit a relatively strong absorption at ~870 nm ( $\epsilon \sim 1,600 \text{ M}^{-1}\text{cm}^{-1}$ ). These complexes and the related family *cis*-[Rh<sub>2</sub>(form)<sub>2</sub>(L)<sub>2</sub>]<sup>2+</sup> (L = diimine ligand) will also be presented. In addition to the results of the photocatalysis and electrocatalysis for the generation of H<sub>2</sub> from aqueous media, time-resolved methods (ultrafast and ns-ms) were used to characterize the excited states of Rh<sub>2</sub>(form)<sub>4</sub> and [Rh<sub>2</sub>(form)<sub>2</sub>(L)<sub>2</sub>]<sup>2+</sup> (L = diimine) complexes to provide information on the nature of the reactive excited state. The results are consistent with excitation into a ligand-to-ligand charge transfer state (formamidinate-to-diimine), <sup>1</sup>LLCT, which decays to the reactive <sup>3</sup>MC (metal-centered) state. We are currently investigating the mechanism of the reaction and tuning the ligands to optimize photocatalytic properties.



## Understanding the effect of catalyst on the photovoltage of an electrodeposited n-Si/SiO<sub>x</sub>/Co/CoOOH photoanode for water oxidation

James C. Hill, Alan T. Landers, and Jay A. Switzer  
 Department of Chemistry and Materials Research Center  
 Missouri University of Science and Technology  
 Rolla, Missouri 65409-1170

A simple and inexpensive electrodeposition method is introduced to fabricate a highly efficient n-Si/SiO<sub>x</sub>/Co/CoOOH photoanode for the photoelectrochemical oxidation of water to oxygen gas. The photoanode generates a 0.47 V photovoltage, 35 mA/cm<sup>2</sup> short-circuit photocurrent density, 0.62 fill factor, and 10.2% conversion efficiency with 100 mW/cm<sup>2</sup> simulated sunlight. The interfacial energetics are quantitatively analyzed. The photoanode has a barrier height of 0.91 eV, compared with the 0.71 eV barrier height that is expected for a solid-state Schottky barrier. This leads to a 270 mV enhancement of the photovoltage, which is attributed to an adventitious 0.5 nm thick SiO<sub>x</sub> tunnel junction that minimizes surface states. The n-Si/SiO<sub>x</sub>/Co/CoOOH photoanode functions as an efficient solid-state metal-insulator-semiconductor (MIS) photovoltaic cell in series with a low overpotential water-splitting electrochemical cell.

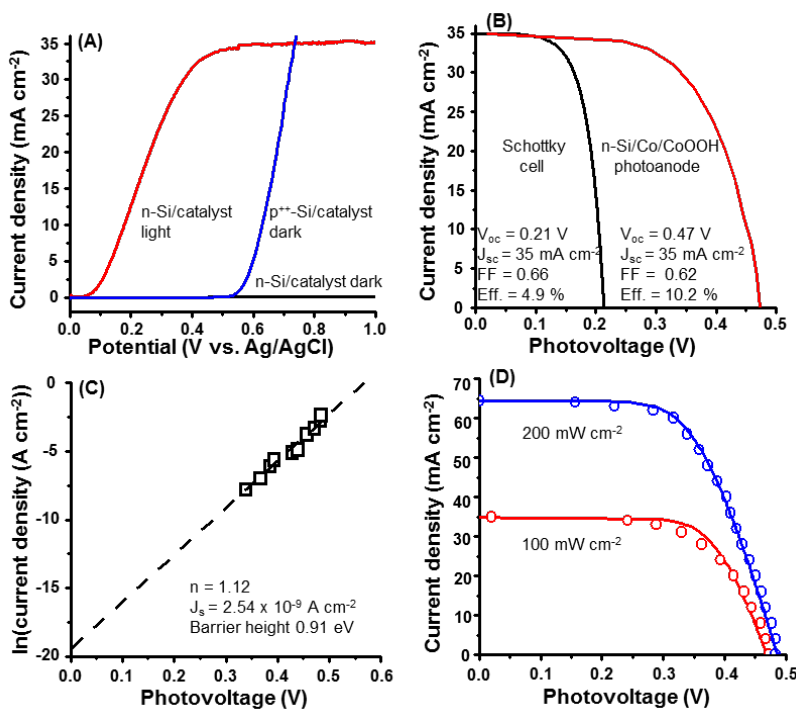


Fig. 1 – Photoelectrochemical performance of the n-Si/SiO<sub>x</sub>/Co/CoOOH photoanode. (A) Linear sweep voltammetry comparing n-Si in the dark (black), p<sup>++</sup>-Si/Co/CoOOH in the dark (blue), and n-Si/SiO<sub>x</sub>/Co/CoOOH under 100 mW/cm<sup>2</sup> AM 1.5 irradiation (red) in 1 M KOH at a 10 mV/s scan rate. (B) Calculated photoresponse of an n-Si/Co Schottky cell with a barrier height of 0.71 eV (black), and measured photoresponse of the n-Si/SiO<sub>x</sub>/Co/CoOOH photoanode under 100 mW/cm<sup>2</sup> AM 1.5 irradiation (red). (C) ln(J)-V plot collected by measuring the limiting photocurrent and photovoltage of photoanode at different light intensities. The photoanode has a diode quality factor of 1.12 and a dark saturation current density of 2.54 × 10<sup>-9</sup> A/cm<sup>2</sup>. (D) Measured (o) and simulated (solid line) photoresponse of the photoanode under (red) 100 mW/cm<sup>2</sup> and (blue) 200 mW/cm<sup>2</sup> AM 1.5 irradiation.



## Reactivity Mechanisms in New Cobalt Catalysts for Proton Reduction

Debashis Basu, Marco Allard, Xuetao Shi, Shivnath Mazumder,  
H. Bernhard Schlegel\* and Cláudio N. Verani\*

Department of Chemistry  
Wayne State University  
Detroit, Michigan 48202

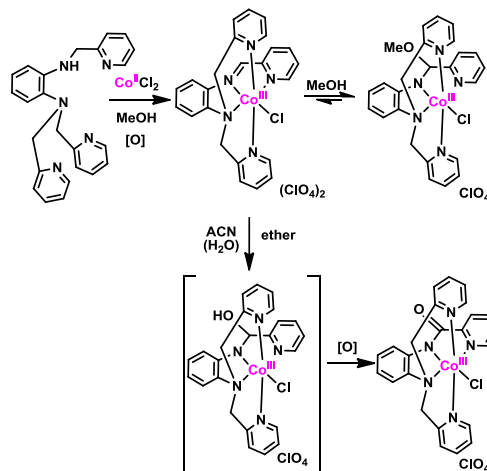
The Verani and Schlegel groups have been partners in the development of groundbreaking work toward the design of new architectures based on earth-abundant transition metals and capable of water splitting.

The work prioritizes the design of manganese, iron, and cobalt species with new ligands, the understanding of their electronic and electrochemical behavior and their testing toward water oxidation and proton reduction. This poster will offer a detailed overview on the trends observed for reactivity mechanisms and proton-reduction catalysis summarized in our oral presentation.

We will start on the collaboration between Basu (experiment) and Allard (calculations) to understand the role of ligand substitution on the overpotential of cobalt complexes with electroactive phenolate-rich  $[N_2O_3]$  donor type ligands, where appropriate substituents on phenylenediamine or phenolate moieties decrease the Co-based potentials.

We will then discuss the work of Basu (experiment) and Shi (calculations) on the energetics of axial ligand dissociation in cobalt oximes, where we reexamine the order of redox vs. chemical events leading to the catalytic Co(I) species.

Finally we will discuss the results obtained by Basu (experiment) and Mazumder (calculations) on the chemical conversions ( $=O$  and  $-OH$  insertion) of a cobalt complex with a new pendant-arm  $[N_2N'_3]$  polypyridyl ligand, where we observe that amines yield imines and amides unless a methyl protective group is used. Interestingly, all three species show some degree of catalytic activity. A schematic reaction coordinate for this last topic is shown.



## Photosystem I-Molecular Catalyst Complexes for Light-Driven Hydrogen Production: New Acceptor Protein Based Strategies for Hybrid Formation

Lisa M. Utschig, Sunshine C. Silver, Sarah R. Soltau, Jens Niklas, Karen L. Mulfort, David M. Tiede, and Oleg G. Poluektov  
Chemical Sciences and Engineering Division  
Argonne National Laboratory  
Argonne, IL 60439

Natural photosynthetic energy research is aimed at resolving fundamental mechanisms of photochemical energy conversion in photosynthetic proteins and using this information in the design of bio-inspired materials for the generation of solar fuels.

We are developing exciting new approaches for solar fuel production that link Nature's finely tuned photosynthetic machinery with synthetic first-row transition metal *molecular* catalysts to create hybrid complexes that use visible light to rapidly produce hydrogen from water. Novel hybrid architectures were realized by simple self-assembly of the photosynthetic reaction center protein Photosystem I (PSI) with the well-known cobaloxime  $\text{Co}(\text{dmgH})_2\text{pyCl}$  and nickel diphosphine  $[\text{Ni}(\text{P}_2^{\text{Ph}}\text{N}_2^{\text{Ph}})_2](\text{BF}_4)_2$  molecular hydrogen electrocatalysts. The resultant complexes provide the first examples of light-driven hydrogen production from synthetic molecular catalysts linked to PSI and, importantly, these hybrids function at near neutral pH in completely aqueous conditions.

Additionally, we have developed a strategy for incorporating the Ni molecular catalyst with the native acceptor protein of PSI, flavodoxin. Photocatalysis experiments with this modified flavodoxin demonstrate a new mechanism for biohybrid creation that involves protein-directed delivery of a

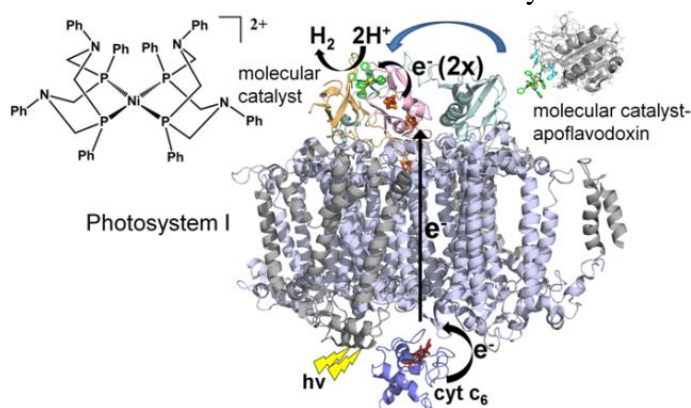


**Figure 1.** Photocatalytic scheme of  $\text{H}_2$  production from a PSI-Ni molecular catalyst hybrid complex and Ni-ApoFlavodoxin.

molecular catalyst to the reducing side of PSI for light-driven catalysis. This approach provides the potential for self-repair of the biohybrid system with a mechanism for introducing fresh catalyst to the acceptor end of PSI. In ongoing investigations, we are examining covalent linkage of catalysts to the second acceptor protein of PSI, ferredoxin. Long term goals of this project involve developing methodologies to spectroscopically probe the molecular catalyst electronic structure in protein environments and characterize interprotein-catalyst ET pathways.

## Studies on the <sup>3</sup>MLCT Excited State and Catalytic Water Oxidation Properties of Mono and Multimetallic Ruthenium Complexes

Cláudio N. Verani, John F. Endicott, H. Bernhard Schlegel

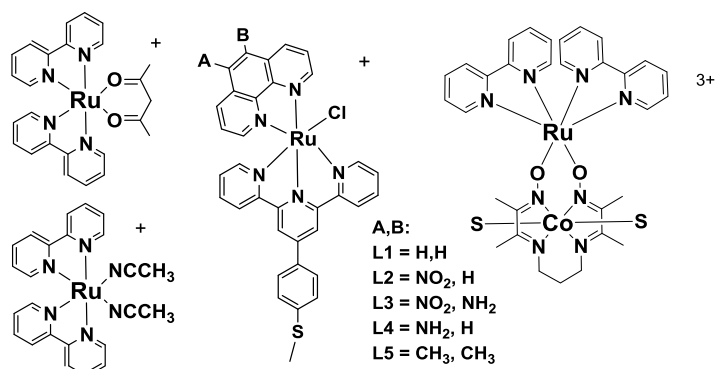
Department of Chemistry  
Wayne State University  
Detroit, Michigan 48202

Our research is focused on the requirements for integrating active center, antennae, and acceptor modules into a single molecule. The current emphasis is on obtaining a better understanding of the electronic and redox properties of monometallic modules and multimetallic assemblies for water splitting in-bulk and on surfaces.

We will start with the analysis of the trends observed in the <sup>3</sup>MLCT excited state properties of ruthenium complexes by the Endicott and Schlegel groups, and summarized in our oral presentation for several series of Ru(II)-pyridyl and polypyridyl complexes. DFT-based assignments indicate that the energies, orbital compositions, and electronic distributions in the Franck-Condon excited states and the reactive triplet excited states do not always correlate in monometallic complexes. The calculated emission spectra, including energies and vibronic bandshapes are in very good agreement with the 77 K spectra and indicate that increases in higher energies in vibronic sideband amplitudes results from the “tuning” of the <sup>3</sup>MLCT excited state energies with respect to the energy of the bpy ligand ππ-ππ\* energy gap and the different mixings of bpy and <sup>3</sup>MLCT orbitals.

We will then discuss the efforts by the Verani and Schlegel groups towards the development of catalysts for water splitting by a series of unsymmetrical ruthenium complexes [(terpy-R)Ru(phen-X)Cl]PF<sub>6</sub> where terpy-R = 4’-(4-methylmercaptophenyl)-2,2’:6’2’’-terpyridine and phen-X = H (**1**), X = 5-nitro (**2**), X = 5,6-dimethyl (**3**), and X = 3,4,7,8-tetramethyl (**4**). The electrochemical properties of these complexes indicate that the first reduction potential of **2** is comparatively lower than that of the other complexes. This trend is supported by DFT calculations where a decrease in the HOMO-LUMO gap is observed for **2**. The turnover numbers of these complexes indicate that EWGs on phenanthroline decrease the catalytic activity. The initial rate of dioxygen evolution was measured using a Clark electrode and higher initial rate is observed for **3** than for **1**. The <sup>1</sup>HNMR and mass analysis of **1** isolated after catalysis suggest the catalytic core is intact, although the methylthio-substituent on terpyridine is oxidized.

Finally we will discuss efforts to build up and study homo- and heterometallic assemblies based on such ruthenium motifs.



## Photoinitiated Charge Separation and Transport in Self-assembled Charge Conduits

Michael R. Wasielewski, Vladimir Roznyatovskiy, Yi-Lin Wu, Raanan Carmieli, Scott M. Dyar, and Kristen E. Brown

Department of Chemistry, Northwestern University  
Evanston, IL 60208

Photoactive molecules for solar fuels production and organic photovoltaics (OPVs) require significant molecular order to achieve high performance. We are currently developing covalently-bound, donor-acceptor building blocks that self-assemble into  $\pi$ -stacked segregated hole and electron charge conduits. In one example, we have prepared a potassium-ion-induced guanine-quadruplex as a supramolecular platform for controlled assembly of electron donor-acceptor system. A monodisperse,  $C_4$ -symmetric octamer of a guanine-erylene-3,4,9,10-bis(dicarboximide) conjugate (Fig. 1, **GPDI**, **1**) was prepared in tetrahydrofuran. The two layers of cyclic **GPDI** tetramers adopt a nearly eclipsed relationship (*H*-aggregation) revealed by small- and wide-angle X-ray scattering, NMR spectroscopy, and steady-state UV-Vis absorption. Following photoexcitation of the PDI moiety in the quadruplex, charge separation occurs in  $\tau_{CS} = 98 \pm 12$  ps to give  $G^{+•}$ -PDI $^{-•}$  that recombines in  $\tau_{CR} = 1.2 \pm 0.2$  ns, which is  $> 100$  times longer than that in the monomeric **GPDI** dyad. The transient absorption spectrum of  $G^{+•}$ -PDI $^{-•}$  within the **GPDI**-quadruplex shows that the PDI $^{-•}$  radical anion is delocalized over the neighboring PDI units. In a second example, **2**, having a central zinc *meso*-tetraphenyltetraabenzoporphyrin (ZnTBTPP) electron donor to which four perylene-3,4,9,10-bis(dicarboximide) (PDI) electron acceptors are linked via xylyl-phenyl spacers was prepared. Small- and wide-angle x-ray scattering measurements indicate that **2** self-assembles in toluene solution into a  $\pi$ -stacked structure having an average of twelve molecules of **1** (**1**<sub>12</sub>). The xylyl-phenyl spacer between ZnTBTPP and each PDI controls the electronic coupling so that photoexcitation of **1**<sub>12</sub> results in rapid single-step electron transfer ( $\tau = 73$  ps) to give long-lived ZnTBTPP $^{+•}$ -PDI $^{-•}$  ( $\tau = 169$  ns). Time-resolved EPR (TREPR) spectroscopy shows that charge transport occurs within the segregated hole and electron charge conduits leading to an average 26 Å electron-hole separation distance.

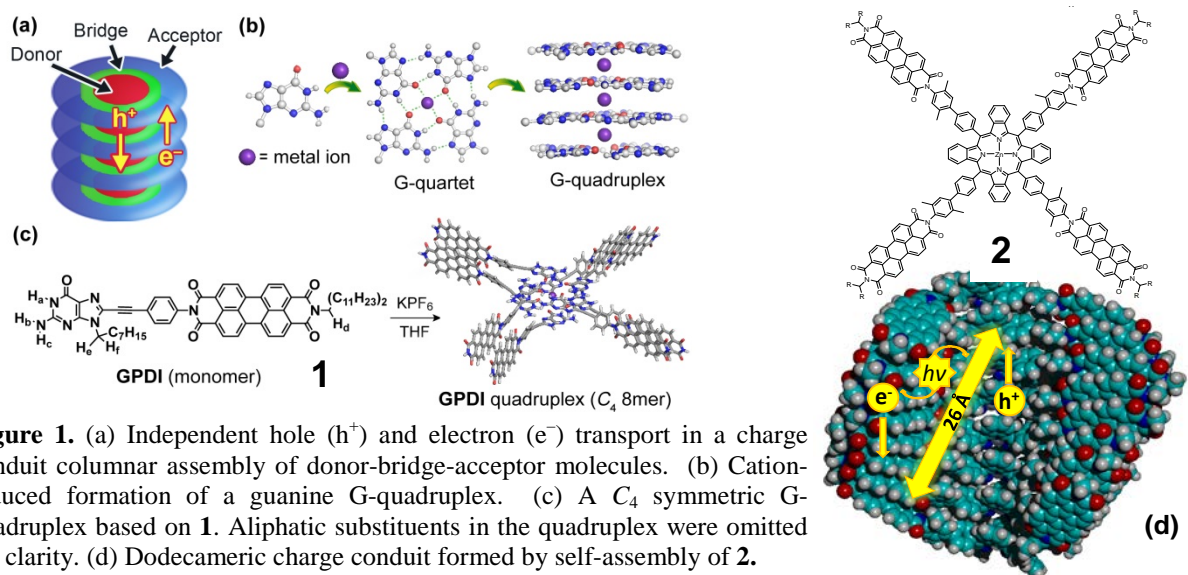


**Figure 1.** (a) Independent hole ( $h^+$ ) and electron ( $e^-$ ) transport in a charge conduit columnar assembly of donor-bridge-acceptor molecules. (b) Cation-induced formation of a guanine G-quadruplex. (c) A  $C_4$  symmetric G-quadruplex based on **1**. Aliphatic substituents in the quadruplex were omitted for clarity. (d) Dodecameric charge conduit formed by self-assembly of **2**.

## Exciton Delocalization at Nanoscopic Organic/Inorganic Interfaces

Matthew Frederick, Victor Amin, Rachel Harris, Ken Aruda, Shengye Jin, and Emily A. Weiss  
Department of Chemistry  
Northwestern University  
Evanston, IL 60208-3113

This poster describes the mechanisms by which organic surfactants – in particular phenyldithiocarbamate (PTC) and its derivatives and thiophenolate (TP) and its derivatives – couple electronically to the delocalized states of semiconductor quantum dots (QDs). This coupling reduces the confinement energies of excitonic carriers, and, in the case of PTC, the optical bandgap of metal chalcogenide QDs by up to 1 eV by selectively delocalizing the excitonic hole. The reduction of confinement energy for the hole is enabled by the creation of interfacial electronic states near the valence band edge of the QD. The PTC case illuminates the general minimal requirements for surfactants to achieve observable bathochromic or hypsochromic shifts of the optical bandgap of QDs: frontier orbitals with energies near the relevant semiconductor band-edge, the correct symmetry to mix with the orbitals of the relevant band, and an adsorption geometry that permits spatial overlap between the orbitals of the ligand and those of the relevant band. NMR measurements indicate that the magnitude of exciton delocalization, as measured by the effective increase in excitonic radius,  $\Delta R$ , increases nonlinearly with surface coverage of PTC and substituted PTCs. Transient absorption measurements on complexes of QDs and zinc-porphyrins show that *bis*-PTC molecules are effective cross-linking ligands for enhancing yields of electron transfer within donor-acceptor complexes.

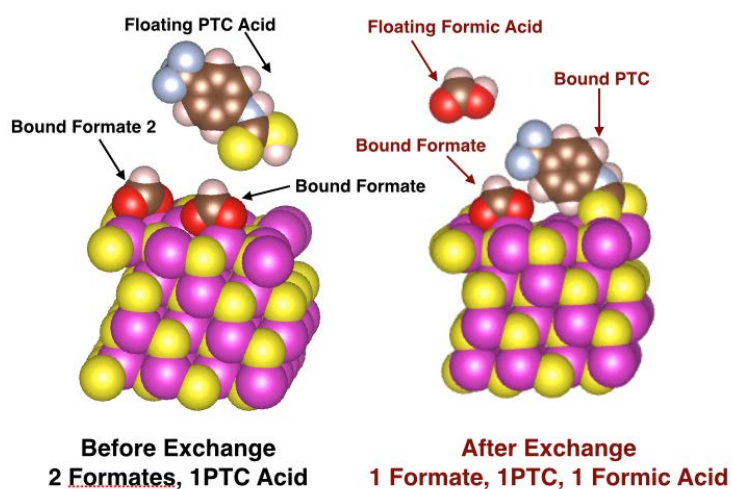


**Figure 1.** Segment of a CdS lattice with two bound formate molecules (left) and with one of the formate molecules replaced with a dithiocarbamate. The ligand exchange influences the electronic structure and, in turn, the optical spectra of nanostructures comprising these basic lattice units.



## *List of Participants*



## Participants List – 36<sup>th</sup> Solar Photochemistry Research Meeting

John Asbury  
Pennsylvania State University  
Department of Chemistry  
University Park, PA 16801  
814-863-6309  
jba11@psu.edu

Victor Batista  
Yale University  
P.O. Box 208107  
New Haven, CT 06477  
203-432-6672  
victor.batista@yale.edu

Andrew Bocarsly  
Princeton University  
Frick Laboratory  
Princeton, NJ 08544  
609-258-3888  
bocarsly@princeton.edu

Shannon Boettcher  
University of Oregon  
Department of Chemistry  
Eugene, OR 97403  
541-346-2543  
swb@uoregon.edu

Kara Bren  
University of Rochester  
120 Trustee Rd.  
Rochester, NY 14627-0216  
585-275-4335  
bren@chem.rochester.edu

Karen Brewer  
Virginia Polytechnic Institute  
Department of Chemistry  
Blacksburg, VA 24061-0212  
540-231-6579  
kbrewer@vt.edu

Gary Brudvig  
Yale University  
P.O. Box 208107  
New Haven, CT 06477  
203-432-5202  
gary.brudvig@yale.edu

Emilio Bunel

Argonne National Laboratory  
9700 S. Cass Ave.  
Argonne, IL 60439  
630-252-4309  
ebunel@anl.gov

Ian Carmichael  
University of Notre Dame  
223 Radiation Laboratory  
Notre Dame, IN 46556  
574-631-4502  
carmichael.1@nd.edu

Edward Castner  
Rutgers University  
610 Taylor Road  
Piscataway, NJ 08854  
732-445-2564  
ecastner@rutgers.edu

Lin Chen  
Argonne National Lab/Northwestern Univ.  
9700 S. Cass Ave.  
Argonne, IL 60439  
630-252-3533  
lchen@anl.gov

Kyoung-Shin Choi  
University of Wisconsin Madison  
Department of Chemistry  
1101 University Avenue  
Madison, WI 53706  
608-262-5859  
kschoi@chem.wisc.edu

Javier Concepcion  
Brookhaven National Laboratory  
Chemistry Department  
Upton, NY 11973-5000  
631-344-4369  
jconcepc@bnl.gov

Philip Coppens  
University at Buffalo SUNY Buffalo  
732 NSc Complex  
Buffalo, NY 14260-3000  
716-645-4273  
coppens@buffalo.edu

Robert Crabtree

## Participants List – 36th Solar Photochemistry Research Meeting

Yale University  
225 Prospect St.  
New Haven, CT 06520  
203-432-3925  
robert.crabtree@yale.edu

Nada Dimitrijevic  
U.S. Department of Energy  
1000 Independence Ave., SW  
Washington, DC 20585  
301-903-5805  
Nada.Dimitrijevic@science.doe.gov

Linda Doerrer  
Boston University  
590 Commonwealth Ave.  
Boston, MA 02139  
617-358-4335  
doerrer@bu.edu

Kim Dunbar  
Texas A&M University  
Department of Chemistry  
College Station, TX 77843-3255  
979-845-5235  
dunbar@mail.chem.tamu.edu

Richard Eisenberg  
University of Rochester  
Department of Chemistry  
Rochester, NY 14627  
585-275-5573  
eisenberg@chem.rochester.edu

John Endicott  
Wayne State University  
321 Chemistry  
Detroit, MI 48202  
313-5787-2607  
jfe@chem.wayne.edu

Christopher Fecko  
U.S. Department of Energy  
1000 Independence Ave., SW  
Washington, DC 20585  
301-903-1303  
christopher.fecko@science.doe.gov

Susanne Ferrere  
National Renewable Energy Laboratory

15013 Denver West Pkwy.  
Golden, CO 80401  
303-384-6502  
Suzanne.Ferrere@nrel.gov

Arthur Frank  
National Renewable Energy Laboratory  
15013 Denver West Pkwy.  
Golden, CO 80401  
303-384-6262  
Arthur.Frank@nrel.gov

Heinz Frei  
Lawrence Berkeley National Laboratory  
One Cyclotron Road  
Berkeley, CA 94720  
510-486-4325  
HMFrei@lbl.gov

Richard A. Friesner  
Columbia University  
Department of Chemistry  
3000 Broadway, MC 3110  
New York, NY 10027  
212-854-7606  
rich@chem.columbia.edu

Etsuko Fujita  
Brookhaven National Laboratory  
Chemistry Department  
Upton, NY 11973-5000  
631-344-4356  
fujita@bnl.gov

Bruce Garrett  
Pacific Northwest National Laboratory  
P.O. Box 999 (K9-90)  
Richland, WA 99352  
509-372-6344  
bruce.garrett@pnnl.gov

Brian Gregg  
National Renewable Energy Laboratory  
15013 Denver West Pkwy.  
Golden, CO 80401  
303-384-6635  
brian.gregg@nrel.gov

David Grills  
Brookhaven National Laboratory

## Participants List – 36th Solar Photochemistry Research Meeting

Chemistry Department  
Upton, NY 11973-5000  
631-344-4332  
dcgrills@bnl.gov

Thomas Hamann  
Michigan State University  
578 S. Shaw Lane, RM 411  
East Lansing, MI 48824  
517-355-9715  
hamann@chemistry.msu.edu

Alexander Harris  
Brookhaven National Laboratory  
Chemistry Department  
Upton, NY 11973-5000  
631-344-4301  
alex@bnl.gov

Michael Henderson  
Pacific Northwest National Laboratory  
P.O. Box 999, K8-87  
Richland, WA 99352  
509-371 -6527  
ma.henderson@pnl.gov

Craig Hill  
Emory University  
1515 Dickey Dr., NE  
Atlanta, GA 30322  
404-727-6611  
chill@emory.edu

Michael Hopkins  
University of Chicago  
Department of Chemistry  
Chicago, IL 60637  
773-702-6490  
mhopkins@uchicago.edu

Libai Huang  
University of Notre Dame  
223 Radiation Laboratory  
Notre Dame, IN 46556  
573-631-2657  
lhuang2@nd.edu

Prashant Kamat  
University of Notre Dame  
223 Radiation Laboratory

Notre Dame, IN 46556  
574-631-5411  
pkamat@nd.edu

Peter Khalifah  
Stony Brook University  
Department of Chemistry  
Stony Brook, NY 11794-3400  
631-632-7796  
kpete@bnl.gov

Carl Koval  
JCAP Energy Innovation Hub  
116 Jorgensen Laboratory  
MC 132-80  
Pasadena CA 91125  
626-395-3908  
ckoval@caltech.edu

Todd Krauss  
University of Rochester  
120 Trustee Road  
Rochester, NY 14627-0216  
585-275-5093  
krauss@chem.rochester.edu

Frederick Lewis  
Northwestern University  
2145 Sheridan Road  
Evanston, IL 60208  
847-491-3441  
fdl@northwestern.edu

Nathan Lewis  
California Institute of Technology  
1200 E. California Blvd.  
Pasadena, CA 91125  
626-395-6335  
nslewis@caltech.edu

Tianquan Lian  
Emory University  
1515 Dickey Drive NE  
Atlanta, GA 30322  
404-727-6649  
tlian@emory.edu

Rene Lopez  
University of North Carolina  
343 Chapman Hall, Physics Dept.

## Participants List – 36th Solar Photochemistry Research Meeting

Chapel Hill, NC 27713  
919-962-7216  
rln@physics.unc.edu

Stephen Maldonado  
University of Michigan  
930 N. University  
Ann Arbor, MI 48109-1055  
734-647-4750  
smald@umich.edu

Thomas Mallouk  
Pennsylvania State University  
Department of Chemistry  
University Park, P A 16801  
814-863-9637  
tom@chem.psu.edu

Diane Marceau  
U.S. Department of Energy  
1000 Independence Ave., SW  
Washington, DC 20585  
301-903-0235  
diane.marceau@science.doe.gov

Gail McLean  
U.S. Department of Energy  
1000 Independence Ave., SW  
Washington, DC 20585  
301- 903-7807  
gail.mclean@science.doe.gov

Thomas Meyer  
University of North Carolina  
Department of Chemistry  
Chapel Hill, NC 27599-3290  
919-843-8313  
tjmeyer@unc.edu

Ana Moore  
Arizona State University  
Dept. Chemistry and Biochemistry  
Tempe, AZ 85287-1604  
480-965-2747  
amoore@asu.edu

Thomas Moore  
Arizona State University  
Dept. Chemistry and Biochemistry  
Tempe, AZ 85287-1604

480-965-3308  
tmoore@asu.edu

James Muckerman  
Brookhaven National Laboratory  
Chemistry Department  
Upton, NY 11973-5000  
631-344-4368  
muckerma@bnl.gov

Karen Mulfort  
Argonne National Laboratory  
9700 S. Cass Ave.  
Argonne, IL 60439  
630-252-3545  
mulfort@anl.gov

Charles Mullins  
University of Texas at Austin  
Dept. of Chemical Eng. C0400  
Austin, TX 78712  
512-471-5817  
mullins@che.utexas.edu

Djamaladdin Musaev  
Emory University  
1515 Dickey Dr.  
Atlanta, GA 30322  
404-727-2382  
dmusaev@emory.edu

Nathan Neale  
National Renewable Energy Laboratory  
15013 Denver West Parkway  
Golden, CO 8040 1  
303-384-6165  
nathan.neale@nrel.gov

Marshall Newton  
Brookhaven National Laboratory  
Chemistry Department  
Upton, NY 11973  
631-344-4366  
newton@bnl.gov

Daniel Nocera  
Harvard University  
Chemistry & Chem. Biology  
12 Oxford St  
Cambridge, MA 02138

## Participants List – 36th Solar Photochemistry Research Meeting

617-495-8904  
dnocera@fas.harvard.edu

Arthur Nozik  
University of Colorado  
215 UCB  
Boulder, CO 80309  
303-384-6603  
arthur.nozik@colorado.edu

Bruce Parkinson  
University of Wyoming  
1000 E. University  
Laramie, WY 82071  
303-766-9891  
bparkin1@uwyo.edu

Hrvoje Petek  
University of Pittsburgh  
3941 O'Hara Street, G01 Allen  
Pittsburgh, P A 15260  
412-624-3599  
petek@pitt.edu

Oleg Poluektov  
Argonne National Laboratory  
9700 S. Cass Ave.  
Argonne, IL 60439  
630-252-3546  
Oleg@anl.gov

Dmitry Polyansky  
Brookhaven National Laboratory  
Chemistry Department  
Upton, NY 11973  
631-344-4315  
dep@bnl.gov

Oleg Prezhdo  
University of Rochester  
Department of Chemistry  
Rochester, NY 14627  
585-276-5664  
oleg.prezhdo@rochester.edu

Yulia Pushkar  
Purdue University  
525 Northwestern A venue  
West Lafayette, IN 97407  
765-496-3279

ypushkar@purdue.edu

Garry Rumbles  
National Renewable Energy Laboratory  
15013 Denver West Parkway  
Golden, CO 80401  
303-384-6502  
garry.rumbles@nrel.gov

Bernhard Schlegel  
Wayne State University  
Department of Chemistry  
Detroit, MI 48202  
313-577-2562  
hbs@chem.wayne.edu

Russell Schmehl  
Tulane University  
Department of Chemistry  
New Orleans, LA 70118  
504-862-3566  
russ@tulane.edu

Charles Schmuttenmaer  
Yale University  
225 Prospect St.  
New Haven, CT 06520-8107  
203-432-5049  
charles.schmuttenmaer@yale.edu

Mark Spitler  
U.S. Department of Energy  
1000 Independence Ave., SW  
Washington, DC 20585  
301-903-4568  
mark.spitler@science.doe.gov

Jay Switzer  
Missouri University of Science and Technology  
103 Materials Research Center  
Rolla, MO 65409-1170  
573-341-4383  
jswitzer@mst.edu

Randolph Thummel  
University of Houston  
Chemistry Department  
Houston, TX 77204-5003  
713-743-2734  
thummel@uh.edu

## Participants List – 36th Solar Photochemistry Research Meeting

David Tiede  
Argonne National Laboratory  
9700 S. Cass Ave.  
Argonne, IL 60439  
630-252-3539  
tiede@anl.gov

Emily Weiss  
Northwestern University  
2145 Sheridan Rd.  
Evanston, IL 60208-3113  
847-491-3095  
e-weiss@northwestern.edu

William Tumas  
National Renewable Energy Laboratory  
15013 Denver West Parkway  
Golden, CO 80401  
303-384-7955  
bill.tumas@nrel.gov

John Turner  
National Renewable Energy Laboratory  
15013 Denver West Parkway  
Golden, CO 80401-3393  
303-275-4270  
John.Turner@nrel.gov

Claudia Turro  
Ohio State University  
100 W. 18th Ave.  
Columbus, OH 43210  
614-292-6708  
turro@chemistry.ohio-state.edu

Lisa Utschig  
Argonne National Laboratory  
9700 S. Cass Ave.  
Argonne, IL 60439  
630-252-3544  
utschig@anl.gov

Claudio Verani  
Wayne State University  
5101 Cass Ave  
Detroit, MI 48202  
311-577-1076  
cnverani@chem.wayne.edu

Michael Wasielewski  
Northwestern University  
2145 Sheridan Rd.  
Evanston, IL 60208  
847-467-1423  
m-wasielewski@northwestern.edu

## *Author Index*



|                               |                        |
|-------------------------------|------------------------|
| Adams, Rebecca.....           | 156                    |
| Allard, Marco.....            | 157                    |
| Allen, Laura J. ....          | 126                    |
| Amin, Victor.....             | 161                    |
| Aruda, Ken.....               | 161                    |
| Asbury, John B. ....          | 125                    |
| Ashford, Dennis.....          | 24                     |
| Baillargeon, Josh.....        | 5                      |
| Barber, Greg D. ....          | 71                     |
| Bard, Allen J. ....           | 33                     |
| Basu, Debashis.....           | 157                    |
| Batista, Victor S. ....       | 66, 126, 130, 131      |
| Bisquert, Juan.....           | 130                    |
| Bocarsly, Andrew B. ....      | 63                     |
| Boettcher, Shannon W. ....    | 103                    |
| Bren, Kara L. ....            | 77                     |
| Brennan, Bradley J. ....      | 130                    |
| Brewer, Karen J. ....         | 49                     |
| Brown, Kristen E. ....        | 160                    |
| Brudvig, Gary W. ....         | 66, 126, 130           |
| Brunell, Adam ....            | 153                    |
| Brus, Louis.....              | 135                    |
| Burmistrova, Polina.....      | 41                     |
| Cao, Bingfei.....             | 41                     |
| Carmieli, Raanan.....         | 160                    |
| Castner, Jr., Edward W. ....  | 127                    |
| Chamberlin, S.E. ....         | 113                    |
| Chambers, S.A. ....           | 113                    |
| Chen, Lin X. ....             | 16, 117, 142           |
| Chen, Yang.....               | 129                    |
| Chen, Yong-Siou.....          | 138                    |
| Chen, Zheyuan.....            | 140                    |
| Choi, Kyoung-Shin.....        | 38                     |
| Ciston, James.....            | 41                     |
| Concepcion, Javier J. ....    | 106, 128               |
| Coppens, Philip.....          | 129                    |
| Crabtree, Robert H. ....      | 66, 126, 130           |
| Davis, Katherine.....         | 152                    |
| Dimitrijevic, N. M. ....      | 117                    |
| Ding, Wendu.....              | 126                    |
| Dix, Victoria.....            | 44                     |
| Doerrer, Linda H. ....        | 131                    |
| Dogutan, Dilek K. ....        | 92                     |
| Dunbar, Kim R. ....           | 132, 154               |
| Durrell, Alec C. ....         | 130                    |
| Dyar, Scott M. ....           | 160                    |
| Dysart, Jennifer.....         | 71                     |
| Eisenberg, Richard.....       | 77                     |
| Endicott, John F. ....        | 53, 159                |
| Ertem, Mehmed Z. ....         | 131                    |
| Farnum, Byron.....            | 24, 141                |
| Feng, Min.....                | 147                    |
| Ferrere, Suzanne.....         | 89, 133                |
| Frank, Arthur J. ....         | 134                    |
| Fransted, K. ....             | 117                    |
| Frederick, Matthew.....       | 161                    |
| Frei, Heinz.....              | 80                     |
| Friesner, Richard A. ....     | 135                    |
| Fujita, Etsuko.....           | 95, 106, 110, 128, 149 |
| Gao, Haifeng.....             | 137                    |
| Garvey, Timothy.....          | 141                    |
| Graham, Daniel.....           | 92                     |
| Gray, Christopher.....        | 71                     |
| Gregg, Brian.....             | 89, 133                |
| Grieco, Christopher.....      | 125                    |
| Grills, David C. ....         | 95, 110                |
| Gu, Jing.....                 | 63                     |
| Guo, Zhi.....                 | 137                    |
| Gust, Devens.....             | 20, 71                 |
| Halverson, Adam F. ....       | 134                    |
| Hamann, Thomas W. ....        | 5                      |
| Harpham, M. R. ....           | 117                    |
| Harris, Rachel.....           | 161                    |
| Henderson, Michael A. ....    | 113                    |
| Hill, Craig L. ....           | 83                     |
| Hill, James C. ....           | 155                    |
| Hopkins, Michael D. ....      | 136, 148               |
| Hu, Yuan.....                 | 63                     |
| Huang, Huafeng.....           | 41                     |
| Huang, Libai.....             | 137                    |
| Huang, J. ....                | 117                    |
| Hybertsen, Mark.....          | 41                     |
| Ito, Akitaka.....             | 24                     |
| Jang, Song-Rim.....           | 134                    |
| Jarzemska, Katarzyna N. ....  | 129                    |
| Jerome, Steve.....            | 135                    |
| Jin, Shengye.....             | 161                    |
| Kamat, Prashant V. ....       | 138                    |
| Kaspar, T. C. ....            | 113                    |
| Kaveevivitchai, Nattawut..... | 57                     |
| Kern, Meghan.....             | 146                    |
| Khalifah, Peter.....          | 41                     |
| Khatun, Sufia.....            | 127                    |
| King, Lauren.....             | 146                    |
| King, Skye.....               | 49                     |
| Koenigsmann, Christopher..... | 130                    |
| Koepf, Matthieu.....          | 130                    |
| Kokhran, Oleksandr.....       | 142                    |
| Kohler, Lars.....             | 57                     |
| Koval, Carl A. ....           | 11                     |
| Kraus, Ted.....               | 146                    |
| Krauss, Todd D. ....          | 77                     |

|                                  |                   |
|----------------------------------|-------------------|
| Landers, Alan T. ....            | 155               |
| Lapides, Alex.....               | 24                |
| La Porte, Nathan T. ....         | 136               |
| Lee, Byeongdu.....               | 137               |
| Lee, Doyun.....                  | 137               |
| Leed, Nicholas.....              | 132, 154          |
| Lewis, Frederick D. ....         | 139               |
| Lewis, Nathan S. ....            | 41, 44            |
| Li, Zhanyong.....                | 132, 154          |
| Lian, Tianquan.....              | 83, 140           |
| Liang, Min.....                  | 127               |
| Lin, Fuding.....                 | 103               |
| Lofaro, John.....                | 41                |
| Lopez, Rene.....                 | 141               |
| Luo, TengFei.....                | 137               |
| Maldonado, Stephen.....          | 3                 |
| Mallalieu, Hannah.....           | 49                |
| Mallouk, Thomas E. ....          | 71                |
| Manbeck, Gerald.....             | 49                |
| Mandal, Dhritabrata.....         | 5                 |
| Mara, M. W. ....                 | 117               |
| Mardis, Kristy L. ....           | 148               |
| Martin, Jarett.....              | 132               |
| Mazumder, Shivnath.....          | 137               |
| McCool, Nicholas S. ....         | 71                |
| McKone, James.....               | 44                |
| Mendez-Hernandez, Dalvin D. .... | 71                |
| Mercado, Candy.....              | 145               |
| Meyer, Thomas J. ....            | 24                |
| Mi, Qixi.....                    | 41                |
| Mills, Thomas J. ....            | 103               |
| Milot, Rebecca L. ....           | 126, 130          |
| Moore, Thomas A. ....            | 20, 71            |
| Moore, Ana L. ....               | 20, 71            |
| Moravec, Davis B. ....           | 136               |
| Morris, Amanda J. ....           | 63                |
| Muckerman, James T. ...          | 95, 106, 128, 149 |
| Mukherjee, Anusree               | 142               |
| Mulfort, Karen L. ....           | 16, 142, 148, 158 |
| Mullins, C. Buddie.....          | 33                |
| Musaev, Djmaladdin G. ....       | 83                |
| Neale, Nathan R. ....            | 143               |
| Negre, Christian, F. A. ....     | 126, 130          |
| Nepomnyashchii, Alexander.....   | 146               |
| Newton, Marshall D. ....         | 144               |
| Niklas, Jens.....                | 142, 148, 158     |
| Nocera, Daniel G. ....           | 92                |
| Nozik, Arthur J. ....            | 145               |
| O'Faria, Luiz Felipe.....        | 127               |
| Ondersma, Jesse.....             | 5                 |
| Papanikolas, John.....           | 24                |
| Park, Jaehong.....               | 153               |
| Parkinson, Bruce.....            | 146               |
| Petek, Hrvoje.....               | 147               |
| Poluektov, Oleg G. ....          | 16, 142, 148, 158 |
| Polyansky, Dmitry E. ....        | 95, 106, 110, 149 |
| Prezhdo, Oleg V. ....            | 150               |
| Pushkar, Yulia.....              | 151, 152          |
| Qin, Dongdong.....               | 71                |
| Reid, Obadiah.....               | 153               |
| Ripolles, Teresa S. ....         | 130               |
| Rimshaw, Adam D. ....            | 125               |
| Roupelakis, Manolis.....         | 92                |
| Roznyatovskiy, Vladimir.....     | 160               |
| Rumbles, Garry.....              | 153               |
| Saunders, Timothy.....           | 71                |
| Schaller, Richard.....           | 137               |
| Schlegel, H. Bernhard.....       | 53, 157, 159      |
| Schmehl, Russell.....            | 156               |
| Schmittenmaer, Charles A. ....   | 66, 126, 130      |
| Seabold, Jason A. ....           | 143               |
| Shan, Bing.....                  | 156               |
| Shi, Xuetao.....                 | 157               |
| Silver, Sunshine C. ....         | 158               |
| Soltau, Sarah R. ....            | 158               |
| Soman, Suraj.....                | 5                 |
| Specht, Sarah E. ....            | 131               |
| Stamplecoskie, Kevin.....        | 138               |
| Steigerwald, Mike.....           | 135               |
| Stewart, Robert J. ....          | 125               |
| Sun, Hao.....                    | 147               |
| Sushko, P. V. ....               | 113               |
| Svedruzic, Drazenka.....         | 89, 133           |
| Swierk, John R. ....             | 71                |
| Switzer, Jay A. ....             | 155               |
| Tahsini, Laleh.....              | 131               |
| Thummel, Randolph P. ....        | 57                |
| Turner, John A. ....             | 29                |
| Tiede, David M. ....             | 16, 142, 148, 158 |
| Tong, Lianpeng.....              | 57                |
| Torre, Jose A. ....              | 130               |
| Trzop, Elzbieta.....             | 129               |
| Turro, Claudia.....              | 132, 154          |
| Utschig, Lisa M. ....            | 16, 148, 158      |
| Vargas-Barbosa, Nella M. ....    | 71                |
| Verani, Cláudio N. ....          | 53, 148, 157, 159 |
| Villanueva-Cab, Julio.....       | 134               |
| Wang, Limin.....                 | 41                |
| Wang, Y. ....                    | 113               |
| Wasielewski, Michael R. ....     | 160               |
| Watkins, Kevin.....              | 146               |
| Weiss, Emily A. ....             | 161               |

|                            |               |
|----------------------------|---------------|
| Westwood, Mark.....        | 136, 148      |
| White, Michael.....        | 41            |
| Wiensch, Joshua D. ....    | 44            |
| Wiggenhorn, Craig.....     | 44            |
| Witt, Suzanne.....         | 132, 154      |
| Wong, Chris.....           | 137           |
| Wu, Boning.....            | 127           |
| Wu, Kaifeng.....           | 140           |
| Wu, Yi-Lin.....            | 160           |
| Xie, Yuling.....           | 5             |
| Xu, Pengtao.....           | 71            |
| Yan, Lifen.....            | 151, 152      |
| Yan, Yong.....             | 63            |
| Yang, Ye.....              | 140           |
| Zakutayev, Andriy.....     | 145           |
| Zeitler, Elizabeth L. .... | 63            |
| Zhang, Jing.....           | 135           |
| Zhang, Sheng.....          | 24            |
| Zhao, Jin.....             | 147           |
| Zhou, Rongwei.....         | 49            |
| Zhu, Guibo.....            | 151           |
| Zhu, Haiming.....          | 140           |
| Zhu, Kai.....              | 134, 143, 145 |
| Zhu, Yimei.....            | 41            |
| Zong, Ruifa.....           | 57            |
| Zuo, Xiaobing.....         | 137           |

